INTERNATIONAL DOCTORAL
SCHOOL OF THE USC

Sergio
Rodríguez Rodríguez

PhD Thesis

GENOMIC CHARACTERIZATION OF THE BIVALVE PATHOGEN VIBRIO EUROPAEUS

Santiago de Compostela, 2025

Doctoral Programme in Advances in Microbial and Parasitic Biology

TESE DE DOUTORAMENTO

GENOMIC CHARACTERIZATION OF THE BIVALVE PATHOGEN *Vibrio europaeus*

Sergio Rodríguez Rodríguez

Directores: Juan Luis Barja Pérez e Javier Dubert Pérez

Titor: Juan Luis Barja Pérez

PROGRAMA DE DOUTORAMENTO EN AVANCES EN BIOLOXÍA MICROBIANA E PARASITARIA

SANTIAGO DE COMPOSTELA

FINANCIACIÓN

Esta Tesis doctoral es parte del proyecto de I+D+I PID2020-120503RA-I00, financiado por MCIU/AEI/10.13039/501100011033.

Durante el periodo de Tesis he disfrutado de distintos contratos asociados a los siguientes proyectos:

- Control microbiolóxico en minicriaderos de moluscos (Ref: 2017-CP102) Consellería do Mar (Xunta de Galicia)
- Producción de semilla de almeja en batea. Biometría y Monitorización sanitaria (Ref: 2021-CE099) Proameixa Fernandez, SL.
- Programa de Ciencias Mariñas dos plans complementarios de I+D+I do Plan de Recuperación Next Generation. (2022-CP081) Consellería do Mar (Xunta de Galicia).

DECLARACIÓN DEL AUTOR

Yo, Sergio Rodríguez Rodríguez, autor de esta tesis, declaro no tener conflicto de intereses.

AGRADECIMIENTOS

Quiero expresar mi agradecimiento a mis directores de tesis, los Dres. Javier Dubert y Juan Luis Barja. Extiendo también mi reconocimiento a la Dra. Alicia Estévez Toranzo, la Dra. Ana Belén López Dieguez, la Dra. Beatriz Magariños, el Dr. Jesús Romalde, la Dra. Sabela Balboa, la Dra. Susana Prado y también a Celsa por su colaboración y aportes a lo largo del proceso.

Agradecimiento sincero a los incontables compañeros de laboratorio que han compartido poyata o escritorio conmigo a lo largo de todos estos años, incluidos los del Instituto de Acuicultura. En este punto me gustaría hacer una mención especial a Carlos Smith, cuya amistad trascendió el breve periodo que coincidimos en el laboratorio, al que agradezco su interés y apoyo sincero durante todos estos años, y al que le debo una visita desde hace mucho. También a María Cascallar, a la que conocí "dirigiéndole" el TFG y cuya tesis he terminado usando de referencia para pulir muchas cosas de la mía. Gracias por tenerme presente todo este tiempo, por tu apoyo e interés.

Gracias a los técnicos con los que he compartido espacio, especialmente a Berta por proximidad y por haber sido siempre tan amable conmigo, además de haberme enseñado tanto.

Agradezco profundamente a Paulino y Laura Elena por su infinito, desinteresado e incondicional apoyo personal y profesional siempre y, especialmente, por todo el recibido durante la última etapa. Puedo decir con total certeza que sin su respaldo hubiese abandonado este proyecto. A Paulino, gracias por las imprescindibles correcciones y sugerencias, por ayudarme con tantas y tantas dudas metodológicas y conceptuales que sin ti se habrían quedado en el limbo de la incertidumbre. A Laura, por estar siempre disponible al otro lado de la línea ya sea para darme ánimos, consejos, o intercambiar contenido de gatos. Gracias a ambos por sus buenas palabras, por apreciar el trabajo y el esfuerzo que hay detrás.

A mi compañera de vida y de laboratorio Clara "Topi", aunque todo el agradecimiento que te tengo no puede ser expresado con palabras, gracias por haber compartido los muchos sinsabores de este proceso siempre con el pragmatismo del que yo carezco, por tus siempre acertados aportes a la parte científica y estética del trabajo y, en general, por ser una pincelada de luz. Desde el privilegio que supone estar saliendo de esta etapa, te garantizo que al golpito también se llega.

A mi amiga y vecina de laboratorio la Dra. Marta, por incluirme en tu ronda de saludos matinal a pesar de tus recelos iniciales. Gracias por enseñarme a hacer qPCRs, por reírme las gracias, por tirar de mí, por tu constancia, paciencia, lealtad, sincera amistad.

A Carlos, por aguantar pírricamente la turra que damos los habitantes de la burbuja cuando nos juntamos, y por renovar el aire de dentro de la misma con tus anécdotas frescas.

A mi más antigua amiga Sofi, aunque me hayas animado en su momento a retomar esta tesis, como me has aguantado las quejas, sacado innumerables sonrisas, apoyado y escuchado siempre, te perdono. Gracias por hacerme sentir tan conectado a pesar de la distancia.

A Kike y Nacho por estar presentes de forma continuada desde el germen de esta tesis, interés y apoyo incondicional.

A Carlos Vila García por, entre otras muchas cosas, guiarme y ayudarme con la racionalización de este trabajo.

A mi familia por su cariño y empatía. A mi hermano Héctor por sacarme de casa directa e indirectamente tantas y tantas veces y por el apoyo técnico que me diste desde el primer día. A mi madre Ana Mercedes por tu ejemplo de fuerza y cabezonería, así como por cuidar de mi cuando hizo falta. Al resto de mi familia adoptiva, las Elenas y Julia, por acogerme tan bien. A Mona, Poleo, Gofio y también a Maga, aunque ya no esté.

TABLE OF CONTENTS

ABSTRACT

Bivalve hatcheries are a fundamental tool in aquaculture expansion, ensuring the seed demand for shellfish aquaculture. However, the industry faces several challenges, with mortalities caused by opportunistic pathogens of the genus *Vibrio* being one of the most significant bottlenecks. These mortalities, resulting from diseases generally referred as vibriosis, hinder the stable availability of bivalve seed for grow-out, as they primarily affect larval stages, leading to significant economic losses. The pathogenic potential of *Vibrio* species is determined by virulence factors, along with host-dependent and environmental factors. Given the rapid progression of these infections, prevention is considered the main tool against them.

Vibrio europaeus, a recently described species, has been linked to mortalities at different developmental stages of various bivalve species, with a broad geographic distribution. This study examines this species from a genomic perspective, sequencing 39 strains obtained from mollusc hatcheries in various geographic regions and associated with different species and life stages. These strains constitute the entire collection available until the present.

First, the pangenome of *V. europaeus* was constructed with all those genomes, which represents the complete genetic repertoire of a microbial species. It consists of a core genome shared by all strains and an accessory genome, which includes genes not shared across the species. The pangenome of *V. europaeus* was characterized as belonging to a species capable of efficiently adapting to its environment by acquiring exogenous DNA. Additionally, the intraspecific variability of *V. europaeus* was analysed using various methods that utilized the entire genomes (hierarchical clustering of ANIb values), the core genome (phylogeny and SNP count differences), and the accessory genome (hierarchical clustering based on gene presence/absence). This analysis grouped the strains into three main phylogenetic branches with eight clusters. Spanish strains exhibited lower genetic diversity than French strains, suggesting a single radiation event followed by local hatchery dispersal. In contrast, French strains displayed greater variability. Strains from other countries (Chile and the USA) formed distinct clusters, suggesting an intercontinental transmission of the species, likely facilitated by human activities such as seed, juvenile, or mollusc lot trade. Furthermore, the study of clonal strains isolated at Hatchery B allowed researchers to infer a pathogen dissemination model through phytoplankton used as feed.

Second, genes relevant to the ecology of *V. europaeus* and thus with impact on aquaculture management were analysed. Each strain was characterized for genes related to virulence factors, antibiotic resistance, secondary metabolite production, and phage defence systems. Additionally, virulence and defence gene profiles were established, allowing comparisons between strains. Phenotypic assays were also conducted, including virulence challenges in juvenile Japanese clams (*Ruditapes philippinarum*) and antibiotic susceptibility tests. This led to the identification of key virulence factors in this species, such as type II (T2SS) and type VI (T6SS1 and T6SS2) secretion systems, adhesion and colonization factors (MSHA type IV pilus and flagella), antiphagocytosis mechanisms (capsular polysaccharides), enzyme and toxin production, and iron uptake systems (metalloproteases, collagenases, enterobactin, heme receptors, hemolysins, and ABC transporter systems). Additionally, quorum sensing mechanisms (autoinducers-1 and 2) were identified.

By combining *in silico* and phenotypic results on antibiotic resistance, it was determined that the species is resistant to erythromycin and cephalexin by core genes. Some Spanish strains isolated between 2011 and 2012 also showed multidrug resistance to sulfonamides and streptomycin, suggesting horizontal gene transfer of resistance genes. Regarding secondary metabolite clusters, highly conserved families were identified across all strains, including NRPS, RiPP-type, betalactone, arylpolyene, and ectoine, which may play roles in resistance to osmotic and oxidative stress, among other functions. Finally, a large diversity of phage defence systems was identified, highlighting the ability of *V. europaeus* to adapt to phage predation. This poses a challenge for implementing phage-based therapies to prevent vibriosis.

Lastly, the accessory genome of *V. europaeus* was characterized, consisting mainly of plasmids and chromosomal plasticity regions. Among these components, mobile genetic elements were identified, forming the mobilome of the species, which is crucial for bacterial evolution via horizontal gene transfer (HGT). This mechanism facilitates adaptation to specific niches by frequently acquiring genes related to antibiotic resistance, virulence, secondary metabolites, and defence systems. The plasmids were classified as conjugative, mobilizable, or non-mobilizable, while conjugative/mobilizable elements (ICEs/IMEs), prophages, and microsatellites were identified within chromosomal plasticity regions. Additionally, genes of interest identified in previous analyses were assigned to different accessory genome elements.

The plasmids of *V. europaeus* were classified into five groups, with pVE1-related plasmids being the largest and most prevalent plasmid and harbouring numerous genes related to defence,

virulence, and biosynthesis, including an additional T6SSi5 secretion system (T6SS2) apart from the one found in the chromosome (T6SS1). Among the chromosomal RGPs, 78 ICEs/IMEs and 55 prophages were identified, classified into 14 and 10 groups, respectively, primarily associated with defence systems. Approximately 10% of the genes in the *V. europaeus* pangenome were linked to the mobilome. Lastly, in the plasticity regions that could not be classified as part of the mobilome—possibly due to mutations in mobilization genes or unknown mobility mechanisms—a wide variety of genes related to antibiotic resistance, virulence, secondary metabolites, and defence systems were found.

This thesis aims to expand knowledge on the emerging pathogen *V. europaeus* from a genomic approach that determines its intraspecific diversity and evolution, as well as key genetic characteristics related to its virulent potential, resistance to treatments, and genetic transfer mechanisms that enhance its environmental adaptation. Additionally, it seeks to establish a foundation for developing innovative strategies to mitigate its impact on aquaculture, promoting the sustainability of the sector.

RESUMEN

Los criaderos de bivalvos son una herramienta fundamental para garantizar la demanda de los mismos. Sin embargo, la industria se enfrenta a varios problemas, siendo las mortalidades producidas por patógenos oportunistas del género *Vibrio* uno de los cuellos de botella más importantes. Estas mortalidades, consecuencia de las patologías llamadas de forma general vibriosis, impiden la disponibilidad estable de semilla de bivalvos para engorde ya que afectan especialmente a los estadios larvarios, suponiendo grandes pérdidas económicas. El potencial de los vibrios para producir enfermedad está determinado por los factores de virulencia, conjuntamente con factores dependientes del hospedador y ambientales. Dada la rápida progresión de estas infecciones, se considera que la prevención es la principal herramienta contra las mismas. *V. europaeus*, una especie descrita recientemente, se ha vinculado con mortalidades en diferentes etapas de desarrollo de varias especies de bivalvos, abarcando una amplia distribución geográfica. A lo largo de este trabajo se ha estudiado esta especie desde un punto de vista genómica, para lo que se secuenciaron 39 cepas obtenidas de criaderos de moluscos en varias regiones geográficas y asociadas a distintas especies y estadios de vida, y que constituyen toda colección de cepas disponible hasta el momento.

En primer lugar, se ha estudiado conjuntamente todos los genomas mediante la construcción del pangenoma, es decir, el repertorio genético completo de una especie microbiana, que se divide en un genoma central compartido por todas las cepas, y un genoma accesorio, que incluye genes no compartidos por toda la especie. Se ha podido caracterizar el pangenoma de *V. europaeus* como el de una especie capaz de adaptarse eficazmente al ambiente mediante la adquisición de ADN exógeno. Por otro lado, se ha estudiado la variabilidad intraespecífica de *V. europaeus* usando varios métodos que implicaron la utilización de la totalidad de los genomas (clusterización jerárquica de los valores de ANIb), la fracción core (filogenia y diferencia en el número de SNPs), y la fracción accesoria (clusterización jerárquica de la presencia/ausencia de genes), lo que ha permitido separar las cepas en tres ramas filogenéticas principales con ocho clústeres. Las cepas españolas mostraron menor diversidad genética que las francesas, lo que sugiere un evento de radiación único seguido de dispersión en criaderos locales. Por el contrario, las cepas francesas exhibieron mayor variabilidad que las

españolas. Las cepas de otros países (Chile y EE. UU.) se agruparon en clústeres diferenciados, sugiriendo un salto intercontinental de la especie, posiblemente facilitada por actividades humanas, como el comercio de semilla, juveniles, o lotes de moluscos. Además, el análisis de las cepas clonales aisladas en el Criadero B, permitieron inferir un modelo de diseminación del patógeno a través del fitoplancton utilizado como alimento.

En segundo lugar, se estudiaron los genes de interés para la ecología de *V. europaeus* y, por lo tanto, con impacto en la gestión acuícola. Para cada cepa, se caracterizaron los genes relacionados con factores de virulencia, resistencia a antibióticos, producción de metabolitos secundarios y sistemas de defensa anti fagos. Además, se establecieron perfiles de genes relacionados con la virulencia y los sistemas de defensa, permitiendo comparar las cepas entre sí. De forma paralela se realizaron ensayos fenotípicos de las cepas, como desafíos de virulencia en juveniles de almeja japonesa (*R. philippinarum*) y antibiogramas. De esta manera, se identificaron factores de virulencia clave en esta especies, como pueden ser los sistemas de secreción tipo II (T2SS) y tipo VI (T6SS), la adhesión y colonización (MSHA pilus tipo IV y flagelo), antifagocitosis (polisacárido capsular), la producción de encimas, toxinas, y sistemas de captación de hierro (metaloproteinasas, colagenasas, enterobactina, receptores hemo, hemolisinas, collagenasas, enterobactina, receptores hemo, hemolisinas, y sistemas de transporte ABC dependientes de proteínas de unión), y quorum sensing (autoinductores-1 y 2). Por otro lado, mediante la combinación de los resultados *in silico* y los fenotípicos para la resistencia a antibióticos, se determinó que la especie presenta resistencia generalizada a eritromicina y cefalexina. Además, algunas cepas españolas aisladas entre 2011 y 2012 presentan multirresistencia a la sulfonamida y la estreptomicina, sugiriendo una transferencia horizontal de genes de resistencia. En cuanto a los clústeres de metabolitos secundarios, se pudieron encontrar algunas familias muy conservadas en todas las cepas, de los tipos NRPS, tipo RiPP, betalactona, arilpolieno, y ectoina, que pueden tener, entre otros, roles resistencia al estrés osmótico y oxidativo. Por último, se identificó una gran diversidad de sistemas de defensa contra fagos, resaltando la capacidad de *V. europaeus* para adaptarse a la depredación de los mismos. Esto representa un desafío para la implementación de terapias basadas en fagos para prevenir la vibriosis.

Por último, se caracterizó el genoma accesorio de *V. europaeus*, compuesto principalmente por plásmidos y regiones de plasticidad cromosómicas. Entre estos componentes se identificaron elementos genéticos móviles, que conforman el moviloma de la especie, esencial

en la evolución bacteriana mediante transferencia horizontal de genes (HGT). De esta forma, facilitan la adaptación a nichos específicos al incorporar con frecuencia genes de resistencia a antibióticos, virulencia, metabolitos secundarios y sistemas de defensa. Los plásmidos fueron clasificados como conjugativos, movilizables o no movilizables, mientras que se buscaron elementos conjugativos/movilizables (ICEs/IMEs), profagos y microsatélites entre las regiones de plasticidad cromosómicas. Además, se asignaron los genes de interés encontrados en el apartado anterior a los distintos elementos del genoma accesorio. Así, se clasificaron los plásmidos de *V. europaeus* en 5 grupos, siendo pVE1 es el más grande y prevalente, albergando numerosos genes relacionados con sistemas de defensa, virulencia y biosíntesis, incluido un T6SSi5 adicional al que se encuentra en el cromosoma. Además, entre los RGPs cromosómicos se encontraron 78 ICEs/IMEs y 55 profagos, que pudieron ser clasificados en 14 y 10 grupos, respectivamente, y en los que se identificaron, principalmente, sistemas de defensa. De esta forma, se consiguió asociar al moviloma alrededor de un 10% de los genes pertenecientes al pangenoma de *V. europaeus*. Por último, en las regiones de plasticidad que no pudieron ser clasificadas como moviloma, presuntamente por mutaciones en los genes implicados en la movilización o por la existencia de mecanismos de movilidad no conocidos, se encontraron gran variedad de genes de resistencia a antibióticos, virulencia, metabolitos secundarios y sistemas de defensa.

Esta tesis pretende aumentar el conocimiento del patógeno emergente *V. europaeus*, a través de un enfoque genómico que permita determinar su diversidad y evolución intraespecífica, así como características genéticas clave relacionadas con su potencial virulento, resistencia a tratamientos y los mecanismos de transferencia genética que favorecen su adaptación al medio ambiente. Además, se espera establecer una base que contribuya al diseño de estrategias innovadoras para mitigar su impacto en la acuicultura, promoviendo la sostenibilidad del sector.

RESUMO *IN EXTENSO*

Estímase que para o ano 2050, a produción mundial de alimentos debe aumentar entre un 70 % e un 110 % para satisfacer a crecente demanda poboacional, enfrontándose a desafíos como a inestabilidade económica, o cambio climático e a degradación do solo. Neste paradigma, os alimentos de orixe acuática constitúen unha peza clave, xa que o seu consumo global creceu de 28 millóns de toneladas en 1961 a 162 millóns en 2021, aportando o 17 % da ingesta mundial de proteínas animais, chegando ata o 50 % nalgunhas rexións. Porén, a pesca extractiva alcanzou o seu límite de explotación na década de 1990, estancándose nos 80 millóns de toneladas. En 2012, a acuicultura superou en volume á pesca extractiva, momento a partir do cal pasou a ser o principal motor de crecemento na produción de alimentos mariños. Este crecemento mantívose constante, alcanzando un récord de 130,9 millóns de toneladas en 2022, cun valor de 312.800 millóns de dólares. Asia domina a produción acuícola co 87,9 % do total. Os moluscos foron o terceiro grupo de animais acuícolas máis cultivados en 2022, representando o 15,6 % da produción, con 88 especies cultivadas. Os bivalvos, en particular a ostra xaponesa e a ameixa xaponesa, están entre as especies mariñas máis cultivadas a nivel mundial. Porén, o cultivo dun número limitado de especies ameaza a biodiversidade, os hábitats naturais e facilita a propagación de enfermidades e especies invasoras. No contexto europeo, España lidera a produción acuícola co 23,7 % do volume total. Porén, en 2022, a produción mariña seguiu sendo maioritariamente extractiva (74,9 %), mentres que a acuicultura representou só o 25,1 %. O mexillón *Mytilus galloprovincialis* foi a especie máis cultivada con 255.218 toneladas, o 97 % procedentes de Galicia. Aínda que rendible, o seu monocultivo xera baixos marxes de beneficio (0,65 €/kg en 2024). Outras especies como a ostra plana (*Ostrea edulis*), a ostra do Pacífico (*M. gigas*), e as ameixas xaponesa (*R. philippinarum*), fina (*Ruditapes decussatus*) e babosa (*Venerupis corrugata*) teñen menor produción a pesar do seu alto valor comercial, o que resalta a necesidade de diversificar a acuicultura.

Historicamente, os bancos naturais foron a principal fonte de sementes para a acuicultura de bivalvos. Porén, a sobreexplotación, o cambio climático e a contaminación reduciron a súa capacidade de abastecemento. Ante isto, os criadeiros gañaron relevancia, ofrecendo unha serie de vantaxes como un subministro estable, especies melloradas xeneticamente e reducindo a

presión sobre as poboacións silvestres. Ademais, permiten mellorar as condicións de produción, como a temperatura e a dispoñibilidade de alimento, favorecendo sementes máis resistentes e cunha produción máis estable. A pesar das súas vantaxes, os criadeiros enfróntanse a desafíos como a necesidade de ubicacións con auga de alta calidade e custos elevados de explotación. A maior dificultade radica nas mortalidades explosivas producidas por patóxenos oportunistas do xénero *Vibrio*, que constitúen o grupo máis diverso e con maior impacto na industria. As mortalidades producidas por vibrios en bivalvos, coñecidas de forma xeral como vibriose, impiden a dispoñibilidade estable de semente de bivalvos para engorde xa que afectan especialmente aos estadios larvarios, supoñendo grandes perdas económicas. Os criadeiros son, a pesar das súas limitacións, a clave para a sostibilidade e expansión da acuicultura de bivalvos.

As bacterias son esenciais nos ecosistemas mariños, participando no ciclo do carbono e do nitróxeno, estando á súa vez estreitamente ligadas aos bivalvos, xa que son capaces de filtrar grandes volumes de auga. As bacterias ligadas a eucariotas mariños, incluídos os bivalvos, presentan relacións simbióticas cos mesmos, que poden ser comensais, mutualistas ou patóxenas. Así, os bivalvos presentan microbiotas complexas que inclúen unha comunidade residente estable e unha microbiota transitoria, estando, especialmente esta última, influída por factores ambientais. Como xa comentamos, as bacterias patóxenas do xénero *Vibrio* adoitan formar parte da comunidade bacteriana transitoria dos bivalvos. O xénero *Vibrio* é un grupo diverso de bacterias Gram-negativas, móbiles e anaerobias facultativas, pertencentes á familia *Vibrionaceae*. Actualmente, conta con 152 especies descritas, organizadas en 35 clados segundo análise de secuencias de xenes esenciais (MLSA). Os patóxenos *Vibrio* que afectan bivalvos agrúpanse en varios clados, incluíndo Anguillarum, Harveyi, Mediterranei, Orientalis, Pectenicida e Splendidus, afectando diversas etapas do desenvolvemento de moluscos como ostras, ameixas e mexillóns.

O desenvolvemento da vibriose está altamente relacionado coa existencia dunha serie de moléculas, compoñentes estruturais e características implicadas na patoxénese, que constitúen unha peza clave na aparición e desenvolvemento da enfermidade. Entre os factores de virulencia presentes en vibrios patóxenos de bivalvos atopamos: (i) toxinas, incluíndo endotoxinas como o LPS, que provoca apoptose en hemocitos, e exotoxinas como hemolisinas e metaloproteasas, esenciais para a invasión e degradación de tecidos, (ii) encimas como fosfolipasas e quitinases, que contribúen á degradación de membranas celulares e estruturas do hóspede, (iii) adhesinas, que facilitan a adhesión a hemocitos e a colonización de superficies tisulares, (iv) motilidade e

quimiotaxe, que permite ao *Vibrio* moverse de forma autónoma a entornos como os tecidos do hóspede, favorecendo a infección, (v) evasión inmune, que comprende mecanismos como a variabilidade do antíxeno O no LPS e a inhibición da fagocitose, que permite á bacteria sobrevivir á acción dos hemocitos, (vi) formación de biofilmes, agregados densos de microorganismos nunha matriz de exopolisacáridos que protexen ás bacterias e facilitan a resistencia a antibióticos, (vii) *quorum sensing*, un sistema de comunicación bacteriana baseado en autoinductores que regulan a expresión xénica en función da densidade celular, influíndo na virulencia e formación de biofilmes, (viii) sistemas de secreción, que transportan substancias que desempeñan funcións clave na patoxenicidade e competencia microbiana, e (ix) adquisición de ferro, o que lles permite sobrevivir en medios con dispoñibilidade limitada deste metal, como o interior dos bivalvos.

Ademais da existencia de factores de virulencia no patóxeno, o desenvolvemento da vibriose depende de factores ambientais que teñen influencia no desempeño destes factores de virulencia, as dinámicas nas poboacións de vibrios e na predisposición do hóspede. Así, observouse que as poboacións de *Vibrio* varían estacionalmente, correlacionándose positivamente coa temperatura. Ademais, a temperatura parece estar relacionada cun aumento na expresión de xenes de virulencia na maioría dos casos. Outro factor ambiental clave é a salinidade, que, ademais de modular as poboacións de vibrios dunha forma non tan clara como a temperatura, influencia a motilidade, colonización e expresión de xenes asociados á virulencia. Por outra banda, estes factores ambientais, e outros como a presenza de contaminantes, poden xerar estrés no hóspede, debilitando o seu sistema inmunitario e favorecendo o desenvolvemento de enfermidades. Finalmente, algunhas especies de bivalvos son máis susceptibles á vibriose que outras, dependendo da súa eficiencia inmunolóxica e do seu desenvolvemento, sendo as etapas larvarias máis susceptibles á vibriose debido ao desenvolvemento incompleto do seu sistema inmunitario, sendo máis vulnerables durante a fase de asentamento.

A patoxénese da vibriose en larvas de bivalvos, ou proceso polo cal un patóxeno causa dano ao hóspede, desenvólvese en tres fases: a fase de incubación, a fase de difusión rápida e a fase de mortalidade aguda. A infección xeralmente entra a través do sistema dixestivo e propágase a outros órganos, causando necrose e dexeneración. Algúns vibrios poden colonizar tecidos sen causar enfermidade inicialmente, pero volvense patóxenos ao adquirir plasmidos.

Ademais, os vibrios poden utilizar a hemolinfa para estender a infección a outros órganos e tecidos, o que compromete as defensas inmunolóxicas do hóspede e leva á súa morte.

Dada a rápida progresión destas infeccións, considérase que a prevención é a principal ferramenta contra as mesmas. Esta prevención inclúe o mantemento dunhas condicións óptimas ao longo das distintas fases de cultivo, como poden ser a temperatura, salinidade e densidade de animais, o que implica unha redución do estrés dos animais e unha menor propensión á enfermidade. Porén, hai outros enfoques, que poden ser complementarios, que teñen como estratexia a eliminación total da carga bacteriana da auga do criadeiro. Así, son comúns procesos de desinfección como UV-C, ozonización e cloración, que teñen como desvantaxe ser operacionalmente custosos, perder eficacia en determinadas condicións como a presenza de partículas na auga ou xerar formas tóxicas para os bivalvos. Existen alternativas sen estas desvantaxes, como a fotodinámica antimicrobiana, que involucra a xeración de formas de osíxeno de vida curta, moi reactivas contra microorganismos. En calquera caso, as estratexias que involucran a eliminación total da carga bacteriana da auga dificilmente conseguen este obxectivo, xa que un criadeiro non é unha instalación axénica, existindo fontes de bacterias como os reprodutores e o plancto. Ademais, o desequilibrio da microbiota xerado por estes métodos pode favorecer o aumento de bacterias oportunistas, incluídos vibrios patóxenos.

Outro enfoque implica o uso de antibióticos que, debido ao rápido desenvolvemento da vibriose, usáronse en criadeiros como profilaxe. O emprego de antibióticos fomenta a aparición e diseminación de resistencias que supoñen un risco para a saúde animal e humana, o que propiciou a redacción de normativa europea regulando o seu uso. Probióticos e nanopartículas demostraron ter unha eficacia variable e, nalgúns casos, chegaron a mostrar toxicidade para as larvas. Ademais, requiren estudos adicionais para garantir a súa seguridade e viabilidade económica a grande escala. Por outra banda, as bacterias demostraron adaptarse rapidamente á depredación por fagos, polo que a aplicación da terapia fágica a escala industrial en criadeiros supón un desafío. Por último, existen estratexias como o *immune priming*, consistente na activación da memoria defensiva dos bivalvos por estimulación do seu sistema inmunitario innato mediante bacterias inactivadas ou subcompostos específicos das mesmas, ou a selección xenética de bivalvos resistentes que destacan polo seu potencial contra a vibriose, aínda que necesitan máis investigación para poder ser implementadas de forma efectiva na industria.

V. europaeus, unha especie descrita recentemente, vinculouse con mortalidades en diferentes etapas do desenvolvemento de varias especies de bivalvos, abarcando unha ampla

distribución xeográfica. Ao longo deste traballo estudouse esta especie dende un punto de vista xenómico, para o que secuenciáronse 39 cepas obtidas de criadeiros de moluscos en varios países e asociadas a distintas especies e estadios de vida, e que constitúen toda a colección de cepas dispoñible.

En primeiro lugar, estudáronse conxuntamente todos os xenomas mediante a construción do panxenoma, é dicir, o repertorio xenético completo dunha especie microbiana, que se divide nun xenoma central compartido por todas as cepas e un xenoma accesorio, que inclúe xenes non compartidos por toda a especie. Pudemos establecer que o panxenoma de *V. europaeus* comprende 9.860 xenes, o cal é comparable con outros patóxenos mariños do xénero *Vibrio*, como *Vibrio anguillarum* e *V. tapetis*. Ademais, puidose establecer que se trata dun panxenoma aberto, mediante o estudo da relación entre os xenes comúns, ou *core*, e os presentes só nun subconxunto de cepas, ou accesorio. Este panxenoma aberto permitiu caracterizar a *V. europaeus* como unha especie capaz de adaptarse eficazmente ao ambiente mediante a adquisición de ADN exóxeno, favorecido pola riqueza microbiana en ambientes altamente favorables como os criadeiros. Por outra banda, atopamos que *V. europaeus* presenta unha maior proporción de xenoma *core* no seu panxenoma que o doutras especies cun rango máis amplo de hóspedes, como é o caso de *V. anguillarum*, *Vibrio tapetis* e *Vibrio fluvialis*, o cal encaixa coa observación de que maiores proporcións de xenoma *core* son propias de especies máis especializadas. Por outra banda, estudouse a variabilidade intraespecífica de *V. europaeus* usando varios métodos que implicaron a utilización da totalidade dos xenomas (clusterización xerárquica dos valores de ANIb), a fracción *core* (filoxenia e diferenza no número de SNPs) e a fracción accesoria (clusterización xerárquica dos perfís de presenza/ausencia de xenes), o que permitiu separar as cepas en tres ramas principais con oito clústeres. A clusterización xerárquica dos perfís de presenza/ausencia de xenes da fracción accesoria permitiu observar diferenzas entre cepas moi próximas en clasificacións que usaron unicamente o xenoma *core*, o cal apunta a unha rápida adquisición horizontal de xenes. Estas diferenzas no xenoma accesorio das cepas poden incluír xenes relevantes para a ecoloxía da bacteria, en aspectos como a virulencia, a resistencia a antibióticos, a síntese de metabolitos secundarios e a defensa contra fagos, polo que estudaremos estes aspectos nos sucesivos capítulos. Por outra banda, as cepas españolas mostraron menor diversidade xenética que as francesas, o que suxire un evento de radiación único seguido de dispersión en criadeiros locais. Pola contra, as cepas francesas exhibiron maior variabilidade, a pesar de que a maioría foron

illadas case simultaneamente nun mesmo entorno. As cepas doutros países (litoral do Pacífico en Chile e EE. UU.) agruparon en clústeres diferenciados, suxerindo un salto intercontinental da especie, posiblemente facilitado por actividades humanas, como o comercio de larvas ou lotes de moluscos. Ademais, obtivéronse resultados compatibles cunha diseminación do patóxeno a través do fitoplancto utilizado como alimento en criadeiros, o cal pode axudar a deseñar estratexias de control para o patóxeno.

En segundo lugar, estudáronse os xenes de interese para a ecoloxía de *V. europaeus* e, polo tanto, con impacto na xestión acuícola. Para cada cepa, caracterizáronse os xenes relacionados con factores de virulencia, resistencia a antibióticos, produción de metabolitos secundarios e sistemas de defensa antifagos. Ademais, establecéronse perfís de xenes relacionados coa virulencia e os sistemas de defensa, permitindo comparar as cepas entre si, en función dos seus xenes de interese accesorios. De forma paralela realizáronse ensaios fenotípicos das cepas, como desafíos de virulencia en xuvenís de ameixa xaponesa (*R. philippinarum*) e antibiogramas. Deste xeito, atopouse que arredor dun 60% dos xenes relacionados coa virulencia pertencían ao xenoma core, tendo un papel central no desempeño patoxénico da especie. Estes xenes puideron ser englobados en distintas clases de factores de virulencia, como resistencia a ácidos, adherencia, antifagocitose, formación de biofilms, quimiotaxe e motilidade, enzimas, captación de ferro, quorum sensing, sistemas de secreción e toxinas, incluíndo factores de virulencia como os sistemas de secreción tipo II (T2SS) e tipo VI (T6SS), o pilus MSHA tipo IV e o flaxelo, o polisacárido capsular, metaloproteínas, colaxenases, enterobactina, receptores hemo, hemolisinas e sistemas de transporte ABC dependentes de proteínas de unión, e autoindutores-1 e 2 relacionados co quorum sensing. Por outra banda, mediante a combinación dos resultados *in silico* e os fenotípicos para a resistencia a antibióticos, determinouse que a especie presenta resistencia xeneralizada a eritromicina e cefalexina. Ademais, algunhas cepas españolas illadas entre 2011 e 2012 presentan multirresistencia á sulfonamida e á estreptomicina relacionada coa presenza dos ARGs aph(3")-Ib e aph(6)-Id, e sul2, respectivamente, suxerindo unha transferencia horizontal de xenes de resistencia. En canto aos clústeres de metabolitos secundarios, puidéronse atopar algunhas familias moi conservadas en todas as cepas, dos tipos NRPS, tipo RiPP, betalactona, arilpolieno e ectoína, que poden ter, entre outros, roles de resistencia ao estrés osmótico e oxidativo. Por último, identificouse unha gran diversidade de sistemas de defensa contra fagos, que incluían sistemas adaptativos, innatos, de infección abortiva, de sinalización e de mecanismo

descoñecido. Do total de 49 sistemas de defensa atopados no pangenoma de *V. europaeus*, a dGTPasa foi a única atopada en todos os xenomas, resaltando a capacidade da especie para adaptarse á depredación dos mesmos. Isto representa un desafío para a implementación de terapias baseadas en fagos para previr a vibriose.

Por último, caracterizouse o xenoma accesorio de *V. europaeus*, composto principalmente por plásmidos e rexións de plasticidade cromosómicas, elementos que potencialmente conteñen o mobiloma da especie. A importancia dos elementos móbiles reside en que facilitan a adaptación a nichos específicos ao incorporar con frecuencia xenes de resistencia a antibióticos, virulencia, metabolitos secundarios e sistemas de defensa e son, ademais, a principal forza que impulsa a evolución dos xenomas bacterianos, dada a ausencia de reprodución sexual. Para a extracción dos plásmidos, deseñouse unha estratexia *ad hoc* que implicou a comparación dos contigs coas secuencias de plásmidos atopados nos xenomas cerrados da especie, así como por análise e curado dos contigs non aliñados con rexións cromosómicas de ditas cepas. Para a extracción das rexións de plasticidade cromosómica, extraéronse os clústeres de xenes accesorios mediante panRGP. Entre estes compoñentes identificáronse elementos xenéticos móbiles, que conforman o mobiloma da especie, esencial na evolución bacteriana mediante transferencia horizontal de xenes (HGT), mediante a detección de homólogos de xenes relacionados coa mobilidade xenética, como son as relaxasas, integrases e recombinases. Outros elementos móbiles como profagos e os seus satélites foron identificados mediante a utilización de programas específicos. Para definir este mobiloma, os plásmidos clasificáronse como conxugativos, mobilizables ou non mobilizables, mentres que se buscaron elementos conxugativos/mobilizables (ICEs/IMEs), profagos e microsatélites entre as rexións de plasticidade cromosómicas. Ademais, realizouse unha busca dos xenes de interese atopados no apartado anterior tanto nos plásmidos como nas rexións de plasticidade. Así, determinouse que todos os plásmidos de *V. europaeus* son potencialmente móbiles, podendo ser clasificados en 5 grupos, sendo pVE1 o máis grande e prevalente, albergando numerosos xenes relacionados con sistemas de defensa, virulencia e biosíntese, incluído un T6SS similar ao que se atopa no cromosoma, e que podería estar relacionado coa competencia con outras bacterias. Ademais, entre os RGPs cromosómicos atopáronse 78 ICEs/IMEs e 55 profagos, que puideron ser clasificados en 14 e 10 grupos en base á similitude da súa secuencia, respectivamente, e nos que se identificaron, principalmente, sistemas de defensa contra fagos. Desta forma, conseguíuse asociar ao mobiloma arredor dun 10 % dos xenes pertencentes ao panxenoma de *V.*

europaeus, o cal é comparable ao atopado en *Vibrio crassostreae*, outro patóxeno de bivalvos. Finalmente, nas rexións de plasticidade que non puideron ser clasificadas como mobiloma, presuntamente por mutacións nos xenes implicados na mobilización, perda dos mesmos xenes por atoparse no borde de contigs ou pola existencia de mecanismos non coñecidos, atopáronse gran variedade de xenes de resistencia a antibióticos, virulencia, metabolitos secundarios e sistemas de defensa. Ademais, identificouse unha rexión variable, localizada no chamado "spot 16", que contén xenes do LPS, polo que está relacionada co glicotipo das cepas, e que ten potencial no desenvolvemento de estratexias de *immune priming* para a prevención da vibriose causada por esta especie.

Esta tese pretende aumentar o coñecemento do patóxeno emerxente *V. europaeus*, a través dun enfoque xenómico que permita determinar a súa diversidade e evolución intraespecífica, así como características xenéticas clave relacionadas co seu potencial virulento, resistencia a tratamentos e os mecanismos de transferencia xenética que favorecen a súa adaptación ao medio ambiente. Ademais, espérase establecer unha base que contribúa ao deseño de estratexias innovadoras para mitigar o seu impacto na acuicultura, promovendo a sustentabilidade do sector.

ABBREVIATIONS

ADSP	Anti-phage defence system profile
ANI	Average nucleotide identity
ARG	Antibiotic resistance genes
BGC	Biosynthetic Gene Cluster
COG	Cluster of Orthologous Group
EPS	Extracellular polymeric substances
FSW	Filtered sea water
GCF	Biosynthetic gene cluster family
GFP	Green fluorescent protein
GI	Genomic Island
HGT	Horizontal gene transfer
HMW	High-molecular weight
ICE	Integrative and conjugative element
IME	Integrative and mobilizable element
LPS	Lipopolysaccharide
MARTX	Multifunctional-Autoprocessing Repeats-in-Toxin
MGE	Mobile genetic element
ML	Maximum likelihood
MPF	Mating pair formation
MSHA	Mannose-sensitive hemagglutinin
NRPS	Non-ribosomal peptide synthetase

PCA	Principal component analysis
PICI	Phage inducible chromosomal island
PKS	Polyketide synthase
PLE	PICI-like elements
PSU	Practical salinity units
PTU	Plasmid taxonomic unit
RGP	Region of genomic plasticity
RiPP	Post-translationally modified peptide product
RT	Room temperature
RTX	Repeats in toxin
SNP	Single nucleotide polymorphism
T2SS	Type II secretion system
T3SS	Type III secretion system
T4CP	Type IV coupling protein
T4CP	Type IV coupling protein
T4SS	Type IV secretion system
T6SS	Type VI secretion system
VF	Virulence factor
VFC	Virulence factor class
VFP	Virulence factor profile

INTRODUCTION

1.1 Bivalve aquaculture production

It is estimated that by 2050, global food production must increase by 70 to 110% to grant population requirements. This increase must take place in a context of inequality in access to food due to the constant increase in the world population, economic instability, changes in trade policies and in production techniques, and environmental problems such as climate change and soil degradation, which entail risks to food security, especially for low-income communities (van Dijk et al. 2021).

Diversity and characteristics to constitute a healthy diet make aquatic food a viable solution to the demand current and future demand increases (FAO 2024b). Thus, the global consumption of aquatic animal foods increased from 28 million tons in 1961 to 162 million tons in 2021, and it is expected to continue growing (FAO 2024b; Bjørndal, Dey, and Tusvik 2024). At present, aquatic foods supposes the 17% of mean per capita intake of animal protein, being up to 50% in some African and southeast Asian states (FAO 2024b). In the 1990s, extractive production reached the maximum sustainable yield, stagnating at around 80 million tons, therefore the sustained growth in aquatic food production is due to aquaculture. Thus, aquaculture production surpassed extractive production in volume in 2012, while if we consider only animal production it did so in 2022 (FAO 2024b).

Following the general trend, global aquaculture production reached a new record in 2022 with 130.9 million tons, with an estimated value of USD 312.8 billion, of which 94.4 million tons corresponded to animals, with an estimated value of USD 295.7 billion. This figure places 2022 as the second year with the highest aquaculture animal production, behind 2018 with 96.5 million tons, and the first in which it exceeds the volume of aquatic animals captured, which are estimated at 91 million tons. Asian countries continued to lead the production of cultured animals in 2022, with 5.9 million tons, that supposes the 87.9 % of the global production (FAO 2024b).

In 2022, molluscs were the third most abundant group of animals produced through aquaculture with 1 million tons, representing 15.6%, including 88 taxonomically recognized species (FAO 2024). However, molluscs are overrepresented among animals cultivated in marine or coastal environments. Thus, among the 20 declared animals most cultivated in marine or coastal environments in 2024 appears 7 species of bivalves (Table 1) (FAO 2024a). Despite the large number of farmed mollusc species, a few species dominate the market, especially the Pacific oyster and the Manila clam. This lack of diversity has consequences in the loss of biodiversity of natural molluscs, habitat destruction and the introduction of diseases and exotic species. (Mckindsey et al. 2007; Peng et al. 2021; Tan et al. 2023).

Table 1. Evolution of production, in terms of weight (x10k t), of the 20 most produced animal taxonomically recognized species in marine and coastal environments in 2022. Bivalve species are marked in bold.

Species	2012	2013	2014	2015	2016	2017	2018	2019	2020	2021	2022
Magallana gigas	442	462	480	498	528	557	582	592	607	648	688
Litopenaeus vannamei	251	255	294	313	343	412	435	476	516	563	605
R. philippinarum	362	372	384	388	418	423	414	402	427	434	443
Salmo salar	206	207	233	238	225	236	242	263	272	290	287
Chanos chanos	87	98	98	101	108	103	119	115	117	117	110
Sinonovacula constricta	69	69	75	76	80	86	85	87	86	86	85
Penaeus monodon	66	71	70	73	70	73	75	72	72	74	76
Mytilus chilensis	24	24	24	21	30	34	37	38	40	42	43
Anadara granosa	38	44	43	43	43	40	44	45	46	41	41
Sparus aurata	14	16	16	17	19	22	23	26	28	32	34
Oncorhynchus kisutch	16	15	16	14	12	18	17	22	22	23	26
Argyrosomus regius	9	10	12	14	16	18	20	23	25	25	26
Dicentrarchus labrax	15	15	16	16	19	22	24	26	28	30	29
Apostichopus japonicus	16	19	19	20	20	22	18	18	20	23	26

Trachinotus ovatus	11	11	11	11	12	14	15	16	16	24	25
Oncorhynchus mykiss	33	24	23	20	21	18	19	21	23	21	24
Lateolabrax japonicus	12	12	11	12	14	16	17	18	20	20	22
Patinopecten yessoensis	19	17	19	25	22	14	18	16	17	19	20
Mytilus edulis	18	17	17	16	17	16	16	17	15	17	16
Scylla paramamosain	12	13	13	14	15	15	16	16	16	15	15

Spain is the main European producer of aquaculture products, with 23.7% of the total volume. Despite this, in Spain, sea food production is primarily extractive, with 74.9%, while aquaculture occupied the remaining 25.1% in 2022 (APROMAR 2023). The most abundant species in aquaculture production was the mussel (*M. galloprovincialis*), with 255,218 tons in 2022, representing an estimated value of 159.3 million euros. This mussel production depends of the traditional culture in Galicia, which produced 97% in 2022. The monoculture of this species, although generating important profits, has low profits per unit of production, standing at around 0.65 euros per kg in 2024, and making Spain the fourth largest aquaculture producer. Other notable cultured species include flat oyster (*O. edulis*) and Pacific oyster (*M. gigas*; formerly *Crassostrea gigas*), with a combined production volume of 1463 tons in 2022, as well as Manila clam (*R. philippinarum*), grooved carpet clam (*R. decussatus*), and pullet carpet clam (*V. corrugata*), with a combined production volume of 993 tons in 2022. These species, although they have a high market value, have reduced productions in relation to their potential (APROMAR 2023). In this sense, there is a pressing need to diversify the sector by implementing cultivation of new species that help to revalue it (Cai et al. 2023).

1.2 Role of mollusc hatcheries in bivalve production

Traditionally, natural banks have been the most important source of seed for bivalve aquaculture production. However, many natural breeding areas lack the capacity to meet the growing demand for seed, which has led many of these banks to overexploitation, often exceeding their sustainable limits (Olivares-Bañuelos 2018). On the other hand, urban development and demographic pressures, together with the generation of environmental problems such as climate change and eutrophication, reduce the capacity of the environment to supply seeds (Brown, Therriault, and Harley 2016; Olivares-Bañuelos 2018; Gobler et al. 2022). Finally, the availability of seed from natural banks is strongly conditioned by the natural reproductive cycles of the species, as well as by the quality and viability of natural spawning (Olivares-Bañuelos 2018).

The challenges in obtaining bivalve seed from natural sources have led to the increased use of specialized facilities known as hatcheries (Helm, Bourne, and Lovatelli 2004). Currently, hatcheries play a crucial role in supporting bivalve aquaculture in regions with high production, as *M. gigas* in China (Li et al. 2011). Hatcheries offer several advantages, including a reliable supply of seeds, providing farmers with consistent access to seeds earlier in the growing season compared to natural collection methods. Additionally, hatcheries can produce specific varieties, including exotic or genetically improved types, which may not be available in natural banks, enhancing growth potential and adaptability to local conditions. Advances in technology have also made hatcheries more economically viable, often becoming the primary source of seeds for commercial aquaculture in certain regions. Furthermore, hatcheries reduce pressure on natural bivalve populations, promoting sustainability as many wild populations are nearing unsustainable levels. In addition, hatcheries can optimize seed production conditions, such as temperature and food availability, resulting in healthier, more resilient seeds (Olivares-Bañuelos 2018). Lastly, the use of hatcheries for seed production allows implementing selective breeding to improve growth rate, disease resistance, and resilience towards environmental perturbation (Nascimento-Schulze et al. 2021).

However, seeds production in bivalve hatcheries faces a series of difficulties that limits it expansion. First, bivalve hatcheries require suitable locations to carry out the activity. The most important factor is the possibility of obtaining good quality water all over the year, with the temperature, salinity and dissolved oxygen within the ranges for the target species to grow. This

usually implies proximity to the coast, which requires favorable government regulation. Although waters of inappropriate quality can be remedied to suit the physiological needs of the target species, these processes are usually economically expensive, further increasing the difference with the cost of obtaining natural seed (Olifirenko and Rutta 2024).

Conversely, sensitivity of bivalves to contaminants and toxic substances at trace concentrations, can cause abnormal development and slow growth, especially in larvae. These contaminants can come from the intake of seawater when it comes from surface waters or near the sediment, since these layers can accumulate hydrocarbons, heavy metals, proteins and lipids. On the other hand, products used to disinfect facilities or water, such as hypochlorite and ozone, are directly toxic to larvae. (Jones 2006).

However, the greatest difficulty in producing bivalve larvae is the presence of bacterial pathogens in the bacterial load associated with the facilities, causing pathologies. This problem is related, firstly, to the optimal physicochemical parameters for the development of bivalve larvae and seed, which favours the growth of a wide spectrum of microorganisms originating from the water and phytoplankton inputs in the form of food, or from the breeders, including opportunistic pathogens (Prado et al. 2005; Dubert, Barja, and Romalde 2017). Secondly, with the capacity of many of these microorganisms to generate biofilms, which favours their association with the facilities and makes their control difficult (Karunasagar, Otta, and Karunasagar 1996; Miller et al. 2015; Almatroudi et al. 2016).

1.3 The role of bacteria in marine ecosystems: a focus on shellfish microbiota

Bacteria constitute a ubiquitous group of microorganisms in the marine environment, inhabiting the water column, sediments, and the surfaces, tissues, and organs of eukaryotic organisms. They play a fundamental role in driving a multitude of ecological processes (Bik et al. 2016; Huang et al. 2021; Minich et al. 2022; Masanja et al. 2023; McCauley et al. 2023; Harbeitner et al. 2024). Both cyanobacteria and heterotrophic bacteria are integrally involved in the oceanic carbon cycle. Cyanobacteria contribute to atmospheric carbon fixation through photosynthesis, while heterotrophic bacteria play a central role in the hydrolysis of polysaccharides derived from phytoplankton degradation, which generates particulate organic

carbon. Additionally, they facilitate the mobilization of dissolved organic carbon to higher trophic levels through the microbial loop (Azam et al. 1983; Salazar and Sunagawa 2017; Giljan et al. 2023). Various bacterial groups also participate in the complex marine nitrogen cycle, which underpins marine productivity. The biogeochemical processes within this cycle involving bacteria include atmospheric nitrogen fixation, multiple nitrification pathways, nitrate/nitrite ammonification or dissimilatory nitrate reduction to ammonium, denitrification, and anaerobic ammonium oxidation (Pajares and Ramos 2019).

Bacteria associated with eukaryotic organisms engage in symbiotic relationships that can be commensal, mutualistic, or pathogenic in nature (Pierce and Ward 2018). Bivalves host a variable and complex bacterial microbiota, with bacterial concentrations exceeding by an order of magnitude those found in the surrounding environment (Cavallo, Acquaviva, and Stabili 2008; Pierce and Ward 2018). The ability of bivalves to filter large volumes of water for feeding exposes them to a wide array of bacteria, including both free-living species and those associated with particles (Pierce and Ward 2018). The bacterial complexity in bivalves is enhanced by the presence of a transient microbiota, which is temporally variable and influenced by environmental changes and host interactions with the environment (Fig. 1). This transient microbiota is particularly affected by seasonal changes, closely linked to variations in water temperature. Temperature has been shown to correlate with bacterial taxonomic and functional diversity, as well as bacterial abundance, with the genus *Vibrio* being especially favoured (Pierce and Ward 2018; 2019; Paillard et al. 2022; Gignoux-Wolfsohn et al. 2024). In contrast, the resident bivalve microbiome comprises the stable bacterial community persisting over time within an individual. These communities can vary between individuals depending on dietary patterns or environmental conditions (Pierce and Ward 2018; Akter et al. 2023).

Bacterial communities exhibit compositional differences across the various organs of bivalves (Masanja et al. 2023). For instance, the gills and the pallial cavity of oysters have been found to harbour a higher diversity of bacteria compared to the digestive glands or gonads. This difference is likely attributable to a greater proportion of transient bacteria resulting from direct contact with the surrounding water (Pierce and Ward 2018).

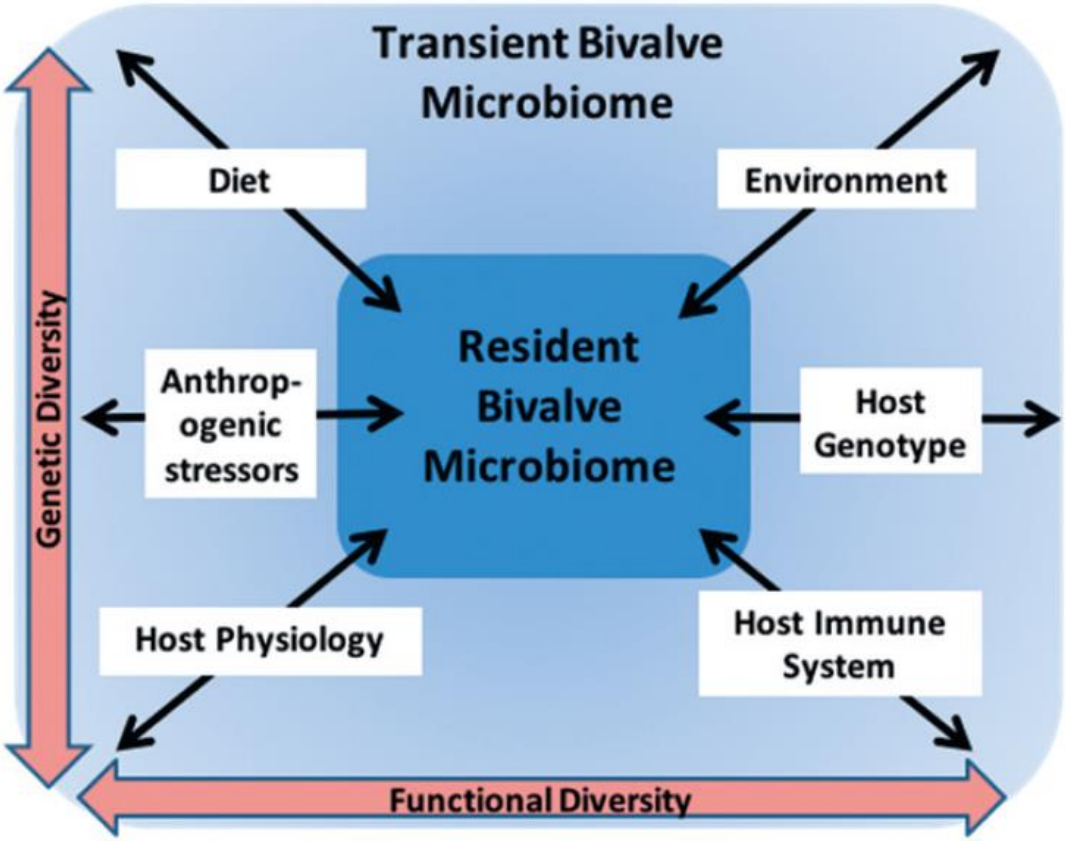

Figure 1. Dynamics of resident and transient microbiota affecting functional and genetic diversity (Pierce and Ward 2018) (Explicit permission from the editor; Annex 1).

The functional role of the microbiota in bivalves remains unclear; however, various studies suggest that it may confer a range of beneficial effects on host enantiostasis and niche adaptation. The most notable effects include:

(i) Pathogen resistance through mechanisms such as resource competition in the digestive tract, production of antimicrobial substances, secretion of cell-signalling molecules, or regulation of host gene expression (García et al. 2014; Modak and Gomez-Chiarri 2020; Ringø 2020).

(ii) Production of digestive enzymes that aid in the breakdown of complex polysaccharides, as seen in *Vibrio halioticoli* in abalones. Moreover, those are essential in xylophagous species such as those in the family Teredinidae (Sawabe 2006; Betcher et al. 2012; Dai et al. 2022; Masanja et al. 2023).

(iii) Direct resistance to thermal stress through the production of heat shock proteins, chaperones, and antioxidants (Masanja et al. 2023).

Some commensal bacteria in bivalves possess pathogenic potential, leading to disease and mortality depending on complex interactions among intrinsic and extrinsic factors within the environment-host-pathogen-microbiota system (Fig. 2) (Zannella et al. 2017; Paillard et al. 2022). Intrinsic, host-dependent factors include species, population, genotype, developmental stage, and the composition of the associated microbiota. In contrast, extrinsic factors pertain to environmental conditions such as temperature, salinity, organic matter availability, and the presence of contaminants (Zannella et al. 2017; Paillard et al. 2022). The strong dependence on host-independent factors suggests that many bacterial pathogens of bivalves function as opportunistic pathogens. Notable examples include *Nocardia crassostreae* and *Roseovarius crassostreae*, which cause nocardiosis and Roseovarius Oyster Disease, respectively (Maloy et al. 2007; Engelsma, Roozenburg, and Joly 2008; Carella et al. 2013). However, bacterial pathogens of the genus *Vibrio* represent the most significant group in terms of species diversity and their overall impact (Paillard, Roux, and Borrego 2004).

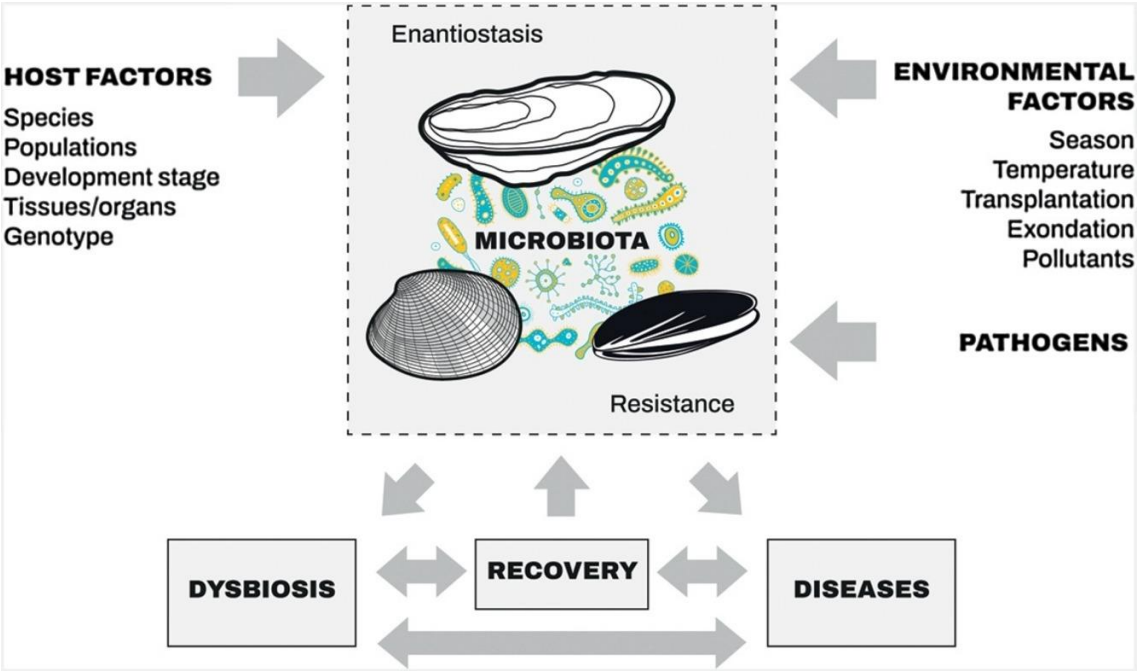

Figure 2. Diversity of factors influence bivalve microbiota, capable to generate dysbiosis, diseases and recovery (Paillard et al. 2022) (Elsevier 5925830163124; Annex 1).

1.4 Bivalve pathogens in the diverse genus Vibrio. *V. europaeus* characteristics

The genus *Vibrio* comprises Gram-negative bacteria that are generally small, motile bacilli, either straight or curved. They are mesophilic, facultative anaerobes, and typically oxidase- and catalase-positive. These bacteria commonly grow on the selective/differential medium TCBS (thiosulfate-citrate-bile-sucrose). *Vibrio* belongs to the class Gammaproteobacteria, within the family Vibrionaceae, which also includes the genera *Aliivibrio*, *Allocatenococcus*, *Allomonas*, *Corallibacterium*, *Echinimonas*, *Enterovibrio*, *Grimontia*, *Listonella*, *Lucibacterium*, *Photobacterium*, *Salinivibrio*, and *Veronia* (Farmer III et al. 2015; Hettiarachchi et al. 2018; Gomez-Gil et al. 2021). The genus is highly diverse, currently comprising 152 described species (Parte et al. 2020). The most recent taxonomic classification of *Vibrio*, based on multilocus sequence analysis (MLSA) of eight housekeeping genes (*ftsZ*, *gapA*, *gyrB*, *mreB*, *pyrH*, *recA*, *rpoA*, and *topA*), organizes the species into 35 distinct clades (Fig. 3) (Jiang et al. 2021).

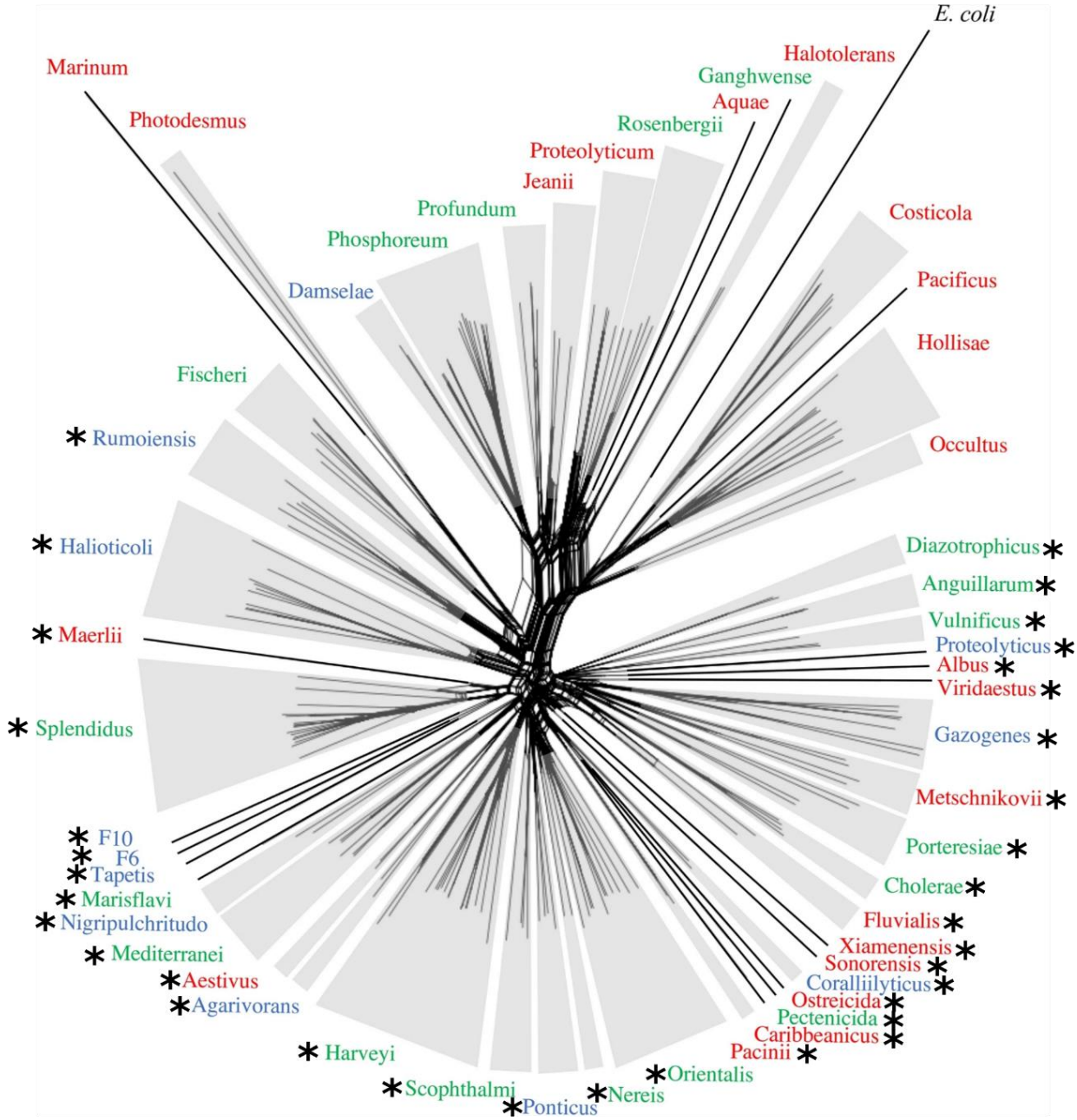

Figure 3. Clade classification of 191 Vibrionaceae species constructed by the MLSA analysis of 8 housekeeping genes. Asterisk indicates *Vibrio* clades. Adapted from (Jiang et al. 2021) (Springer Nature 5925830830104; Annex 1).

Vibrio pathogens of bivalves belong to Anguillarum, Coralliilyticus, Harveyi, Mediterranei, Orientalis, Pectenicida and Splendidus clades (Table 2) (Beaz-Hidalgo et al. 2010; Destoumieux-Garzón et al. 2020).

Table 2. Relation of *Vibrio* species pathogens to bivalves in different development stages.

Clade	Vibrio pathogen	Host	References
Anguillarum	*V. anguillarum*	*M. gigas* larvae	(Jeffries 1982)
		M. edulis larvae	(Wang et al. 2021)
		M. galloprovincialis larvae	(Anguiano-Beltrán, Lizárraga-Partida, and Searcy-Bernal 2004)
		O. edulis larvae	(Jeffries 1982; Lodeiros et al. 1987)
	Vibrio aestuarianus	*M. gigas* adults	(Garnier et al. 2007; Coyle et al. 2023)
		Cerastoderma edulis adults	(Garcia et al. 2021)
Harveyi	*Vibrio alginolyticus*	*M. gigas* adults	(Yang et al. 2021)
		Magallana hongkongensis adults	(Mao et al. 2021)
		Perna viridis adults	(Laith et al. 2021)
		R. decussatus larvae	(Gómez-León et al. 2005)
	Vibrio harveyi	*Scapharca broughtonii* adults	(Wei et al. 2019)
	V. neocaledonicus	*P. yessoensis* adults	(Geng et al. 2022)
Mediterranei	*V. mediterranei*	*Sinonovacula constricta* larvae and juveniles	(Fan et al. 2023)
		Magallana sikamea larvae and juveniles	(Fan et al. 2023)
		Pinna nobilis juveniles	(Prado et al. 2020)
Orientalis	*Vibrio bivalvicida*	*Argopecten purpuratus* larvae	(Rojas et al. 2019)
		Donax trunculus larvae	(Dubert, Romalde, Prado, et al. 2016)
		O. edulis larvae	(Dubert, Romalde, Prado, et al. 2016)
		R. decussatus larvae	(Dubert, Romalde, Prado, et al. 2016)
		R. philippinarum larvae	(Dubert, Nelson, Spinard, et al. 2016)
	V. europaeus	*A. purpuratus* larvae	(Rojas et al. 2021)
		M. gigas spat	(Saulnier et al. 2010; Travers et al. 2014)
		O. edulis larvae	(Prado, Dubert, and Barja 2015)

		R. decussatus larvae and adults	(Dubert, Nelson, Spinard, et al. 2016)
		R. philippinarum larvae, spat and juveniles	(Prado, Dubert, and Barja 2015; Dubert, Nelson, et al. 2016; Martinez et al. 2022)
	Vibrio tubiashii	*M. gigas* larvae	(Hasegawa et al. 2008)
		Crassostrea virginica larvae	(Richards et al. 2015)
		Babylonia areolate adults	(Dai et al. 2022)
		Mercenaria mercenaria spat	(Estes et al. 2004)
Pectenicida	*V. pectenicida*	*Pecten maximus* larvae	(Lambert et al. 1998; Kesarcodi-Watson et al. 2012)
Splendidus	*V. chagasii*	*A. purpuratus* larvae	(Urtubia et al. 2023)
	V. crassostreae	*M. gigas* juveniles and adults	(Bruto et al. 2017; Piel et al. 2020)
		M. edulis larvae	(Islam et al. 2022)
	Vibrio cyclitrophicus	*Mytilus coruscus* adults	(Li et al. 2019)
	Vibrio kanaloae	*S. broughtonii* adults	(Huang et al. 2021)
	Vibrio splendidus	*A. purpuratus* larvae	(Rojas et al. 2015)
		M. gigas spat and juveniles	(Le Roux et al. 2002; Wang et al. 2021)
		Mytillus edulis larvae	(Wang et al. 2021)
		Patinopecten yessoensisis larvae	(Liu et al. 2015)
		R. decussatus larvae	(Gómez-León et al. 2005)
		R. philippinarum adults	(Le Roux et al. 2002)
	V. tasmaniensis	*M. gigas juveniles*	(Bruto et al. 2017)
		M. edulis larvae	(Islam et al. 2022)
		P. yessoensisis larvae	(Liu et al. 2015)
Coralliilyticus	*Vibrio coralliilyticus*	*M. gigas* larvae	(Richards et al. 2015; Kim, Jun, Giri, Kim, et al. 2020; Kim, Jun, Giri, Chi, et al. 2020; Ushijima et al. 2022)
		C. virginica larvae	(Richards et al. 2015)
		M. galloprovincialis larvae and adults	(Balbi et al. 2019)
		O.edulis larvae	(Kesarcodi-Watson et al. 2012)
		P. maximus larvae	(Kesarcodi-Watson et al. 2012)
		Perna canaliculus adults	(Nguyen et al. 2018)
		Tridacna crocea adults	(Xu et al. 2020)
	Vibrio neptunius	*O. edulis* larvae	(Prado et al. 2005; Galvis, Barja, et al. 2021)

		R. philipinarum larvae and adulsts	(Galvis, Ageitos, et al. 2021)
Ostreicida	*Vibrio ostreicida*	*M. gigas* spat and larvae	(Prado et al. 2014)
Tapetis	*Vibrio tapetis*	*R. philippinarum* adults	(Paillard and Maes 1990)
		R. decussatus adults	(Paillard and Maes 1990)

Within the *Orientalis* clade, *V. europaeus* emerged from the reclassification of *V. tubiashii* subsp. *europaeus* as a new species, based on a comprehensive study employing multilocus sequence analysis (MLSA) of eight housekeeping genes, *in silico* DNA-DNA hybridization (eDDH), phenotypic and chemotaxonomic characterization through MALDI-TOF-MS (Matrix-Assisted Laser Desorption/Ionization Time-Of-Flight Mass Spectrometry) and fatty acid methyl ester (FAME) analysis (Dubert, Romalde, Spinard, et al. 2016). Currently, *V. europaeus* is recognized as an etiological agent in outbreaks of vibriosis affecting clam and oyster hatcheries in France and Spain, with subsequent detection in Chile (Rojas et al. 2021). This species is capable of causing significant impacts on bivalve aquaculture, as it not only induces mass larval mortality but also exhibits pathogenicity in adult stages, leading to substantial economic losses (Prado et al. 2005; Travers et al. 2014). From a phenotypic perspective, *V. europaeus* is a motile, facultative anaerobic, Gram-negative, with oxidase and catalase activities, susceptible to the vibriostatic agent O/129, and sensitive to ampicillin (AMP10). It can reduce nitrates to nitrites and grow on TCBS (thiosulfate-citrate-bile salts-sucrose agar). However, it lacks lysine decarboxylase, valine arylamidase, cysteine arylamidase, acid phosphatase, naphthol-AS-BI-phosphohydrolase activities, as well as lipase and esterase-lipase activity, and cannot hydrolyze ONPG (o-nitrophenyl-β-D-galactopyranoside). Regarding its utilization of carbon sources, *V. europaeus* is incapable of metabolizing aspartic acid and citrate but can utilize glucose, melibiose, gluconic acid, sucrose, D-mannitol, and D-galactose. It is unable to metabolize myo-inositol and putrescine but can metabolize tyrosine and L-citrulline. Furthermore, it ferments salicin but cannot ferment arbutin or D-turanose. It does not grow at temperatures of 4°C or 35°C, nor at 8% salinity (Prado, Dubert, and Barja 2015; Dubert, Romalde, Spinard, et al. 2016).

1.5 Role of Virulence Factors in virulence of *Vibrio*

The degree of damage intensity caused by a pathogen to its host is known as virulence. The ability of a bacterial pathogen to inflict such damage depends on the presence of what are termed virulence factors, components capable of harming a susceptible host, which are encoded by multiple genes involved in a multifactorial molecular strategy (Paillard, Roux, and Borrego 2004; Casadevall and Pirofski 2009). Virulence factors play a role in the ability of the pathogen to invade the host, evade host defences, proliferate within the host environment, counteract immune responses, acquire iron and nutrients from the environment, and respond to environmental changes. Understanding these virulence factors and their roles in pathogenesis is critical for developing sustainable disease management strategies and distinguishing between virulent and non-virulent strains (Dubert, Barja, and Romalde 2017a; Vandeputte et al. 2024).

Although most virulence factors participate in various processes, both related and unrelated to virulence, they are often categorized into functional groups (Casadevall and Pirofski 2009). The primary categories of virulence factors associated with vibrios affecting bivalves are as follows:

(i) **Toxins:** In general, toxins can be classified into endotoxins and exotoxins. Endotoxins are components of the outer membrane, while exotoxins are a group of soluble proteins secreted by bacteria that can enter host cells and alter their physiology (Vandeputte et al. 2024). Endotoxins are part of the lipopolysaccharide (LPS) complex, which is released when the pathogen's cell wall breaks down, either through autolysis or external lysis, leading to hemocyte apoptosis (Nguyen et al. 2019). On the other hand, exotoxins are not essential for bacterial survival, but they are often crucial for disease production. This, combined with their high presence in mobile genomic elements such as phages and plasmids, explains the existence of *Vibrio* species with both pathogenic and asymptomatic strains (Casadevall and Pirofski 2009; Hossain et al. 2020). The most abundant toxins in the *Vibrio* genus are hemolysins, which cause the lysis of erythrocytes and other blood cells, as well as tissue damage in vertebrates. Although there are no studies specifically addressing the role of hemolysins in bivalve vibriosis, they have been described in pathogenic strains, including *V. europaeus* (Le Roux et al. 2009; Spinard et al. 2016). Additionally, proteolytic toxins are crucial for virulence in

bivalves. These toxins assist bacteria in invading host tissues and can degrade proteins, making amino acids available for the pathogen's growth and survival, such as the metalloprotease VtpA in *V. tubiashii* (Hasegawa et al. 2008; Vandeputte et al. 2024). Metalloproteases have also been found to inhibit the host's immune response, such as Vam in *V. aestuarianus*, which inhibits immune responses and is cytotoxic to hemocytes (Labreuche et al. 2010). Furthermore, in the specific case of *V. europaeus*, the metalloprotease VemA aids in the colonization of bivalve mucus, enhancing the infection process (Martinez et al. 2022). Lastly, there are critical toxins involved in the virulence of pathogenic vibrios in bivalves, such as the MARTX complex (Multifunctional-Autoprocessing Repeats-in-Toxin), whose involvement in the virulence of *V. splendidus* strains in oysters has been demonstrated, although the specific mechanism remains unknown (Bruto et al. 2018).

(ii) **Enzymes:** Enzymes play a significant role in microbial virulence by targeting host components and causing tissue damage, thereby facilitating infection and providing nutrients for the microbes (Casadevall and Pirofski 2009). In addition to the aforementioned proteolytic enzymes, there are phospholipases, such as VnpA in *V. neptunius*, which facilitate its ability to infect and cause disease by degrading cell membranes, as well as chitinases, such as those present in *V. tapetis*, which seemingly enable the utilization of chitin, a component of the shell organic matrix, as a carbon source (Galvis, Barja, et al. 2021).

(iii) **Adhesins:** Adhesins, also known as adhesion factors, are microbial molecules that facilitate attachment to surfaces as part of the invasion, colonization, and hemocyte survival processes (Paranjpye et al. 2007; Duperthuy et al. 2011), which are critical steps for infection and growth, making them key virulence factors. Adhesins include a variety of chemical structures such as proteins, polysaccharides, and cell wall components. For instance, it has been found that the porin OMPu is essential for the attachment of *V. splendidus* to oyster hemocytes as part of its pathogenic process (Duperthuy et al. 2011). Additionally, fiber-like transmembrane structures known as pili, specifically type IV pili and mannose-sensitive hemagglutinin (MSHA) type IV pili, as well as lateral flagella, are involved in surface colonization and persistence in bivalves (Kirov 2003; Paranjpye and Strom

2005; Paranjpye et al. 2007; Vezzulli et al. 2015;). Finally, the presence of LPS contributes to the hydrophobicity of the pathogen, thereby facilitating attachment to cell membranes (Lee and Yii 1996).

(iv) **Motility and Chemotaxis:** Motility refers to the ability of an organism to move independently using metabolic energy, which enables pathogens to adapt to new environments, invade host tissues, and spread. Bacteria often rely on flagella for movement, which also play a crucial role in attachment and biofilm formation (Casadevall and Pirofski 2009). Two types of motility occur: (i) swimming in liquid media, mediated by the polar flagellum, and (ii) swarming on solid surfaces, mediated by the lateral flagella (Karlsen et al. 2008). On the other hand, chemotaxis, the movement of an organism in response to a chemical stimulus, allows organisms to navigate toward favourable environments or away from harmful substances. Chemotaxis involves membrane receptors, such as the Methyl-accepting Chemotaxis Proteins family, regulators like CheA, CheB, and CheR, and flagella to drive the movement (Zboralski and Filion 2020; Ushijima et al. 2022). During vibriosis, chemotaxis plays a role in the initial infection, leading to the colonization of mucosal surfaces. For example, it has been demonstrated that *V. europaeus* exhibits positive chemotaxis toward the mucus of juvenile clams (Martinez et al. 2022), and possibly also in the colonization of various organs during the infection process. Regarding vibriosis in bivalve larvae, mechanisms similar to those described for other pathogens, such as *V. anguillarum* in fish, and *V. harveyi* and *Vibrio parahaemolyticus* in adults of *Haliotis tuberculata*, *Haliotis discus ssp. hannai*, and *Ostrea chilensis*, have been speculated (Dubert, Nelson, Spinard, et al. 2016).

(v) **Immune Evasion:** Immune evasion is the ability of bacteria to escape the host's immune system, which in the case of bivalves consists of immune-competent cells, or hemocytes, and various immune effectors and soluble factors produced by them. Escaping immune recognition allows bacteria to inhabit the hemolymph or use it as a medium for expansion during disease development (Parizadeh et al. 2018). Several mechanisms are involved in immune evasion: the hypervariability of the *wbe* region, which encodes the immune-recognizable portion of the O-antigen LPS, has been proposed as a feature that allows pathogen survival

under the selective pressure exerted by hemocytes (Wildschutte et al. 2010). Furthermore, some pathogenic vibrios of bivalves, such as *V. splendidus*, *V. aestuarianus*, and *V. tubiashii*, or their extracellular products, are capable of altering the function of hemocytes, decreasing their adhesion and phagocytosis (Labreuche et al. 2006; Tanguy et al. 2013; Mersni-Achour et al. 2014; Cheikh et al. 2016). Although the mechanisms behind this alteration are poorly studied, the activity of the metalloprotease Vam in *V. aestuarianus* has been linked to the alteration of hemocyte morphology by affecting the cytoskeleton, which is involved in phagocytosis (Labreuche et al. 2010). On the other hand, some pathogenic bacteria can survive inside host cells, evading the immune response. As previously mentioned, *V. splendidus* can adhere to hemocytes through the OMPu porin, after which it is phagocytosed, surviving through the expression of antioxidants and by altering lysosomal membranes and blocking the formation of acid vacuoles, ultimately causing the cytolysis of the hemocyte (Duperthuy et al. 2011; Balbi et al. 2013). Actively killing hemocytes is considered a mechanism of immune evasion, for which there are various molecular mechanisms. For instance, *V. crassostreae*, through direct contact with the hemocyte, employs an unidentified protein with cytotoxic effects, while *V. tasmaniensis* requires a Type 6 Secretion System (T6SS) to carry out this cytotoxicity (Rubio et al. 2019; Piel et al. 2020).

(vi) **Biofilm Formation:** Biofilms are dense aggregates of microorganisms within an exopolysaccharide matrix, playing a critical role in the pathogenesis of certain infectious diseases. Microbes in biofilms exhibit distinct gene expression compared to their planktonic counterparts, affecting properties such as cell surface characteristics and biosynthetic capacity. Biofilm formation is interconnected with processes such as quorum sensing, adherence, and signalling. Biofilms can form on biotic or abiotic surfaces, through a dynamic process consisting of the following steps: (i) Reversible attachment: the initial binding of the bacterium to a surface, dependent on environmental conditions; (ii) Irreversible adhesion: irreversible adhesion involves membrane adhesins, creating a more stable structure; (iii) Formation of small colonies: The formation of an exopolysaccharide matrix corresponds to the early development of the biofilm structure, and its formation is dependent on quorum sensing; (iv) Biofilm maturation: the biofilm continues to

grow and mature, developing a complex structure that includes channels and clusters of cells, which enhances nutrient transport and communication; (v) Cell separation and diffusion: prompted by external or internal factors, some cells in the biofilm detach and disperse, potentially colonizing other areas (Fig. 4) (Liu et al. 2023). The formation of biofilms allows the pathogen to improve its survival in the environment, making it more resistant to antibiotic treatments (Liu et al. 2023). Furthermore, the biofilm structure facilitates the horizontal transmission of genes, including antibiotic resistance and virulence genes (Antonova and Hammer 2011). Finally, biofilm formation contributes to host colonization, enabling survival against antibacterial peptides present in the epithelial mucus, as observed in *V. europaeus* (Martinez et al. 2022) (Fig. 4).

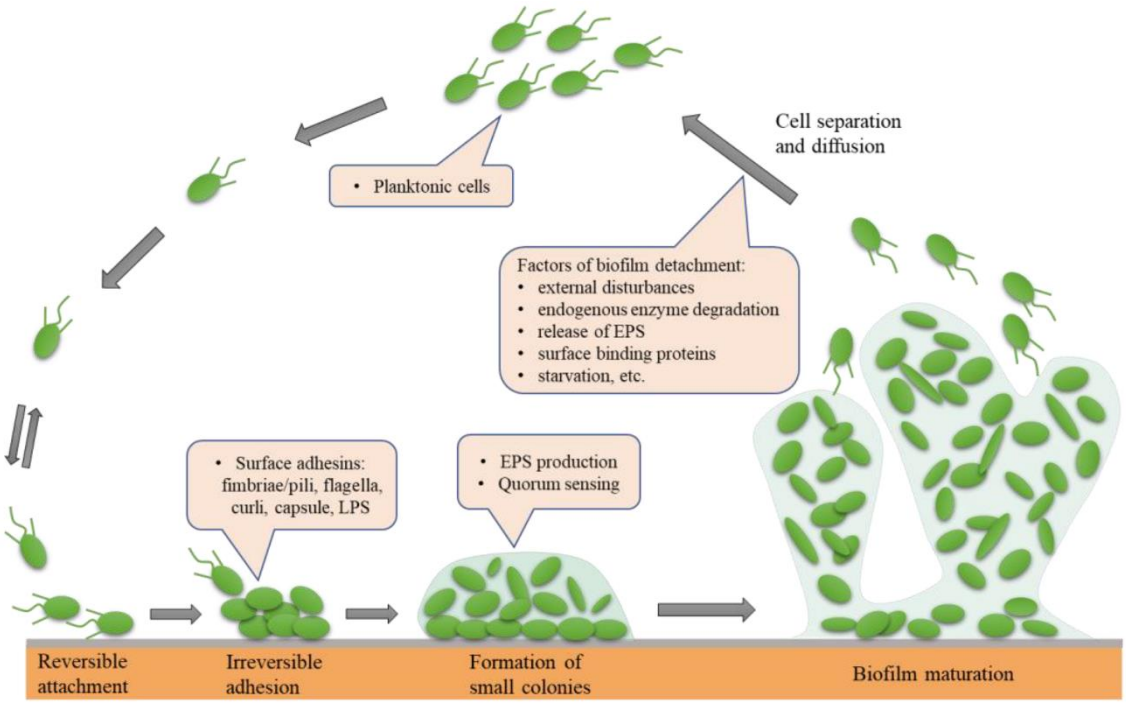

Figure 4. Key phases of the development and formation of biofilm. Adapted from Liu et al. (2023) (Creative Commons Attribution (CC BY 4.0); Annex 1).

(vii) **Quorum Sensing:** Quorum sensing is a form of bacteria-to-bacteria communication that utilizes autoinducers: small signalling molecules capable of modulating bacterial behaviour based on their density. Vibrios employ a unique quorum sensing system involving multiple signalling molecules, known as the multi-channel system. They can produce up to three types of autoinducers:

homoserine lactone (AHL), autoinducer-2 (AI-2), and cholerae autoinducer-1 (CAI-1), which are specifically detected by membrane receptors LuxN, LuxPQ, and CqsS, respectively. This binding triggers a signal transduction pathway that leads to the expression of multiple genes (Defoirdt 2014). In addition to biofilm formation, quorum sensing has implications for the pathogenicity of certain fish pathogens, regulating motility and the secretion of enzymes such as proteases, hemolysins, phospholipases, chitinases, as well as siderophores (Defoirdt 2014; Islam et al. 2022). There is a significant lack of understanding of how quorum sensing regulates virulence in bivalve pathogens, with studies having only been conducted on *V. tasmaniensis* and *V. crassostreae*, where a relationship with motility was found, but not with protease expression (Islam et al. 2022).

(viii) **Secretion Systems**: Vibrios secrete substances through various mechanisms known as secretion systems of types I-VI, which differ in their structure and specific functions (Defoirdt 2014). These systems can be classified into one-step translocation (e.g., T1SS, T3SS, T4SS, and T6SS), where substances are directly transported from the bacterial cytosol to the extracellular space or the target cytoplasm, and two-step translocation (e.g., T2SS and T5SS), where an intermediate step occurs in the periplasmic space (Defoirdt 2014; Y. Luo et al. 2023). The secretion systems show a variable relationship with the pathogenicity of *Vibrio*, being implicated in other virulence factors: (i) **T1SS**: Although this system is the least associated with virulence, atypical forms have been shown to be involved in the secretion of MARTX toxins in several pathogenic *Vibrio* species (Vandeputte et al. 2024); (ii) **T2SS**: This system is involved in various pathogenic processes, including tissue degradation, immune evasion, and biofilm formation through the secretion of extracellular polymeric Substances (EPS) and matrix proteins (Cianciotto and White 2017; Vandeputte et al. 2024); (iii) **T3SS**: This system plays a prominent role among the secretion systems with implications in *Vibrio* virulence, being responsible for the injection of toxic effectors into eukaryotic cells, causing morphological changes and cell death (Osorio 2018; Vandeputte et al. 2024); (iv) **T4SS**: Although its primary function is the horizontal gene transfer, a clear relationship with the virulence of *V. tapetis* in *R. philippinarum* has been observed, although the specific mechanism remains unclear (Rahmani et al. 2021). In other

Gram-negative bacterial groups, the T4SS has been found to participate in bacterial-bacterial competition and the delivery of toxins into eukaryotic cell cytoplasm (Bhatty, Gomez, and Christie 2013; Souza et al. 2015); (v) **T5SS**: Despite being widely distributed in bacteria, information regarding its prevalence and involvement in the virulence of *Vibrio* is limited, though it may be implicated in adherence to host cells or the extracellular matrix, invasion of host cells, immune evasion, cytotoxicity, protease activity, and biofilm formation, often in collaboration with other secretion systems (Abby et al. 2016; Pena et al. 2019; Luo et al. 2023); and (vi) **T6SS**: Several functions of this secretion system are related to virulence. Thus, T6SS is involved in the antibacterial activity of pathogens, causing dysbiosis in complex microbial communities and promoting infection. Furthermore, T6SS effectors can disrupt host cell membranes, interfering with host signalling pathways during infection, manipulating the cytoskeleton, and evading innate immunity (Lin et al. 2021). In the case of bivalve pathogens, the involvement of a T6SS in the destruction of eukaryotic cells by injecting various toxic effectors into them has been demonstrated (Mass, Cohen, Gerlic, et al. 2024). As mentioned earlier, T6SS has been identified as a mediator of cytotoxicity in hemocytes in *V. crassostreae* and *V. tasmaniensis* (Rubio et al. 2019; Piel et al. 2020).

(ix) **Iron Acquisition**: Due to the importance of iron for bacterial growth, bacteria possess various mechanisms to acquire it from several bacterial sources (Wandersman and Delepelaire 2004). This active iron acquisition enables bacteria to thrive in environments with iron deficiency or low availability, such as eukaryotic tissues, where part of the iron is confined within transport or storage molecules (Braun and Hantke 2011). In bivalves, these forms include heme groups, transferrins, and ferritins (Huan et al. 2014; Taniguchi, Dobbs, and Dunn 2017; Gianazza et al. 2021). Thus, many pathogenic vibrios of bivalves are capable of synthesizing these mechanisms, such as *V. neptunius*, which synthesizes the siderophores piscibactin and amphibactin, and *V. tubiashii*, which encodes the siderophore vibrioferrin and the hemophore HutA (Beaubrun et al. 2011; Galvis, Ageitos, et al. 2021; Dai et al. 2022).

1.6 Additional key drivers of *Vibrio* populations, virulence, and pathogenicity

As previously mentioned, the ability of vibrios to cause disease and death results from a highly complex system in which, in addition to the ability to express virulence factors, a variety of environmental and host-dependent factors are involved (Zannella et al. 2017; Paillard et al. 2022).

It is widely recognized that *Vibrio* populations are subject to seasonal variations that affect both their composition and abundance (Romero et al. 2014; López-Hernández et al. 2015; Neu et al. 2021; Hartwick et al. 2021). Among these seasonal parameters, temperature appears to play a particularly important role in the increase of microbiota associated with the *Vibrio* genus, suggesting that temperature influences both the growth rate and pathogenicity (Elston et al. 2008; Romero et al. 2014), being clearly linked to the occurrence of marine fauna mortality events (Vezzulli et al. 2010). In general, high temperatures modulate the pathogenicity of *Vibrio* by increasing the expression of virulence-associated genes, which enhance bacterial virulence. However, exceptions exist, such as the case of hemolysin and siderophore production in *V. kanaloae* (Huang et al. 2021). Several virulence factors related to motility, host degradation, secretion of effectors with anti-eukaryotic activity, antimicrobial resistance, and transcriptional regulation have been identified as positively temperature-correlated in *V. coralliilyticus* (Kimes et al. 2012; Ushijima et al. 2018; Mass, Cohen, Podicheti, et al. 2024). Similarly, *Vibrio harveyi* increases its expression of lytic enzymes, secretion systems involved in the mobilization of virulence elements, and proteins involved in biofilm formation, motility, and quorum sensing (Montánchez et al. 2019; Lee et al. 2023).

Similarly, variations in salinity affect the composition of marine bacterial communities, including those associated with bivalves (Conceição et al. 2021; Dai et al. 2023). The relationship between *Vibrio* and salinity is more complex than that with temperature, with a clear species-dependent pattern reflecting adaptation to different niches. On one hand, several studies conducted in natural environments have observed changes in *Vibrio* populations, with a positive correlation to salinity, including an increase in human pathogenic vibrios such as *Vibrio cholerae* and *V. parahaemolyticus* (Kopprio et al. 2017; Fernández-Juárez et al. 2024), whereas *Vibrio vulnificus* increases in brackish waters but may disappear during events of high salinity (Randa, Polz, and Lim 2004; Froelich et al. 2012; Fernández-Juárez et al. 2024). In recirculating systems, it has been observed that while there are changes in microbiota composition with

varying salinity, shrimp pathogens such as *V. parahaemolyticus*, *V. owensii*, and *V. campbellii* are favored by medium salinity concentrations (15 psu) (Bauer et al. 2021).

This adaptation to the niche is also observed when studying the relationship between the pathogenicity of marine vibrios and salinity, where it serves as a trigger to switch key processes in disease development. Thus, salinity appears to play an important role in the activation of motility and colonization mechanisms of the shrimp pathogen *V. harveyi*. On one hand, it has been found that the flagellation genes *fliA*, *flrB*, and *fliR*, involved in adhesion, biofilm formation, motility, and flagella synthesis, have increased expression at low salinity (8 psu), whereas some genes of the flagellin subunits, as well as the flagellar protein FilL and chitinase, are activated at high salinities (40 psu), suggesting the importance of this parameter in the activation of host searching and colonization (Qi et al. 2022; Kloska et al. 2022). On the other hand, *Vibrio salmonicida*, the causative agent of cold-vibriosis in fish, exhibits salinity-dependent motility. Salinities that are compatible with the external environment activate motility, enabling host colonization, while salinities compatible with the host's internal environment trigger a flagellin protein shutdown, promoting energy conservation that allows the pathogen to thrive and develop cold-vibriosis (Karlsen et al. 2008; Nørstebø et al. 2017). It has been demonstrated that the tricarboxylic acid cycle and the flagellar assembly pathway, involved in adhesion to fish mucus in *V. alginolyticus*, are sensitive to abiotic changes, including salinity (Wang et al. 2015; Huang et al. 2016). The expression of the genes *flrA*, *flrB*, and *flrC*, which are part of the flagellar assembly pathway, increases at salinities of 8 and 45 psu, compared to salinities of 15 to 35 psu (Luo et al. 2016). Furthermore, high salinities play a role in the onset of EMS/AHPND (Early Mortality Syndrome/Acute Hepatopancreatic Necrosis Disease) in shrimp, caused by virulent strains of *V. parahaemolyticus* carrying a plasmid that encodes the binary toxin PirAB (Hossain et al. 2020). It has been shown that the expression of PirA, a component of the PirAB binary toxin, increases when the bacteria grow at salinities of 35 psu, while it is almost nonexistent at 20 psu (López-Cervantes et al. 2021).

Environmental variables also have an effect on the host, favoring the appearance of disease when they act as stressors. Thus, high temperatures have been linked to increased oxidative stress, immune response, elevated host metabolic expenditure, and disturbance of the gut microbiota, which facilitates pathogen entry and disease development (Forberg et al. 2012; Li et al. 2023; Lee et al. 2023; Tian et al. 2024). Similar to what is described for temperature, there is a synergistic effect between host salinity changes and bacterial infection, favouring disease

development and mortality. For example, it has been observed that low salinity stress promotes mortality in oysters infected with *V. alginolyticus*, due to gut microbiota disruption that allows pathogen proliferation, excessive inflammatory response, and consequent immune dysregulation (Li et al. 2022). Similarly, salinity changes that affect the innate defence mechanisms of *Haliotis diversicolor supertexta* have been shown to favor disease onset when confronted with *V. parahaemolyticus* (Cheng, Juang, and Chen 2004).

On the other hand, certain bivalve species are more susceptible to vibriosis than others. These differences in susceptibility reflect variations in the immune efficiency of each species, as demonstrated by studies on the hemocytes of *M. galloprovincialis*, which exhibit a greater ability to kill *Vibrio* bacteria compared to those of *M. gigas* (Cheikh et al. 2016). Regarding host development, it has been shown that adult animals exhibit greater genetic resistance to *Vibrio* infections (Dégremont et al. 2020; Zhai et al. 2021; Nordio et al. 2021; Dietrich et al. 2022).

1.7 Pathogenesis of *Vibrio* infection in bivalves

Pathogenesis refers to the process by which a pathogen causes harm to its host (Paillard, Roux, and Borrego 2004). Although mortality associated with vibriosis has been reported at all developmental stages of bivalves, the larval stages are more susceptible to such events, with a possible explanation being incomplete immune development (Tirapé et al. 2007). Within the larval stages, the greatest vulnerability occurs during the settlement phase, e.g., when there is a transition from a planktonic to a benthic lifestyle. In aquaculture production, this may be related to the higher concentration of pathogenic bacteria present at the tank bottom, associated with moribund larvae or organic detritus, joined with the lower resistance of the larval stages to vibriosis (Romalde 2012; Dégremont et al. 2020; Zhai et al. 2021; Nordio et al. 2021; Dietrich et al. 2022). The first descriptions of vibriosis in bivalves date back to the 1960s, when bacillary necrosis was reported in larvae of various bivalve species. Signs of this bacillary necrosis appear 4-5 hours after exposure to the pathogen and consist of the extension of the velum and impaired motility (Beaz-Hidalgo et al. 2010). Later, Elston y Leibovitz (1980) established a classification of vibriosis in bivalve larvae based on developmental stage and specific signs: (i) Pathogenesis I, which occurs at all larval stages, leading to the loss of swimming ability and colonization of the mantle and pallial cavity, (ii) Pathogenesis II, which affects the veliger larva, resulting in damage to the velum and swimming, as well as visceral atrophy, and (iii)

Pathogenesis III, which affects the pediveliger larva, causing loss of swimming ability and progressively leading to visceral atrophy and lesions in the digestive tract organs.

In the specific case of larval vibriosis caused by *V. europaeus*, Dubert, Nelson et al. (2016) conducted infection tracking using bacteria labelled with GFP. It was established that the infection caused by these pathogens develops in three distinct stages. During the first stage, the pathogens colonize the digestive tract through what is believed to be a chemotactic response to one or more compounds from this organ. After two hours of proliferation, the pathogenic vibrios spread through the visceral cavity from the dorsal to the ventral region (second stage), eventually colonizing the entire larva between 14 and 24 hours (third stage), after which 100% mortality was reached by 36 hours. Associated with this infectious peak, bacterial aggregations, or swarming, are commonly observed around the dead and moribund larvae. Anyway, after the first 2-4 hours, the infection process in irreversible. The larval pathogenesis described is consistent with that observed by Rojas et al. (2019) for *V. bivalvicida* in *A. purpuratus* larvae using the same methodology.

Pathogenesis studies of vibriosis in bivalve larvae suggest that the pathogen enters through the digestive system. Furthermore, Wang et al. (2021) studied the infection of *M. edulis* larvae by *V. splendidus* and *V. anguillarum*, using also bacteria labelled with green fluorescent protein (GFP) alongside with histopathological analyses (Fig. 5). Three phases of infection were established: First, Phase I, also known as the incubation phase, is characterized by the initial colonization of the larval stomach, presumably through the capture of bacteria and food particles by the larval velum. This initial colonization of the digestive tract begins 6 hours after exposure to the pathogen, a period required for the bacteria to degrade the stomach's mucus layer. Disruption of the digestive epithelium was confirmed by histopathology. The infection then progresses to Phase II, termed the rapid diffusion phase, which occurs between 36 and 48 hours after exposure. During this phase, vibrios spread extensively to nearby organs, particularly the ventral region of the larva, causing necrosis in the digestive organs and velum degeneration, along with disorganized stomach cilia. Finally, Phase III, or the acute mortality phase, occurs between 72 and 96 hours after pathogen exposure. This phase is characterized by larval mortality resulting from extensive damage caused by the infection, culminating in the complete degradation of the larval soft tissues.

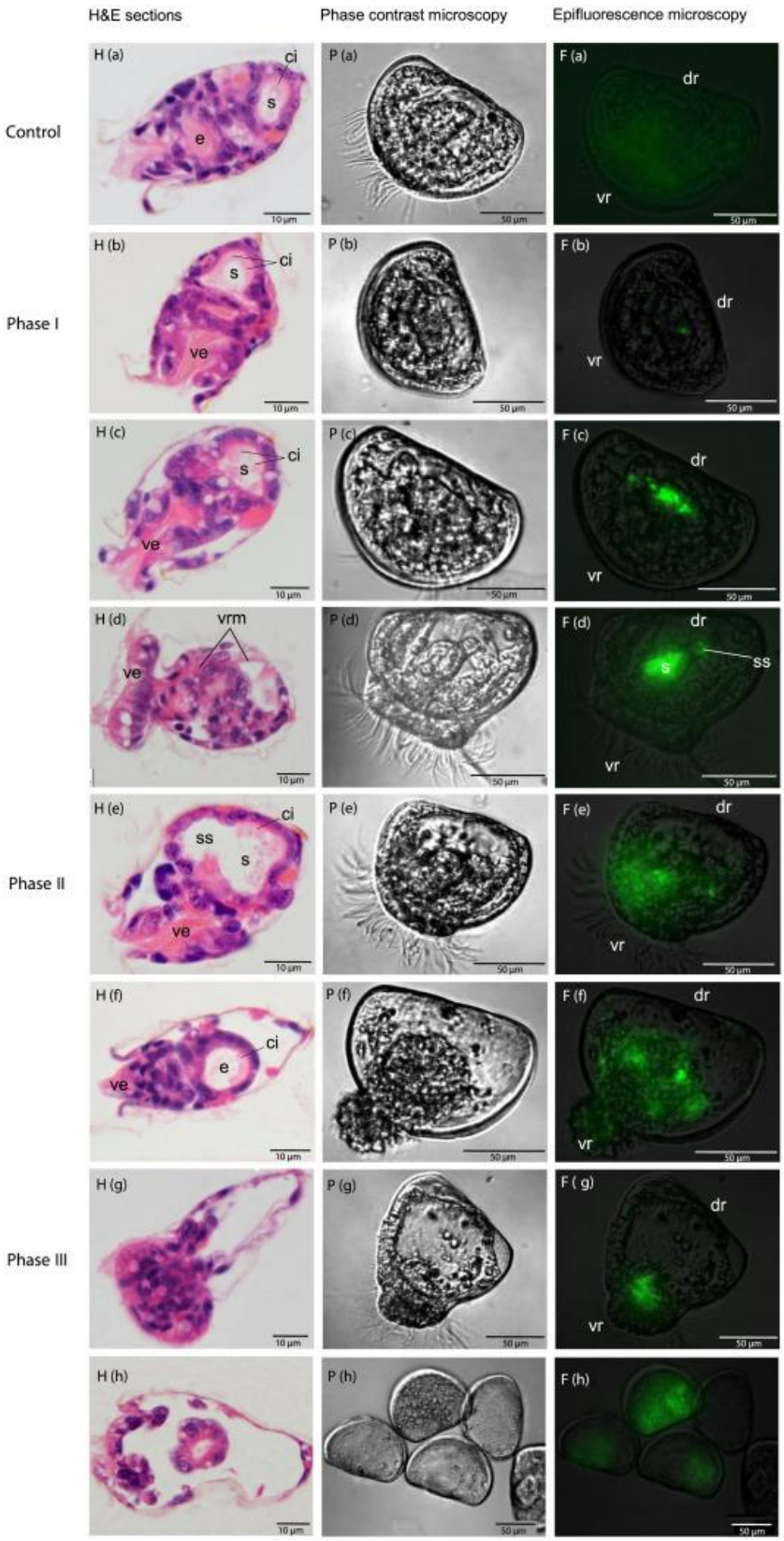

Figure 5. Vibriosis progression in *M. edulis* larvae, by histological observation (H b-h), phase contrast (P a-h), and epifluorescence microscopy (F b-h) (Wang et al. 2021) (Elsevier 5925840589316; Annex 1).

As previously mentioned, the *Vibrio*-host dynamics is complex and dependent on multiple factors. Thus, vibrios that cause vibriosis in non-larval stages may be part of the transient microbiota or be previously associated with host tissues without causing disease (Destoumieux-Garzón et al. 2020). In the case of *V. crassostreae*, its ability to colonize various oyster tissues, including the hemolymph, has been demonstrated, where it can establish itself without causing disease, becoming pathogenic through the acquisition of a plasmid (Bruto et al. 2017). On the other hand, Parizadeh et al. (2018) demonstrated that *V. aestuarianus* can remain asymptomatic in oysters, particularly during the colder months. Furthermore, it has been shown that bivalves can filter bacteria present in the water column, whether associated with particles or not, and these bacteria may either be digested, expelled in feces, or survive and spread to other organs (Cabello, Espejo, and Romero 2005; Parizadeh et al. 2018). The occurrence of early tissue damage in organs outside the digestive tract when bivalves are subjected to bath challenges with pathogenic vibrios raises the possibility of alternative infection routes. In addition to affections in the digestive tract, Loor et al. (2023) found damage in the abductor muscles and gills of juvenile oysters infected with *V. coralliilyticus*, which included infiltration of inflammatory cells into the interstitium of the abductor muscle bundles and damage to the gill filaments, ranging from cilia loss to structural degeneration, with infiltration of hemocytes. Meanwhile, Parizadeh et al. (2018) observed lysis of the sub-epithelial connective tissue in the mantle, as well as hemocyte lysis and/or infiltration by hemocytes and/or hemocyte agglutination in hemolymph vessels.

Regardless of the origin of the infection, pathogenic vibrios spread to other organs, using the hemolymph as a medium for proliferation and colonization of additional tissues, while simultaneously inducing lysis of the hemolymph, thereby compromising the host's immune defences (Cabello, Espejo, and Romero 2005; Parizadeh et al. 2018). The damage associated with the systemic infection resulting from this colonization of other organs and connective tissues leads to host mortality (Parizadeh et al. 2018; Destoumieux-Garzón et al. 2020).

1.8 Vibriosis management in bivalve aquaculture

Bivalve aquaculture presents a series of particularities that complicate the management of infectious diseases. First, the rapid progression of vibriosis in bivalve larvae limits the use of remediation strategies (Dubert, Nelson, Spinard, et al. 2016). Additionally, the lack of an acquired immune system in invertebrates has prevented the use of vaccines (Yang et al. 2021). Finally, the grow-out phase, which involves juveniles and adults, is typically carried out in the natural environment, making the application of treatments unfeasible. As a result, prevention remains the primary approach for combating these diseases.

The most widely used approaches for preventing vibriosis in bivalve hatcheries are those aimed at completely eliminating the bacterial load from the water. Thus, all modern hatcheries are equipped with a water filtration and disinfection system. The filtration system generally consists of the following components: (i) primary filtration: this involves various mechanical filters for the retention of large particles (>20-40 μm), typically a sand filter or a rotating drum filter if the water is directly sourced from the sea or a recirculation system, combined with a series of progressively smaller cartridge filters capable of retaining smaller particles (>10 μm). In hatcheries that source water from wells, primary filtration occurs naturally as the water passes through porous rock or sediments; (ii) secondary filtration: this employs filters capable of retaining particles larger than 1 μm; (iii) disinfection: commonly, UV-C radiation (direct photolysis), ozone, chlorination, or heat are used (Castagna 1983; Helm, Bourne, and Lovatelli 2004; Jorquera et al. 2002; Teitge et al. 2020), although there are less costly alternatives, both in terms of materials and operational procedures, as well as more bivalve-friendly options, such as photodynamic antimicrobial chemotherapy. This method involves the release of porphyrin-type photosensitizers that, upon exposure to light, generate a highly reactive and short-lived singlet oxygen ($^1O_2$), capable of killing pathogens (Malara et al. 2017).

As previously mentioned, the rapid development of vibriosis in bivalve larvae makes treatment with antibiotics unviable (Dubert, Nelson, Spinard, et al. 2016). However, there is a prophylactic use of antibiotics, especially in regions with lax regulations (Campa-Córdova et al. 2005; Baralla et al. 2021; Hossain et al. 2022). Furthermore, the use of antibiotics in aquaculture is associated with risks, such as the development of resistance due to the fixation of antibiotic resistance genes (ARGs), which can be horizontally transferred to other bacteria, including human pathogens (Hossain et al. 2022). Additionally, antibiotics lose their

effectiveness when pathogens are forming biofilms, and do not prevent their formation (Karunasagar, Otta, and Karunasagar 1996; Barja et al. 2023). The significant impact of antibiotic use in aquaculture has led to strong regulations in the European Union, including the prohibition of chloramphenicol, nitrofurans, and furazolidone in aquaculture (Lulijwa, Rupia, and Alfaro 2020).

The nonspecific elimination of bacteria from the hatchery water is an unattainable goal and may favour opportunistic bacteria. Hatcheries are not axenic environments, as bacteria enter from various sources, such as the broodstock, which can transmit part of their microbiota to the offspring, and phytoplankton (Dubert, Barja, and Romalde 2017a). Additionally, bacteria, including pathogenic vibrios, are capable of forming biofilms on culture surfaces, making them resistant to a variety of treatments and serving as a source of bacterial dispersal (Karunasagar, Otta, and Karunasagar 1996). Finally, such measures can lead to an imbalance in the composition of the microbiota, with opportunistic pathogens being favoured due to the lack of competition (Schulze et al. 2006). In contrast, maintaining appropriate culture conditions, such as optimal temperature and salinity, along with low stocking densities, constitutes an important preventive resource against vibriosis, as environmental stressors contribute to the susceptibility of bivalves to developing bacterial diseases (Guo and Ford 2016; Zannella et al. 2017; Sanches-Fernandes, Sá-Correia, and Costa 2022).

Bacteriophage prophylactic therapy refers to the use of viruses (bacteriophages or phages) that specifically infect and kill bacteria as a means of preventing bacterial infections. In aquaculture, it is emerging as a promising alternative to antibiotics due to its specificity, high efficiency, and environmental friendliness (Oliveira et al. 2012; Richards 2014; Liu et al. 2022). However, phage therapy also has a number of drawbacks. First, the evolutionary pressure exerted by phages on bacteria leads to the continuous emergence of resistance against them (Hampton, Watson, and Fineran 2020). To delay the development of resistance and reduce the specificity of these treatments, multiple phages are administered together in what is known as phage cocktails (Mateus et al. 2014; Richards et al. 2021). On the other hand, phages can mediate horizontal gene transfer between bacteria, including antibiotic resistance genes (ARGs), raising concerns about the potential consequences in natural environments and human health (Liu et al. 2022; Hossain et al. 2022). Finally, there are challenges related to the technical viability of such therapies, including methods for the production, delivery, preservation, and large-scale administration of phages (Richards et al. 2021; Liu et al. 2022).

The use of bacterial strains as probiotics, that is, administered live to generate a benefit for the host by modifying its microbiota or the environment (Verschuere et al. 2000), has been proposed as an alternative strategy to the use of antibiotics and other chemicals. Although studies on the efficacy of probiotics in preventing vibriosis in bivalves are scarce compared to those available for other aquaculture species, a variety of bacterial species have been identified that can improve survival during vibriosis. These bacteria include *Alteromonas*, *Pseudoalteromonas*, *Aeromonas*, *Bacillus*, *Roseobacter*, *Phaeobacter*, and *Vibrio* (Prado, Romalde, and Barja 2010; Ringø 2020). While probiotics can provide various benefits to the host, such as improvements in water quality and growth enhancement, the main mechanisms involved in improving survival to vibriosis are the production of antibacterial substances and competition with pathogens (Sohn et al. 2016). The effectiveness of probiotics is highly species-specific, with improvements in survival observed in *scallop* larvae treated with the probiotic bacteria *Phaeobacter inhibens* and *Bacillus pumilus* when challenged with *V. coralliilyticus*, while they were ineffective in northern quahogs, razor clams, and blue mussels (Sohn et al. 2016). Among these variable effects, some probiotics, such as *Phaeobacter gallaeciensis*, can be toxic to larvae (Ruiz-Ponte et al. 1999). On the other hand, the effectiveness of probiotics can be influenced by environmental factors such as temperature and salinity. These variables affect the physiological state of bivalves and their interaction with probiotics, adding complexity to their use (Sohn et al. 2016).

Among the promising prophylactic treatments for the prevention of vibriosis in bivalve hatcheries is the use of nanoparticles, tiny elements typically ranging in size from 1 to 100 nm, with unique physical and chemical properties due to their small size and high surface area. Nanoparticles are attractive for biological applications because of their high surface-to-mass ratio, quantum properties, and ability to absorb and transport compounds such as drugs and proteins. In aquaculture, they show potential for preventing microbial growth and reducing bacterial infections with minimal risk of resistance. However, their toxicity to aquatic organisms and the risks of accumulation requires further studies, as well as the economic feasibility of large-scale production. While there are no specific studies on the use of nanoparticles to control pathogenic *Vibrio* populations in bivalve hatcheries, bactericidal effects of copper, silver, and gold nanoparticles, growth inhibition with zinc nanoparticles, and antibiofilm activity of copper nanoparticles have been observed in various *Vibrio* species affecting fish and crustaceans (Sem et al. 2023).

Despite the absence of adaptive immunity in invertebrates, the recent increase in knowledge about their immune memory has enabled the development of pathogen protection strategies equivalent to vaccination in fish. (Yang et al. 2021). The process begins when the immune system encounters a pathogen for the first time. Hemocytes use specific receptors to recognize pathogen antigens (e.g., peptidoglycans or LPS), triggering their growth and specialization to better engulf and destroy pathogens in future encounters. The immune system also develops memory, enabling faster and stronger responses to similar pathogens later. This memory includes sustained production of immune molecules and improved receptor diversity, which helps the immune system recognize and clear the pathogen more effectively. Finally, long-lasting defence molecules, such as antimicrobial peptides, provide ongoing protection, ensuring a stronger response to future infections (Yang et al. 2021). Additionally, the protection generated by immune priming can be passed on to offspring through what is known as trans-generational immune priming. However, negative consequences for both parties have been observed, likely due to fitness costs (Tetreau et al. 2019). Immune priming has primarily been studied in arthropods, though there are also studies in bivalves. For example, immune memory in *M. gigas* against *Vibrio* has been demonstrated when the bivalve is prepared through injection of sublethal doses, heat-killed, or formalin-inactivated bacteria (Zhang et al. 2014; Arfatahery et al. 2024; Wang et al. 2024). On the other hand, in immune priming against Ostreid herpes virus *1* (*OsHV-1*), the duration of this protection has been estimated at least 5 months, which could serve as a partial solution to the inability to treat bivalves once they are growing in the natural environment (Lafont et al. 2017).

Disease resistance in marine molluscs is heritable and can be improved through selective breeding. This approach is becoming increasingly prevalent in mollusc aquaculture, which could accelerate genetic advancements using genomic tools (Roch 1999; Potts et al. 2021). Currently, breeding programs have been developed for the production of bivalves resistant to infection, particularly from parasites, such as *Bonamia ostreae* and *Marteilia sydneyi*, and viruses such as *OsHV-1* (Jiang et al. 2024). A positive response to selection has been found to increase resistance to *V. aestuarianus*, *V. coralliiyticus*, *V. harveyi*, and *V. alginolyticus* in *M. gigas* (Dégremont et al. 2020; Nordio et al. 2021; Zhai et al. 2021; Dietrich et al. 2022). As genomic technologies continue to advance, there is potential for more effective breeding strategies to enhance *Vibrio* resistance, which could lead to improved sustainability in molluscan aquaculture (Potts et al. 2021).

OBJECTIVES

The overall objective of this work is to expand the genomic knowledge of the emergent mollusc pathogen *V. europaeus*, enabling the development of future prevention and control strategies. To this end, a genomic approach will be employed, involving the whole genome sequencing and analysis of all *V. europaeus* strains identified to the date. To achieve this general objective, the following specific objectives have been defined:

1. To determine the intraspecific diversity of *V. europaeus* and construct its pangenome. This will enable the identification and characterization of core and accessory genes, providing genomic insights into the intra-specific diversity of the species, evolutionary history, and potential strategies to mitigate its impact on aquaculture.
2. To annotate the genes of the *V. europaeus* pangenome and determine their classification as core or accessory genes. This will facilitate the evaluation of their roles in virulence, secondary metabolite production, and resistance to potential preventive treatments (e.g., antibiotics and phage therapy), as well as the analysis of genetic diversity among *V. europaeus* strains based on the accessory genome.
3. To characterize the structural organization of the of the accessory genome of *V. europaeus*, including the plasticity regions and its mobile genetic elements, including plasmids, prophages, and integrative and conjugative elements. This analysis will assess the distribution of genes and elements of interest identified in the accessory genome, providing insights into the species' evolution, mobilome composition, and the mechanisms of horizontal gene transfer that contribute to bacterial survival and adaptation under environmental stress.

MATERIAL AND METHODS

1.1.1 Strains origin

All strains identified to date as *V. europaeus* (n=39) were used for the pangenome reconstruction, including 36 *V. europaeus* strains sequenced in this study and three genomes retrieved from NCBI (strains 071316F, NPI-1 and CECT8426; Table 1).

Table 1.1. Main features of all strains identified to date as *V. europaeus*.

Strain	Source	Location	Year	Mortalities *2	Reference
EX1	*O. edulis* larvae	Hatchery A (Galicia, Spain)	Jul/85	Y	A
PP-654	*O. edulis* larvae	Hatchery B (Galicia, Spain)	Mar/01	Y	B
PP-660	*O. edulis* larvae	Hatchery B (Galicia, Spain)	Mar/01	Y	B
PP-635	*O. edulis* seawater tank	Hatchery B (Galicia, Spain)	Mar/01	Y	B
CECT8136*1	*O. edulis* seawater tank	Hatchery B (Galicia, Spain)	Mar/01	Y	B
CECT8427*1	*H. tuberculata* spat	Hatchery C (Normandy, France)	Jan/2004	Y	C,D
CECT8426*1	*M. gigas* spat	Hatchery D (Nouvelle-Aquitaine, France)	Jun/07	Y	C,D
07/038 2T2	*M. gigas* spat	Hatchery D (Nouvelle-Aquitaine, France)	Aug/2007	Y	C,D
07/108 T1	*M. gigas* spat	Hatchery D (Nouvelle-Aquitaine, France)	Aug/2007	Y	D
07/110 T1	*M. gigas* spat	Hatchery D (Nouvelle-Aquitaine, France)	Aug/2007	Y	C,D
07/112 T1	*M. gigas* spat	Hatchery D (Nouvelle-Aquitaine, France)	Aug/2007	Y	D
07/115 T2	*M. gigas* spat	Hatchery D (Nouvelle-Aquitaine, France)	Aug/2007	Y	-
07/116 T1	*M. gigas* spat	Hatchery D (Nouvelle-Aquitaine, France)	Aug/2007	Y	D

07/117 T1	*M. gigas* spat	Hatchery D (Nouvelle-Aquitaine, France)	Aug/2007	Y	C,D
07/120 T1	*M. gigas* spat	Hatchery D (Nouvelle-Aquitaine, France)	Aug/2007	Y	D
07/121 1T1	*M. gigas* spat	Hatchery D (Nouvelle-Aquitaine, France)	Aug/2007	Y	-
PP2-843	*R. philippinarum* spat	Hatchery E (Galicia, Spain)	Nov/08	Y	B
PP2-978	*R. philippinarum* spat	Hatchery E (Galicia, Spain)	Nov/08	Y	B
2909	*R. decussatus* seawater tank	Hatchery B (Galicia, Spain)	May/11	Y	E
2895	*R. decussatus* seawater tank	Hatchery B (Galicia, Spain)	May/11	Y	E
2930	*R. decussatus* larvae	Hatchery B (Galicia, Spain)	May/11	Y	E
2951	*R. decussatus* larvae	Hatchery B (Galicia, Spain)	May/11	Y	E
2945	*R. decussatus* seawater tank	Hatchery B (Galicia, Spain)	May/11	Y	E
2967	*R. decussatus* larvae	Hatchery B (Galicia, Spain)	May/11	Y	E
2968	*R. decussatus* seawater tank	Hatchery B (Galicia, Spain)	May/2011	Y	E
2969	*R. decussatus* larvae	Hatchery B (Galicia, Spain)	May/2011	Y	E
2971	*R. decussatus* seawater tank	Hatchery B (Galicia, Spain)	May/2011	Y	E
2974	*R. decussatus* larvae	Hatchery B (Galicia, Spain)	May/2011	Y	E
2975	*R. decussatus* seawater tank	Hatchery B (Galicia, Spain)	May/2011	Y	E
3454	*D. trunculus* larvae	Hatchery B (Galicia, Spain)	May/2012	Y	-
3492	*D. trunculus* seawater tank	Hatchery B (Galicia, Spain)	Jun/2012	Y	-
3610	*R. decussatus* broodstock	Hatchery B (Galicia, Spain)	Jul/2012	Y	F
3614	*R. decussatus* eggs	Hatchery B (Galicia, Spain)	Jul/2012	Y	F
NPI1	*A. purpuratus* larvae	Hatchery F (Coquimbo, Chile)	Feb/2015	Y	-
071316F	Seawater	Netarts Bay (Oregon, US)	Jul/2016	N	-
L2	*P. rhomboides* larvae	Hatchery B (Galicia, Spain)	Mar/2018	Y	-

L3	*E. arcuatus* larvae	Hatchery B (Galicia, Spain)	Mar/2018	Y	-
L4	*E. arcuatus* larvae	Hatchery B (Galicia, Spain)	Mar/2018	Y	-
L20	*R. philippinarum* larvae	Hatchery B (Galicia, Spain)	May/2018	Y	-

*[1]Synonymous names: *V. europaeus* CECT8136=PP-638 (Prado, Dubert, y Barja 2015); *V. europaeus* 04/002 1T2 = CECT8427 and *V. europaeus* 07/118 T2 (CECT8426) (Travers et al. 2014); *[2] Strains isolated from mortalities (see references for more information). References: A (Lodeiros et al. 1987); B (Prado, Dubert, y Barja 2015); C (Saulnier et al. 2010); D (Travers et al. 2014); E (Dubert et al. 2017); F (Dubert et al. 2016).

1.1.2 DNA extraction, whole genome sequencing and assembly

Two sequencing approaches were followed for genome assembly:

(i) Short-read sequencing. 150 bp paired-end Illumina sequencing was performed in the *V. europaeus* strains (n=36) for assembling at the contig level (Table 1.1). Strains were grown overnight in Trypto–Casein Soy agar supplemented with 2% (w/v) sodium chloride (TSA–2, Condalab) at 25ºC. Subsequently, a single colony was picked and grown under the same bacterial culture conditions but in broth (TSB-2) with vigorous shaking. High-molecular weight (HMW) DNA was extracted from an aliquot of the overnight culture (200 µl) using the DNeasy Blood & Tissue Kit (QIAGEN) following the manufacturer instructions. Quantity, quality and integrity of each DNA extraction was evaluated using NanoDrop One (Thermo Scientific), Qubit (Thermo Scientific) and by electrophoresis in a 1% (w/v) agarose gel. Genomic libraries and sequencing (HiSeq4000 sequencer, Illumina) were performed by the SNPsaurus company. Quality of Illumina reads was performed using Trimmomatic (Bolger, Lohse, and Usadel 2014) and paired-end short reads were assembled at contig level using SPAdes 3.15.4 using default arguments (Prjibelski et al. 2020).

(ii) Long-read sequencing (Pacific Biosciences, PacBio, or Oxford Nanopore Technologies, ONT). Four representative strains (the type strain, CECT8136 and the isolates CECT8427, PP2-843 and EX1; Table 1.1) were long-read sequenced to achieve high resolution assemblies including polishing with Illumina reads. For this, each bacterial strain was grown as described previously and HMW DNA was extracted from

4 ml of an overnight culture using Qiagen Genomic-tips 100/G kit (QIAGEN). Quantity, quality, and integrity of HMW DNA extractions was evaluated as described above. CECT8136, CECT8427 and PP2-843 strains were sequenced using a PacBio Sequel II sequencer (PacBio) by SNPsaurus, while EX1 genome was sequenced in our lab using MinION sequencer using the Rapid sequencing gDNA-barcoding kit (ONT). Assemblies from PacBio and ONT reads were performed using *de novo* long-read assembler Flye (Kolmogorov et al. 2019) and polished by Racon (Vaser et al. 2017). Finally, each assembly was polished using Illumina reads with Pilon using default arguments (Walker et al. 2014). Thus, a total of six whole genome chromosome-level assemblies (CECT8136T, CECT8427, PP2-843 and EX1 sequenced in this study; and NPI-1 and CECT8426 retrieved from NCBI) were used in this study for pangenome analyses (Table 1.1).

1.1.3 Genome annotation and pangenome construction

Each genome assembly (n=39; Table 1.1) was annotated by Prokka 1.14.4 using default arguments (Seemann 2014). The gff3 file was used to construct the *V. europeus* pangenome using Roary 3.13.0, with the core gene alignment with MAFFT option (Page et al. 2015). The core genome was constructed including those genes that were present in the 100% of the *V. europaeus* genome strains, while the accessory genome was further classified as shell core, soft and cloud genome if a gene was present in the 95-99%, 15-95% or 0-15% of the genomes respectively. Genes classified into core, shell core, soft or cloud fractions were plotted with ggplot2 3.3.6 R package (Wickham 2016).

The micropan R package (Snipen and Liland 2015) was used to determine if the *V. europaeus* pangenome was open or closed by the calculation of the Heaps alpha value setting 1000 permutations and results plotted as described above.

Gene sequences from each pangenome fraction (e.g., core, shell core, soft and cloud) were retrieved from the Roary's *pan_genome_reference* file using SeqKit 2.1.0 (Shen et al. 2016). Subsequently, each gene was functionally annotated using reCOGnizer 1.7.0 using default arguments (Sequeira et al. 2022) to obtain the distribution of Cluster of Orthologous Group (COG) categories within the *V. europaeus* pangenome. The percentage of genes assigned to the different COG categories per

pangenome fraction was calculated and the resulting matrix was plotted in a heatmap using the ComplexHeatmap 2.11.1 R package (Gu 2022).

Identification of tRNAs and rRNAs from each genome assembly was done using tRNAscan-SE 2.0.1 (Chan et al. 2021) and barrnap 0.9 (https://github.com/tseemann/barrnap) using default arguments, respectively.

1.1.4 Phylogenomic comparisons: phylogenetic tree, SNPs identification and Average Nucleotide Identity (ANI) calculations

Genes from the core fraction of each genome assembly (n=39), previously aligned by Roary 3.13.0 using MAFFT, was used to build a phylogenomic tree with IQ-TREE (Nguyen et al. 2015) based on the maximum likelihood (ML) algorithm with the UNREST model by bootstrapping over 1000 replications and the phylogenomic tree was visualized in iTOL v6.6 (Letunic and Bork 2021).

Single nucleotide polymorphisms (SNPs) were identified across the core genes alignment created with MAFFT using an *ad hoc* Phyton script (available in https://github.com/sergio-c-r/core-snps/blob/main/snp_dif.py).

Average nucleotide identity (ANI) among the different *V. europaeus* genome assemblies was calculated by PYANI 0.2.11 (Pritchard et al. 2016) with default parameters and plotted in a heatmap as described above.

A hierarchical clustering was using to construct a dendrogram of the accessory gene profiles was constructed using the stats package in R, based on the presence/absence matrix generated by Roary. To illustrate the presence/absence genes profiles, these were plotted as a heatmap using the R package ComplexHeatmap 2.11.1, and plot together the dendrogram. Finally, a principal component analysis (PCA) based on the presence/absence matrix of pangenome genes was computed by R.

1.1.5 Experimental infections

A total of 38 *V. europaeus* strains (71316F was not available in our bacterial collection; Table 1.1) were tested in virulence challenges using Manila clam (*R.*

philippinarum) juveniles (14±1 mm). Virulence challenges were performed following the infection protocol described by Martínez et al. (Martínez et al., 2022) and *V. breoganii* C5.5 was used as negative control. Briefly, bacterial strains were grown overnight and bacterial suspensions were made in sterile sea water (SSW) adjusted to OD_{600}=1 and confirmed by decimal dilution series onto TSA–2 plates (~10^8 CFU ml^{-1}). Experimental challenges included two steps:

(i) Infection: tanks were filled with filtered seawater (FSW; 0.22 µM Nalgene Rapid–Flow, Thermo Scientific) containing a bacterial suspension adjusted to a final concentration of 10^7 CFU ml^{-1}. Subsequently, 15 Manila clam juveniles were added to each tank and kept for 24 h at room temperature (RT=~20ºC) for active bacteria filtration. Experimental challenges were performed in triplicate.

(ii) Post–infection: challenged juveniles were taken out from the infection tanks and maintained for 8 h at RT to internalize the bacteria within the pallial cavity. Then, juveniles were transferred to "fresh tanks" filled with 200 ml FSW and maintained at RT with aeration. Mortalities were monitored at 8 h, 20 h, 32 h, 44 h, 56 h, 68 h and 80 h post–infection and clams were immediately removed when the valves were open (dead juveniles), or siphons were not retracted following stimulation (moribund juveniles) and were recorded as a percentage of survival. FSW was renewed once per day (or if it was turbid).

1.1.6 *In silico* identification of the virulence genes

Genes related to virulence were identified in each *V. europaeus* genome (n=39) using the VFDB database using default arguments (Liu et al. 2021). An additional set of well-known proteins whose role in virulence was experimentally demonstrated was included in the analyses by BLASTp comparisons. The resulting presence-absence matrix was used to plot a heatmap as described above.

Subsequently, a principal component analysis (PCA) was performed using the prcomp function available in R base, and plotted with ggplot2 to compare the virulence genes belonging to the non-core fractions among the different *V. europaeus* strains.

1.1.7 Characterization of the antibiotic resistance profile

Antibiotic resistance profiles were obtained based on the consensus obtained between the *in silico* and *in vitro* analyses, and plotted in a presence-absence matrix using ComplexHeatmap 2.11.1:

(i) Search for antibiotic resistance genes was performed using the web-based servers RGI 5.2.1 (McArthur et al. 2013) using the CARD database being considered only strict and perfect matches (bitscore > 500), and ResFinder 4 (Bortolaia et al. 2020) with 80% of threshold and minimum length.

(ii) Available bacterial strains (n=38) were grown as described above and antibiograms were carried out by the disc diffusion method on Müeller–Hinton agar (Oxoid) supplemented with 1% NaCl (MHA-1) with commercial discs (Oxoid, UK). The antibiotics tested were tetracycline (TE, 30 µg), oxytetracycline (OT, 30 µg), cephalexin (CN, 30 µg), ampicillin (AMP, 10 µg), amoxycillin (AML, 25 µg), erythromycin (E, 15 µg), enrofloxacin (ENR, 5 µg), flumequine (UB, 30 µg), cefoxitin (FOX, 30 µg), chloramphenicol (C, 30 µg), florfenicol (FFC, 30 µg), streptomycin (S, 10 µg), sulfonamide (SULDD, 25 µg) and gentamicin (CN ,10 µg). After incubation (24 h at 25ºC), the zones of inhibition around the discs were measured and compared against recognized zone size ranges established by the manufacturer for specific antimicrobial agents.

1.1.8 Search for secondary metabolite biosynthetic gene clusters

Biosynthetic gene clusters (BGC) were identified in each bacterial genome (n=39) using antiSMASH 7.0 web server (https://antismash.secondarymetabolites.org/) with default parameters and considering only strict findings. Genetic diversity within each BGC cluster among the 39 strain genomes was evaluated using BIG-SCAPE 1.1.5 using default arguments (Navarro-Muñoz et al. 2020), including the determination of biosynthetic gene cluster families (GCF). To deep into the intra-family sequence diversity of BGCs, the minimum and the average of BGC pairs belonging to the same phylogenetic cluster were estimated from each GCF using the Jaccard Index values obtained with BIG-SCAPE. To visualize the internal diversity of the GCFs, a vector image was generated by joining for each GCF the phylogenetic tree and the schemes of

their respective BGCs generated by BIG-SCAPE, for which an *ad hoc* python script was used (available at https://github.com/sergio-c-r/BIG-SCAPE_merge). To simplify the images, branches with no diversity were manually collapsed.

1.1.9 Characterization of anti-phage defence systems

All genome assemblies (n=39) were individually analysed using the following web-based servers: Defence-Finder (Tesson et al. 2022) and PADLOC v1.1.0 (v1.4.0) (Payne et al. 2022) with CRISPRDetect option (Biswas et al. 2016). A consensus between Defence-Finder and PADLOC outcomes was shown with an absence-presence matrix and a PCA was performed with each strain profile as described above.

1.1.10 Identification of plasmids

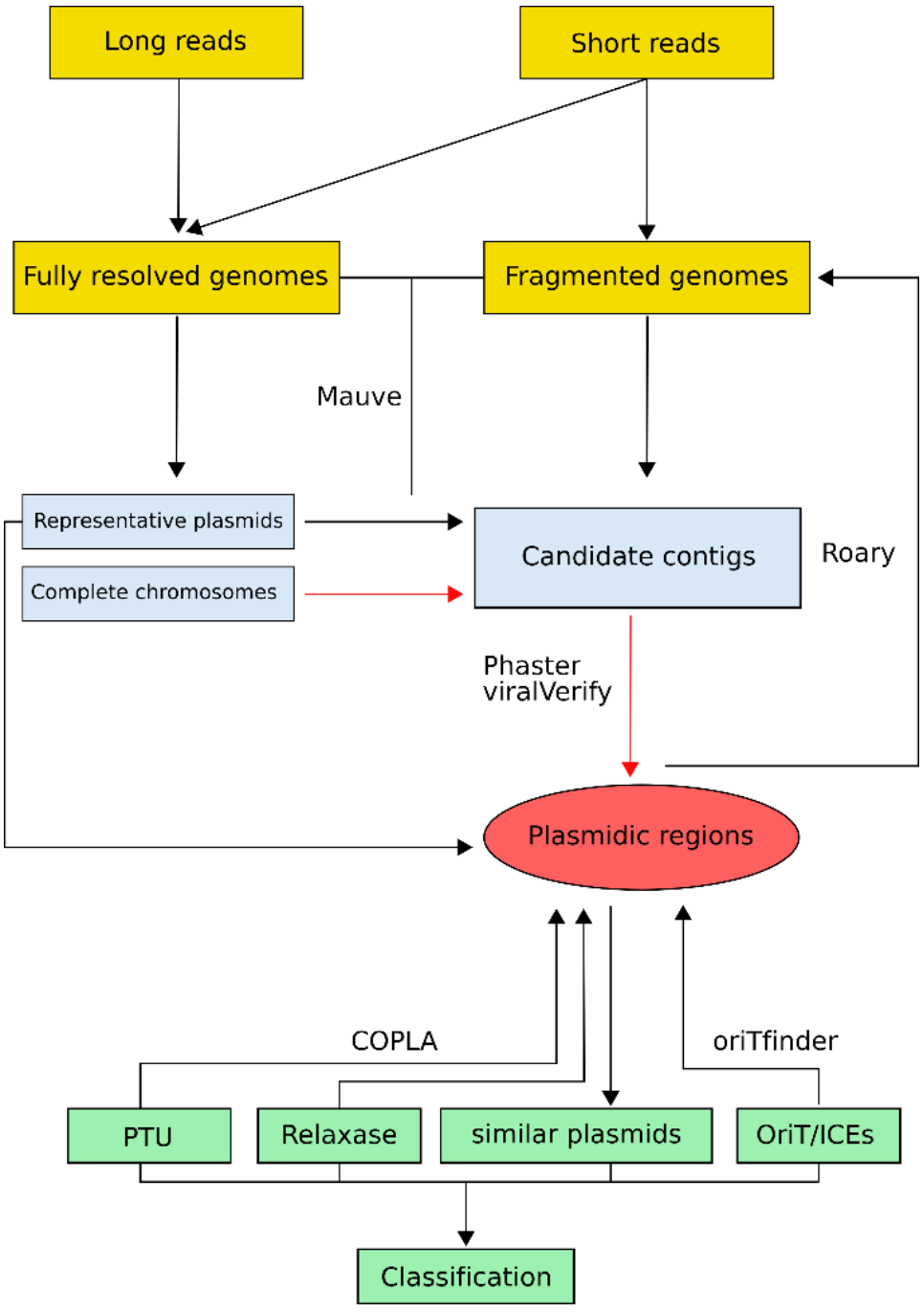

Figure 3.1. Bioinformatic workflow to identify and classify plasmids from the contigs. Red arrows represent deletion of elements. Genome assemblies from long and/or short reads were described in Chapter 1 and represented in yellow. Software used in each step is also indicated.

Fully resolved genomes (CECT 8136, CECT 8427, CECT 8426, PP2-843, EX1, and NPI-1 strains; Table 1.2) assembled from long-reads yielded whole plasmids (hereinafter referred to as representative plasmids). Plasmids from genome assemblies at scaffold (n=32; Table 1.2) and contig levels (n=1; Table 1.2) were identified by aligning contigs/scaffolds against each fully resolved genome using Mauve 2.4.0 with default parameters (match seed weight 15) (Darling et al. 2004) (Fig. 3.1). Contigs aligned with representative plasmids were designated as candidate contigs. On the other hand, contigs not aligned with the bacterial representative chromosomes were subjected to further analyses. Then, those contigs were analyzed using Phaster (https://phaster.ca/) (Arndt et al. 2016) and viralVerify 1.1 (https://github.com/ablab/viralVerify), and discarded if positive match was found. To ensure the detection of true plasmidic regions, an additional search was performed by subtracting previously detected plasmidic sequences from genomes (Fig. 3.1). Then, homology between plasmid genes and the remaining genomes was assessed with Roary as explained in Chapter 1.

Plasmidic regions, including representative and putative plasmids, were analysed with COPLA 1.0 with default parameters (Redondo-Salvo et al. 2021) to find the closest relative plasmids and to be classified according the following criteria: (i) a plasmid taxonomic unit (PTU) and (ii) their relaxases via MOBscan (Garcillán-Barcia et al. 2020). Finally, OriTfinder and ICE finder 1.0 (Li et al. 2018; Liu et al. 2019) were used to evaluate if plasmids are non-mobilizable, mobilizable or conjugative (Fig. 3.1).

Among the plasmids identified, pVE1-related plasmids were distributed across the 38 *V. europaeus* genomes analysed. pVE1-related plasmids were aligned with Mauve using default parameters (Darling et al. 2004), and the consensus sequence was obtained with Jalview (Waterhouse et al. 2009). This consensus sequence was used as reference to visualize and plot all pVE1-related sequences using the GView server (https://server.gview.ca/). Additionally, genes related to virulence, antibiotic resistance, biosynthetic gene clusters and anti-phages defence systems, identified previously in Chapter 2, as well as integrative and conjugative elements, were identified on each plasmid.

3.1.1 Identification of chromosomic RGPs

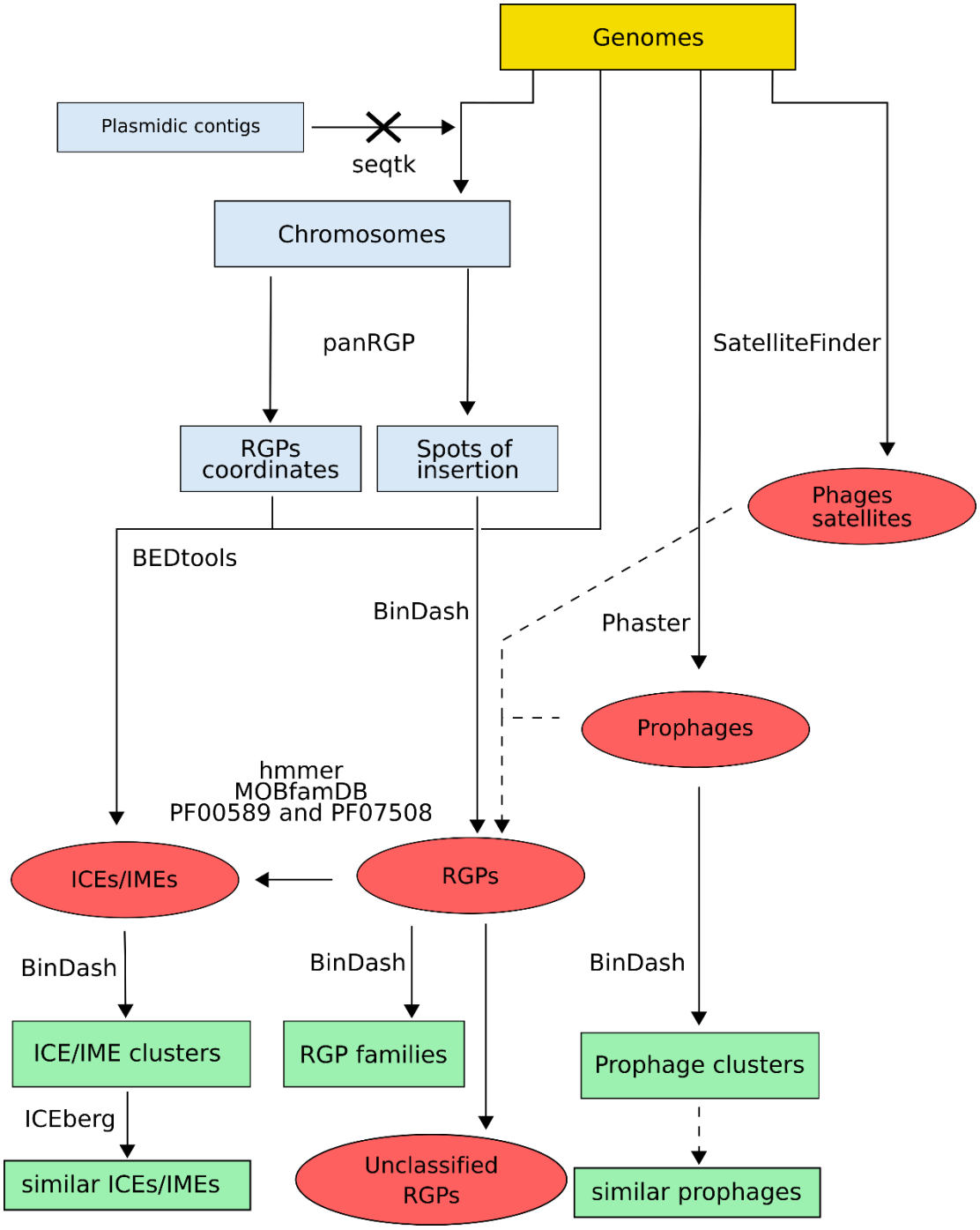

Figure 3.2. Bioinformatic workflow to identify and classify chromosomic RGPs, ICEs/IMEs, prophages, and phage satellites. Red arrows represent deletion of elements. Methodology described in other chapters are represented in yellow. The processes that required the establishment of homologies with BLAST are indicated with dashed lines.

Plasmids identified as described above were removed from genome assemblies using seqtk (https://github.com/lh3/seqtk) (Fig.3.2). Then, resulting chromosomes were reannotated with Prokka as described in Chapter 1. The obtained gff3 files were used to identify all the chromosomal RGPs with panRGP, using default arguments (Bazin et al. 2020). The RGPs genomic coordinates obtained with panRGP were used to extract the sequences from the chromosomic contigs, using the getfasta utility from BEDtools 2.31.1 (Quinlan and Hall 2010), and subsequently annotated with Prokka for further analysis (Fig. 3.2).

Final dataset was curated to remove chromosomic RGPs associated to chromosomic MGEs such as ICEs/IMEs, prophages and phage satellites for further analyses as described below and this dataset designated as unclassified chromosomic RGPs. To evaluate the chromosomic RGPs diversity, the mutation distance and the Jackard Index of each pair of RGPs were calculated with BinDash 1.0 using default arguments (Zhao 2019). Pairs of RGPs with Jaccard Index value higher than the arithmetic mean were used to construct a network of RGPs using Cytoscape 3.10.0 (Shannon et al. 2003) (Fig. 3.2). The relationship between RGPs not assigned to a spot of insertion (hereafter designated as decontextualized RGPs) and the fragmentation of the genome was studied by calculating of the Kendall rank correlation coefficient between the number of fragments of the *V. europaeus* genomes (contigs or scaffolds) and the proportion of decontextualized RGPs, using R.

1.1.11 Identification of ICEs/IMEs, prophages and phage satellites

ICEs/IMEs, prophages and phage satellites were identified from the bacterial genomes (Fig. 3.2) such as:

(i) **ICEs/IMEs:** RGP proteome obtained with Prokka was examined with hmmer 3.4 (http://hmmer.org/) to search for relaxases, integrases, and recombinases using the MOBfamDB (Garcillán-Barcia et al. 2020) and the Pfam accessions PF00589 and PF07508, respectively (Fig. 3.2). RGPs with homologs for relaxase and integrase/recombinase were considered as a putative ICE/IME. Putative ICE/IME were clustered by calculating the Jaccard Index using BinDash 1.0 (Zhao, 2019) with a cut-off similarity value of 0.95 and clusters (C1-C14) were plotted in a heatmap using the

ComplexHeatmap 2.11.1 R package (Gu 2022). The distribution of the different ICEs/IMEs clusters (clusters composed of more than one ICE/IME) within bacterial hosts was shown by the construction of a hierarchical edge bundling plot using the ggraph 2.1.0 R package (https://ggraph.data-imaginist.com) combined with the phylogenetic tree based on the core genome (see Chapter 1). Additionally, the Multigeneblast comparison method available in the ICEberg 3.0 database online tool (https://tool2-mml.sjtu.edu.cn/ICEberg3) was used to search similar ICEs/IMEs (Fig. 3.2). Finally, RGPs identified as ICEs/IMEs were removed from the RGP sequences pool for further analysis.

(ii) **Prophages:** prophages were identified by Phaster (Arndt et al. 2016) and only "intact" matches (high number of coding DNA sequences (CDS) of a region attributable to prophages, and presence of phage-related genes) were considered as prophages for further analysis (Fig. 3.2). In order to study the similarity among detected prophages, the Jaccard Index between pairs of sequences was calculated with same methodology and criteria described above for ICEs/IMEs. The nucleotide sequences of identified prophages were queried in the nt NCBI database using megaBLAST to look for similar prophages (Camacho et al. 2009) (Fig. 3.2). Resulting prophages were associated with the RGPs previously identified by megaBLAST (Camacho et al. 2009) and removed from the RGP pool for further analysis.

(iii) **Phage satellites:** Detection of phage satellites was carried out using SatelliteFinder (https://galaxy.pasteur.fr/root?tool_id=toolshed.pasteur.fr/repos/fmareuil/satellitefinder/SatelliteFinder/0.9) (Abby et al. 2014) (Fig. 3.2). The obtained phage satellites were associated with the RGPs previously identified by megaBLAST using default arguments (Camacho et al. 2009), and removed from the RGP pool for further analysis.

1.1.12 Gene annotation of the accessory genome

The enrichment of genes identified in Chapter 2 and related to virulence, antibiotic resistance, anti-phages defence, and secondary metabolism production was determined in plasmids, ICEs/IMEs, prophages, phage satellites and unclassified chromosomic RGPs. Nucleotide sequences of these regions were used to construct a database with the makeblastdb

application of BLAST+, using default arguments in both cases (Camacho et al. 2009). Then, genes of interest were blasted (blastn) against our database using megaBLAST using default parameters (Camacho et al. 2009). For RGPs, results were manually marked in the networks of RGPs obtained previously and summarized and plotted as a bubble plot with the ggplot2 3.3.6 R package (Wickham 2016).

Two different T6SSs (T6SS1 and T6SS2) were identified in Chapter 2. T6SS1 was encoded by the chromosome 1 and T6SS2 was only located in the pVE1-related plasmids. Thus, T6SS was characterized in SecReT6 3.0 (Zhang et al. 2023) using the nucleotide sequences from the CECT8136 genome as reference. A phylogenetic analysis of T6SS1 and T6SS2 was performed: (i) the complete T6SS dataset available in the SecReT6 3.0 database was downloaded and filtered to retain only the NCBI accession sequences containing T6SSs type i5 (accessed on May 13, 2024), as well as the genomic coordinates of these systems; (ii) T6SS sequences were extracted from the nucleotide sequences obtained from NCBI and the CECT8136 genome using the getfasta utility from BEDtools 2.31.1 (Quinlan and Hall 2010) and GBK files obtained with Prokka as described in Chapter 1; (iii) GBK files were used to construct a T6SS core-protein phylogeny with CORASON (https://github.com/nselem/corason), using the *tssB* gene and the T6SS sequence of CECT8136 as references, with default parameters. The resulting Newick tree was visualized in iTOL v6.6 (Letunic and Bork 2021). The Scalable Vector Graphics (SVG) file containing the phylogenetic tree with the T6SS synteny was manually modified to show the minimal clade containing the chromosomic (T6SS1) and plasmidic (T6SS2) T6SS sequences of *V. europaeus*.

1.1.13 Distribution of accessory genetic elements among the pangenome accessory fractions

The nucleotide sequences of plasmids, ICEs/IMEs, prophages, phage satellites and unclassified chromosomic RGPs corresponding to each *V. europaeus* genome were separated into multifasta to study their distribution in the accessory fractions of the pangenome (soft core, shell genes, and cloud genes; Chapter 1). These multifasta files were annotated with Prokka (Seemann 2014) to obtain a ffn file with the protein-coding sequences. Subsequently, these ffn files were compared using megaBLAST using default arguments (Camacho et al. 2009) with the ffn file corresponding to each strain

(obtained in Chapter 1). Gene ID of perfect matches were assigned to an accessory genome fraction using the gene_presence_absence.csv file generated by Roary (Page et al. 2015) as described in Chapter 1 and an *ad hoc* Phyton script (https://github.com/sergio-c-r/gene-freq-from-roary/blob/main/converge).

CHAPTER 1: EVOLUTIONARY HISTORY AND PANGENOME OF THE MARINE MOLLUSCS PATHOGEN *Vibrio europaeus*

1.1 Introduction

The term bacterial pangenome has been defined as the whole gene repertoire of a microbial species (McInerney, McNally, and O'Connell 2017). Advances in the study of the bacterial pangenome have had an impact on the understanding of the genomic adaptations of bacteria to environments, and its implications in taxonomy and evolution (Liao et al. 2021; Fu et al. 2021; Simonsen 2022). The determination of a pangenome reflects indeed the diversity within a bacterial taxon, but also enables the identification of shared genes across strains or lineages, usually known as the core genome, while the accessory genome would encompass the heterogeneity of genomes across strains or populations (McInerney, McNally, and O'Connell 2017). The core genome can intersect at various taxonomic levels providing the genomic basis of the species phylogeny and is composed by genes fundamental for bacterial survival (McInerney, McNally, and O'Connell 2017). The accessory genome enables the bacterial adaptation to ecological niches, providing the variability underlying specific traits such as a virulence, phage defence systems or antimicrobials resistance (Jackson et al. 2011; Vassallo et al. 2022).

Pangenome inspection is especially interesting for studying pathogenic strains in activities with high-economic impact such as aquaculture. Bivalve aquaculture is the second most important activity within the world aquaculture and its expansion is constrained (i) by the negative impact of bacterial diseases such as vibriosis promoted by different *Vibrio* spp., specially at hatchery level, endangering the continuous supply of seed to shellfish beds for grow-up and harvesting (Prado et al. 2005; Dubert, Barja, y Romalde 2017); and (ii) the lack of effective and eco-friendly treatments to fight those pathogens (Dubert, Barja, and Romalde 2017b). Despite this, the pangenome studies about bacterial pathogens affecting bivalve aquaculture are scarce (Dias et al. 2018). Among *Vibrio* pathogens, *V. europaeus* is an emergent species with great impact on bivalve aquaculture worldwide affecting the most important molluscs species reared even at different stages of development in the main producer countries such as Spain, France, Chile or US (Prado et al. 2005; Mersni-Achour et al. 2014; 2014b; Prado,

Dubert, and Barja 2015; Dubert et al. 2017; Rojas et al. 2021). This emergent pathogen has been responsible of mortality events in different mollusc species, such as clams (*R. decussatus*, *R. phillipinarum, D. trunculus*, *Ensis arcuatus*, and *Politapes rhomboides*), oysters (*M. gigas* and *O. edulis*), scallops (*A. purpuratus*) or abalones (*H. tuberculata*) (Prado et al. 2005; Mersni-Achour et al. 2014; Travers et al. 2014; Prado, Dubert, and Barja 2015; Dubert, Romalde, Spinard, et al. 2016; Rojas et al. 2021).

The aim of this Chapter was to characterize the pangenome of the bivalve pathogen *V. europaeus* to gain knowledge about genomics on this species, and to use this information to minimize its negative impact in aquaculture. For this purpose, all the existing *V. europaeus* strains were whole genome sequenced using Illumina short-read and, in some cases, also by third generation sequencing to obtain fully resolved and accurate assemblies. Finally, core and accessory genes were identified and inspected to elucidate basic questions related to evolution and intra-specific variability.

1.2 Results

1.2.1 Pangenome description

The features of *V. europaeus* strains used in this study are summarized in Table 1.2. The *V. europaeus* pangenome was composed by a total of 9860 gene clusters and it was open according to the alpha value obtained (0.68) (Fig. 1.1). Among these gene clusters, the 39% (3846 gene clusters) was assigned to the core genome, whereas 61% (n=6014 gene clusters) belonged to the accessory genome (Fig. 1.2A and B). Within the accessory genome, the 26%, 4% and 70% was assigned to the shell, soft, and cloud gene fractions respectively (Fig. 1.2A and B). The main source of cloud genes proceeds from the French strains (CECT8427=666 genes; 07/115 T2==617 genes; 07/038 2T2=487 genes; 07/117 T1=468 genes; 07 108 T1=455 genes; CECT8426=321 genes; and 07/120 T1=316 genes), two Spanish strains (EX1=388 genes and PP2-843=320 genes) and the American strain (071316F=542 genes) (Fig. 1.2A).

Table 1.2. Genomic information (assembly level and accession number) of *the V. europaeus* strains (n=39) used in this study.

Strain	Assembly*1	CDS	Accession number
EX1	comp (4)	4936	CP180205-CP180207
PP-654	cont (38)	4921	JAPFJT000000000.1
PP-660	cont (34)	4891	JAPFJS000000000.1
PP-635	cont (38)	5014	JAPFJR000000000.1
CECT8136T*1	comp (4)	4936	LUAX00000000.1
CECT8427*1	comp (4)	4941	JAPFJQ000000000.1
CECT8426*1	comp (3)*2	4935	GCA_015654285.1
07/038 2T2	cont (44)	5008	JAPFJP000000000.1
07/108 T1	cont (43)	4887	JAPFJO000000000.1
07/110 T1	cont (43)	4880	JAPFJN000000000.1
07/112 T1	cont (36)	4878	JAPFJM000000000.1
07/115 T2	cont (47)	4856	JAPFJL000000000.1
07/116 T1	cont (37)	4851	JAPFJK000000000.1
07/117 T1	cont (37)	4908	JAPFJJ000000000.1
07/120 T1	cont (41)	4998	JAPFJI000000000.1
07/121 1T1	cont (39)	4883	JAPFJH000000000.1
PP2-843	comp (4)	5086	GCA_028447005.1
PP2-978	cont (32)	5015	JAPFJF000000000.1
2909	cont (34)	5019	JAPFJE000000000.1
2895	cont (33)	4884	JAPFJD000000000.1
2930	cont (36)	4952	JAPFJC000000000.1
2951	cont (37)	4944	JAPFJB000000000.1
2945	cont (33)	4844	JAPFJA000000000.1
2967	cont (33)	5015	JAPFIZ000000000.1
2968	cont (34)	4940	JAPFIY000000000.1
2969	cont (37)	4941	JAPFIX000000000.1
2971	cont (35)	4943	JAPFIW000000000.1
2974	cont (39)	5124	JAPFIV000000000.1
2975	cont (35)	4941	JAPFIU000000000.1
3454	cont (45)	5205	JAPFIT000000000.1
3492	cont (45)	5203	JAPFIS000000000.1
3610	cont (40)	5199	JAPFIR000000000.1
3614	cont (40)	5129	JAPFIQ000000000.1
NPI1	comp (3)*2	4811	GCA_013154935.1
071316F	cont (85)*2	4923	VTYH00000000.1
L2	cont (40)	5049	JAPFIP000000000.1
L3	cont (40)	5011	JAPFIO000000000.1
L4	cont (36)	4881	JAPFIN000000000.1

L20	cont (37)	5011	JAPFIM000000000.1

*[1]Assembly level: cont (contig), compl (full resolved); *[2] Assemblies from other studies (See references in Table 1)

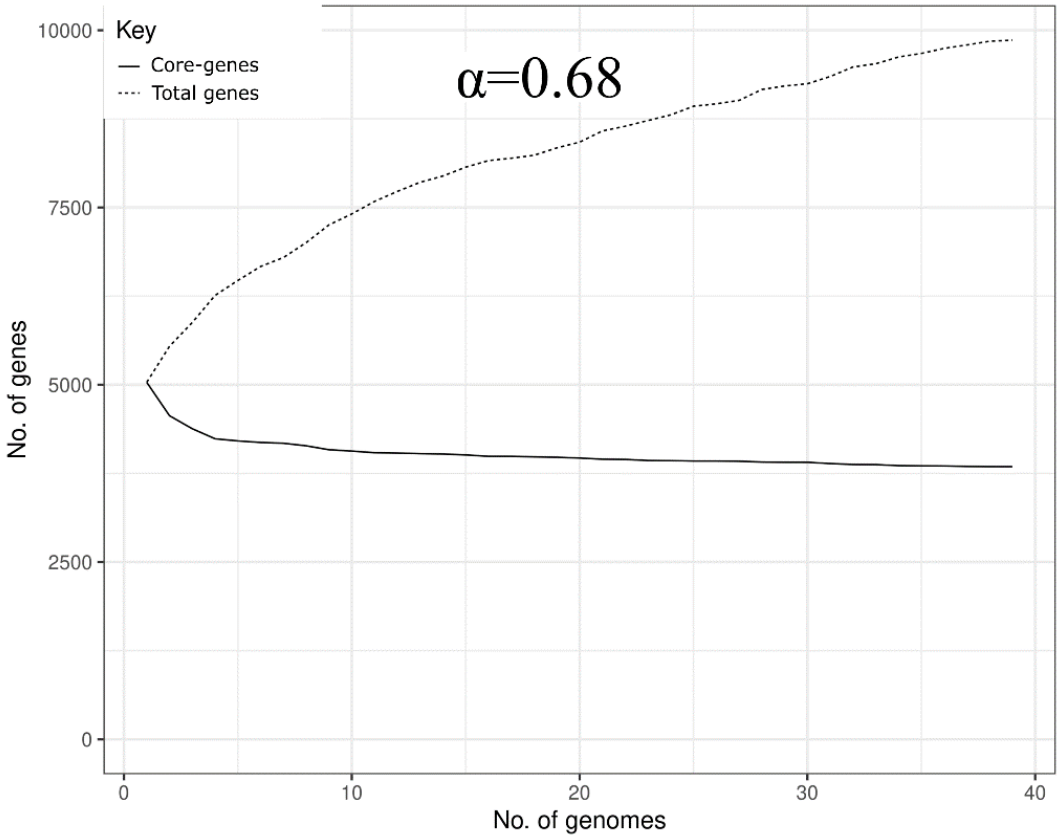

Figure 1.1. Relation between the number of genes (core and total) and the number of genomes. α coefficient value of Heap's Law for conserved curve is shown.

The 69% of the pangenome (n=6781 genes) was accurately assigned to specific COG functions, representing the 61%, 3%, 12% and 24% of the core, shell core, soft, and cloud fractions, respectively (Fig. 1.2C). Core genes were more abundant (>50%) than the accessory genes in most COG categories (Fig. 1.2C) such as “cytoskeleton” (100%), “energy production and conversion” (89%), “inorganic ion transport and metabolism” (81%), “signal transduction mechanisms” (78%), “translation, ribosomal structure and biogenesis” (77%), “amino acid transport and metabolism” (77%), “coenzyme transport and metabolism” (74%), “carbohydrate transport and metabolism” (71%), “nucleotide transport and metabolism” (68%), “function unknown” (66%), “transcription” (64%), “lipid transport and metabolism” (62%), “cell motility” (61%), “posttranslational modification, protein turnover, chaperones” (61%), and “general function prediction only” (56%). The COG functions where accessory genes were predominant (>50%), always involved the cloud category as the most abundant, and included “Cell cycle control, cell division, chromosome partitioning”, “Defence mechanisms”, “Extracellular structures”, “Intracellular trafficking, secretion, and vesicular transport”, “Mobilome: prophages, transposons”, “Replication, recombination and repair” and “Secondary metabolites biosynthesis, transport and catabolism” (Fig. 1.2C).

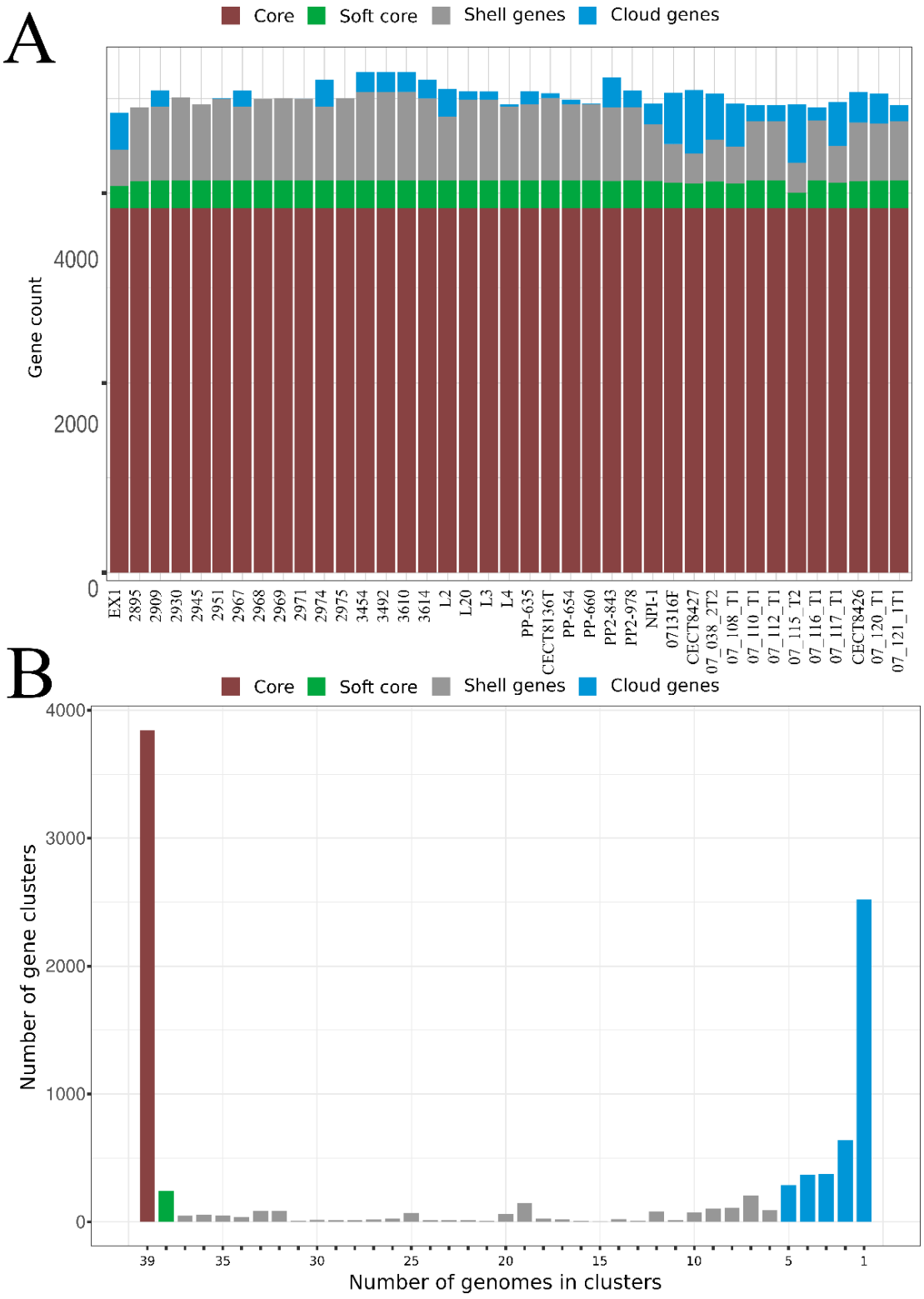

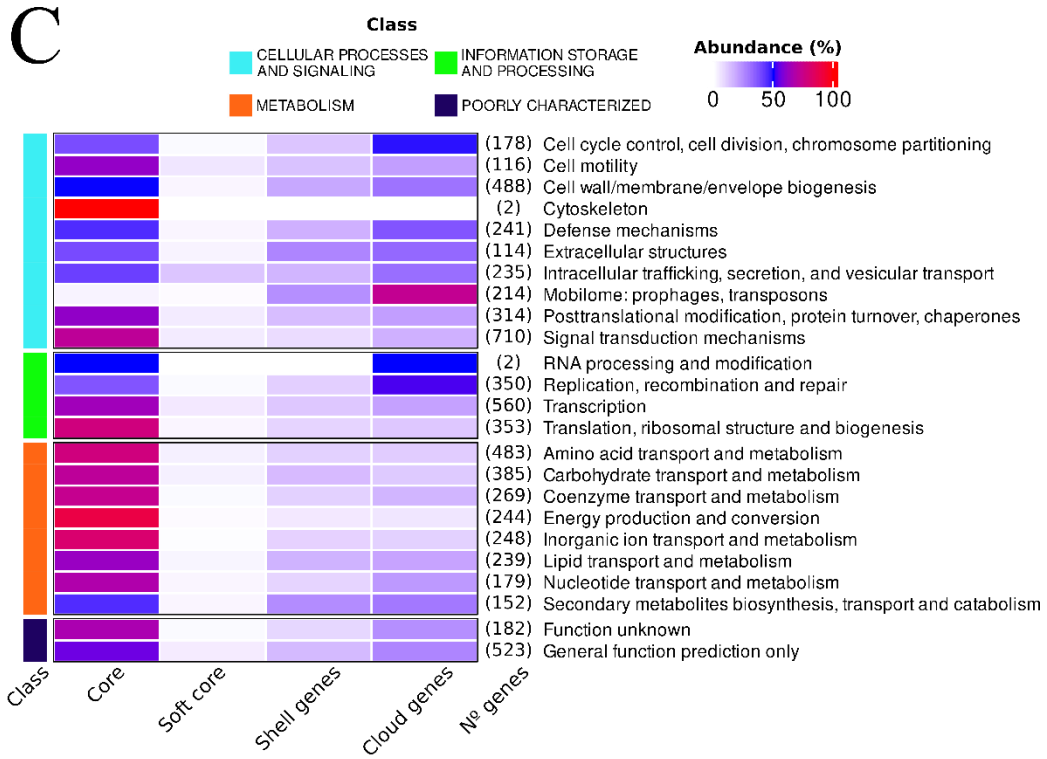

Figure 1.2. Main features of the *V. europaeus* pangenome. (A) Gene fraction (core, shell core, soft and cloud) profiles. (B) Frequency distribution of gene clusters throughout the pangenome. (C) Percentage of genes related with COG general functions found in core, soft core, shell, and cloud fractions of pangenome.

Differences in the number of RNA coding genes were found between the six chromosome-level assembled genomes and the Illumina's assemblies. Among the Illumina assemblies, tRNAs ranged from 88 (071316F) to 122 (CECT8427) (Table 1.3) with an average of 106 tRNAs/genome. However, the six highly contiguous chromosome-level assembled genomes encoded the highest number of tRNAs, ranging from 118 tRNAs (CECT8136 and NPI-1) to 122 tRNAs (CECT8427), (Table 1.3). Furthermore, rRNAs from Illumina assemblies displayed a lower copy number (1 copy for 16S rRNA, 1-4 copies for 5S rRNA and 1-2 for 23S rRNA) than the fully resolved genomes (9-10 copies for 16S rRNA, 10-11 copies for 5S rRNA and 9-10 copies for 23S rRNA) (Table 1.4).

Table 1.3. tRNAs found from the *V. europaeus* genomes used in this study. Strains with fully resolved genomes are marked with asterisks.

Strain	tRNAs decoding Standard 20 AA	tRNAs with undetermined/unknown isotypes	Predicted pseudogenes	Total tRNA
07/038 2T2	101	2	3	106
07/108 T1	100	1	0	101
07/110 T1	106	1	0	107
07/112 T1	106	0	0	106
07/115 T2	107	0	1	108
07/116 T1	107	0	0	107
07/117 T1	102	1	1	104
07/120 T1	101	0	2	103
07/121 1T1	108	1	0	109
071316F	85	0	3	88
2895	104	2	0	106
2909	97	1	2	100
2930	97	3	1	101
2945	98	2	0	100
2951	100	3	0	103
2967	100	1	1	102
2968	101	3	0	104
2969	101	2	0	103
2971	105	3	1	109
2974	97	1	1	99
2975	101	3	0	104
3454	95	2	0	97
3492	102	3	0	105

3610	99	3	0	102
3614	102	3	0	105
CECT8136T*	116	2	0	118
CECT8426*	119	0	2	121
CECT8427*	121	0	1	122
EX1*	118	0	1	119
L2	101	2	1	104
L20	97	3	0	100
L3	100	3	1	104
L4	103	3	0	106
NPI-1*	116	1	1	118
PP2-843*	119	1	1	121
PP2-978	102	1	2	105
PP-635	100	3	0	103
PP-654	100	2	0	102
PP-660	100	3	0	103

Table 1.4. rRNAs found from the *V. europaeus* genomes used in this study. Strains with fully resolved genomes are marked with asterisks.

Strain	16S rRNA	5S rRNA	23S rRNA
07/038 2T2	1	2	1
07/108 T1	1	3	1
07/110 T1	1	3	1
07/112 T1	1	3	1
07/115 T2	1	1	1
07/116 T1	1	3	1
07/117 T1	1	2	1
07/120 T1	1	1	1
07/121 1T1	1	2	1
071316F	1	1	1
2895	1	2	1
2909	1	3	1
2930	1	2	1
2945	1	2	1
2951	1	3	1
2967	1	2	1
2968	1	3	1
2969	1	2	1
2971	1	2	1
2974	1	2	1
2975	1	4	2
3454	1	2	1
3492	1	2	1
3610	1	2	1
3614	1	2	1
CECT8427*	10	11	10
CECT8136T*	9	10	9
CECT8426*	10	11	10
EX1*	10	11	10
L2	1	2	1
L20	1	3	1
L3	1	2	1
L4	1	2	1
NPI-1*	9	10	9
PP2-843*	10	10	10
PP2-978	1	3	1
PP-635	1	2	1
PP-654	1	3	1
PP-660	1	2	1

1.2.2 Phylogeny and genetic differentiation between strains

The phylogenomic tree based on the concatenated sequences of the core-genes showed a topology with three main branches containing a total of eight robust clusters (boostrap value=100; terminal or sub terminal branches distance > 0.006): branch I (cluster I), branch II (cluster II) and branch III (clusters III-VIII), being clusters I and II differenced in sub clusters (boostrap value=100; terminal branches distances from 0.0003 to 0.0025) (Fig. 1.3). Cluster I was the largest group (n=25 strains), and it was exclusively constituted by Spanish strains distributed in two sub-clusters (Ia=19 strains; Ib=6 strains) (Table 1.1). These strains were isolated from two Spanish hatcheries (Hatchery B=23 strains; Hatchery E=2 strains), in different years (2001, 2008, 2011 and 2018) and from a broad host range (Table 1.1) covering all stages of the bivalve life stages including eggs (*R. decussatus*), larvae (*O. edulis*, *R. decussatus*, *D. trunculus*, *P. rhomboides* or *E. arcuatus*), spat of (*R. philippinarum*) and adults (*R. decussatus*) and directly from the seawater associated to culture tanks.

These phylogenetic relationships were supported by ANIb values (Fig. 1.4), higher than 0.979 in all pairwise comparisons, and around 0.995 for the strains belonging to the same cluster including between closely related sub-clusters.

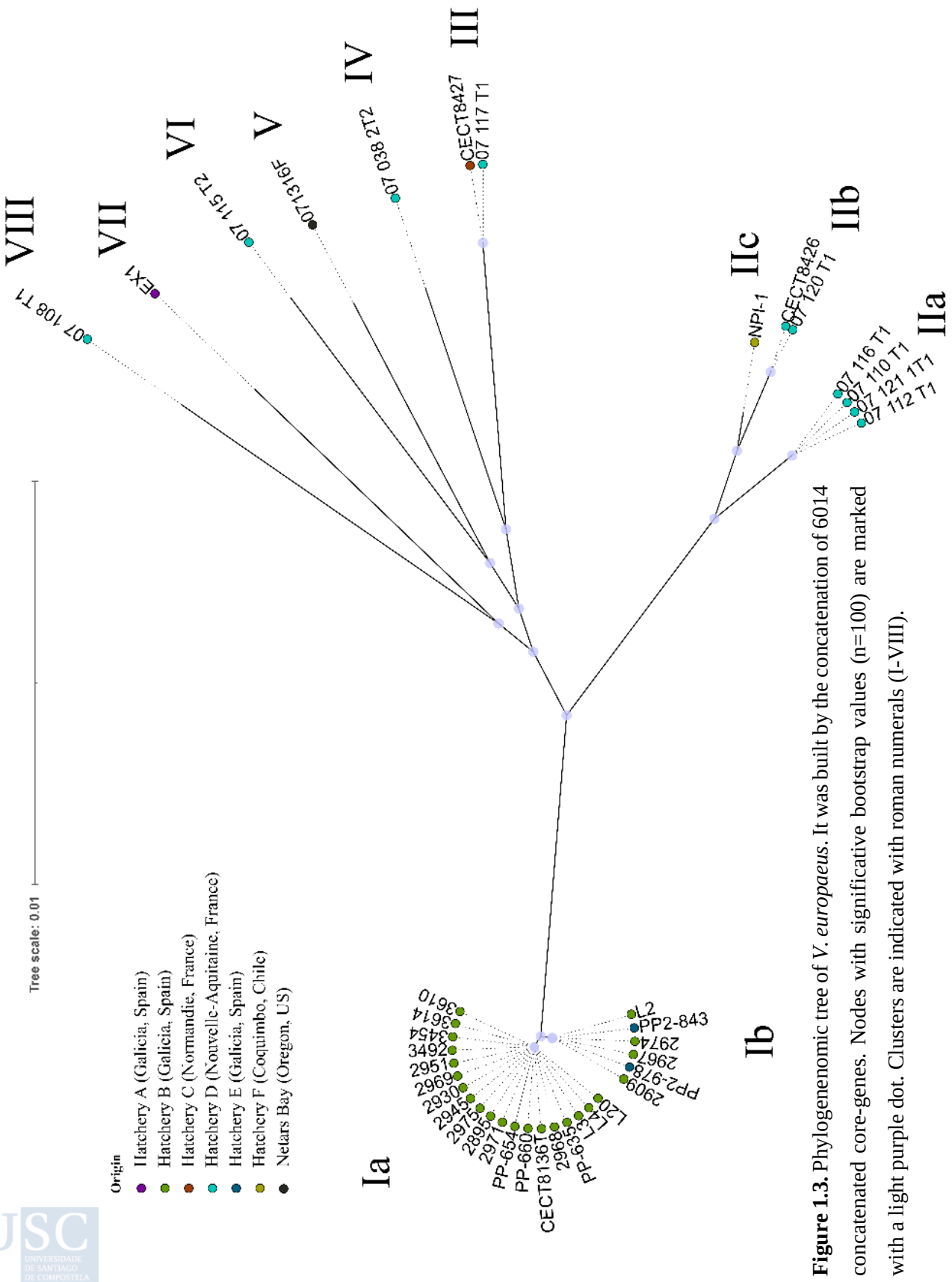

Figure 1.3. Phylogenenomic tree of *V. europaeus*. It was built by the concatenation of 6014 concatenated core-genes. Nodes with significative bootstrap values (n=100) are marked with a light purple dot. Clusters are indicated with roman numerals (I-VIII).

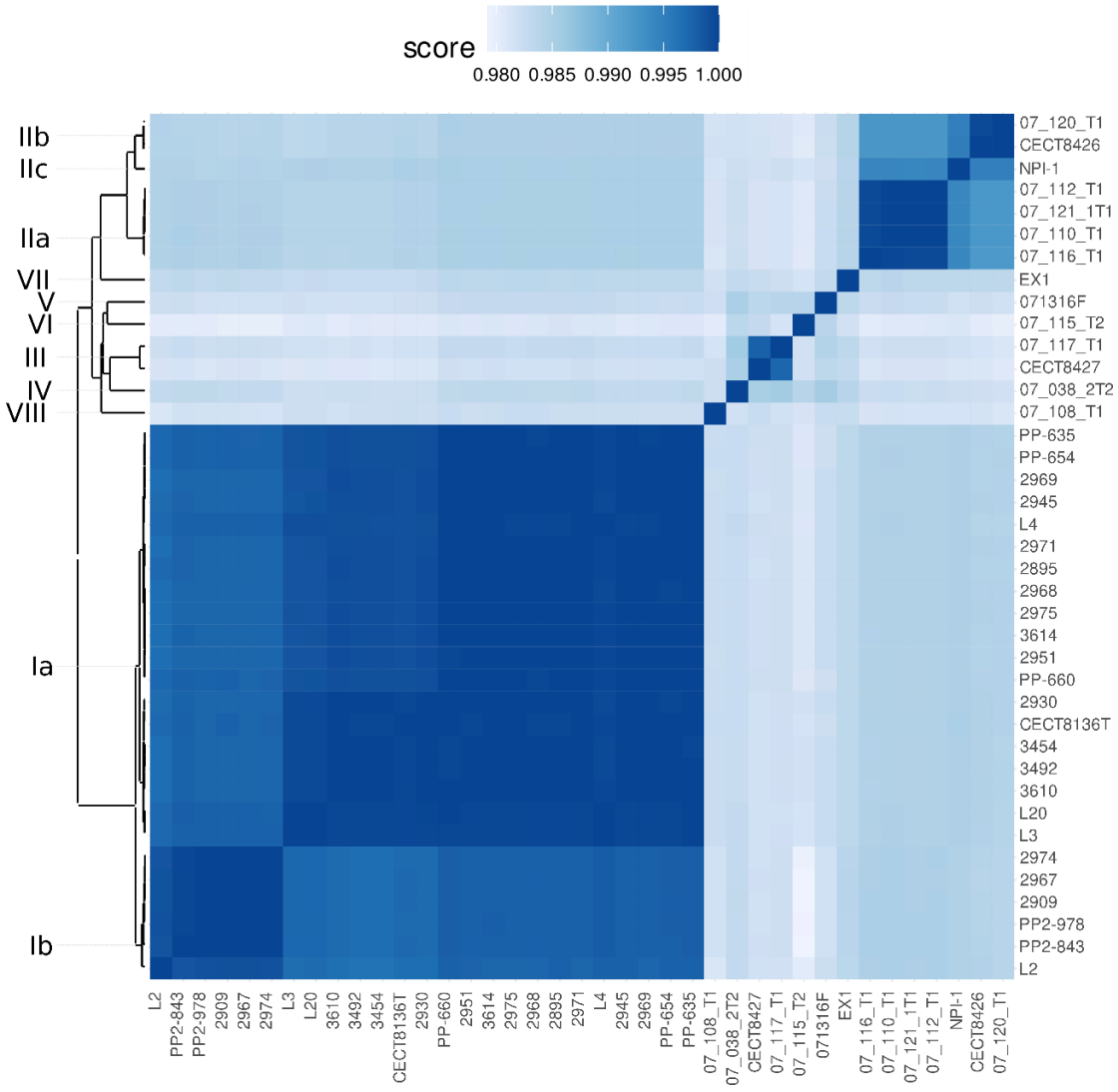

Figure 1.4. ANI heatmap of *V. europaeus* strains with hierarchical clustering.

A complementary analysis to establish genetic differentiation and diversity within and between clusters and strains was done using the SNPs detected in the coding regions of the genomes of the 39 strains. According to this analysis (Fig. 1.5A), the genetic diversity within sub-clusters was low including a maximum of 197 SNPs among the strains belonging to the sub-cluster Ia (CECT8136T vs. 2968) and 162 SNPs to the sub-cluster Ib (2974 vs. L2), and more than 2300 SNPs between those sub-clusters. Based on the core-genome SNP dataset, some clonal strains could be identified coming from: (i) the same bivalve species culture (not necessarily in the same sampling date) in the sub-cluster Ia (3454 and 3492, 0 SNPs; 2895, 2930, 2945, 2951, 2969, 2971 and 2975: 1-2 SNPs; (i) L3 and L4: 5 SNPs; and PP-654 and PP-660: 1 SNP) and sub-cluster Ib (2909, 2974 and 2967: 1 SNP; and PP2-843 and PP2-978: 14 SNPs); (ii) from broodstock to the offspring after spawning: 0 SNPs, 3610/3614 (Table 1.1); (iii) different hatcheries, hosts and/or dates (Table 1.1), for example: 3 SNPs between PP2-978 and 2909/2974/2967; 5 SNPs between L20 and L3/L4; 1 SNP between 3454/3492 and 3610/3614; 5 SNPs between 2895/2930/2945/2951/2969/2971/2975 and 3454/3492 or 6 SNPs with 3610/3614; 19 SNPs between PP-654/PP-660 and L20, L3 and L4. In contrast, there were SNP differences among strains isolated from the same sampling despite they were assigned to the same sub-cluster, such as 89 SNPs between PP-635 and PP-660/PP-654 or 146 SNPs between PP-635 and CECT8136; and (118 SNPs between 2968 and 2895/2930/2945/2951/2969/2971/2975).

EX1, the only Spanish strain located out of cluster I, constituted a well-differentiated group in the branch III (cluster VII; Fig. 1.3). EX1 was the oldest *V. europaeus* strain (year=1985) and the unique isolated from the Spanish Hatchery A (Table 1.1).

Despite the same origin of most French strains (n=10/11; Table 1.1), they exhibited much more genetic diversity than the Spanish strains (Fig. 1.3), being distributed in six different clusters: branch II (cluster II=sub-clusters IIa, IIb and IIc) and branch III (clusters III, IV, VI and VIII). Within the cluster IIa, the strains 07/110 T1, 07/112 T1, and 07/121 T1 were nearly clonal (<2 SNPs), and they were differentiated by >55 SNPs with the strain 07/116 T1 (Fig. 1.5B). Within the sub-cluster IIb, 28 SNPs were found between the strain 07/120 T1 and CECT8426 (Fig. 1.5B). Cluster III (Fig. 1.3) was formed by two strains (07/117 T1 and CECT8427) from two different origins (Hatchery

D and Hatchery C, located in Nouvelle-Aquitaine and Normandy respectively) and hosts (*C. gigas* spat and the non-bivalve species *H. tuberculata*) and 182 SNPs were identified among them (Fig. 1.5B). Other strains isolated from Hatchery D (07/138 2T2, 07/115 T2 and 07/108 T1) constituted by themself independent clusters (clusters IV, VI and VIII) supported by differences of more than 50k SNPs with their contemporary strains belonging to sub-cluster IIa, IIb and cluster III (Fig. 1.5B).

Despite the Chilean strain NPI-1 was closely related to sub-cluster IIb, it constituted an independent group (sub-cluster IIc; Fig. 1.3) supported by a difference of 11.208 SNPs (Fig. 1.5B).

The American strain 071316F was the only one non-isolated from a hatchery environment and it also grouped in an independent cluster (cluster V), sharing a node with the French strain 07/115 T2 (Fig. 1.3).

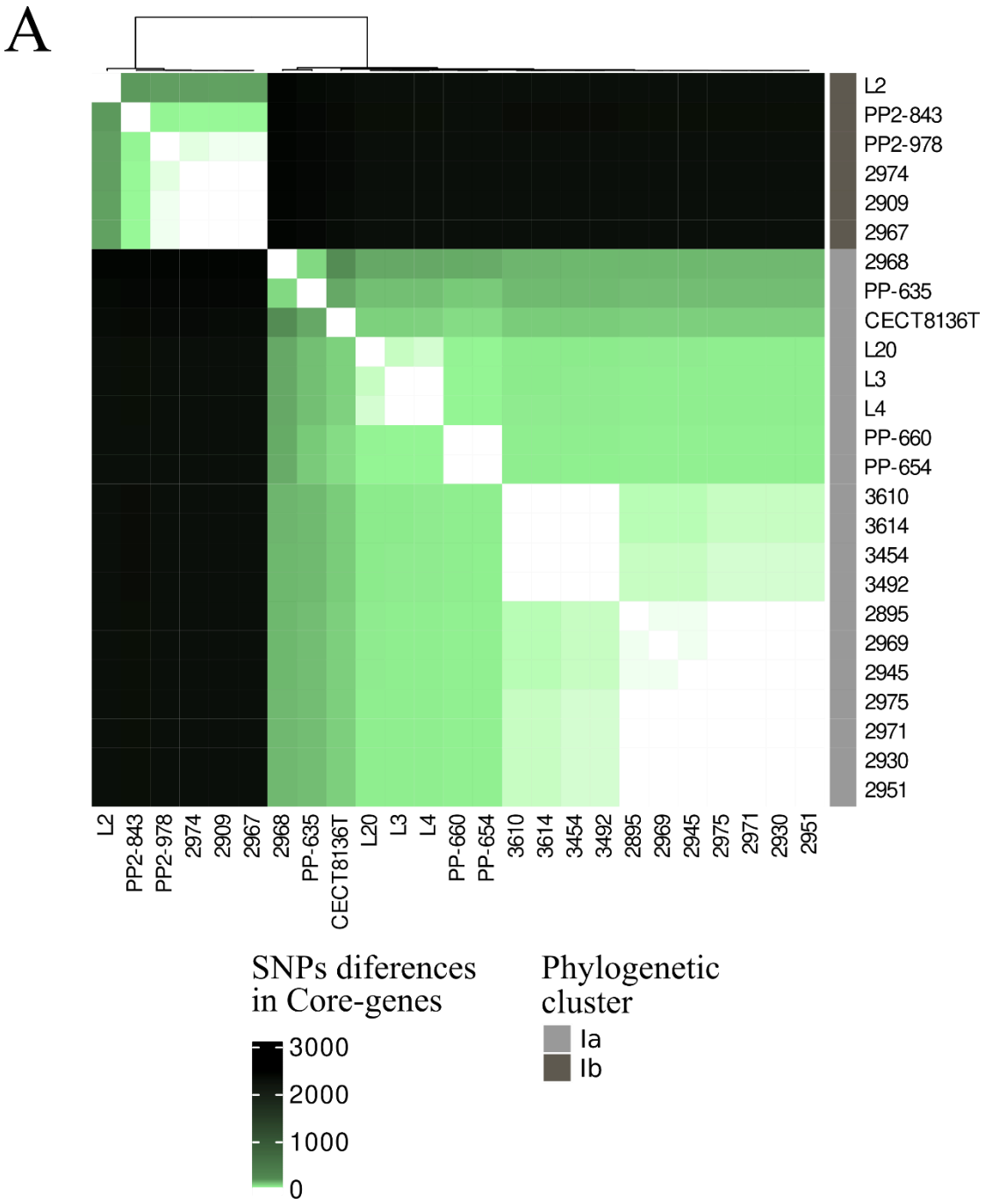

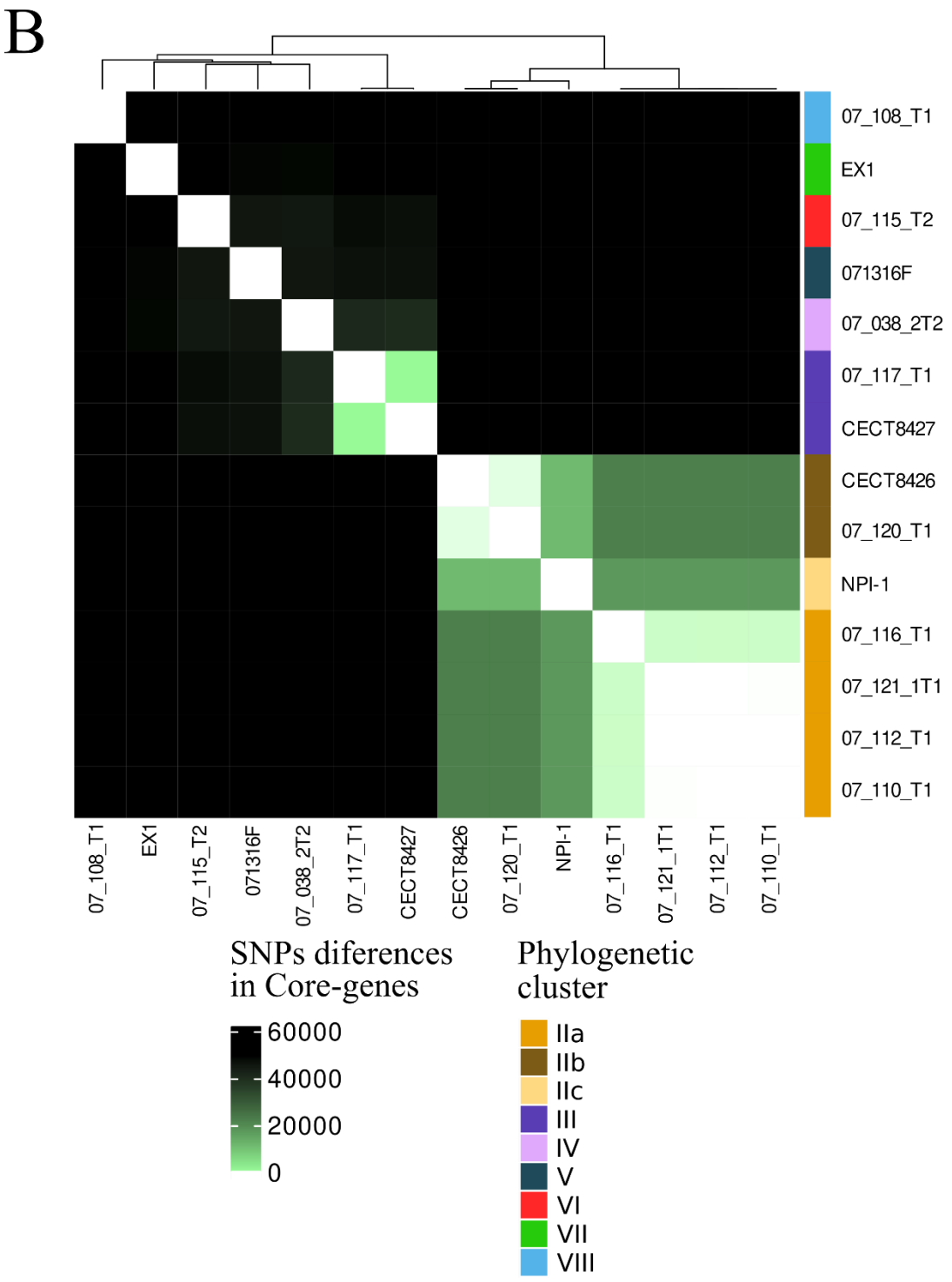

Figure 1.5. Heatmaps showing the genetic variability represented as SNP differences in core-genes of *V. europaeus* strains belonging: (A) Sub-clusters Ia and Ib; (B) Clusters from II to VIII. In both heatmaps, phylogenetic clusters and sub-clusters of the strains are shown in the right bar.

Analysis of the accessory genes encoded by different strains revealed a clustering similar with the clusters established through the core genome phylogeny (Fig 1.6A).

PCA of the accessory genes revealed a higher variability within the same cluster than the observed from the core genome clusters (Fig. 1.3 and 1.6B), This is the case of the strains of the phylogenetic subcluster Ia, which showed some specific gene blocks of the accessory genome, but, at the same time, homogeneous within clades; see for instance the clades (2930, 2969, 2975, 2951, 2971, 2895, 2945) vs (PP-654, PP-660); or the specific block in the subcluster Ib of the clade constituted by strains PP2-843 and 2974 vs (2967, 2909, PP2-978) (Fig 1.6A and B).

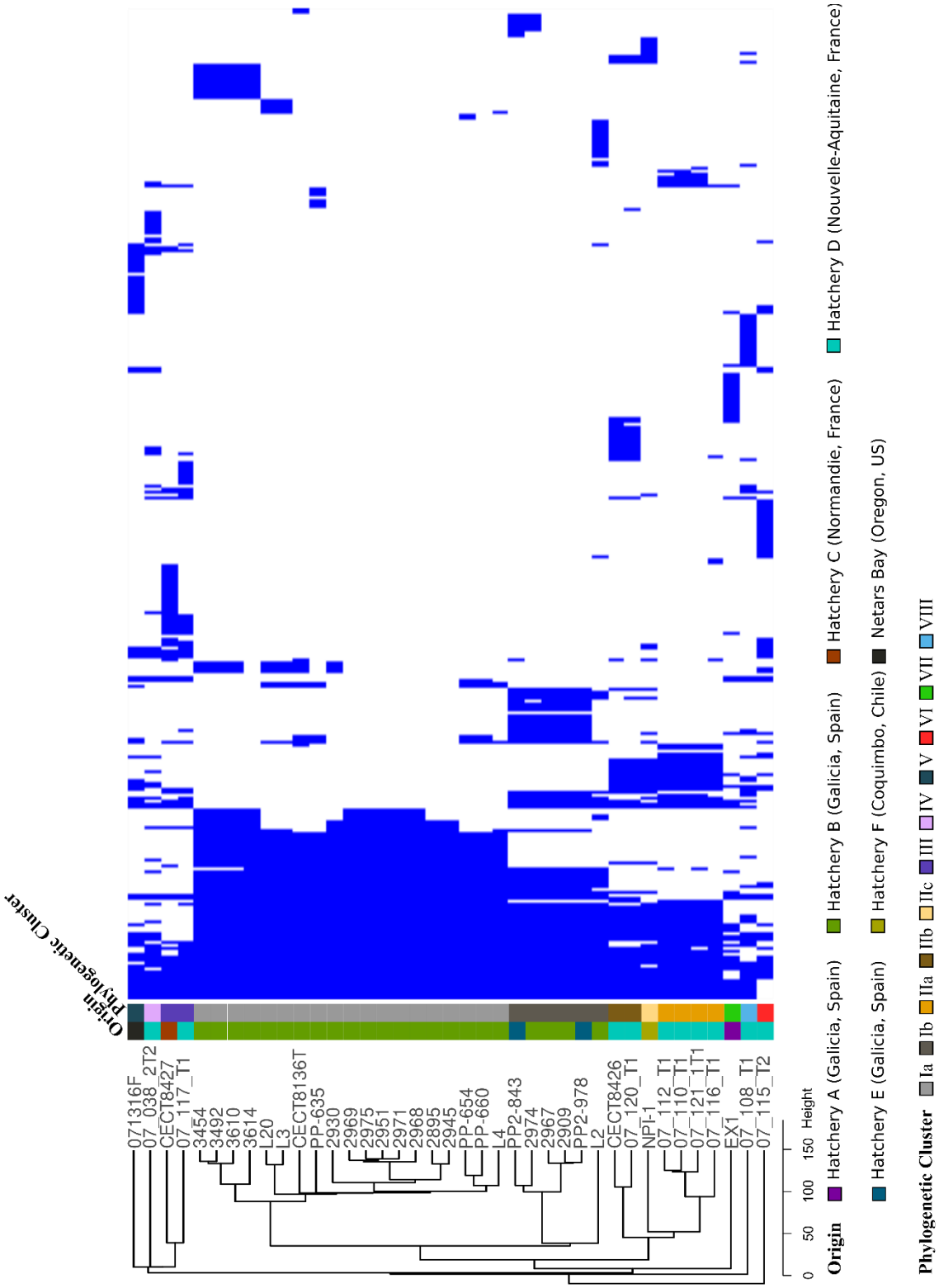
Origin
Phylogenetic Cluster
071316F
07_038_2T2
CECT8427
07_117_T1
3454
3492
3610
3614
L20
L3
CECT8136T
PP-635
2930
2969
2975
2951
2971
2968
2895
2945
PP-654
PP-660
L4
PP2-843
2974
2967
2909
PP2-978
L2
CECT8426
07_120_T1
NPI-1
07_112_T1
07_110_T1
07_121_1T1
07_116_T1
EX1
07_108_T1
07_115_T2
0 50 100 150 Height
Origin
Hatchery A (Galicia, Spain)
Hatchery B (Galicia, Spain)
Hatchery C (Normandie, France)
Hatchery D (Nouvelle-Aquitaine, France)
Hatchery E (Galicia, Spain)
Hatchery F (Coquimbo, Chile)
Netars Bay (Oregon, US)
Phylogenetic Cluster
Ia
Ib
IIa
IIb
IIc
III
IV
V
VI
VII
VIII

B

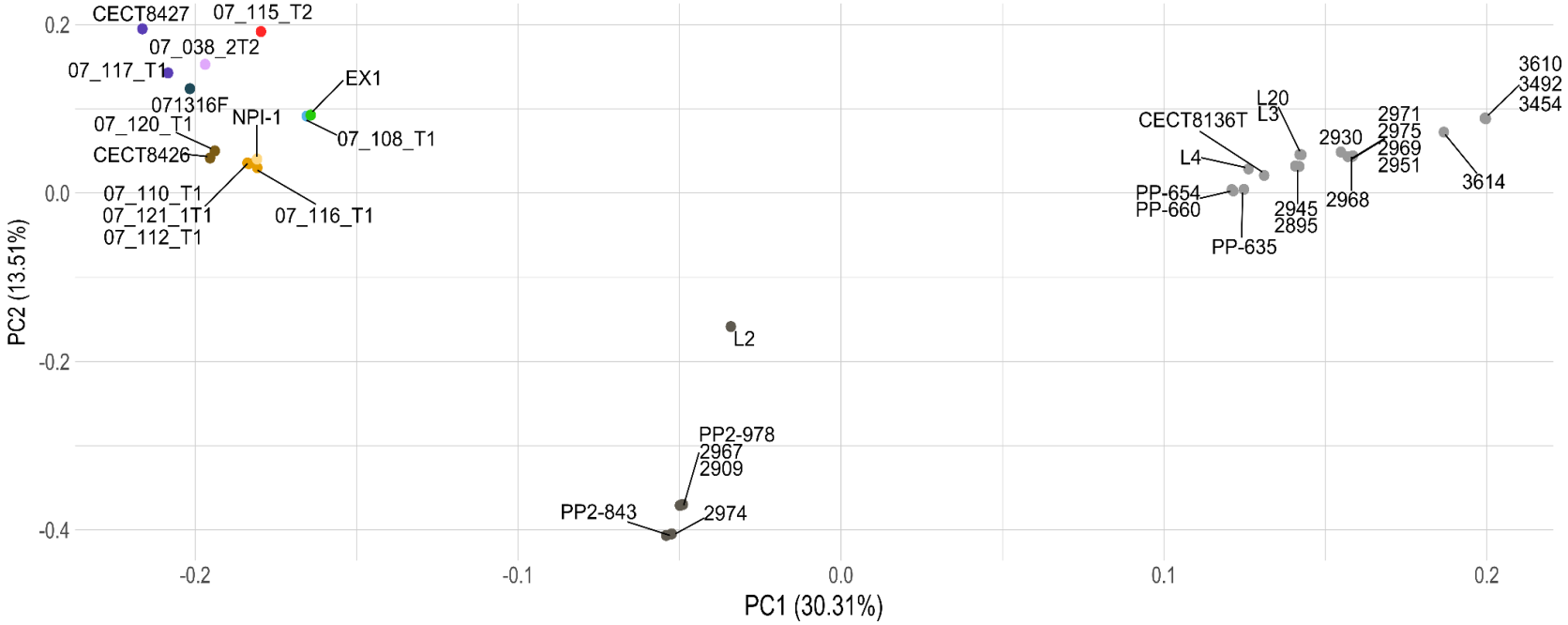

Fig 1.6. Pangenome analysis of *V. europaeus* accessory genomes. (A) Presence/absence matrix showing the *V. europaeus* accessory genomes profiles. (B) PCA of the accessory genes profiles. Strains are sorted according to the dendrogram plotted to the left.

1.3 Discussion

As pangenome metrics fits to a dynamic adaptative model, large pangenome size might be associated with the ability to colonize new ecological niches, as well as reflect high effective population sizes (Maistrenko et al. 2020). Pangenomes for species of the genus *Vibrio* show a broad size range (Dias et al. 2018; Hansen, Kudirkiene, and Dalsgaard 2020; Guardiola-Avila et al. 2021; Zheng et al. 2022; Du et al. 2022) reflecting high genomic diversity within the genus, which matches with its well-known ecological diversity (Nathamuni et al. 2019; Sampaio et al. 2022). The pangenome of *V. europaeus* comprehends 9860 genes, which is comparable to other *Vibrio* pangenomes such as the multi host pathogens *V. anguillarum* (9537 genes) and *V. tapetis* (11213 genes) (Dias et al. 2018; Hansen, Kudirkiene, and Dalsgaard 2020).

Since the core genome size differs between prokaryotes groups, the percentage of core genes in the pangenome seems to be strongly related to their evolutionary history and lifestyle. Thus, free-living species with high degree of dispersion have a small proportion of core genomes (McInerney, McNally, and O'Connell 2017). *V. europaeus* exhibits a higher proportional core genome (39.00%) than other marine broad host-range *Vibrio* pathogens, such as *V. anguillarum* (28.24%) and *V. tapetis* (29.90%) (Dias et al. 2018; Hansen, Kudirkiene, and Dalsgaard 2020). In addition, it is noteworthy that this percentage is significantly higher than that observed in the human and marine pathogen *V. fluvialis* (15.36%) (Zheng et al. 2022). The proportion of core genes of *V. europaeus* aligns with its apparently restricted mollusc host range (Lodeiros et al. 1987; Mersni-Achour et al. 2014; Prado, Dubert, and Barja 2015; Dubert et al. 2017; Rojas et al. 2021).

V. europaeus strains were isolated from environments associated to mollusc hatcheries. Bacteria circulate among production compartments within the hatcheries, and there is also an external influx of bacteria from either the broodstock, open waters or the phytoplankton used as food (Dubert, Barja, and Romalde 2017b). Also, environmental conditions, particularly the elevated levels of organic matter, contribute to the development of microbial communities within mollusc hatcheries (Timmins-Schiffman et al. 2021; Ishaq et al. 2023). These environments favour species with a high capacity to acquire exogenous DNA, which implies high rate of horizontal gene transfer as *V. europaeus* and other opportunistic bacterial species (Mira 2010; Rouli et al. 2015).

From a functional perspective, it is remarkable that most of the pangenome COG functions assigned to *V. europaeus* genes were associated with core genes, reflecting the presence of basal functions of the species in the core genome. Gene functional profiles of the pangenome fractions is conserved across bacterial species, being the core genome enriched in niche-related functions while the accessory genome in specialized functions (Hyun, Monk, and Palsson 2022).

A substantial difference on the abundance of structural RNAs (tRNA and rRNA) were found between the six long-read sequencing assemblies and those sequenced with short-read Illumina technology. The six chromosome-level assembled genomes showed the highest number of RNAs, probably due to the limitations of short-read to identify different genes of the same family, especially if they are tandemly arranged (Miyamoto et al. 2014).

The capacity of a pangenome to reflect the full genomic diversity of a species is limited by the number and nature of strains employed for its construction, and it should be evaluated when comparing pangenomes of different species (Andrey et al. 2011). Analysis of the core genome allowed to evaluate the evolutionary history and intraspecific diversity of *V. europaeus*. For example, the Spanish strains belonging to phylogenetic sub-clusters Ia and Ib displayed a lower genetic variability in core genes than the French strains. Similarly to what was described for the radiation event of the clonal type of the bacterium *V. parahaemolyticus* Sequence Type 3 by Campbell et al. (2024), we can assume that those Spanish populations came from a monophyletic radiation event, and that it was recently dispersed artificially or naturally throughout the hatcheries under study (Hatchery B and E). In contrast, French strains exhibited a higher variability than the Spanish strains, even though the geographical and temporal distribution of its isolation were more restricted (10/11 in Hatchery D in 2007). In the case of Chilean strain NPI-1, its closeness to strains of sub-cluster IIb strongly suggest an intercontinental transference of *V. europaeus*, probably mediated by the anthropic movement of mollusc spats, broodstoks or phytoplankton stocks.

In addition, the monitoring of the clonal strains in Hatchery B allowed to hypothesize the potential reservoir of this bacteria in the hatchery. Broodstock, phytoplankton or seawater are proposed as key players in the *Vibrio* dissemination within the hatchery environment (Dubert et al., 2017). Strain 3610 was isolated from *R.*

decussatus broodstock conditioned a constant temperature and continuously fed with a mixture of phytoplankton produced in the hatchery (Dubert et al., 2015; 2016). For the spawning induction, those broodstocks were placed in a tray with UV-sterilized seawater and additional stimuli were provided by adding gametes stripped from one of the conditioned bivalves and mixture of phytoplankton (Dubert et al., 2016). After fertilization, the embryos were transferred to larval culture tanks filled with filtered UV-irradiated seawater and no food was supplied during embryo incubation. Thus, a vertical transmission of clonal strains (SNPs=0) was demonstrated from *R. decussatus* broodstock (strain 3610) to eggs (strains 3614) (Fig. 1.7), discarding in this case other potential sources of bacterial contamination such as the seawater tank or food. Then, how could *V. europaeus* colonize those broodstocks? The hypothesis for which *V. europaeus* form part of the regular microbiota is discarded because it was only isolated from the broodstock fed with the mixture of phytoplankton but not from those depurated with seawater in absence of food (Dubert et al., 2016). It is important to remark that the same phytoplankton diet based on a mixture of *Isochrysis galbana*, *Diacronema lutheri*, *Tetraselmis suecica*, *Chaetoceros* sp. and *Skeletonema marinoï* was previously supplied to other larval cultures reared in May'11 and May-June'12 (Dubert et al., 2017) from which some clonal strains (1-6 SNPs) to the isolates 3610/3614 were isolated (Fig. 1.7). Thus, we hypothesized that phytoplankton is the main source of *V. europaeus* to the larval cultures, directly supplied to the larval tanks as food or by a vertical transmission from broodstock previously feed with this mixture of phytoplankton. Once in the larval tank, *V. europaeus* could survive the water changes forming biofilms on the inner tank as reported with other *Vibrio* pathogens (Prado et al., 2014). Also, the exchange of phytoplankton stocks and broodstock among hatcheries can justify the finding of clonal strains in different Spanish hatcheries.

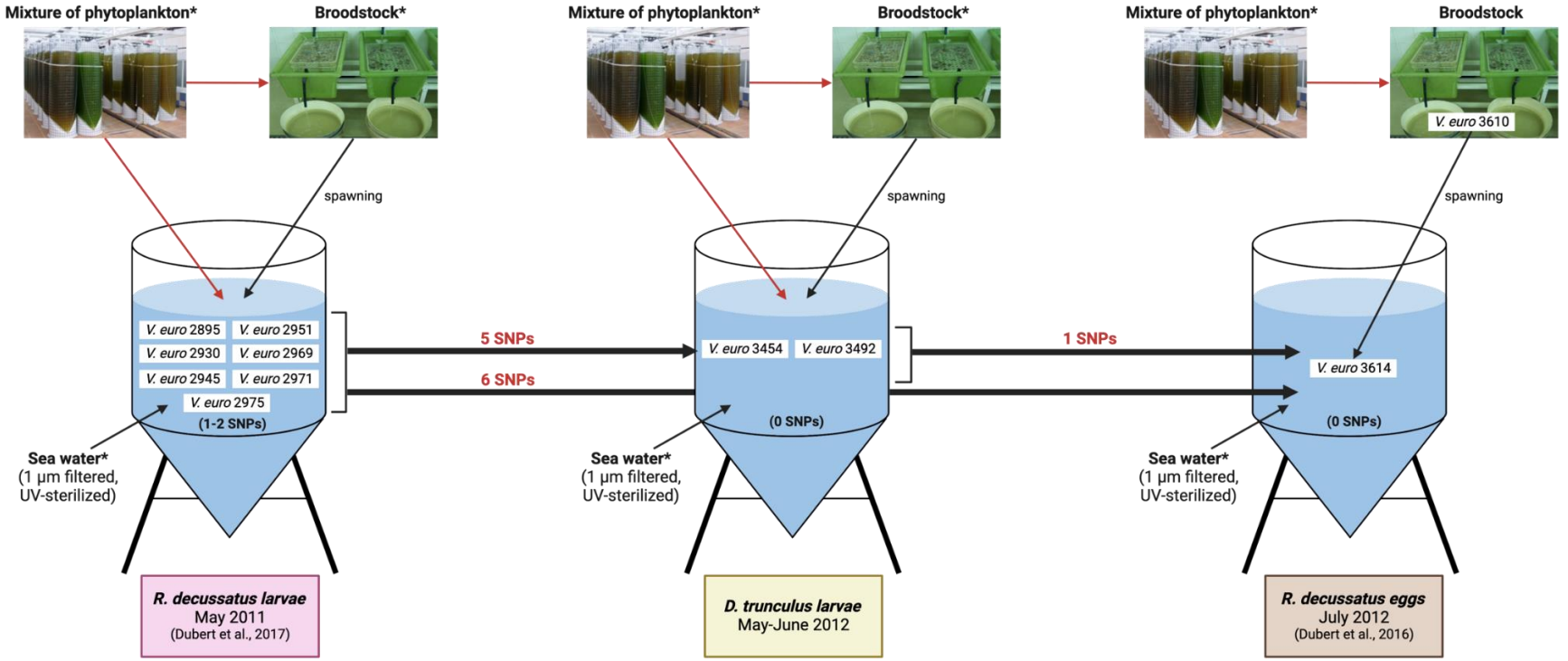

Fig 1.7. Hypothesis about the *V. europaeus* source to larval cultures from the clonal strains isolated from hatchery B. Broodstock were induced by thermal shock plus addition of microalgae and gonad extracts. Mixture of phytoplankton (*Isochrysis galbana*, *Diacronema lutheri*, *Tetraselmis suecica*, *Chaetoceros* sp. and *Skeletonema marinoi*) was produced in the hatchery and it was used to feed larvae and broodstocks (red line) but not to eggs. SNPs among the contemporary strains were showed in brackets and between the strains isolated from different bivalve cultures on the arrows in red. Asterisks mean no-microbiological samples were taken.

CHAPTER 2: IDENTIFICATION OF *V. europaeus* GENES WITH POTENTIAL IMPACT ON AQUACULTURE ENVIRONMENTS

2.1 Introduction

Among the more than 130 described species of the genus *Vibrio*, several of them are capable of producing mortality outbreaks, commonly known as vibriosis, in bivalve populations, both wild and cultivated (Sanches-Fernandes, Sá-Correia, and Costa 2022). Vibriosis is recognized as one of the main bottleneck affecting early bivalve production, carried out in hatcheries, which means great losses for the industry (Gray et al. 2022). Vibrios are commonly considered as opportunistic pathogens, with differences in their inter and intraspecific virulence (Li et al. 2018; Naknaen et al. 2024). This variability is closely linked to virulence factors (VFs), implied in different infection stages, including those related to adherence, invasion and survival in the environment of the host (Shapiro-Ilan et al. 2005; Le Roux, Wegner, and Polz 2016; Parizadeh et al. 2018; Destoumieux-Garzón et al. 2020). A diverse range of VFs has been identified in *Vibrio* species pathogenic to aquatic animals, including flagellum, biofilm formation, iron uptake, lipopolysaccharides, quorum sensing, secretion systems and enzymes such as proteases, lipases, DNases, chitinases and hemolysins (Frans et al. 2011; Natrah et al. 2011; Osei-Adjei, Huang, and Zhang 2018; B. Yang et al. 2021; Nurhafizah et al. 2021; Choi and Choi 2022; Choi and Choi 2022). Until the present study, some VFs have been identified in *V. europaeus*, such as the metalloprotease VemA, the main protein of the extracellular products, and the T3SS and T6SS (Mersni-Achour et al. 2014; Spinard et al. 2016; Martinez et al. 2022).

The economic losses in the industry caused by vibriosis have led to an indiscriminate use of antibiotics, often as a prophylactic treatment (Baralla et al. 2021; Hossain et al. 2022). This has led to the acquisition of resistance genes, which are easily disseminated among bacteria through horizontal gene transfer mechanisms (Pepi and Focardi 2021). This gene transfer poses a threat to human health, the environment and fisheries, but it also reduces the available treatments for commercial aquaculture putting food safety and nutrition at risk (Schar et al. 2021). The generation of resistance and its associated risks has led to strong regulation by the European Union with the prohibition of chloramphenicols, nitrofurans, and frurazolidone in aquaculture, although the majority of large producers, especially the Asian ones, are not taking

measures in this regard (Lulijwa, Rupia, and Alfaro 2020; Hossain et al. 2022). Numerous species of vibrios isolated from aquaculture environments have been shown to be resistant to antibiotics, including ampicillin, amoxicillin-clavulanic, gentamycin, imipenem, cefotaxime, cefuroxime, meropenem, and trimethoprim/sulfamethoxazole (Nurhafizah et al. 2021; Sanches-Fernandes, Sá-Correia, and Costa 2022; Ferri et al. 2024; Sharma et al. 2024). Previous studies found no antibiotic resistance in two French strains of *V. europaeus* (CECT8426 and CECT8427) being sensitive to flumequine, erythromycin, chloramphenicol, gentamicin, kanamycin, tetracycline, sulphamethoxazole/trimethoprim, streptomycin, sulfonamides, and trimethoprim (Mersni-Achour et al. 2014).

As alternatives to the use of antibiotics, some microorganism-based therapies have been proposed as an eco-friendly alternative to prevent or treat vibriosis in aquaculture. This is the case of phage therapy, which has been tested in the laboratory against pathogens such as *V. alginolyticus*, *V. coralliilyticus*, and *V. tubiashii* (Kalatzis et al. 2018; Doron et al. 2018; Richards et al. 2021; Liu et al. 2022). However, phage therapy presents practical problems for its application. One of these problems is the existence of a bacterial immune system, composed of multiple defence systems with a variety of mechanisms (Doron et al. 2018; Chevallereau and Westra 2022; Hochhauser, Millman, and Sorek 2023). These systems are highly dynamic, boosting an arm-race through a co-evolution between bacteria and phages that implies the appearance of resistance by the host and new survival strategies by the phages (R. Liu et al. 2022; Murtazalieva et al. 2024). A deep understanding of the immune response to phages will be critical for advancing phage therapy, potentially leading to the discovery of new biological mechanisms (Federici, Nobs, and Elinav 2021).

The aim of this Chapter was to annotate the genes of the *V. europaeus* pangenome and to determine its affiliation to the core or accessory genome. This allowed: (i) to evaluate the role of those genes over the virulence, production of secondary metabolites or the resistance to potential preventive treatments such as antibiotic or phage therapy; and (ii) to study the genetic variability among *V. europaeus* strains based on the analyses of the annotated-genes associated to the accessory genome.

2.2 Results

2.2.1 Pathogenicity of *V. europaeus*: infection challenges and virulence factors

According to the virulence challenges, all the *V. europaeus* strains tested (n=38) were virulent against Manila clam juveniles. Survival rates ranged from 0-7% in most cases (32/38 strains), 22-27% for 3/38 strains (CECT8427, 07/116 T1 and 2967) and 9-16% for 3/38 strains (07/121 1T1; 2968 and 2969) (Fig. 2.1A).

A total of 231 genes (Fig. 2.1B; Table 2.1) were identified as putative virulence factors from the *V. europaeus* pangenome and they were distributed in 15 virulence factor classes (VFC1-15) (Fig. 2.1B and C). The 75% of the virulence factors (Fig. 2.1B and C) were assigned to three classes (VFC 14, secretion systems; VFC 5, chemotaxis and motility; VFC 2, adherence) and the remaining ones (VFC 1, 3, 4, 6-13 and 15) harboured each less than 6%, ranging from 5.6% (toxins, VFC 13) to 0.4% (VFC classes constituted by one gene: VFC 4, biofilm formation; VFC 8, glycosylation system; VFC 11, nutritional factors).

Among these genes, 59.3% (n=137) were assigned to the core genome (Fig. 1B and 1C). Core virulence genes were found in the most abundant VFC and were related to: (i) VFC 1, acid resistance: urease (*ure*B and *ure*G); (ii) VFC 2, adherence: mannose-sensitive hemagglutinin (MSHA) type IV pilus (*mshA*-H, *msh*J, *msh*L-M), type IV pilus (*pil*B and *pil*D) and tad locus (*tad*A and *tad*A2); (iii) VFC 3, antiphagocitosis: capsular polysaccharide (*wbf*U, *wbf*V and *wbf*Y); (iv) VFC 4, biofilm formation: AdeFGH efflux pump/transport autoinducer (*ade*G); (v) VFC 5, chemotaxis and motility: flagella (*che*A, *che*B, *che*R, *che*V, *che*W, *che*Y and *che*Z; *fil*M; *fla*A-G and *fla*I; *flg*A-M; *flh*A, *flh*B, *flh*F and *flh*G; *fli*A, *fli*D-J, *fli*L and fliN-S; *flr*A-C; *mot*A-B and *mot*X-Y); (vi) VFC 7, enzymes: metalloproteinases (*vem*A and *prt*V) and collagenases (*col*A and *col*P); (vii) VFC 10, iron uptake: enterobactin (*vct*A) and heme receptors (*hut*A) and periplasmic binding protein-dependent ABC transport systems (*vct*C, *vct*D, *vct*G and *vct*P); (viii) VFC 13, quorum sensing: autoinducer 1 (*cqs*A) and 2 (*lux*S); (ix) VFC 14, secretion systems: type 2 secretion system (T2SS; *eps*C-M), VAS type 6 secretion systems (T6SS; *vas*A-K; tssE; *imp*B/*vip*A and *imp*C/*vip*B; *hcp* and PAAR repeat protein); (x) VFC 15, toxins: thermostable direct hemolysin (*tlh*), phytotoxin coronatine, hemolysin (*hly*III) and other five hemolysins. In contrast, some VFC such as endotoxins (VFC 6), glycosylation system (VFC 8), immune evasion (VFC 9), nutritional factors (VFC 11) and others (VFC 12) did not contain any gene assigned to the core-genome.

Table 2.1. Virulence factors found in *V. europaeus* pangenome. Core virulence-related genes were indicated in bold. Virulence factor classes (VFCs) are numbered according to Fig. 2.1.

VFclass	Virulence factors	Related genes
Adherence (VFC 2)	Mannose-sensitive hemagglutinin (MSHA type IV pilus)	*mshA*, *mshB*, *mshC*, *mshE*, *mshG*, *mshH*, *mshI*, *mshJ*, *mshK*, *mshL*, *mshM*, *mshN*.
	Type IV pilus	*pilA*, *pilB*, *pilC*, *pilD*.
	Curli fibers(*Escherichia*)	***csgG***
	LPS-O-antigen (P. aeruginosa)(*Pseudomonas*)	*tviB*, *tviB*(2), *hisF2*.
	Tap type IV pili(*Aeromonas*)	*tapQ*
	The tad locus(*Haemophilus*)	***tadA***, ***tadA*(2)**
	Type IV pili(*Yersinia*)	*pilW*
Antiphagocytosis (VFC 3)	Capsular polysaccharide	*cpsA*, *cpsC*, *rmlA*, *rmlB*, *rmlC*, *rmlD*, *wbfT*, *wbfU*, *wbfV/wcvB*, *wbfY*.
	Capsule (*Klebsiella*)	*uge*
Chemotaxis and motility (VFC 5)	Flagella	***cheA***, ***cheA*(2)**, ***cheB***, ***cheR***, ***cheV***, ***cheW***, ***cheY***, ***cheZ***, ***filM***, ***flaA***, ***flaB***, ***flaC***, ***flaD***, ***flaE***, ***flaG***, ***flaI***, ***flgA***, ***flgB***, ***flgC***, ***flgD***, ***flgE***, ***flgF***, ***flgG***, ***flgH***, ***flgI***, ***flgJ***, ***flgK***, ***flgL***, ***flgM***, ***flgN***, ***flhA***, ***flhB***, ***flhF***, ***flhG***, ***fliA***, ***fliD***, ***fliE***, ***fliF***, ***fliG***, ***fliH***, ***fliI***, ***fliJ***, *fliK*, ***fliL***, ***fliN***, ***fliO***, ***fliP***, ***fliQ***, ***fliR***, ***fliS***, ***flrA***, ***flrB***, ***flrC***, ***motA***, ***motB***, ***motX***, ***motY***.
Enzyme (VFC 7)	Metalloproteinase	***hap/vvp***, ***prtV***
	Collagenase	***colA***, ***colP***
Iron uptake (VFC 10)	Enterobactin receptors	***vctA***
	Heme receptors	***hutA***
	Periplasmic binding protein-dependent ABC transport systems	*vctC*, *vctD*, *vctG*, *vctP*, *vctP*(2)
	Pyoverdine(*Pseudomonas*)	*pvdY*
Quorum sensing (VFC 13)	Autoinducer-2	***luxS***

	Cholerae autoinducer-1	***cqsA***
Secretion system (VFC 14)	EPS T2SS	*epsC*, *epsE*, *epsF*, *epsG*, *epsH*, *epsI*, *epsJ*, *epsK*, *epsL*, *epsM*, *gspD*
	T3SS1 secreted effectors	Undetermined, *vopQ*
	T3SS1	*sycN*, *tyeA*, *vcrD*, *vcrG*, *vcrH*, *vcrR*, *virF*, *virG*, *vopB*, *vopN*, *vscA*, *vscB*, *vscC*, *vscD*, *vscF*, *vscG*, *vscI*, *vscJ*, *vscK*, *vscL*, *vscN*, *vscO*, *vscQ*, *vscR*, *vscS*, *vscT*, *vscU*, *vscX*, *vscY*, *vxsC*.
	VAS effector proteins	*hcp-2*, *hcp-2*(2), *vgrG-2*, *vgrG-2(2)*, *vgrG*-2(3), *vgrG*-3
	VAS T6SS secretion system	***vasA***, ***vasB***, ***vasC***, ***vasD***, ***vasE***, ***vasF***, ***vasG***, ***vasH***, ***vasJ***, ***vasK***, ***tssE***, ***impC/vipB***, ***ipmB/vipA***, *impA*, ***impA*(2)**, *hcp*, *hcp*(2), **hcp(3)**, *impB/vipA*, ***impB/vipA*(2)**, *impC/vipB*, ***impC/vipB*(2)**, ***impC/vipB*(3)**, *tssE*, ***tssE*(2)**, *impG/vasA*, ***impG/vasA*(2)**, *impH/vasB*, ***impH/vasB*(2)**, *tssH*, ***tssH*(2)**, *impI/vasC*, ***impI/vasC*(2)**, *vasD*, ***vasD*(2)**, *impJ/vasE*, ***impJ/vasE*(2)**, *impK/vasF/ompA/motB*, ***impK/vasF/ompA/motB* (2)**, *icmF/vasK*, ***icmF/vasK*(2)**, PAAR-repeat_protein, **PAAR-repeat_protein(2).**
	T3SS(*Aeromonas*)	*ati1*
Toxin (VFC 15)	RTX toxin	*rtxB*, *rtxD*
	V.cholerae cytolysin	*hlyA*
	Phytotoxin coronatine(*Pseudomonas*)	***alaX***
	Phytotoxin phaseolotoxin(*Pseudomonas*)	*cysC1*
	The repeat in toxin (RTX)(*Aeromonas*)	*rtxE*
	Hemolysin	**aerolysin**, **Hemolysin**, **Putative hemolysin**, **Putative hemolysin 2**, ***HlyIII***, **Hemolysins or related proteins containing CBS domains.**
Acid resistance (VFC 1)	Urease(*Helicobacter*)	***ureB***, ***ureG***
Biofilm formation (VFC 4)	AdeFGH efflux pump/transport autoinducer(*Acinetobacter*)	***adeG***
Endotoxin (VFC 6)	LOS(*Haemophilus*)	*kdsA*, *kpsF*

	LPS(*Bordetella*)	*bplA*
Glycosylation system (VFC 8)	O-linked flagellar glycosylation(*Campylobacter*)	*pseB*
Immune evasion (VFC 9)	Capsule(*Neisseria*)	*ctrD*
	Capsule(*Acinetobacter*)	*pseI, pseF, pseC, wbpD, tviB(3), pseB(2), vipB/tviC, wbpP*
Nutritional factor (VFC 11)	Allantoin utilization(*Klebsiella*)	*allA*
Others (VFC 12)	O-antigen(*Yersinia*)	*manA, wcaG*

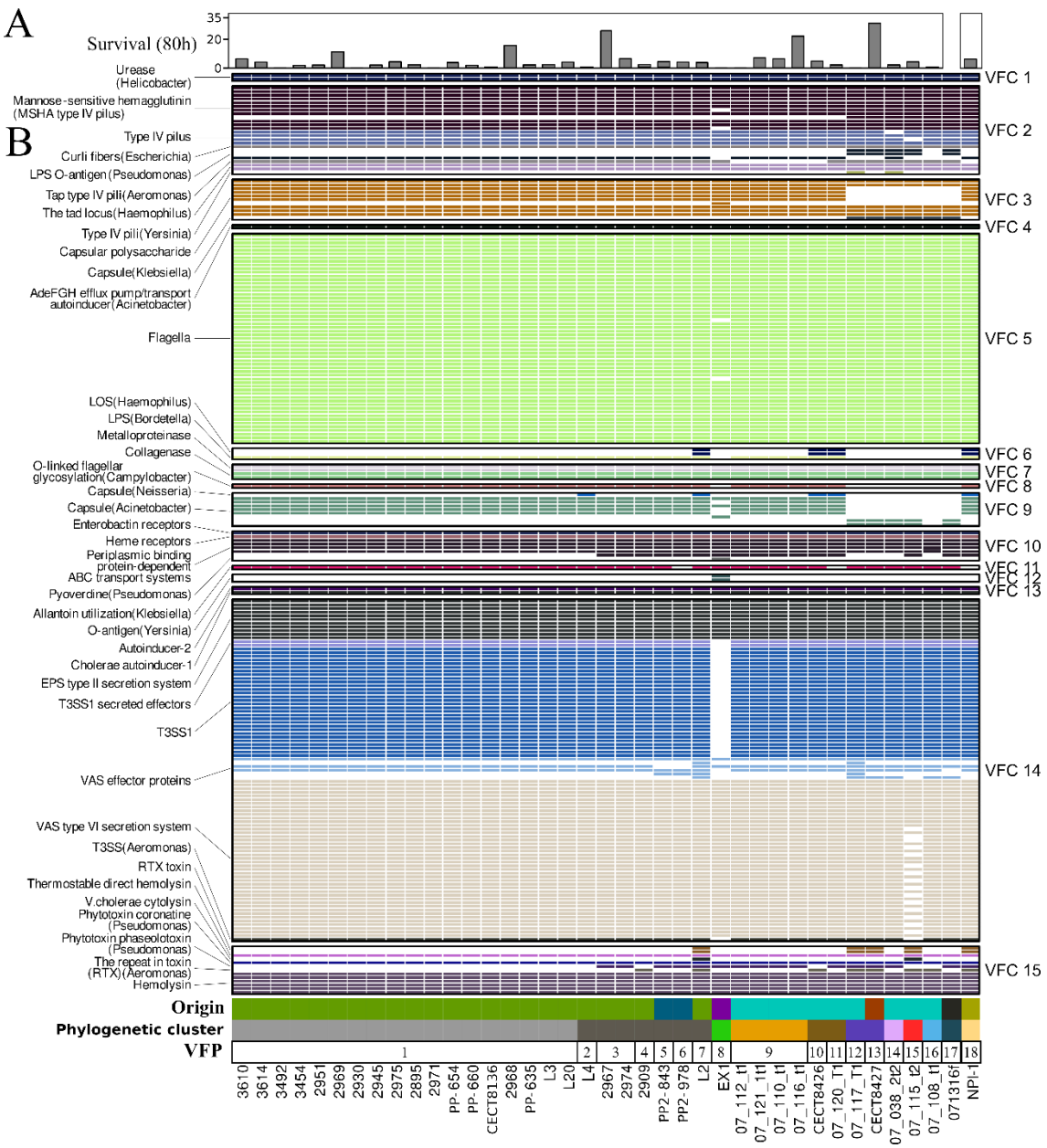

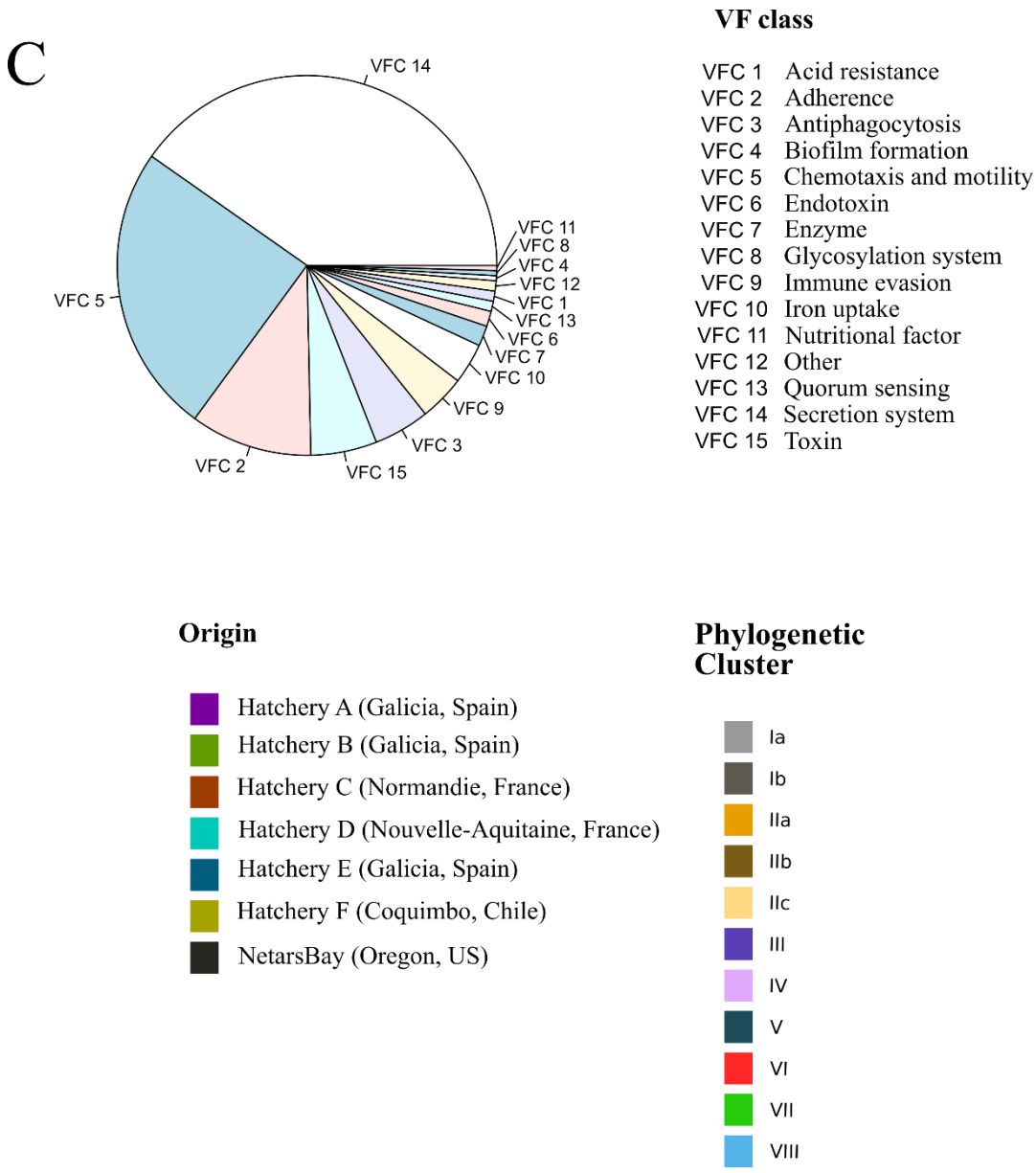

Figure 2.1. Characterization of virulence genes identified from *V. europaeus* genomes: (A) Percentage of survival of Manila clam juveniles after *V. europaeus* infection (B) Presence/absence of virulence genes. (C) Relative abundance of the different Virulence Factor classes (VFCs) in the *V. europaeus* pangenome. VFs (Virulence Factors) associated with these genes are indicated on the left and VFCs on the right. Geographical origin of the *V. europaeus* strains, as well as their phylogenetic cluster and virulence factors profiles (VFP) stablished in Fig. 2.2 are indicated at the bottom.

The PCA analysis based on the non-core virulence factors revealed the existence of genetic differentiation among the 39 strains with the 18 different virulence factors profiles (VFP) identified. Analyses of the VFPs revealed a higher genetic variability among strains (Fig. 2.2A), than the found in the core-genome analyses described in Chapter I and from we have defined eight clusters based on the core-genome (I: Ia and Ib; II: IIa, IIb and IIc; III-VIII).

In the Spanish strains isolated from Hatchery B (sub-clusters Ia and Ib) and Hatchery E (sub-cluster Ib), a total of five and two distinctive VFPs, respectively, were identified (Fig. 2.1B). Sub-cluster Ia was only constituted by strains isolated from Hatchery B and most of those strains (n=18/19) showed a homogeneous profile (VFP 1; Fig. 2.1B), regardless of the sampling date/host, and shared a total of 70 non-core virulence factor genes (Fig. 2.2B; Table 2.1). However, the strain L4 was exclusively associated with VFP2 because it encoded an additional non-core gene, the immune evasion gene *ctr*D (Fig. 2.1B and 2.2A), absent even in its clonal strains. Sub-cluster Ib included strains isolated from hatcheries B (2909, 2967 and 2974) and E (PP2-843 and PP2-978) (Fig. 2.1B), and three and two different VFPs were identified from the strains isolated in Hatchery B and E respectively (Fig. 2.1A): VFP 3 (2967 and 2974), VFP 4 (2909), VFP 5 (PP2-843), VFP 6 (PP2-978) and VFP 7 (L2) (Fig. 2.2B). All these strains shared 69 non-core virulence factors (Fig. 2.1B and 2.2B; Table 2.1). Despite the core-genome clonality found in the strains 2967, 2974, 2909, PP2-843, and PP2-978, they differed in the presence/absence of some genes, for example the VAS effector protein coding genes *vgr*G-2 (present in 2967, 2974 and 2909) and *vgr*G-2_3 (present in PP2-978), the toxins coding genes *cys*C1 (present in the strains 2967, 2974 and PP2-978) or *rtx*E (present only in 2909), and the allantoin utilization gene *all*A (present in 2967, 2974, 2909 and PP2-843) (Fig. 2.1B; Table 2.1). Interestingly, the strain L2 (VFP 7; Fig. 2.1A) harboured the highest number of virulence genes (n=82) among the *V. europaeus* strains and it included 13 additional non-core virulence genes such as those encoding an additional VAS effector proteins of the T6SS encoded in the accessory genome (*hcp*-2_2, *vgrG-2*, *vgrG-2_3* and *vgrG-3*), toxins (*rtx*B, *rtx*D, *rtx*E, *hly*A and *cys*C1), endotoxins (*kds*A and *kps*F), immune evasion (*ctr*D) and allantoin utilization (*all*A) (Fig. 2.1A; Table 2.1).

These results revealed the co-existence of different VFPs in the same environment, such as VFP 5 and VFP 6 formed by the closely related phylogenetic strains PP2-843 and PP2-978, respectively (Hatchery E; Nov/2008). This was also observed in Hatchery B along the time series (2001-2018) (Fig. 2.2B): VFP 1 was always detected, being the unique profile in Mar/2001, May/2012, Jun/2012 and Jul/2012 and it co-existed with VPF 3 and VPF 4 in May/2011 and with VFP 2 and VFP 7 in Mar/2018.

The only Spanish strain isolated from hatchery A (EX1; Table 1.1), encoded the lowest number of non-core virulence genes (n=38; VFP 8) because it was the only one without the T3SS genes in their genome (Fig. 2.1B and 2.2A; Table 2.1).

French strains isolated from Hatchery D showed a higher VFP variability than the Spanish strains, coexisting 8 different VFP in a same environment (Fig. 2.1B). Sub-cluster IIa (07/112 T1, 07/121 1T1, 07/110 T1, and 07/116 T1) (Fig. 2.1A) showed the same profile (VFP 9; Fig. 2.2A) sharing 71 additional non-core genes (Fig. 2.1B). However, this was very different in sub-cluster IIb where the strains CECT8426 and 07/120 T1 (Fig. 2.1B), although sharing 72 non-core genes, differed in the type 4 pili *tap*Q and the toxin *cys*C1 (only present in 07/120 T1) and *rtx*E and *all*A (only present in CECT8426), supporting its position in the PCA as independent profiles (VFP 10 and VFP 11) (Fig. 2.1B and 2.2A; Table 2.1). Strains 07/117 T1 and CECT8427, isolated from Hatchery D and C, respectively, and belonging to cluster III, showed independent virulence factor profiles (VFP 12 and VFP 13; Fig. 2.1A) since they differed in the type IV pili *pil*W and VAS effectors, such as *hcp*-2_*2* and *vgrG*2_3, present only in the strain 07/117 T1 (Fig. 2.1B and 2.2A). The other three strains isolated from hatchery D (07/038 2T2, 07/115 T2 and 07/108), which constituted by themselves three independent clusters in the core phylogeny (clusters IV-VIII; Fig 2.1B), held their own VFPs (VFP 14-16; Fig. 1B). Interestingly, we have found two different T6SS: one encoded in the core-genome (T6SS1) and the other one (T6SS2) encoded in the accessory genome because it was harboured by most of *V. europaeus* strains only with the exception of the French strain 07/115 T2. For this reason, 07/115 T2 encoded a lower number of non-core virulence genes (n=57; VFP 15; Fig. 2.1B) than their contemporary strains.

Although they do not harbour unique genes, the American strains constituted two completely different VFPs (071316F, VFP 17; NPI-1, VFP 18; Fig. 2.1B).

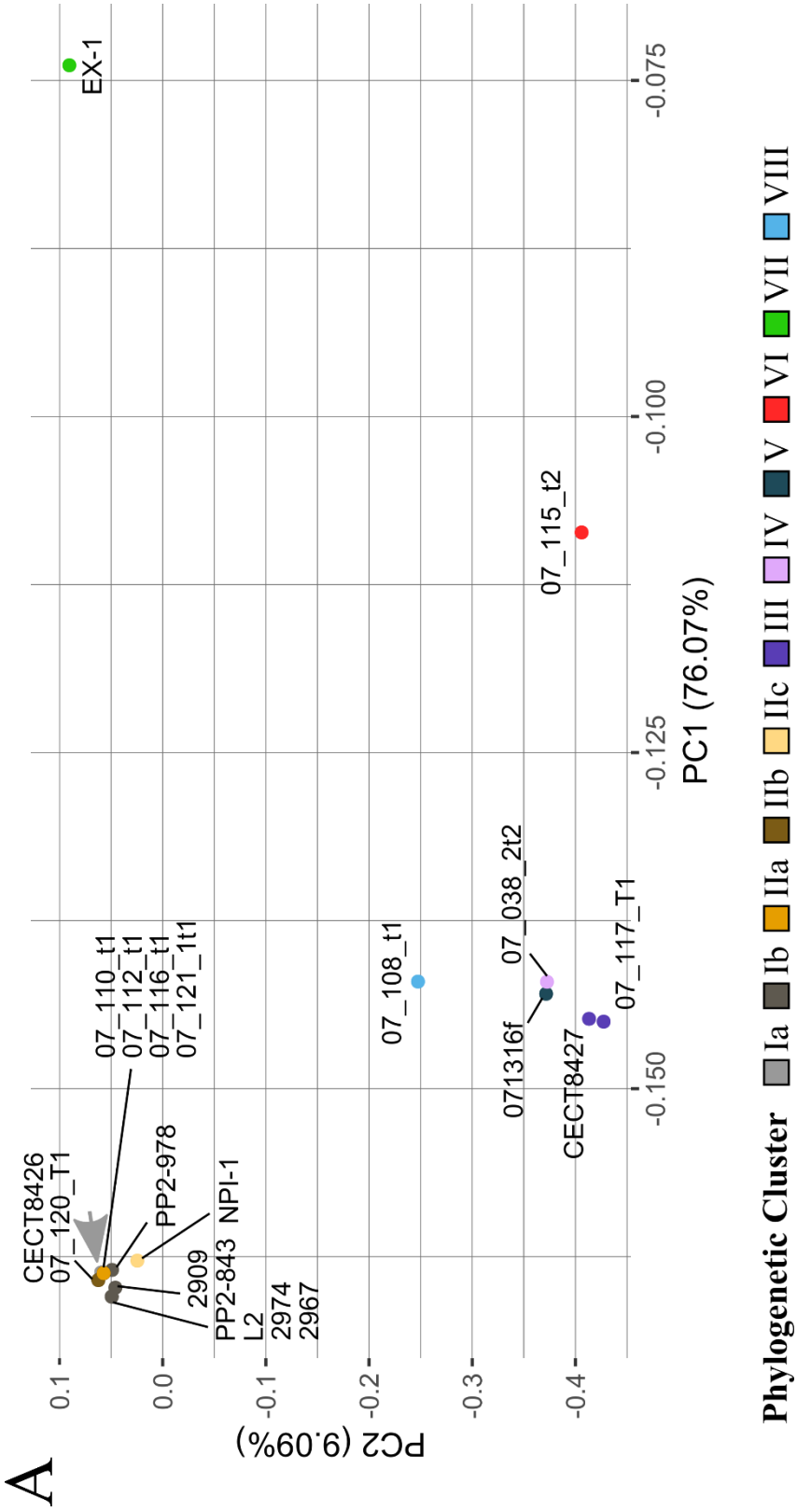

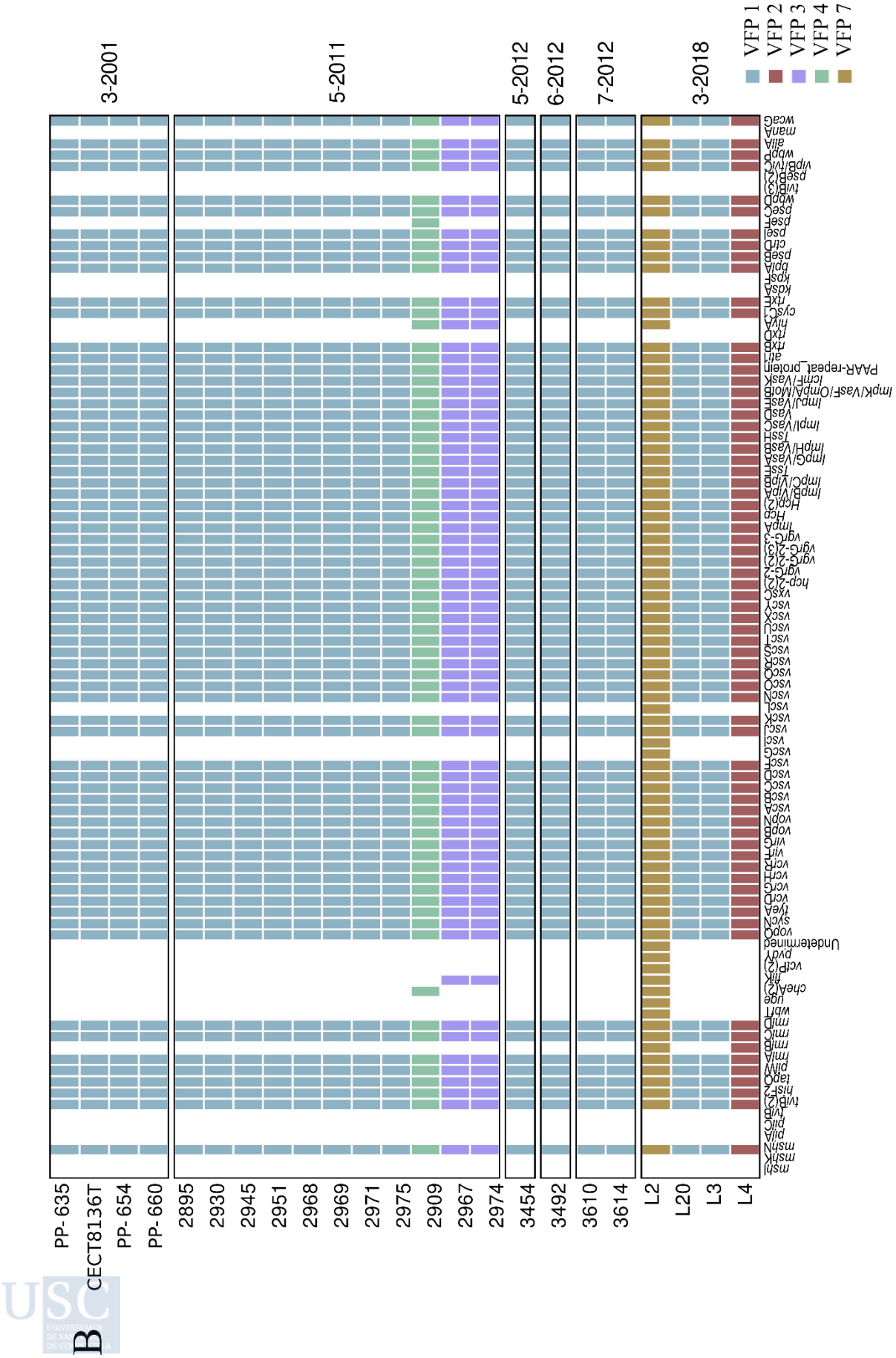
B
3-2001
5-2011
5-2012
6-2012
7-2012
3-2018
VFP 1
VFP 2
VFP 3
VFP 4
VFP 7
PP-635
CECT8136T
PP-654
PP-660
2895
2930
2945
2951
2968
2969
2971
2975
2909
2967
2974
3454
3492
3610
3614
L2
L20
L3
L4
msh
msK
msN
pilA
pilC
tviB
tviB(2)
tagQ
pilW
rmlA
rmlB
rmlC
rmlD
wbtT
uge
cheA(2)
flik
vctP(2)
pvdY
Undetermined
vopQ
sycN
tyeA
vcrD
vcrG
vcrH
vcrR
virF
virG
vopB
vopN
vscA
vscB
vscC
vscD
vscF
vscG
vscI
vscJ
vscK
vscL
vscN
vscO
vscQ
vscR
vscS
vscT
vscU
vscX
vscY
vxsC
hcp-2(2)
vgrG-2
vgrG-2(2)
vgrG-2(3)
vgrG-3
tmpA
Hcp
Hcp(2)
impB/VipA
impC/VipB
tssE
impG/VasA
impH/VasB
tssH
impI/VasC
VasD
impJ/VasE
impK/VasF/OmpA/MotB
icmF/VasK
PAAR-repeat_protein
atiA
rxb
rxD
hlyA
cysC1
rxE
ksaA
kpsF
bplA
psiB
ctrD
pseI
pseF
pseC
wbpD
tviB(3)
pseB(2)
VipB/VipC
wbpP
allA
manA
wcaG

Figure 2.2. (A) Genomic variability of *V. europaeus* strains based on their virulence factors profiles (VFPs). (B) Temporal evolution (2001-2018) of VFPs encoded by *V. europaeus* strains isolated from Hatchery B. Phylogenetic core-genome clusters were showed in different color in PCA. Strains codes belonging to cluster Ia (light gray) were omitted for readability and its location were labelled with a light gray arrow. In Fig. 2B, presence/absence of accessory virulence-related genes were displayed in rows.

2.2.2 Antibiotic resistance profiles

A concordance between the *in silico* and phenotypic results was required to stablish the final antibiotic resistance profile. For example, all *V. europaeus* strains (n=38) were resistant to erythromycin (E, 15 µg) according to the disc diffusion method, which agreed with the presence of the antibiotic resistance gene (ARG) CRP (Fig. 2.3). The strains 3454, 3492, 3610 and 3614 were also resistant to streptomycin (S, 10 µg) and sulfonamide (SULDD, 25 µg) by the presence of the ARGs aph(3")-Ib and aph(6)-Id genes and *sul2* gene, respectively, in their genomes (Fig. 2.3).

Some discrepancies were found between *in silico* and phenotypic results, and thus *in silico* data were curated with the results obtained by the disc-diffusion method. For example, despite no cephalosporin resistance gene was found in CARD and ResFinder database, all *V. europaeus* (n=38) strains were resistant to cephalexin on MHA-1 plates. On the other hand, some resistance genes found by *in silico* analyses rendered a negative phenotypic result: (i) *floR* gene was identified in the genomes of the strains 3454, 3492, 3610 and 3614 by ResFinder (identities ranged from 98.19%-98.27%), however, they were sensitive to florfenicol (FFC, 30 µg); (ii) suggestive tetracycline resistance genes were found in all strains in both databases (gene identity >85%), however they were sensitive to tetracycline (TE, 30 µg).

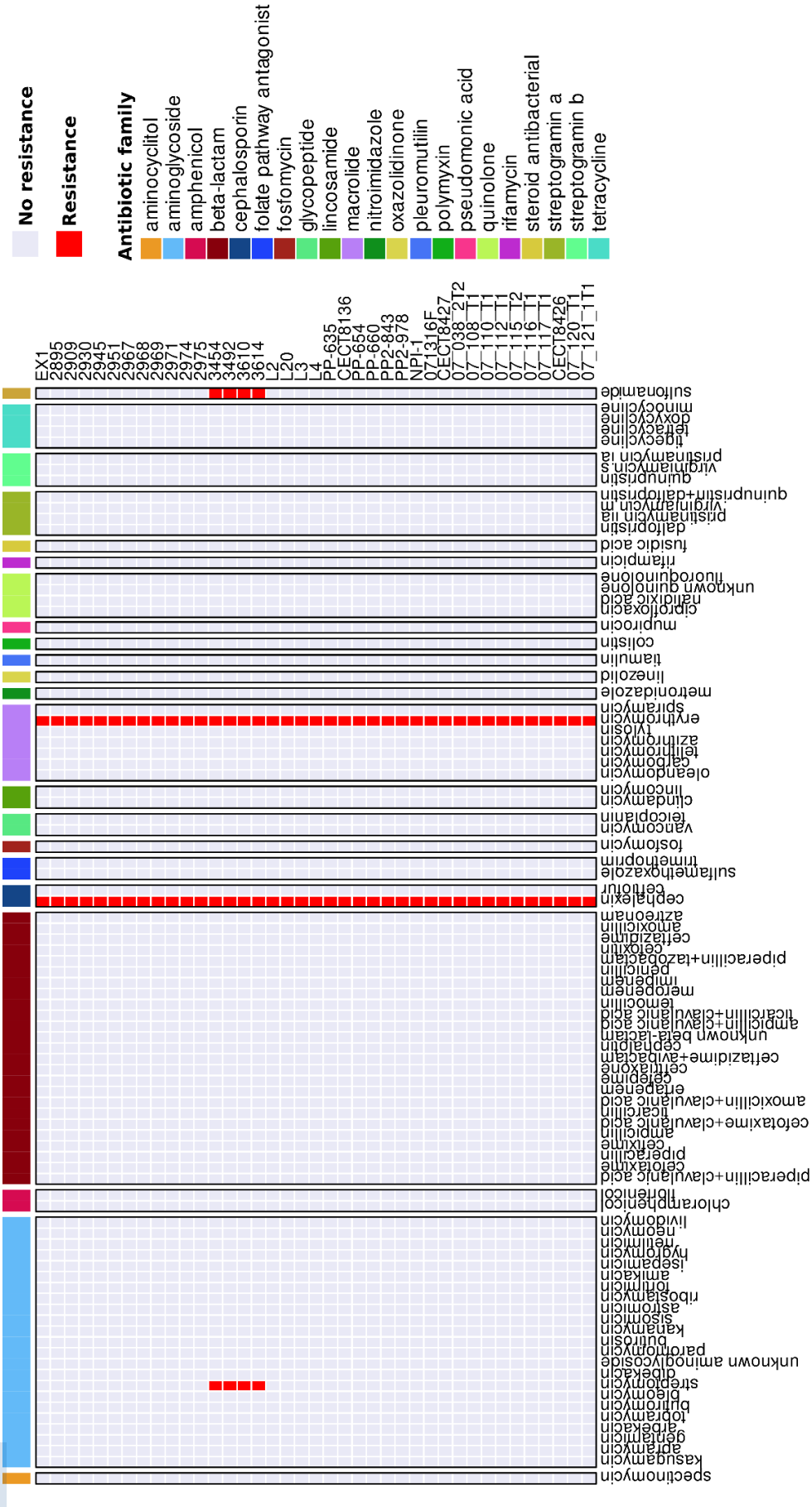

Figure 2.3. Antibiotic resistance phenotypes of the *V. europaeus* strains. Antibiotics are depicted by columns and grouped by antibiotic families as indicated in the right legend

2.2.3 Characterization of secondary metabolite biosynthetic gene clusters

V. europaeus genomes encoded a total of 254 biosynthetic gene cluster (BGCs). Most of the strains encoded 6-7 BGCs, ranging from the 5 BGCs encoded by the French strain 07/115 T2 (cluster VI) to the 8 BGCs of the American strain 071316F (cluster V) (Fig. 2.4 and Fig. 2.5).

Study of the intra-BGC diversity allowed its classification in four major classes: PKS-NRP hybrids (14.57%), RiPPs (15.75%), NRPS (15.75%), and Others (53.94%). Within those classes, 12 biosynthetic gene clusters families (GCF) could be defined (Fig. 2.4 and 2.5): GCF1 and GCF2 presumably produces PKS-NRP hybrids; GCF3 and GCF4 post-translationally modified peptides (RiPPs); GCF5 and GCF6, non-ribosomal peptide synthetases (NRPS); GCF7 and GCF8, ectoine; GCF9, arylpolyene-NRPS hybrids; GCF10, butyrolactone; GCF11, betalactone; GCF12, arylpolyene.

GCF4, GCF6, GCF11 and GCF12 contains BGCs of all the *V. europaeus* strains analysed and thus they were assigned to the core-genome (Fig. 2.4 and 2.5). GCF1, GCF2, GCF7, GCF8, and GCF9 are conformed by sequences of just a subset of strains (Fig. 2.4 and 2.5): GCF1 and GCF9, cluster Ia; GCF2, clusters Ib, IIa-c, III, IV, V, and VII; GCF7, clusters Ia, IIa-c, III, VIII, and IV; GCF8, clusters Ib, IIa-b, V, VI, VII. Moreover, out of three GCFs singletons found, GCF3 and GCF5 were only encoded by the strain 071316f (US; phylogenetic cluster V), whereas GCF10 was only detected in the strain 07/108 T1 (France; phylogenetic cluster VIII) (Fig. 2.4). According to antiSMASH results, GCF5 present a 100% similarity to the siderophore amphibactin B biosynthetic gene cluster of *V. neptunius*, and GCF12 present an 85-90% similarity to arylpolyene Vf BGC of *Aliivibrio fischeri* ES114.

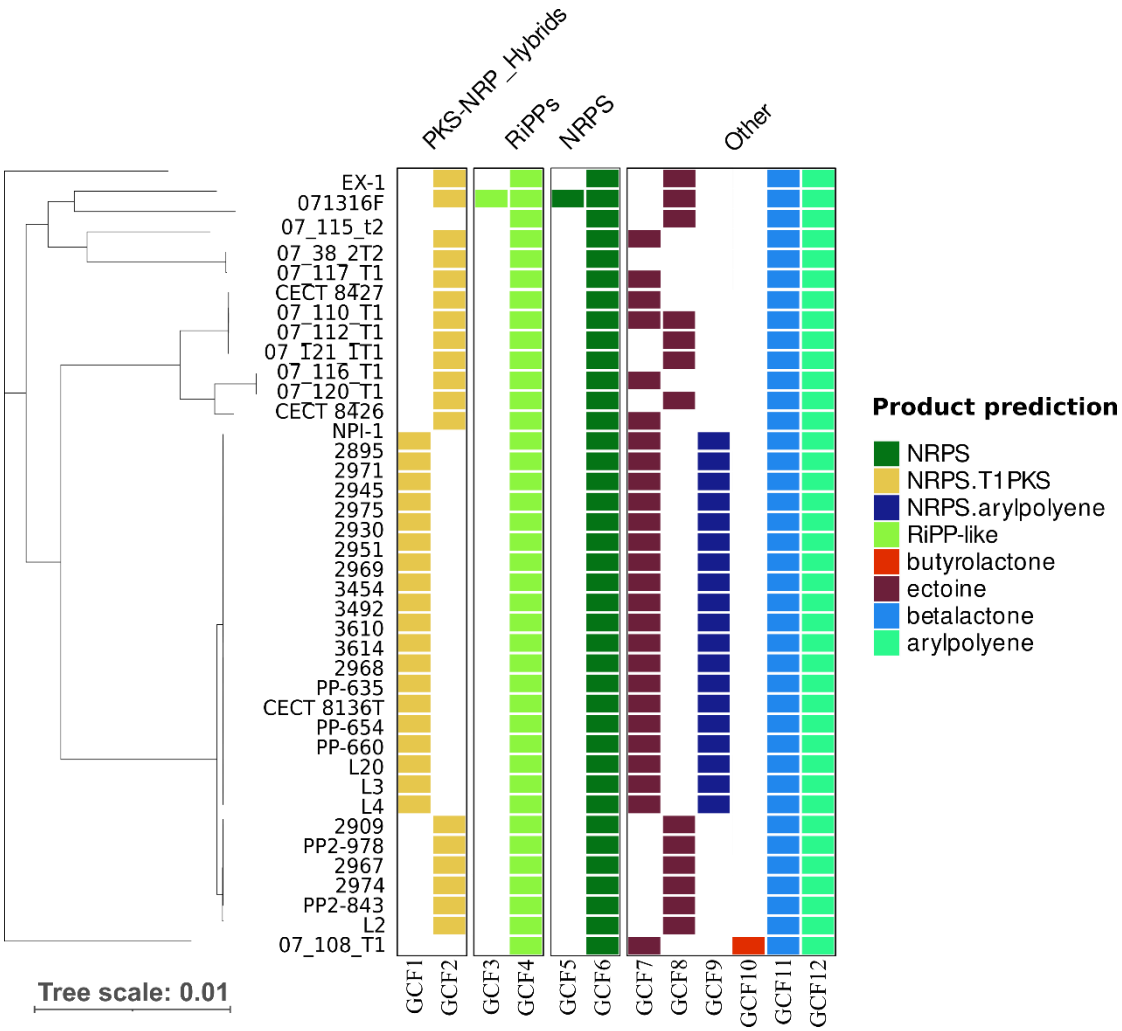

Figure 2.4. Heatmap showing the GCFs located along *V. europaeus* strains. Colour indicates the product prediction of the BGCs. The phylogenetic tree previously obtained with the core genome was reshaped and plotted on the left.

To study the intra-family sequence diversity of BGCs, minimum Jaccard Index and mean between BGC pairs belonging the same phylogenetic cluster were computed. More diverse families showed a minimum Jaccard Index lower than 0.5: GCF8 (0.27), GCF7 (0.25), GCF2 (0.32), GCF5 (0.46), and GCF3 (0.44). In contrast, a high similarity was found for GCF11 (0.51), GCF12 (0.58), and GCF9 (0.88) and GCF1 (0.99), both only encoded by the strains belonging to phylogenetic cluster Ia (Fig. 2.4 and 2.5). Regarding the phylogenetic dependency of BGCs, all strains belonging the same phylogenetic cluster based on the core-genome showed a high BGC homogeneity (>0.90), being the more diverse GCF2 (0.91), and GCF11 (0.97) (Fig. 2.5).

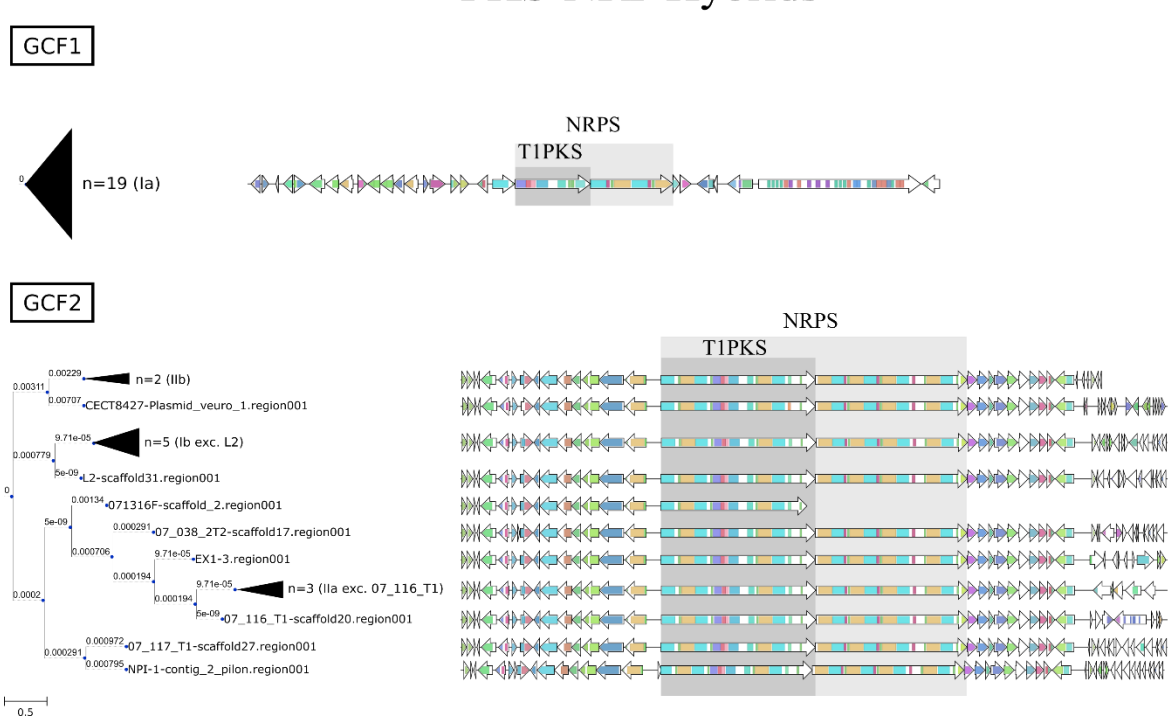
PKS-NRP Hybrids
GCF1
NRPS
T1PKS
n=19 (Ia)
GCF2
NRPS
T1PKS
n=2 (IIb)
CECT8427-Plasmid_veuro_1.region001
n=5 (Ib exc. L2)
L2-scaffold31.region001
071316F-scaffold_2.region001
07_038_2T2-scaffold17.region001
EX1-3.region001
n=3 (IIa exc. 07_116_T1)
07_116_T1-scaffold20.region001
07_117_T1-scaffold27.region001
NPI-1-contig_2_pilon.region001
0.5

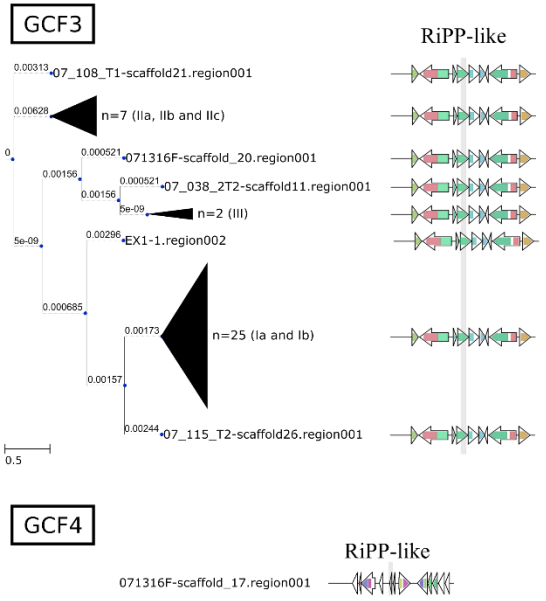
RiPPs
GCF3
RiPP-like
07_108_T1-scaffold21.region001
n=7 (IIa, IIb and IIc)
071316F-scaffold_20.region001
07_038_2T2-scaffold11.region001
n=2 (III)
EX1-1.region002
n=25 (Ia and Ib)
07_115_T2-scaffold26.region001
0.5
GCF4
RiPP-like
071316F-scaffold_17.region001

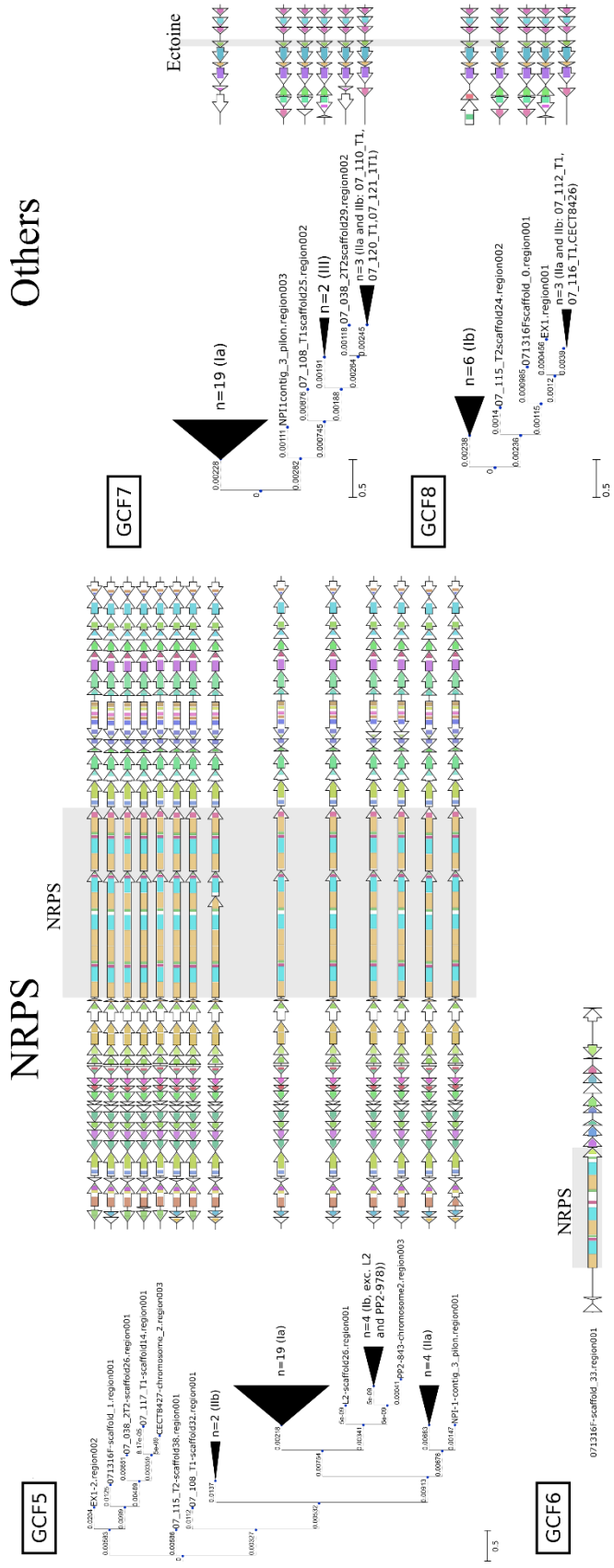
Others
Ectoine
GCF7
n=19 (Ia)
n=2 (III)
n=3 (IIa and IIb: 07_110_T1, 07_120_T1,07_121_1T1)
GCF8
n=6 (Ib)
n=3 (IIa and IIb: 07_112_T1, 07_116_T1,CECT8426)
NRPS
NRPS
GCF5
n=2 (IIb)
n=19 (Ia)
n=4 (Ib, exc. L2 and PP2-978))
n=4 (IIa)
GCF6
NRPS

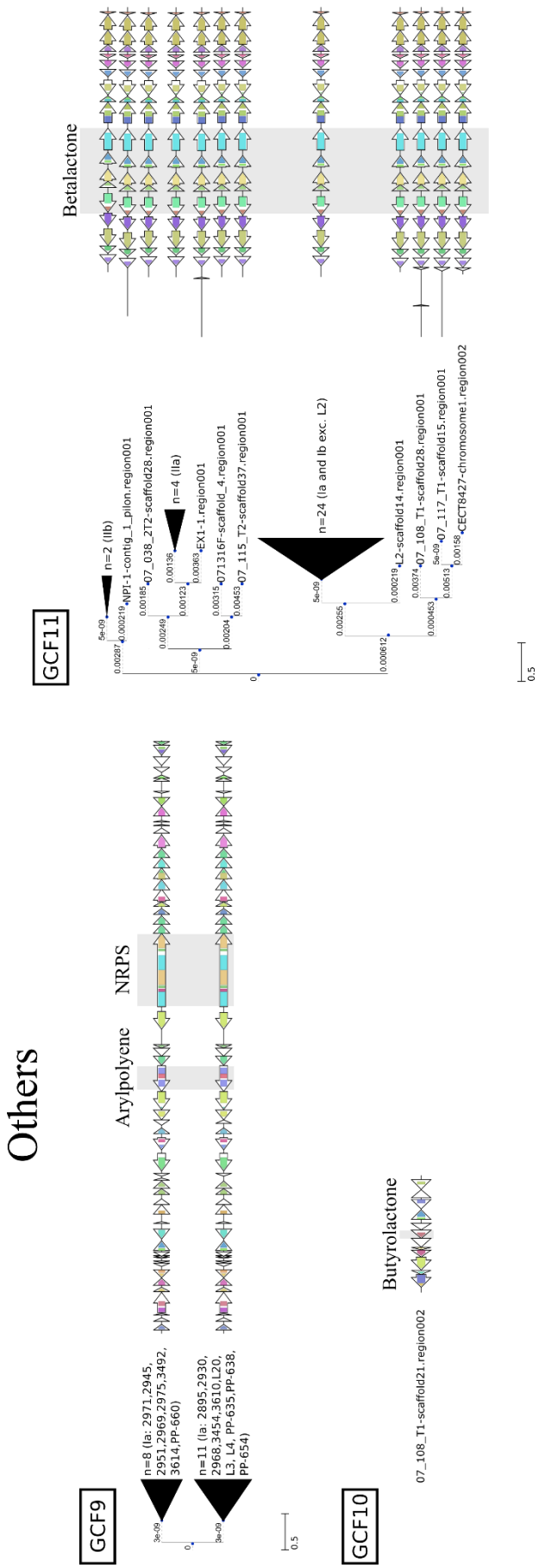
Others
GCF9
n=8 (Ia: 2971,2945, 2951,2969,2975,3492, 3614,PP-660)
n=11 (Ia: 2895,2930, 2968,3454,3610,L20, L3, L4, PP-635,PP-638, PP-654)
Arylpolyene
NRPS
GCF10
Butyrolactone
07_108_T1-scaffold21.region002
GCF11
Betalactone
n=2 (IIb)
NPI-1-contig_1_pilon.region001
07_038_2T2-scaffold28.region001
n=4 (IIa)
EX1-1.region001
Q71316F-scaffold_4.region001
07_115_T2-scaffold37.region001
n=24 (Ia and Ib exc. L2)
L2-scaffold14.region001
07_108_T1-scaffold28.region001
07_117_T1-scaffold15.region001
CECT8427-chromosome1.region002

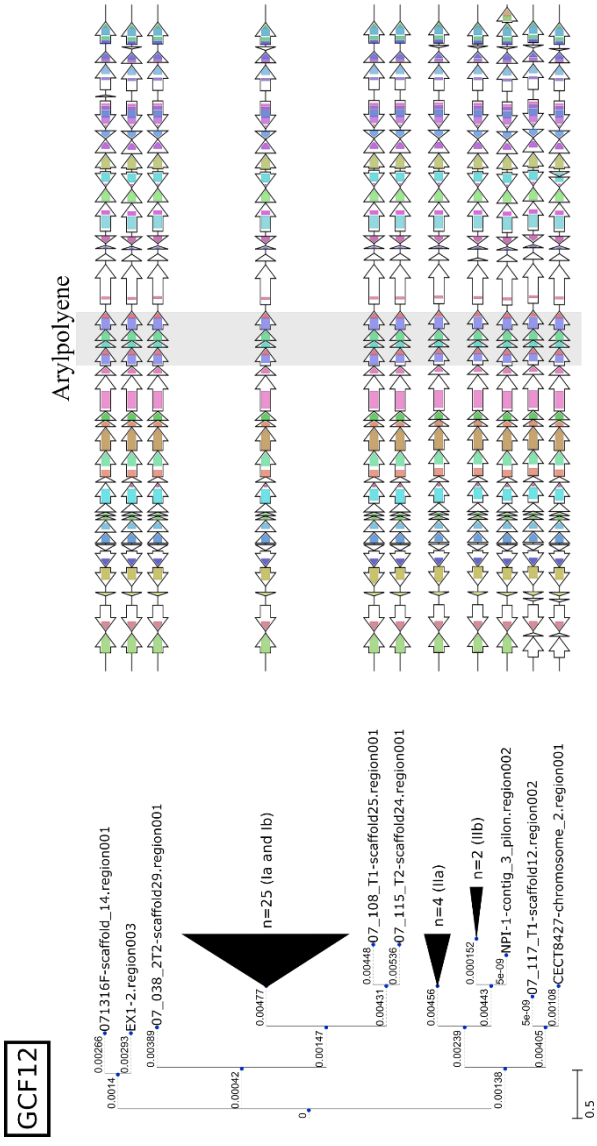

Figure 2.5. Phylogenetic reconstruction of the 12 biosynthetic gene clusters families (GCF 1-12) associated to the different major classes. Branches conformed by identical sequences were collapsed. Gene schemes obtained with antiSMASH for each BGC are displayed together with their corresponding branches, and core biosynthetic genes were shaded.

2.2.4 Characterization of anti-phage defence systems encoded by *V. europaeus*

V. europaeus genomes were enriched in phage defence systems: a total of 49 systems were identified among the studied genomes (Fig. 2.6). Only the dGTPase system was common to all strains indeed (Fig. 2.6). Interestingly, Gao Hhe system was absent only in the French strain 07/115 T2 (Fig. 2.6). However, most of the anti-phage defence systems were non-core, and PCA analyses revealed the genetic variability among *V. europaeus* strains is mainly determined by the anti-phage defence systems in comparison with other accessory genes such as virulence, ARG or BGCs because 20 different anti-phage defence system profiles (ADSP) were found in the accessory genome (Fig. 2.7A).

Among the Spanish strains isolated from Hatchery B and Hatchery E, seven (ADSP 1-7) and two (ADSP 8-9) different ADSPs were identified, respectively (Fig. 2.6 and 2.7A). Within the strains belonging to sub-cluster Ia (n=19; Hatchery B, Fig. 2.6), the oldest strains isolated in this hatchery (CECT8136, PP-654, PP-660 and PP-635; Mar/2001, Fig. 2.6) encoded eight defence systems (dGTPase, Gabija, Gao Hhe, Gao Qat, Gao Upx, PD T7 1, PD T2 7 and RM type I; ADSP 1). However, they constituted two ADSP (ADSP 1 and 2) because PP-635 harboured five additional copies of the Gao Qat system and two copies of the CBASS II, respectively (ADSP 2). Those eight defence types were remained along time in the *V. europaeus* strains belonging to sub-cluster Ia isolated from Hatchery B and new defence systems were added, such as BREX I, Lamassu Fam, Rloc, RM type IV and Rst 3HP in ADSP 3 (2895, 2930, 2945, 2951, 2969, 2971, 2975, and 2968, isolated in May/2011; 3454 in May/2012 3492 in June/2012 and 3610 and 3614, in July/2012; Fig. 2.7B) or Lamassu Fam and RM type IV in ADSP 4 (L3, L4 and L20, isolated in Mar/2018; Fig. 2.6).

Within the sub-cluster Ib, the four strains (2909, 2967, 2974 and L2) isolated from hatchery B contained three ADSPs (ADSP 5, 2909 and 2967; ADSP 6, 2974; ADSP 7, L2). Interestingly, ADSP 4 and ADSP 5 were closely related to the two Spanish strains isolated from hatchery E (ADSP 8, PP2-843; ADSP 9, PP2-978; Fig. 2.6 and 2.7A). In fact, those five strains (2909, 2967, 2974, PP2-843 and PP2-978) shared 14 defence systems BREX I, CBASS II, dGTPase, Gabija, Gao Hhe, Lamassu Fam (two copies), NLR like bNACHT09, PD lambda 5, PD T7 2, Retron II, RM type I, RM type IV and SspBCDE. The latter was the defence profile of the strain PP2-978 (ADSP 9), but additional systems were encoded by the remaining strains such as: PP2-843 (RosmerTA;

ADSP 8), 2909 and 2967 (PD T4 7; ADSP 5) or 2974 (PD T4 7 and RosmerTA; ADSP 6) which constituted the most protected *V. europaeus* strain against phage predation with 16 full systems. On the other hand, L2 was the other strain to sub-cluster Ib and it showed a very different profile than its contemporary strains L3, L4 and L20 (Fig. 2.6). L2 (ADSP 7) harboured a total of eight defence systems (CBASS II, dGTPase, Gao Hhe, Hachiman, NLR like bNACHT09, PD T4 7, PfiAT, and RM type I) and it was the only *V. europaeus* strains encoding the PfiAT system.

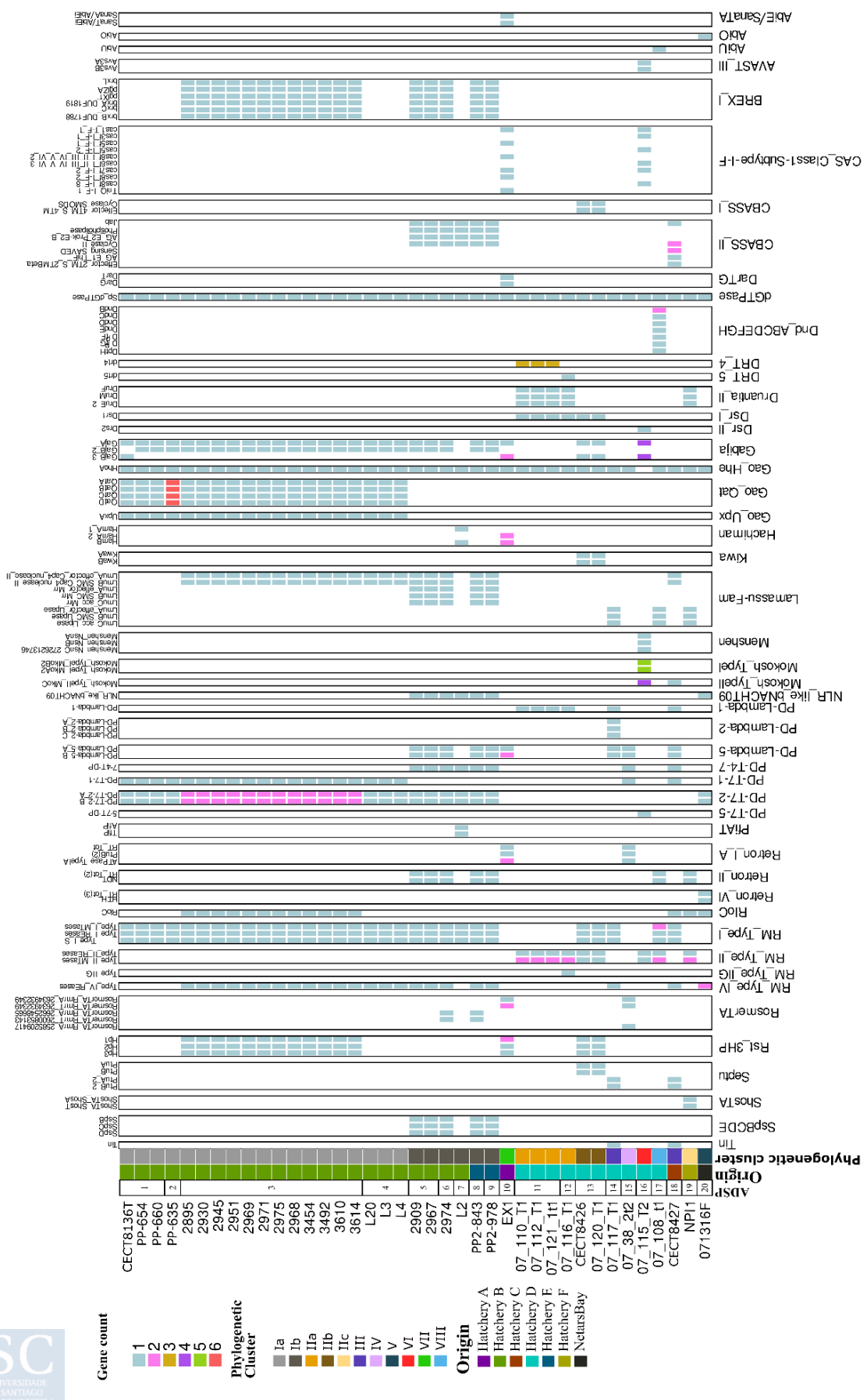
CECT8136T
PP-654
PP-660
PP-635
2895
2930
2945
2951
2969
2971
2975
2968
3454
3492
3610
3614
L20
L3
L4
2909
2967
2974
L2
PP2-843
PP2-978
EX1
07_110_T1
07_112_T1
07_121_1t1
07_116_T1
CECT8426
07_120_T1
07_117_T1
07_38_2t2
07_115_T2
07_108_1t1
CECT8427
NPI1
071316F
ADSP
Origin
Phylogenetic cluster
Tin
SspBCDE
ShosTA
Septu
RsI_3HP
RosmerTA
RM_Type_IV
RM_Type_IIG
RM_Type_II
RM_Type_I
RloC
Retron_VI
Retron_II
Retron_I_A
PfiAT
PD-T7-2
PD-T7-5
PD-T7-1
PD-T4-7
PD-Lambda-5
PD-Lambda-2
PD-Lambda-1
NLR_like_bNACHT09
Mokosh_TypeII
Mokosh_TypeI
Menshen
Lamassu-Fam
Kiwa
Hachiman
Gao_Upx
Gao_Cat
Gao_Hhe
Gabija
Dsr_II
Dsr_I
Druantia_II
DRT_5
DRT_4
Dnd_ABCDEFGH
dGTPase
DarTG
CBASS_II
CBASS_I
CAS_Class1-Subtype-I-F
BREX_I
AVAST_III
AbiU
AbiO
AbiE/SanaTA
Gene count
1
2
3
4
5
6
Phylogenetic Cluster
Ia
Ib
IIa
IIb
IIc
III
IV
v
VI
VII
VIII
Origin
Hatchery A
Hatchery B
Hatchery C
Hatchery D
Hatchery E
Hatchery F
NetarsBay

Figure 2.6. Heatmap showing the set of anti-phage defence systems encoded by *V. europaeus*. Components are coloured by the number of copies and grouped by a specific defence system. Geographical origin of the *V. europaeus* strains, the phylogenetic cluster based on the core genomes and the anti-phage defence system profiles (ADSPs) are indicated on the left.

As observed in the virulence profiles related to the Spanish strains isolated in Hatchery B and E, different ADSPs coexisted to effectively protect the *V. europaeus* population from the phage predation in the same environment, e.g. ADSP 8 (PP2-843) and ADSP 9 (PP2-978) (Fig. 2.6). In Hatchery B, the genetic variability was evaluated along a time series (2001-2018) (Fig. 2.7B). ADSP variability along the time series was higher than the observed for the virulence profiles (=5 different VFP types *vs* 7 different ADSP types) and there was no correspondence among them (Fig. 2.7A and B). ADSP 1 and ADSP 2 profiles co-existed in Mar 2001 (Fig. 2.7B). ADSP 1 evolved by the addition/deletion of new defence systems, including new profiles such as: (i) ADSP 3 (Fig. 2.7B). ADSP 3 coexisted with ADSP 5 and 6 in May 2011, where it was unique in strains isolated 2012 (Fig. 2.7B); or ADSP 4, which coexisted with ADSP 7 (Fig. 2.7B). Additional copies of some defence systems were encoded by some strains such as the five additional copies of Gao Qat system (PP-635; ADSP 2) or the duplicated PD_T7_2 in all the strains with the ADSP 3 (Fig. 2.6 and 2.7B).

On the other hand, the Spanish strain EX1 (cluster VII), isolated from Hatchery A, showed an exclusive ADSP (ADSP 10), and the DarTG and SanaTA systems were only identified in this genome (Fig. 2.6).

French strains isolated from hatchery D also showed high variability, supporting the coexistence of seven different profiles in the same hatchery (ADSP 11-17) (Fig. 2.6). Within the sub-cluster IIa, three strains 07/110 T1, 07/112 T1 and 07/121 1T1 encoded seven systems such as dGTPase, and three copies of Drt 4, Druantia II, Dsr I, Gao Hhe, PD lambda I and RM type II (ADSP 11). The remaining strain belonging to this sub-cluster (07/116 T1) showed a similar profile to ADSP 11 (only lacking DRT 4); however, it harboured two additional systems being the only *V. europaeus* strains encoding the DRT 5 and RM type IIG systems (ADSP 12) (Fig. 6 and 7A). Strains belonging to sub-cluster IIb (CECT8426 and 07/120 T1) included the ADSP 13 (Fig. 2.6 and 2.7A) encoding 10 systems (CBASS I, dGTPase, Dsr I, Gabija, Gao Hhe, Kiwa, RM type I,

RM type II, Rst 3HP and Septu). The remaining strains isolated from Hatchery D (Fig. 2.6) such as 07/117 T1 (cluster III), 07/038 2T2 (cluster IV), 07/115 T2 (cluster VI) and 07/108 T1 (cluster VIII) contained independent ADSPs (ADSP 14-17) with exclusive defence systems, for example: (i) PD-Lambda-2 system only encoded by 07/117 T1 (ADSP 14); (ii) Retron IA system only encoded by 07/038 2T2 (ADSP 15), which it is the strain with the lowest number of defence systems with only six full systems; (iii) AVAST III, Dsr II, Menshen and Mokosh_Type I only encoded by 07/115 T2 (ADSP 16); (iv) AbiU and Dnd ABCDEFGH systems only encoded by 07/108 T1 (ADSP 17).

The only French strain isolated from a different hatchery (CECT8427; Hatchery C, Normandy; Fig. 2.6) showed an independent ADSP (ADSP 18; 11 defence systems: CBASS II, dGTPase, Gao Hhe, Lamassu Fam, PD-lambda 1, PD-lambda 5, PD-T7 1, RloC, RM_Type_I, RM Type IV and Septu) and it was the only one with two copies of the genes of CBASS (Fig. 2.6). The American strains NPI-1 (Chile; cluster IIc) and 071316F (US; cluster V) showed exclusive ADSPs encoded for a total of 7 (ADSP 19) and 9 (ADSP 20) (Fig. 2.7A) defence systems respectively. Interestingly, some defence systems were only harboured by those strains such as AbiO and Retron VI systems only encoded by the strain 071316F or ShosTA system by the Chilean strain NPI-1.

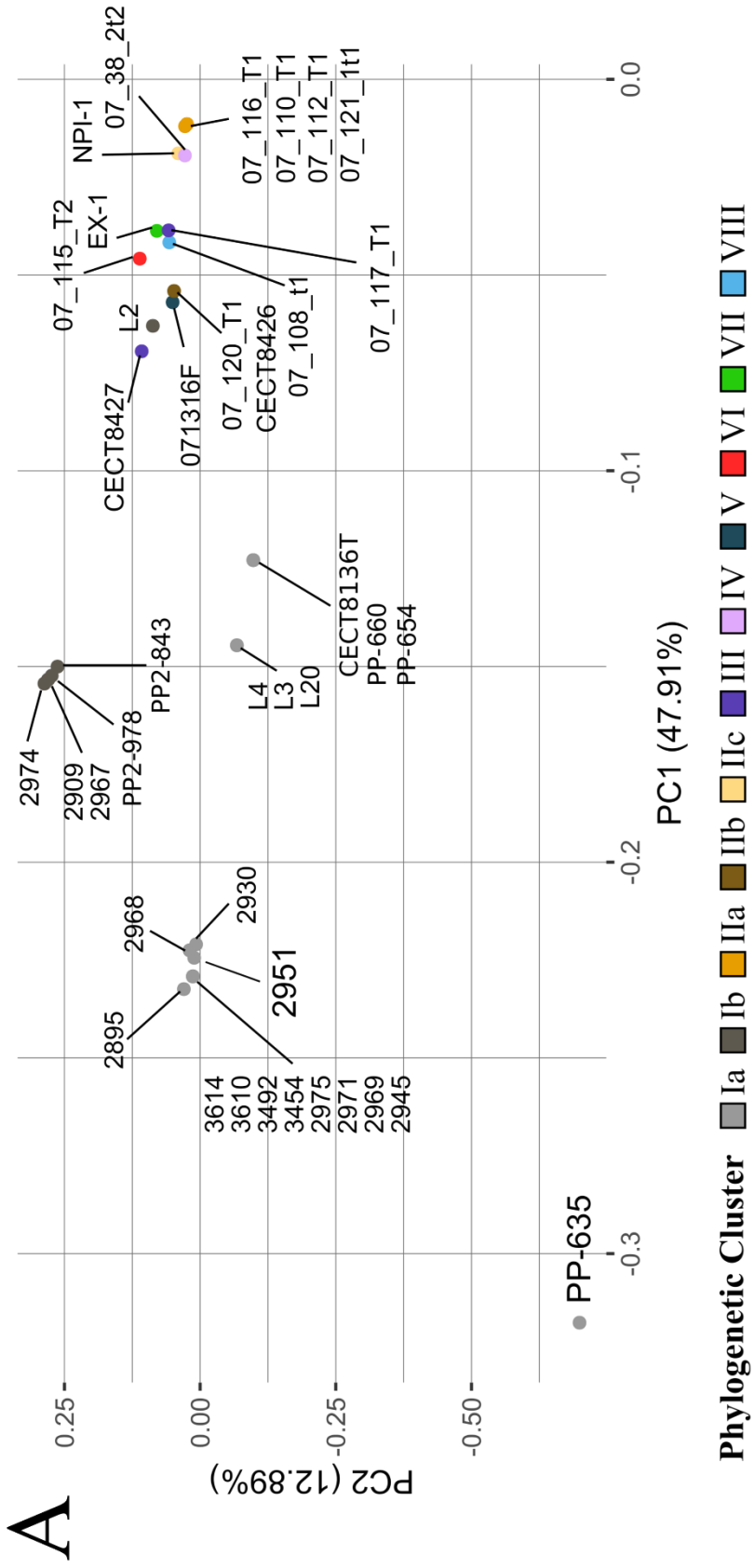
A
PC2 (12.89%)
0.25
0.00
-0.25
-0.50
PC1 (47.91%)
0.0
-0.1
-0.2
-0.3
Phylogenetic Cluster
Ia
Ib
IIa
IIb
IIc
III
IV
V
VI
VII
VIII
07_115_T2
EX-1
NPI-1
07_38_2t2
07_116_T1
07_110_T1
07_112_T1
07_121_1t1
CECT8427
L2
071316F
07_120_T1
CECT8426
07_108_t1
07_117_T1
2974
2909
2967
PP2-978
PP2-843
L4
L3
L20
CECT8136T
PP-660
PP-654
2895
2968
2930
2951
3614
3610
3492
3454
2975
2971
2969
2945
PP-635

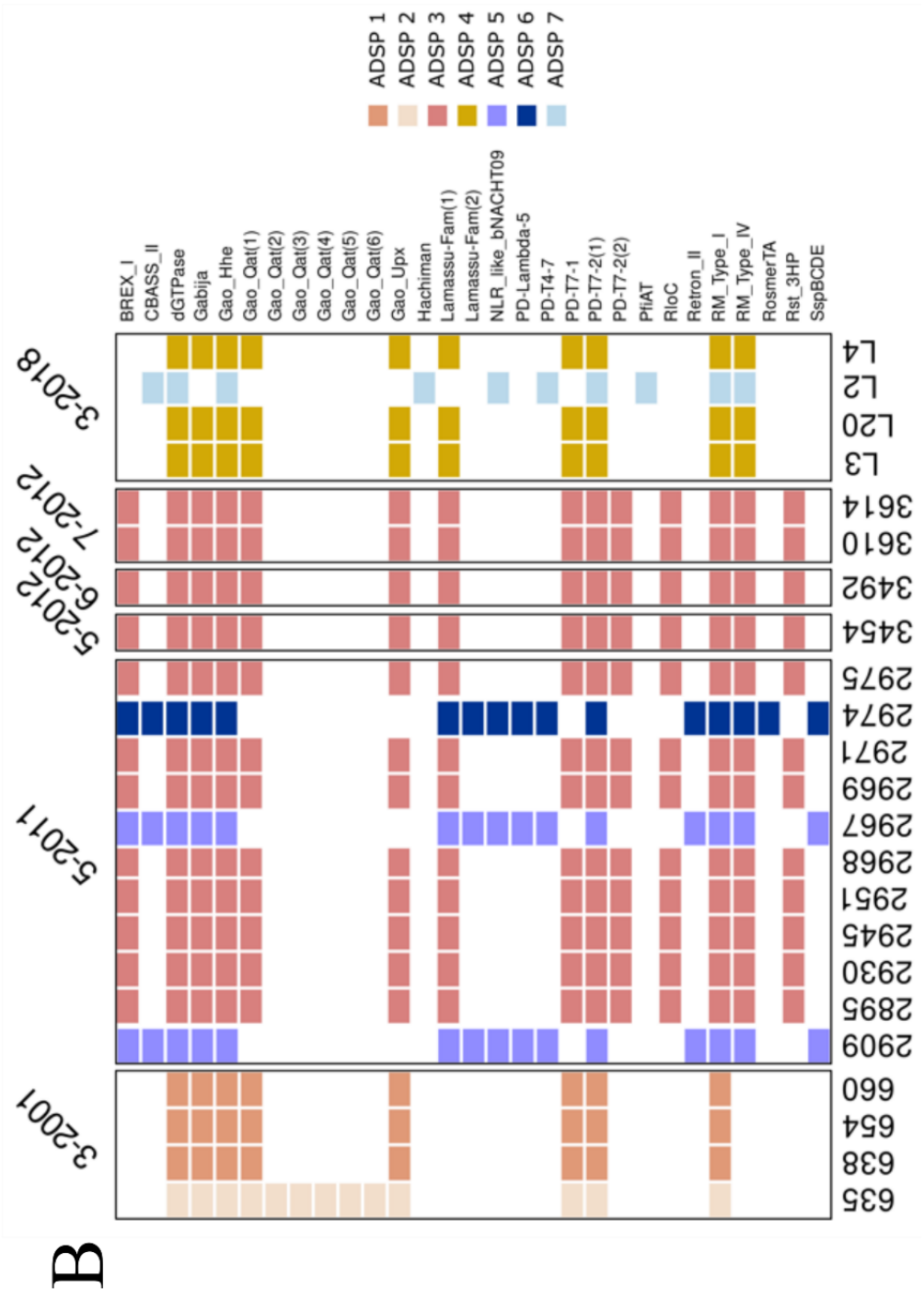

Figure 2.7. Variability of ADSPs in *V. europaeus* strains. **(A)**: PCA based on ADSPs. Colour represents the phylogenetic cluster of the strain **(B)**: Heatmap showing the temporal evolution of ADSPs (marked with different colours) in strains isolated from hatchery B.

2.3 Discussion

Analyses of the virulence genes revealed that 60% of those genes belonged to the core genome. It is important to remark that all *V. europaeus* strains were highly virulent towards Manila clam juveniles. However, different percentage mortalities were found among bacteria encoding the same virulence factor profiles (e.g. VFP 3: 2967 vs. 2974). Those differences can be supported by some bias related to the experimental infections such as the genetic diversity of the juvenile's stock or bacteria inoculum.

The high virulence of *V. europaeus* is indeed a key feature of our bacterial collection, and thus, it is expected that critical virulence factors are encoded in the core genome. Bacterial pathogenic capacity depends on the concurrence of various genomic virulence factors (Casadevall and Pirofski 2009). In the case of *Vibrio* involving in bivalves mortalities, pathogenesis depends on a combination of different factors, such as successful chemotaxis, adherence and a first colonization of bivalve tissues; survival to bivalve immune system and proliferation in hemolymph; colonization of the connective tissue, and a loop of proliferation and nutrient acquisition, which finally causes tissular disruption and host death (Parizadeh et al. 2018; Destoumieux-Garzón et al. 2020). This sequence of facts fits with that found on previous studies of *V. europaeus* pathogenesis (Dubert, Nelson, Spinard, et al. 2016b; Martinez et al. 2022) and with the core virulence genes observed in this study. Basis on our comparative analyses, we hypothesized that the pathogenic capacity of *V. europaeus* depends on successful host adhesion and colonization (MSHA type IV pilus and flagella) (van der Woude and Bäumler 2004; Paranjpye and Strom 2005; Aagesen and Häse 2012; Konieczna et al. 2012; Zhu, Kojima, and Homma 2013; He et al. 2015; Pu and Rowe-Magnus 2018), antiphagocytic (capsular polysaccharide), nutrient acquisition (metalloproteinases, collagenases, enterobactin, heme receptors, periplasmic binding protein-dependent ABC transport systems, type 2 secretion system, VAS type 6 secretion systems, thermostable

direct hemolysin, phytotoxin coronatine, and hemolysins) (Miyoshi and Shinoda 2000; Mey and Payne 2001; Mey et al. 2002; Aagesen and Häse 2012; Miyoshi 2013; Galvis, Barja, et al. 2021; Akhtar and Turner 2022), and it is conceivable modulated by quorum sensing (autoinducer-1 and 2). Additionally, the participation of core genes belonging to incomplete virulence factors, such as urease, tad locus, type IV pilus, and biofilm formation in *V. europaeus* pathogenicity is unclear. Conversely, accessory genes associated with immune evasion (VCF 9) may lead to increased diversity in capsular polysaccharides within *V. europaeus*, enhancing its ability to circumvent host immune defences and ensuring survival in hemolymph (Chatzidaki-Livanis, Jones, and Wright 2006; Shu et al. 2009; Nakhamchik et al. 2010). It is important to note that virulence factors of *V. europaeus* were strictly analysed here by comparative genomics. However, genetic manipulation is essential to demonstrate the role of those gene in virulence.

Due to their presence in all strains, fundamental pathogenic effectors seem to be driven by the core-secretion systems T2SS and T6SS. Virulence-related functions of T2SS includes the participation in attachment, biofilm formation and colonization, as well as the secretion to the extracellular medium of proteins capable to produce tissue disruption, such as proteases, pectinases, phospholipases, lipases, and toxins (Sandkvist 2001; Cianciotto and White 2017). In the other hand, T6SS is a cell-to-cell injector which participates in bacteria-bacteria competition and pathogenesis, existing numerous effects described in eukaryotic cells including adhesion modification, stimulating internalization, cytoskeletal rearrangements, and evasion of host innate immune responses (Smith et al. 2020; Feria and Valvano 2020). Interestingly, the redundancy of T6SS structural components found in most *V. europaeus* strains encoded in both pangenome fractions is not an unusual phenomenon in Bacteria, and may reflects the importance of niche-competition (Sarris et al. 2011; Santos et al. 2020).

The T3SS, a recognized virulence factor of Gram-negative bacteria capable to inject effectors of variable functions into host cells (Cornelis and Van Gijsegem 2000; Park et al. 2004; Osorio 2018), is present in all the *V. europaeus* strains except for the first V. europaeus isolated strain EX1, suggesting a recent horizontal acquisition of that operon (Brown and Finlay 2011). The gene set found in our *V. europaeus* collection correspond to T3SS1 described in *V. parahaemolyticus*, that has been reported to be mainly related to biofilm formation, motility and cytotoxicity (Hiyoshi et al. 2010; Calder et al. 2014).

Due the remarkable absence of T3SS in pathogenic strain EX1, its role in the pathogenicity of the species would deserve further investigation.

Genes *vemA* and *prtV* encoding for M4 metalloproteinases and *colA* and *colP* encoding for collagenases, and seven hemolysin toxins were encoded in the *V. europaeus* core-genome. Metalloproteinases VemA and PrtV and their homologues were found related to virulence factor such as proteolysis and colonization in a broad range of *Vibrio* taxa, such as *V. cholerae*, *V. anguillarum*, *V. aestuarianus*, *V. coralliilyticus*, *V. neptunius*, and *V. splendidus* (Vaitkevicius et al. 2006; Binesse et al. 2008; Hasegawa et al. 2008; Varina et al. 2008; Mo et al. 2010; Galvis, Barja, et al. 2021). In a previous study, Martinez *et al.* (2022) determined that *V. europaeus* type strain CECT8136 mutant defective in the *vemA* gene resulted in a slightly slow pathogenic process in larvae and juveniles of Manila clam and presented a deprecated chemotaxis to the clam mucus.

Accessory genes related to virulence and mainly the anti-phage defence systems associated explained the intra-specific variability of *V. europaeus* in groups formed by more than one strain better than the phylogenetic clusters based on the core-genome. Thus, we could observed genetic differences among clonal strains (clonal strains were previously defined due to the low number SNPs among core genes). Interestingly, several VPFs can coexist in a close temporal and even physical space, as is the case of VFP1 and VFP2 (PC Ia), VFP3 and VFP4 (PC Ib), VFP5 and VFP6 (PC Ib), and VFP10 and VFP11 (PC Iib). Despite the variability of VFPs showed by *V. europaeus* genomes, there are subtle differences in the number of genes, and therefore their relevance on pathogenicity of the species is questionable. The scarcity of virulence-related genes in the accessory genome of *V. europaeus* points to a lesser importance of horizontal gene transfer mechanisms in defining the virulence of this species (Jackson et al. 2011).

All the studied *V. europaeus* strains, only showed resistance to cephalexin and erythromycin and they were sensitive to most of the antibiotics tested. This fits with previous studies that showed high prevalence of macrolides and cephalosporins antibiotic resistance genes among *Vibrio* species, including the aquaculture pathogen *V. parahaemolyticus* (Albini et al. 2022; Ha et al. 2023). Interestingly, erythromycin appears cited as a vibriosis control agent in aquaculture (Campa-Córdova et al. 2006; Dubert, Barja, and Romalde 2017b). It is important to note that four strains isolated from

Spanish Hatchery B between May and July of 2012, were antibiotic multiresistant. This demonstrates that hatcheries are reservoirs of antibiotic resistances genes (Dubert, Osorio, Prado, et al. 2016). Hatcheries and bivalves are optimal environments to stimulate the bacterial acquisition and fixation of antibiotic resistances, due to the extended use of antibiotic compounds to prevent and control bacterial diseases, and the capacity of bioaccumulation of antibiotics in bivalve tissues (Dubert, Barja, and Romalde 2017b; Baralla et al. 2021; Kijewska et al. 2023). This highlights the risk of using antibiotics in shellfish aquaculture to prevent and control bacterial diseases despite most of the antibiotics tested can be useful to fight *V. europaeus* (Dubert, Barja, and Romalde 2017b; Kijewska et al. 2023; Baralla et al. 2021). The genetic basis of resistance to cephalosporins in *V. europaeus* has not been determined in this work, and may be due to specific mutations (Palace et al. 2020).

From an environmental perspective, secondary metabolites are connected to the capacity of the bacteria to occupy its ecological niche, facilitate access to a specific nutrient, competing for resources or stablishing relationships with microorganism (Giubergia et al. 2016; Modolon et al. 2020). Regarding *V. europaeus*, most of the BGCs types shared by all the studied strains (NRPS, RiPP-like, betalactone, arylpolyene, and ectoine) match with those previously described for marine vibrios (Burks et al. 2017; Alex et al. 2021), suggesting its importance for the correct performance in this environment. This idea is reinforced by the coexistence of two GCFs encoding ectoine of which, at least one is present in each *V. europaeus* genome. Thus, identified biosynthetic products common to *V. europaeus* genomes are related with nutrient acquisition and environment adaptation. A highly conserved amphibactin system was found in *V. europaeus* strains (GCF5). The amphibactin system was previously found widespread in commensal and pathogenic *Vibrio* associated to bivalve hemolymph, included *V. europaeus*, being related to the capacity to acquire iron (Galvis et al. 2020). On the other hand, ectoine and arylpoliene role may be related to bacterial fitness in osmotic and oxidative stress (Cimermancic et al. 2014; Czech et al. 2018). Due to its high prevalence in the studied *V. europaeus* strains, the ecological role of the RiPP GCF3, the arylpolyene GCF12, and the PKS-NRP hybrid families GCF1 and GCF2, must be clarified to draw the complete ecological profile of the species.

As we exposed above, our results demonstrated that intra-specific variability is mostly due to the presence of different anti-phage defence systems. This shed light on the vast -and diverse- repertoire of phage defence systems encoded by *V. europaeus*, recently named as defensome (Beavogui et al. 2024). Hence, with the only exception of a dGTPase system, all the *V. europaeus* defensome is part of the accessory genome. According to Hussain et al. (2019), protection is cumulative, and those defence systems constitute a large fraction of the accessory genome, accounting even for more than 90% of the accessory genome among closest relatives. This means the phage defence elements can evolve and transfer from cell to cell without interfering with metabolic processes required to synthesize essential cell surface molecules (Hussain et al. 2021). The association of anti-phage system genes to accessory genome reflects the host's adaptation in the arms-race phage-bacteria. This idea is supported by the presence of multiple defence profiles in a close temporal and physical space, especially in strains belonging the same phylogenetic cluster (Bernheim and Sorek 2020; Rocha and Bikard 2022; Botelho et al. 2023). Understanding the defensome is important when considering the therapeutic use of phages in aquaculture. In this sense, phage therapy could be not effective against *V. europaeus* due to the important and diverse defence arsenal encoded by the accessory genome. Some authors have demonstrated the rapid acquisition of bacterial resistance against phages offers a parallel to the spread of antibiotic resistance on plasmids in bacteria (Hussain et al. 2021). Then, the routine administration of a phage cocktail in shellfish aquaculture could be problematic.

CHAPTER 3: STRUCTURAL ORGANIZATION OF THE ACCESSORY GENOME AND ITS RELATIONSHIP WITH THE MOBILOME OF *V. europaeus*

3.1 Introduction

The accessory genome is formed by: (i) genes that are present in most individuals of the studied clade (known as shell core or persistent genome), conceptually similar to the core genome but it is more adapted to large-scale genomic comparisons as it allows for missing genes due to punctual evolutionary loss events or technical reasons, such as assembly or gene calling artifact (Bazin et al. 2020); (ii) genes that are conserved between some individuals of the group but not most (known as shell soft genome or shell genome) and (iii) genes that are rare within the population and found only in one or a few individuals (known as cloud genome) (Page et al. 2015; Bazin et al. 2020). As most newly acquired genes are expected to arise from horizontal gene transfer (HGT) events, it is expected that most of the genes included in the shell and cloud genomes have a non-vertical origin (Bazin et al. 2020). HGT is a major source of variability in prokaryotic genomes and allows an efficient niche adaptation (Narra and Ochman 2006; Dobrindt et al. 2010). HGT is mediated by three main mechanisms: (i) transformation, which involves the capture of external free DNA by bacteria; (ii) transduction, which involves the mediation of phage components to transfer DNA between bacterial hosts; and (iii) conjugation, the direct transfer of DNA between two adjacent bacteria via pili structures (Thomas and Nielsen 2005).

The accessory genome is organized principally into polymorphic strain-specific DNA segments that are missing in at least one of the genomes analysed (Ogier et al. 2010). These segments are named regions of genomic plasticity (RGPs), which are clusters of genes located in highly variable genomic regions (Ogier et al. 2010; Bazin et al. 2020). RGPs are inserted in spots of insertion, which are more active than the rest of the genome in terms of acquisition rate of new elements and tend to have a much more diverse gene content even between closely related individuals (Bazin et al. 2020). Most of the RGPs arose from HGT and correspond to genomic islands (GIs) (Bazin et al. 2020). GIs are clusters of consecutive genes found in the accessory genome,

characterized by their large size (> 10 Kb) with a different G+C content that the rest of the host's chromosome for recent acquisitions and are often associated with mobile genetic elements (MGEs) (Bazin et al. 2020).

MGEs are genetic material capable of intra- and intercellular mobility and the entire set of MGEs in a genome constitute the microbial mobilome (Carr et al. 2021; Botelho, Cazares, and Schulenburg 2023). The microbial mobilome include transposons, integrons, integrative and conjugative/mobilizable elements (ICEs/IMEs), microsatellites, prophages, plasmids, among others (Siefert 2009; Carr et al. 2021). In some cases, MGEs could progressively lose their capacity to move due to mutation or deletion of the genes that constitute the mobility mechanisms (Bellanger et al. 2014).

Plasmids are extra-chromosomal DNA molecules capable of autonomous replication of chromosomes. Plasmid size is largely variable, from less than one kilobase to megabases, being usually the largest components of the mobilome (Dagan, Artzy-Randrup, and Martin 2008; Siefert 2009; Carr et al. 2021). According to their ability to move, plasmids can be characterized as conjugative, mobilizable or non-mobilizable. Conjugative plasmids are those that encode in their sequence the machinery necessary to be transmitted by conjugation, which it is the most important transfer mechanism of plasmids. This is made up of four components: (i) an origin of transfer (oriT); (ii) a relaxase; (iii) a type IV coupling protein (T4CP); (iv) and a mating pair formation (MPF) complex encoded by the T4SS genes that facilitates the assembly and functionality of the mating channel (Smillie et al. 2010; Thomas and Nielsen 2005). Mobilizable plasmids are those whose transfer is dependent on their association with other conjugative plasmids. This is because they lack at least the MPF and it uses an MPF of another genetic element present in the cell (Smillie et al. 2010). These plasmids tend to be of small size (<30kb) (Siefert 2009; Smillie et al. 2010). Some plasmids are non-mobilizable because they are neither conjugative nor mobilizable (Smillie et al. 2010). They can be transmitted by transduction, natural transformation, or cointegration in mobile plasmids (Smillie et al. 2010). Most very large plasmids are non-mobilizable, with evidence of domestication into secondary chromosomes (Smillie et al. 2010).

ICEs/IMEs are a diverse group of genetic elements found in bacteria that can integrate into the bacterial chromosome or a plasmid, ranged from 10-700 kb for ICEs and 2-50 kb for IMEs (Bellanger et al. 2014; Guédon et al. 2017). ICEs have the ability

to excise from the host genome, transfer through conjugation, and re-integrate into the host DNA. In contrast, IMEs need the conjugation machinery of co-resident conjugative elements to transfer (Bellanger et al. 2014; Delavat et al. 2017).

Prophages are products of the lysogenic cycle of a phage, which involves the insertion of the phage genome into the host. It can be integrated either into the host's genome (integrated phage), or take the form of a linear or circular plasmid (plasmid prophages) (Canchaya et al. 2003). Prophages can return to their active form through the lytic cycle or degenerate into residual forms through the inactivation of their genes (Canchaya et al. 2003).

Phage satellites act as parasites of bacterial phages, using their machinery to transcribe and transmit horizontally between bacteria (de Sousa et al. 2023). Although the molecular mechanisms by which phage satellites exploit helper phages are diverse, they have a significant impact on phage-bacteria interactions. Four families of phage satellites have been identified to the date based on their genetic diversity and taxonomic distributions. These families are P4-like, phage-inducible chromosomal islands (PICI), capsid-forming PICI, and PICI-like elements (PLE) (de Sousa et al. 2023).

MGEs often harbour genes conferring selective advantages, such as virulence genes, antibiotic resistance genes (ARGs) and anti-phage defence systems, which aid to bacterial niche adaptation, shaping bacterial evolution and dissemination of these traits (Rodriguez-Valera, Martin-Cuadrado, and López-Pérez 2016; Carroll and Wong 2018; Patel and Maxwell 2023). These traits act as a trade-off for the survival of MGEs in bacterial genomes, since hosts tend to eliminate unnecessary genetic material to avoid metabolic burden (Dionisio et al. 2005; Carroll and Wong 2018; Ramisetty and Sudhakari 2019; Taylor et al. 2019). For instance, in the case of plasmids, although cryptic plasmids exist, have traditionally been classified by their function such as: (i) Col plasmids, which are involved in bacterial killing; (ii) resistance plasmids, which carry ARGs; (iii) degradative plasmids, which allow the digestion of unusual substrates; or (iv) virulence plasmids, which encode genes involved in pathogenicity (Siefert 2009). In the same way, ICEs/IMEs are also classified according to their function, including fitness islands, virulence islands, secretion islands, defence islands, ecological islands, saprophytic islands, resistance islands, symbiosis islands, metabolic islands, and

symbiosis islands among others identified (Patel 2016; Hochhauser, Millman, and Sorek 2023).

Therefore, understanding the structural organization of the accessory genome might shed light on the evolution of the *V. europaeus* related to the composition of the mobilome and the mechanisms underlying horizontal gene transfer with biological implications for the bacterial survival and adaptation under environmental stress.

3.2 Results

3.2.1 Characterization of the *V. europaeus* plasmidome

The *V. europaeus* plasmidome was formed by a total of 52 plasmids and they were classified around five different groups (Table 3.1): pVE1-like plasmids (size range: 308.9–419.27 kb; n= 38), pVE2-like plasmids (64.02–82.13 kb; n= 8), pVE3-like plasmids (168.72–168.83 kb; n= 4), pVE4 (41.65 kb; n=2), and pVE5 (71.05 kb; n=1).

Plasmids pVE1-like were present in most strains (n=38/39), including Spanish, French (excluding only the strain 07/115 T1), American, and Chilean strains (Table 3.1). Interestingly, pVE1-like plasmids were the only one in 29 strains (Table 3.1.). Some strains harboured two plasmids through the combination of plasmids pVE1-like with other plasmids, such as: (i) pVE2-like (CECT8136 and 2930); (ii) pVE3 (3614); (iii) pVE4 (L3); and (iv) pVE5 (CECT8427) (Table 3.1). In addition, some strains harboured even three plasmids, such as: (i) 3610, 3454, and 3492 (pVE1-like, pVE2-like, and pVE3-like) or L3 and L20 (pVE1-like, pVE2-like, and pVE4) (Table 3.1).

V. europaeus plasmids could not taxonomically classified because any plasmid taxonomic unit (PTU) was identified by COPLA. However, other closely related plasmids were found in the COPLA's database (Table 3.1): (i) p251 (NZ_CP009356.1; *V. tubiashii* ATCC 19109) with pVE1-like; (ii) p57 (NZ_CP009358.1; *V. tubiashii* ATCC 19109) with pVE2-like; and (iii) p1 (CP092386.1; *Vibrio gigantis* LMG 22741) with pVE3-like plasmids. Although no related plasmids were found for pVE4 and pVE5, significative similarities matched in short regions (2% and 1%, respectively, e-value = 0.0) with *V. tubiashii* ATCC 19109 plasmid p48 (CP009359.1) and *Vibrio* sp. THAF190c plasmid pTHAF190c_e (CP045343.1) (Table 3.1).

Despite any oriT sequences were identified from the plasmidome, most of the *V. europaeus* plasmids were conjugatives because most of pVE1-like and all pVE2-like and pVE3-like plasmids encoded the whole conjugative machinery (relaxases; the type IV coupling protein, T4CP; and the gene cluster for the bacterial type IV secretion system, T4SS) (Table 3.1). Interesting exceptions were found in the pVE1-like plasmids (Table 3.1 and Fig. 3.3): (i) pVE1 from the strain 07/108 T1 and from the fully resolved assembly NPI-1, only contained the relaxase gene and, thus, were considered mobilizable (Table 3.1; Fig. 3.3); (ii) some T4CP and T4SS genes were missing in two

strains (NPI-1 and 07_108_t1). In the conjugative pVE1-like, the relaxase and the T4CP genes (TrwB_AAD_bind/TraD; Table 3.1) were located very close on the backbone (Fig. 3.3) and they encoded a T4SS (Table 3.1; Fig. 3.3). On the other hand, pVE4 lacked the T4CP genes and thus it was classified as mobilizable. Interestingly, pVE5 was classified as potentially mobilizable because it encoded the T4SS and T4CP genes but any known relaxase was identified (Table 3.1).

Regarding relaxase families, pVE1-like and pVE2-like plasmids contained a relaxase from the MOBF family, while pVE3-like and pVE4 harboured relaxases from the MOBH and MOBC families (Table 3.1). Interestingly, a second relaxase (MOBC) was found in the pVE1 plasmids of three French strains (07/121 T1, 07/112 T1 and 07/110 T1, belonging to subcluster IIa based on the core-genome phylogeny) (Table 3.1).

Plasmids pVE1-like were indeed the MGEs encoding the highest number of virulence traits, defence systems, and secondary metabolites production and a significant number of anti-phage defence systems (Fig. 3.4). No traits were found in pVE2 to pVE5, while pVE1 annotation revealed a wide variety of traits, accounting in the *V. europaeus* accessory genome the 32.90% of the defence systems, 59.61% of the virulence-related genes, and 94.91% of the BGCs (Fig. 3.4).

Table 3.1. List of plasmids identified in the *V. europaeus* genomes, as well as the elements of the conjugation machinery detected and possible related plasmids.

Strain	Plasmid	Size (kb)	Relaxase	T4CP(n)	MPF(T4SS)	Integrase(n)	Related plasmid
EX1	pVE1	330.1	MOBF	TrwB_AAD_bind, FtsK_SpoIIIE, TraD_N	TraG_F, TraH_F, TraH_F, TraB_F, TraF_F, TraN_F, TraN_F, TrbC_F, TraU_F, TraC_F, TraC_F, TraC_F, TraC_F, TraC_F, TraB_F, TraK_F, TraE_F, TraE_F, TraL_F, TraA_F	Phage_integrase, rve	NZ_CP009356.1
2895		329.0	MOBF	TrwB_AAD_bind	TraA, F_traL, TraE, TraK, F_traB, F_traV, virb4, F_traW, F_traU, F_trbC, F_traN, TraF, F_traF, F_traH, F_traG	Phage_integrase, rve	
2909		386.1	MOBF	TrwB_AAD_bind (2)	TraA, F_traL, TraE, TraK, F_traB, F_traV, virb4, F_traW, F_traU, F_trbC, F_traN, TraF, F_traF, F_traH, F_traG	Phage_integrase	
2930		329.3	MOBF	TrwB_AAD_bind	TraA, F_traL, TraE, TraK, F_traB, F_traV, virb4, F_traW, F_traU, F_trbC, F_traN, TraF, F_traF, F_traH, F_traG	Phage_integrase, rve	
2945		329.0	MOBF	TrwB_AAD_bind	TraA, F_traL, TraE, TraK, F_traB, F_traV, virb4, F_traW, F_traU, F_trbC, F_traN, TraF, F_traF, F_traH, F_traG	Phage_integrase, rve	
2951		329.0	MOBF	TrwB_AAD_bind	TraA, F_traL, TraE, TraK, F_traB, F_traV, virb4, F_traW, F_traU, F_trbC, F_traN, TraF, F_traF, F_traH, F_traG	Phage_integrase, rve	
2967		386.1	MOBF	TrwB_AAD_bind (2)	TraA, F_traL, TraE, TraK, F_traB, F_traV, virb4, F_traW, F_traU, F_trbC, F_traN, TraF, F_traF, F_traH, F_traG	Phage_integrase	
2968		329.0	MOBF	TrwB_AAD_bind	TraA, F_traL, TraE, TraK, F_traB, F_traV, virb4, F_traW, F_traU, F_trbC, F_traN, TraF, F_traF, F_traH, F_traG	Phage_integrase, rve	
2969		329.0	MOBF	TrwB_AAD_bind	TraA, F_traL, TraE, TraK, F_traB, F_traV, virb4, F_traW, F_traU, F_trbC, F_traN, TraF, F_traF, F_traH, F_traG	Phage_integrase, rve	
2971		329.0	MOBF	TrwB_AAD_bind	TraA, F_traL, TraE, TraK, F_traB, F_traV, virb4, F_traW, F_traU, F_trbC, F_traN, TraF, F_traF, F_traH, F_traG,	Phage_integrase, rve	
2974		386.1	MOBF	TrwB_AAD_bind (2)	TraA, F_traL, TraE, TraK, F_traB, F_traV, virb4, F_traW, F_traU, F_trbC, F_traN, TraF, F_traF, F_traH, F_traG	Phage_integrase	
2975		329.0	MOBF	TrwB_AAD_bind	TraA, F_traL, TraE, TraK, F_traB, F_traV, virb4, F_traW, F_traU, F_trbC, F_traN, TraF, F_traF, F_traH, F_traG	Phage_integrase, rve	
3454		330.0	MOBF	TrwB_AAD_bind	TraA, F_traL, TraE, TraK, F_traB, F_traV, virb4, F_traW, F_traU, F_trbC, F_traN, TraF, F_traF, F_traH, F_traG	Phage_integrase, rve	
3492		329.4	MOBF	TrwB_AAD_bind	TraA, F_traL, TraE, TraK, F_traB, F_traV, virb4, F_traW, F_traU, F_trbC, F_traN, TraF, F_traF, F_traH, F_traG	Phage_integrase, rve(2)	
3610		329.1	MOBF	TrwB_AAD_bind	TraA, F_traL, TraE, TraK, F_traB, F_traV, virb4, F_traW, F_traU, F_trbC, F_traN, TraF, F_traF, F_traH, F_traG	Phage_integrase, rve	

3614		329.0	MOBF	TrwB_AAD_bind	TraA, F_traL, TraE, TraK, F_traB, F_traV, virb4, F_traW, F_traU, F_trbC, F_traN, TraF, F_traF, F_traH, F_traG	Phage_integrase, rve	
L2		370.2	MOBF	TrwB_AAD_bind (2)	TraA, F_traL, TraE, TraK, F_traB, F_traV, virb4, F_traW, F_traU, F_trbC, F_traN, TraF, F_traF, F_traH, F_traG	Phage_integrase	
L20		326.8	MOBF	TrwB_AAD_bind	TraA, F_traL, TraE, TraK, F_traB, F_traV, virb4, F_traW, F_traU, F_trbC, F_traN, TraF, F_traF, F_traH, F_traG	Phage_integrase	
L3		326.6	MOBF	TrwB_AAD_bind	TraA, F_traL, TraE, TraK, F_traB, F_traV, virb4, F_traW, F_traU, F_trbC, F_traN, TraF, F_traF, F_traH, F_traG	Phage_integrase	
L4		326.5	MOBF	TrwB_AAD_bind	TraA, F_traL, TraE, TraK, F_traB, F_traV, virb4, F_traW, F_traU, F_trbC, F_traN, TraF, F_traF, F_traH, F_traG	Phage_integrase	
PP-635		326.4	MOBF	TrwB_AAD_bind	TraA, F_traL, TraE, TraK, F_traB, F_traV, virb4, F_traW, F_traU, F_trbC, F_traN, TraF, F_traF, F_traH, F_traG	Phage_integrase	
PP-654		326.4	MOBF	TrwB_AAD_bind	TraA, F_traL, TraE, TraK, F_traB, F_traV, virb4, F_traW, F_traU, F_trbC, F_traN, TraF, F_traF, F_traH, F_traG	Phage_integrase	
PP-660		326.5	MOBF	TrwB_AAD_bind	TraA, F_traL, TraE, TraK, F_traB, F_traV, virb4, F_traW, F_traU, F_trbC, F_traN, TraF, F_traF, F_traH, F_traG	Phage_integrase	
CECT8136		327.2	MOBF	TrwB_AAD_bind	TraA, F_traL, TraE, TraK, F_traB, F_traV, virb4, F_traW, F_traU, F_trbC, F_traN, TraF, F_traF, F_traH, F_traG	Phage_integrase	
PP2-843		389.5	MOBF	TrwB_AAD_bind (2)	TraA, F_traL, TraE, TraK, F_traB, F_traV, virb4, F_traW, F_traU, F_trbC, F_traN, TraF, F_traF, F_traH, F_traG	Phage_integrase	
PP2-978		385.6	MOBF	TrwB_AAD_bind (2)	TraA, F_traL, TraE, TraK, F_traB, F_traV, virb4, F_traW, F_traU, F_trbC, F_traN, TraF, F_traF, F_traH, F_traG	Phage_integrase	
NPI-1		335.7	MOBF	-	-	-	
071316f		309.0	MOBF	TrwB_AAD_bind	TraA, F_traL, TraE, TraK, F_traB, F_traV, TraC_F_IV, virb4, F_traW, F_traU, F_trbC, F_traN, TraF, F_traF, F_traH, F_traG	Phage_integrase	
CECT8427		362.6	MOBF	TrwB_AAD_bind	F_traL, TraE, TraK, F_traB, F_traV, virb4, F_traW, F_traU, F_trbC, F_traN, TraF, F_traF, F_traH, F_traG	Phage_integrase (3), rve	
07/38_2t2		393.6	MOBF	TrwB_AAD_bind	TraA, F_traL, TraE, TraK, F_traB, F_traV, virb4, F_traW, F_traU, F_trbC, F_traN, TraF, F_traF, F_traH, F_traG	Phage_integrase	
07/108_t1		309.0	MOBF	-	-	Phage_integrase	
07/110_t1		395.0	MOBF,MOBC	TrwB_AAD_bind	TraA, F_traL, TraE, TraK, F_traB, F_traV, virb4, F_traW, F_traU, F_trbC, F_traN, TraF, F_traF, F_traH, F_traG	Phage_integrase (3)	
07/112_t1		395.0	MOBF,MOBC	TrwB_AAD_bind	TraA, F_traL, TraE, TraK, F_traB, F_traV, virb4, F_traW, F_traU, F_trbC, F_traN, TraF, F_traF, F_traH, F_traG	Phage_integrase (3)	
07/116_t1		373.1	MOBF	TrwB_AAD_bind	TraA, F_traL, TraE, TraK, F_traB, F_traV, virb4, F_traW, F_traU, F_trbC, F_traN, TraF, F_traF, F_traH, F_traG	Phage_integrase (3), TIGR02224	
07/117_t1		373.2	MOBF	TrwB_AAD_bind (2)	TraA, F_traL, TraE, TraK, F_traB, F_traV, virb4, F_traW, F_traU, F_trbC, F_traN, TraF, F_traF, F_traH, F_traG	Phage_integrase (3), TIGR02224	

8426		419.3	MOBF	TrwB_AAD_bind	TraA, F_traL, TraE, TraK, F_traB, F_traV, virb4, F_traW, F_traU, F_trbC, F_traN, TraF, F_traF, F_traH, F_traG	Phage_integrase	
07/120_T1		415.2	MOBF	TrwB_AAD_bind	TraA, F_traL, TraE, TraK, F_traB, F_traV, virb4, F_traW, F_traU, F_trbC, F_traN, TraF, F_traF, F_traH, F_traG	Phage_integrase	
07/121_1T1		395.0	MOBF,MOBC	TrwB_AAD_bind	TraA, F_traL, TraE, TraK, F_traB, F_traV, virb4(2), F_traW, F_traU, F_trbC, F_traN, TraF, F_traF, F_traH, F_traG, FATA_trsC	Phage_integrase (3)	
CECT8136	pVE2	64.1	MOBF	TrwB_AAD_bind	Orf169_F, TraD_F, TraG_F, TraH_F, TraB_F, TraF_F, TraN_F, TrbC_F, TraU_F, TraW_F, TraC_F, TraC_F, TraV, TraB_F, TraK_F, TraE_F, TraL_F, TraA_F	Phage_integrase	NZ_CP009358.1
2930		64.2	MOBF	TrwB_AAD_bind	Orf169_F, TraD_F, TraG_F, TraH_F, TraB_F, TraF_F, TraN_F, TrbC_F, TraU_F, TraW_F, TraC_F, TraC_F, TraV, TraB_F, TraK_F, TraE_F, TraL_F, TraA_F	Phage_integrase	
3454		65.0	MOBF	TrwB_AAD_bind	TraF_F, TraN_F, TrbC_F, TraU_F, TraW_F, TraC_F, TraV, TraB_F, TraK_F, TraE_F, TraL_F, TraA_F	Phage_integrase	
3492		64.3	MOBF	TrwB_AAD_bind	Orf169_F, TraD_F, TraG_F, TraH_F, TraB_F, TraF_F, TraN_F, TrbC_F, TraU_F, TraW_F, TraC_F, TraC_F, TraV, TraB_F, TraK_F, TraE_F	Phage_integrase	
3610		64.2	MOBF	TrwB_AAD_bind	Orf169_F, TraD_F, TraG_F, TraH_F, TraB_F, TraF_F, TraN_F, TrbC_F, TraU_F, TraW_F, TraC_F, TraC_F, TraV, TraB_F, TraK_F, TraE_F	Phage_integrase	
L20		64.0	MOBF	TrwB_AAD_bind	TraA_F, TraL_F, TraE_F, TraK_F, TraB_F, TraV, TraC_F, TraW_F, TraU_F, TrbC_F, TraN_F, TraF_F, TraB_F, TraH_F, TraG_F	Phage_integrase	
L3		64.2	MOBF	TrwB_AAD_bind	Orf169_F, TraD_F, TraG_F, TraH_F, TraB_F, TraF_F, TraN_F, TrbC_F, TraU_F, TraW_F, TraC_F, TraC_F, TraV, TraB_F, TraK_F, TraE_F	Phage_integrase	
07/115t2		82.1	MOBF	TrwB_AAD_bind	TraA, F_traL, TraE, TraK, F_traB, F_traV, virb4, F_traW, F_traU, F_trbC, F_traN, TraF, F_traF, F_traH, F_traG, T_virB1	Phage_integrase, rve	
3454	pVE3	168.7	MOBH	t4cp2	TraF_F, TraH_F, TraG_F	Phage_integrase	NZ_CP092386.1
3492		168.7	MOBH	t4cp2	TraF_F, TraH_F, TraG_F	Phage_integrase	
3610		168.8	MOBH	t4cp2	TraF_F, TraH_F, TraG_F	Phage_integrase	
3614		168.8	MOBH	t4cp2	TraG_F, TraH_F, TraF_F	Phage_integrase	
L3	pVE4	41.7	MOBC	-	VirD4, VirB11, VirB1, TraJ_I, Tfc2, VirB10, VirB9, VirB8, VirB6, VirB5, VirB4, VirB2	-	-
L20		41.7	MOBC	-	VirD4, VirB11, VirB1, TraJ_I, Tfc2, VirB10, VirB9, VirB8, VirB6, VirB5, VirB4, VirB2	-	
CECT8427	pVE5	71.05	-	t4cp2	Tfc19,Tfc22,Tfc23,Tfc24,Tfc4,TraJ_I,Tfc16,Tfc15,Tfc14,Tfc13,Tfc12,Tfc11,Tfc11,Tfc9,Tfc8,Tfc5,Tfc4,Tfc3,Tfc2	Phage_integrase	-

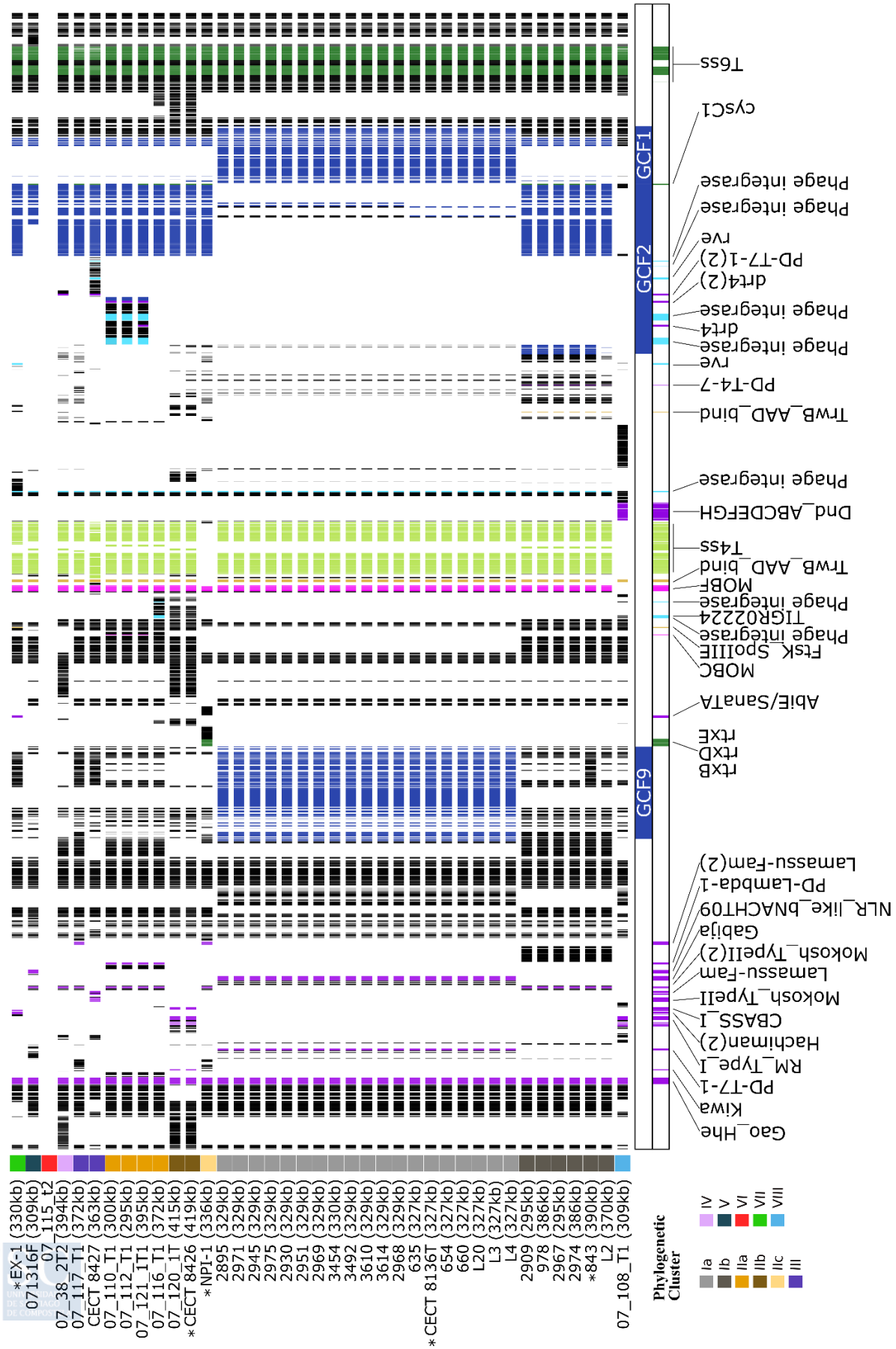
*EX-1 (330kb)
071316F (309kb)
07_115_t2
07_38_2T2 (394kb)
07_117_T1 (372kb)
CECT 8427 (363kb)
07_110_T1 (300kb)
07_112_T1 (295kb)
07_121_1T1 (395kb)
07_116_T1 (372kb)
07_120_1T (415kb)
*CECT 8426 (419kb)
*NPJ-1 (336kb)
2895 (329kb)
2971 (329kb)
2945 (329kb)
2975 (329kb)
2930 (329kb)
2951 (329kb)
2969 (329kb)
3454 (330kb)
3492 (329kb)
3610 (329kb)
3614 (329kb)
2968 (329kb)
635 (327kb)
*CECT 8136T (327kb)
654 (327kb)
660 (327kb)
L20 (327kb)
L3 (327kb)
L4 (327kb)
2909 (295kb)
978 (386kb)
2967 (295kb)
2974 (386kb)
*843 (390kb)
L2 (370kb)
07_108_T1 (309kb)
Phylogenetic Cluster
Ia
Ib
IIa
IIb
IIc
III
IV
V
VI
VII
VIII
GCF1
GCF2
GCF9
Gao_Hhe
Kiwa
PD-T7-1
RM_Type_I
Hachiman(2)
CBASS_I
Mokosh_TypeII
Lamassu-Fam
Mokosh_TypeII(2)
Gabija
NLR_like_bNACHT09
PD-Lambda-1
Lamassu-Fam(2)
rtxB
rtxD
rtxE
AbiE/SanaTA
MOBC
FtsK_SpoIIIE
Phage integrase
TIGR02224
Phage integrase
MOBF
TrwB_AAD_bind
T4ss
Dnd_ABCDEFGH
Phage integrase
TrwB_AAD_bind
PD-T4-7
rve
Phage integrase
drt4
Phage integrase
drt4(2)
PD-T7-1(2)
rve
Phage integrase
Phage integrase
cysC1
T6ss

Figure 3.3. Genetic structure of pVE1-like plasmids. Strains are arranged by phylogenetic cluster (as determined in Chapter 1). Plasmids from fully resolved assemblies are marked with an asterisk, and plasmid sizes are shown in brackets. Traits and conjugative transfer machinery are highlighted with colours: defence systems (purple), BGCs (dark blue) encoding GCF1 and GCF2 PKS-NRP hybrid, and GCF9 arylpolyene-NRPS hybrids (see Chapter 2), virulence genes (dark blue), T6SS (green), relaxase (pink), T4CP (orange), MPF (T4SS) (light green), and integrases (light blue).

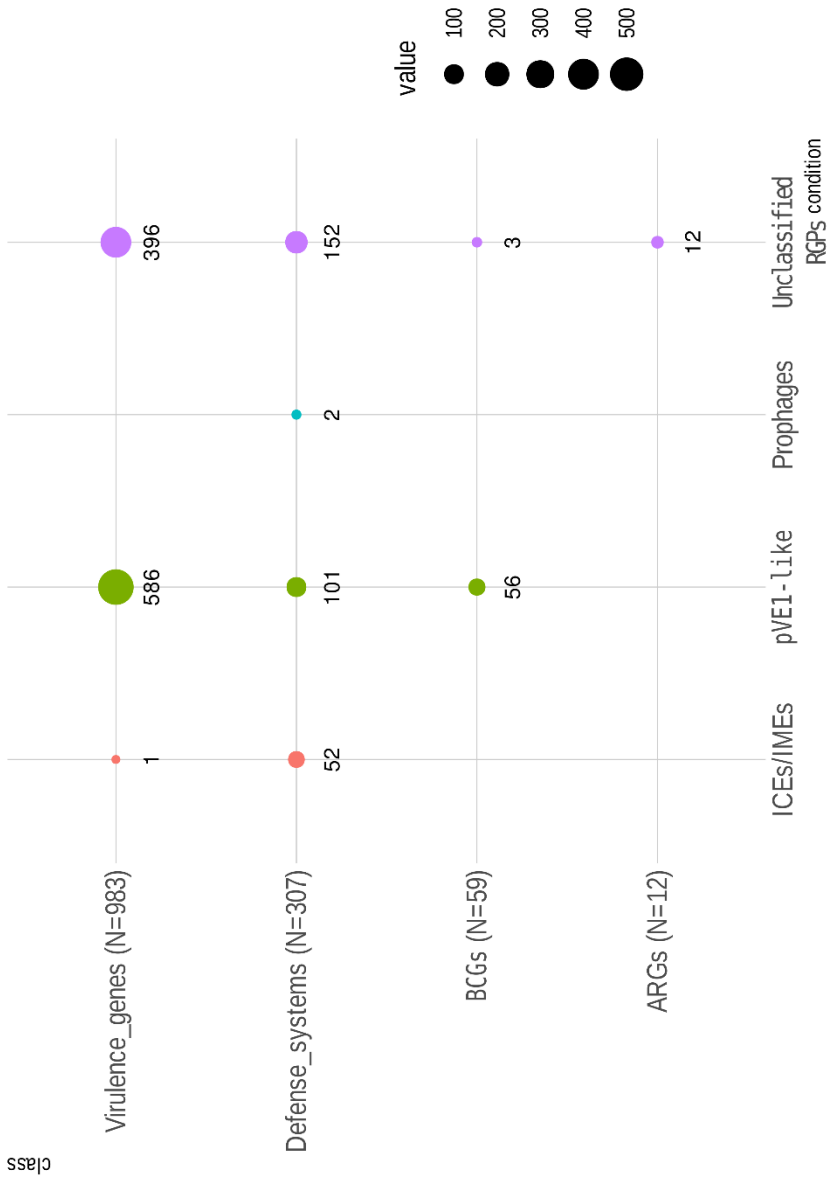

Figure 3.4. Absolute counts of traits found in ICEs/IMEs, plasmids, prophages and unclassified chromosomic RGPs found in *V. europaeus* genomes. Dot size is proportional to the total number of findings.

Strains within the same phylogenetic cluster based on the core-genome (see Chapter 1) exhibited similar defence system profiles in their pVE1-like plasmids (Fig. 3.3). For example, in addition to the Gao_Hhe system which is common to all pVE1-like plasmids, subcluster Ia harbored the Gabija and PD-T7-1 systems, while subcluster Ib the the Mokosh_TypeII systems and PD-T4-7 system, with the exception of the strains 2909 and 2967 which lacked the latter system. Subcluster IIa is characterized by two DRT_4 systems, PD-Lambda-1, and Mokosh_TypeII, though strain 07/116 T1 lacked both copies of DRT_4. Subcluster IIb displays the CBASS_I, Kiwa, and RM_Type_I systems, whereas subcluster IIc features the Lamassu-Fam and Mokosh_TypeII systems. pVE1 plasmids from Cluster III shared a similar defence system profile, including the Lamassu-Fam, PD-T7-1, and Mokosh_TypeII systems, excluding strain 07_117_T1, which lacked PD-T7-1. Cluster IV exclusively harboured the Mokosh_TypeII system, while Cluster V presents the NLR_like_bNACHT09 and Mokosh_TypeII systems. Cluster VII is characterized by the Hachiman and SanaTA systems, and Cluster VIII features the RM_Type_I and Dnd_ABCDEFGH systems (Fig. 3.3).

The most noteworthy discovery regarding virulence in the *V. europaeus* plasmidome was the presence in all pVE1-like plasmids of a complete set of structural components for the T6SS (T6SS2) (Fig. 3.3 and 3.5B), additional to the other T6SS (T6SS1; Fig. 3.5A) encoded in chromosome I (Fig. 4.5B). T6SS1 and T6SS2 synteny was very similar and only differed for the location of the tube-spike genes (TssI/VgrG and PAAR) (Fig. 3.5).

Both T6SS were classified as the i5 subtype and the TssB phylogeny of the 340 i5 T6SSs (338 from the SecReT6 database and the T6SS1 and T6SS2 from *V. europaeus* CECT 8136) clustered T6SS1 and T6SS2 within a common clade of 129 sequences (Fig. 3.6A). TssB1 and TssB2, and TssC1a and TssC2a showed an amino acid sequence homology of 77,06% and 71,40% respectively. However, amino acid sequence comparisons obtained by blastp revealed homologies below 40% among most of the core proteins such as TssA, TssC2(2), TssE, TssF, TssG, TssI/VgrG, TssJ, TssK, TssL and TssM, supporting both systems were different.

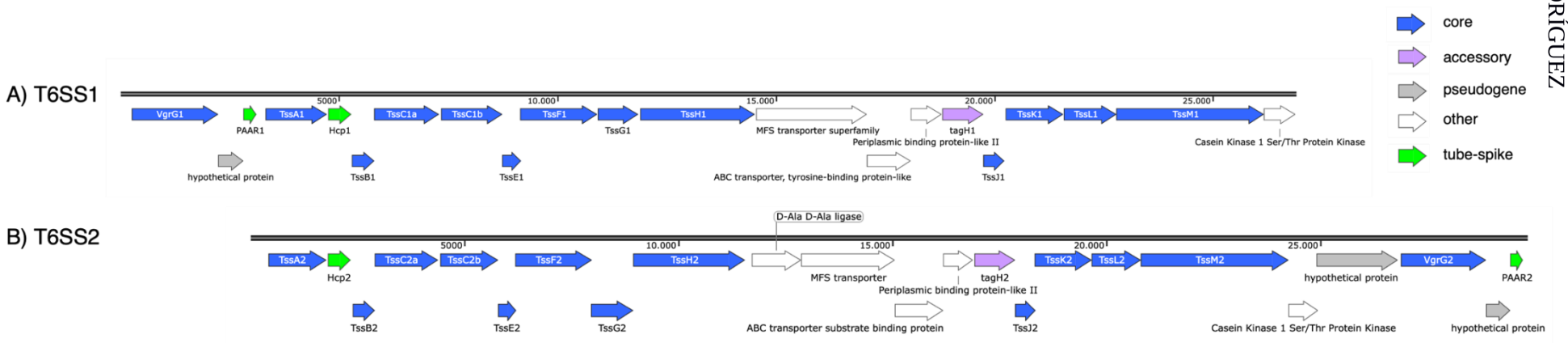

Fig. 3.5. T6SS gene clusters found in *V. europaeus* genomes. T6SS1 (A) and T6SS2 (B) were encoded in the Chromosome I and pVE1-like plasmids respectively. T6SS genes are denoted by arrows indicated the predicted direction of the transcription. Encoded proteins or domains are denoted on the genes.

Interestingly, while some strains harboured two copies of the T6SS i5, only the *V. europaeus* strains and the closely related species *V. tubiashii* ATCC 19109 house one of these copies located on a plasmid and the other one encoded in the chromosome (Fig. 3.6A).

Out of T6SS2, other virulence genes were identified in pVE1-like plasmids such as: (i) the rtx cluster (*rtxB*, *rtxD*, and *rtxE*) encoded by pVE1 of NPI-1; and (ii) single copies of the *cysC1* gene, identified in thirteen pVE1-like plasmids (Fig. 3.3). Interestingly, secondary metabolite biosynthetic genes were mainly encoded by plasmids (Fig. 3.4). Three biosynthetic gene clusters (described in Chapter 2) were present in most pVE1-like plasmids (only with the exception of the 07/108 T1 strain) (Fig. 3.3): GCF1 and GCF2, which encoded PKS-NRP hybrid polyketides and were distributed across all pVE1 plasmids (GCF1 in Cluster Ia and GCF2 in other clusters); and GCF9, which produces arylpolyene-NRPS hybrids and was only found in strains from Cluster Ia (Fig. 3.3).

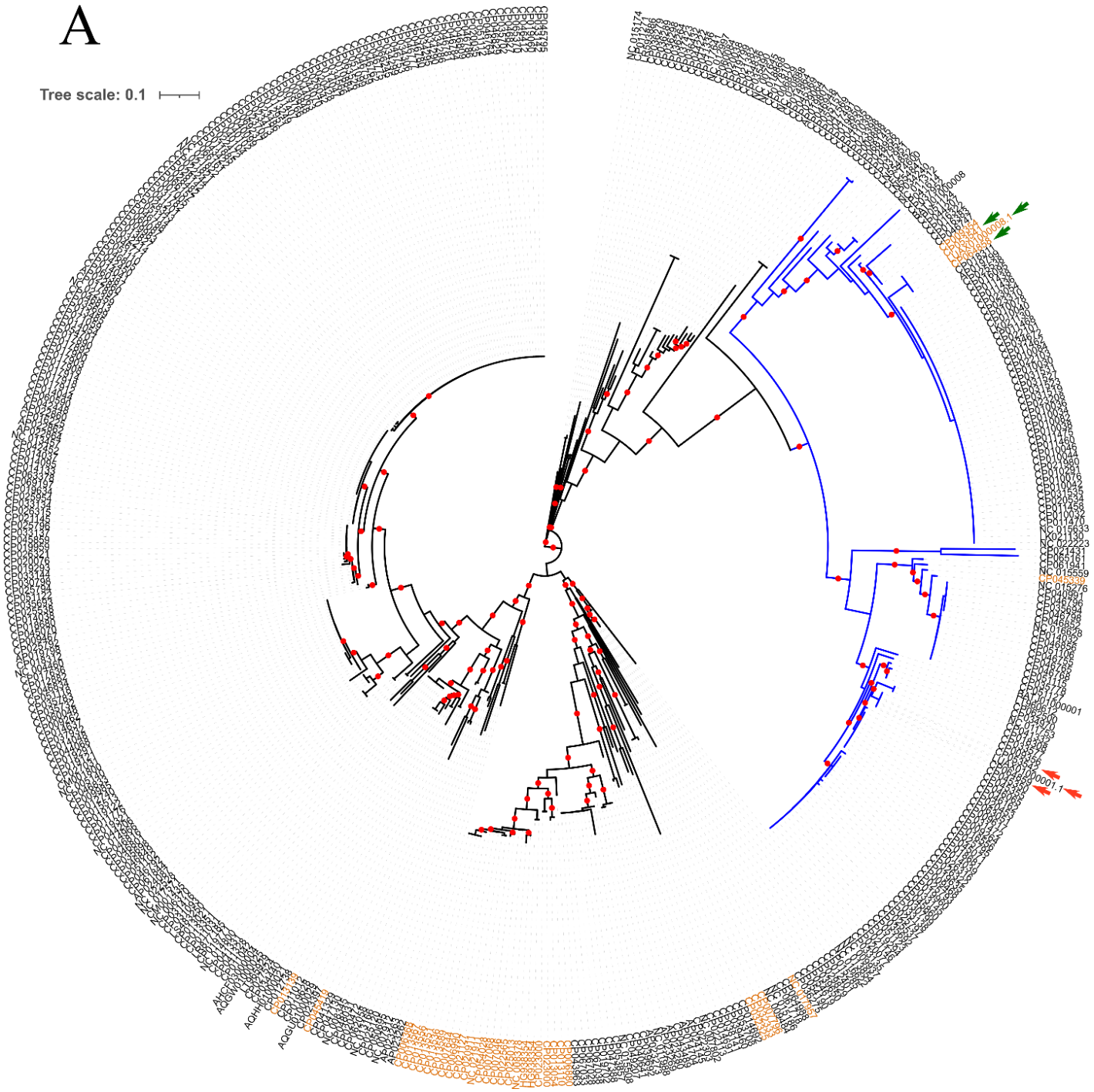

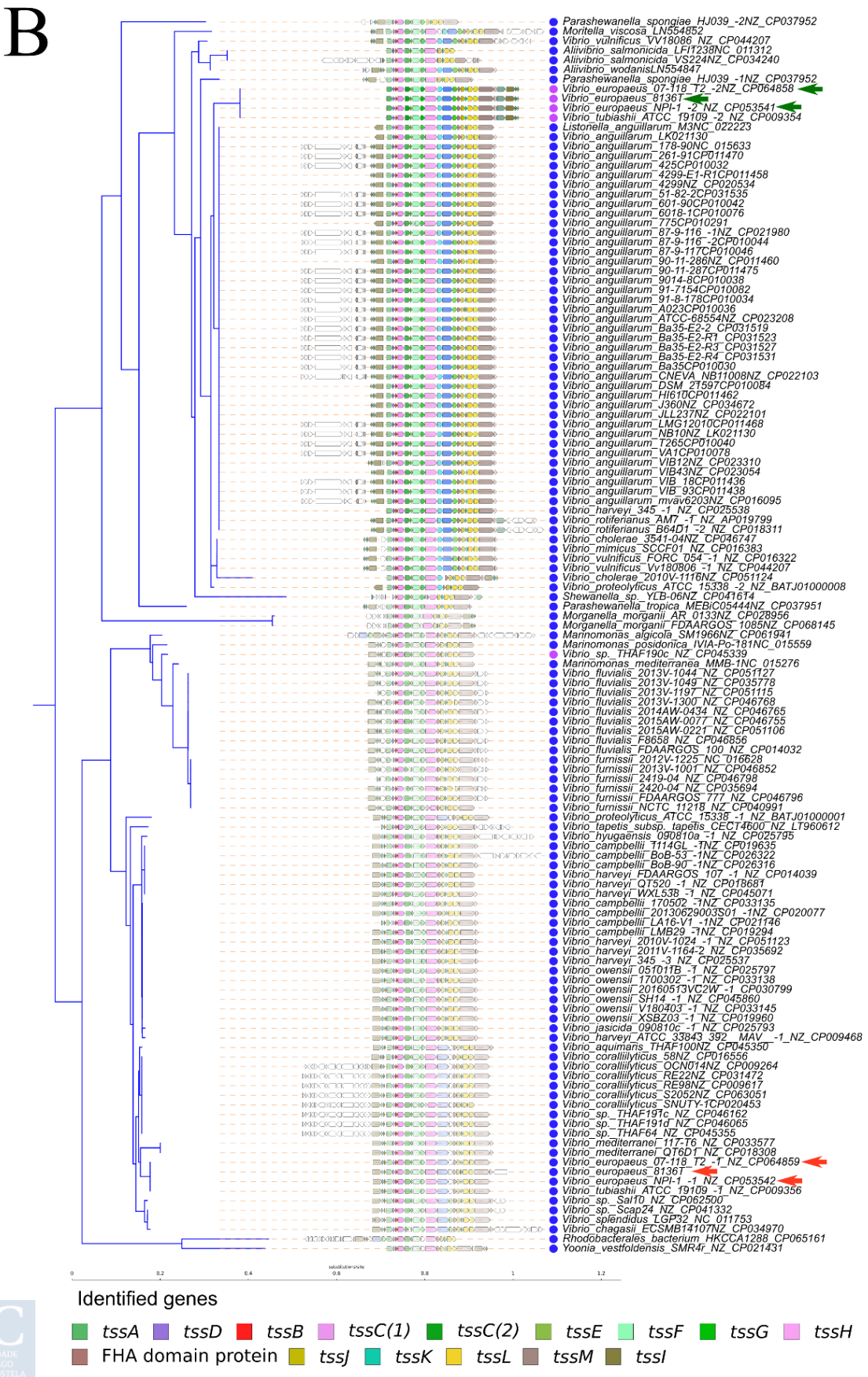
B
Parashewanella_spongiae_HJ039_-2NZ_CP037952
Moritella_viscosa_LN554852
Vibrio_vulnificus_YV18086_NZ_CP044207
Aliivibrio_salmonicida_LFI1238NC_011312
Aliivibrio_salmonicida_VS224NZ_CP034240
Aliivibrio_wodanisLN554847
Parashewanella_spongiae_HJ039_-1NZ_CP037952
Vibrio_europaeus_07-118_T2_-2NZ_CP064858
Vibrio_europaeus_8136T
Vibrio_europaeus_NPI-1_-2_NZ_CP053541
Vibrio_tubiashii_ATCC_19109_-2_NZ_CP009354
Listonella_anguillarum_M3NC_022223
Vibrio_anguillarum_LK021130
Vibrio_anguillarum_178-90NC_015633
Vibrio_anguillarum_261-91CP011470
Vibrio_anguillarum_425CP010032
Vibrio_anguillarum_4299-E1-R1CP011458
Vibrio_anguillarum_4299NZ_CP020534
Vibrio_anguillarum_51-82-2CP031535
Vibrio_anguillarum_601-90CP010042
Vibrio_anguillarum_6018-1CP010076
Vibrio_anguillarum_775CP010291
Vibrio_anguillarum_87-9-116_-1NZ_CP021980
Vibrio_anguillarum_87-9-116_-2CP010044
Vibrio_anguillarum_87-9-117CP010046
Vibrio_anguillarum_90-11-286NZ_CP011460
Vibrio_anguillarum_90-11-287CP011475
Vibrio_anguillarum_9014-8CP010038
Vibrio_anguillarum_91-7154CP010082
Vibrio_anguillarum_91-8-178CP010034
Vibrio_anguillarum_A023CP010036
Vibrio_anguillarum_ATCC-68554NZ_CP023208
Vibrio_anguillarum_Ba35-E2-2_CP031519
Vibrio_anguillarum_Ba35-E2-R1_CP031523
Vibrio_anguillarum_Ba35-E2-R3_CP031527
Vibrio_anguillarum_Ba35-E2-R4_CP031531
Vibrio_anguillarum_Ba35CP010030
Vibrio_anguillarum_CNEVA_NB11008NZ_CP022103
Vibrio_anguillarum_DSM_2T597CP010084
Vibrio_anguillarum_HI610CP011462
Vibrio_anguillarum_J360NZ_CP034672
Vibrio_anguillarum_JLL237NZ_CP022101
Vibrio_anguillarum_LMG12010CP011468
Vibrio_anguillarum_NB10NZ_LK021130
Vibrio_anguillarum_T265CP010040
Vibrio_anguillarum_VA1CP010078
Vibrio_anguillarum_VIB12NZ_CP023310
Vibrio_anguillarum_VIB43NZ_CP023054
Vibrio_anguillarum_VIB_18CP011436
Vibrio_anguillarum_VIB_93CP011438
Vibrio_anguillarum_mvav6203NZ_CP016095
Vibrio_harveyi_345_-1_NZ_CP025538
Vibrio_rotiferianus_AM7_-1_NZ_AP019799
Vibrio_rotiferianus_B64D1_-2_NZ_CP018311
Vibrio_cholerae_3541-04NZ_CP046747
Vibrio_mimicus_SCCF01_NZ_CP016383
Vibrio_vulnificus_FORC_054_-1_NZ_CP016322
Vibrio_vulnificus_Vv180806_-1_NZ_CP044207
Vibrio_cholerae_2010V-1116NZ_CP051124
Vibrio_proteolyticus_ATCC_15338_-2_NZ_BATJ01000008
Shewanella_sp._YLB-06NZ_CP041674
Parashewanella_tropica_MEBiC05444NZ_CP037951
Morganella_morganii_AR_0133NZ_CP028956
Morganella_morganii_FDAARGOS_1085NZ_CP068145
Marinomonas_algicola_SM1966NZ_CP061941
Marinomonas_posidonica_IVIA-Po-181NC_015559
Vibrio_sp._THAF190c_NZ_CP045339
Marinomonas_mediterranea_MMB-1NC_015276
Vibrio_fluvialis_2013V-1044_NZ_CP051127
Vibrio_fluvialis_2013V-1049_NZ_CP035778
Vibrio_fluvialis_2013V-1197_NZ_CP051115
Vibrio_fluvialis_2013V-1300_NZ_CP046768
Vibrio_fluvialis_2014AW-0434_NZ_CP046765
Vibrio_fluvialis_2015AW-0077_NZ_CP046755
Vibrio_fluvialis_2015AW-0221_NZ_CP051106
Vibrio_fluvialis_F8658_NZ_CP046856
Vibrio_fluvialis_FDAARGOS_100_NZ_CP014032
Vibrio_furnissii_2012V-1225_NC_016628
Vibrio_furnissii_2013V-1001_NZ_CP046852
Vibrio_furnissii_2419-04_NZ_CP046798
Vibrio_furnissii_2420-04_NZ_CP035694
Vibrio_furnissii_FDAARGOS_777_NZ_CP046796
Vibrio_furnissii_NCTC_11218_NZ_CP040991
Vibrio_proteolyticus_ATCC_15338_-1_NZ_BATJ01000001
Vibrio_tapetis_subsp._tapetis_CECT4600_NZ_LT960612
Vibrio_hyugaensis_090810a_-1_NZ_CP025795
Vibrio_campbellii_1114GL_-1NZ_CP019635
Vibrio_campbellii_BoB-53_-1NZ_CP026322
Vibrio_campbellii_BoB-90_-1NZ_CP026316
Vibrio_harveyi_FDAARGOS_107_-1_NZ_CP014039
Vibrio_harveyi_QT520_-1_NZ_CP018681
Vibrio_harveyi_WXL53B_-1_NZ_CP045071
Vibrio_campbellii_170502_-1NZ_CP033135
Vibrio_campbellii_20130629003S01_-1NZ_CP020077
Vibrio_campbellii_LA16-V1_-1NZ_CP021746
Vibrio_campbellii_LMB29_-1NZ_CP019294
Vibrio_harveyi_2010V-1024_-1_NZ_CP051123
Vibrio_harveyi_2011V-1164-2_NZ_CP035692
Vibrio_harveyi_345_-3_NZ_CP025537
Vibrio_owensii_05101B_-1_NZ_CP025797
Vibrio_owensii_1700302_-1_NZ_CP033138
Vibrio_owensii_20160513VC2W_-1_CP030799
Vibrio_owensii_SH14_-1_NZ_CP045860
Vibrio_owensii_V180403_-1_NZ_CP033145
Vibrio_owensii_XSBZ03_-1_NZ_CP019960
Vibrio_jasicida_090810c_-1_NZ_CP025793
Vibrio_harveyi_ATCC_33843_392_MAV_-1_NZ_CP009468
Vibrio_aquimarie_THAF100NZ_CP045350
Vibrio_coralliilyticus_58NZ_CP016556
Vibrio_coralliilyticus_OCN014NZ_CP009264
Vibrio_coralliilyticus_RE22NZ_CP031472
Vibrio_coralliilyticus_RE98NZ_CP009617
Vibrio_coralliilyticus_S2052NZ_CP063051
Vibrio_coralliilyticus_SNUTY-1CP020453
Vibrio_sp._THAF187c_NZ_CP046162
Vibrio_sp._THAF191d_NZ_CP046065
Vibrio_sp._THAF64_NZ_CP045355
Vibrio_mediterranei_117-T6_NZ_CP033577
Vibrio_mediterranei_QT6D1_NZ_CP018308
Vibrio_europaeus_07-118_T2_-1_NZ_CP064859
Vibrio_europaeus_8136T
Vibrio_europaeus_NPI-1_-1_NZ_CP053542
Vibrio_tubiashii_ATCC_19109_-1_NZ_CP009356
Vibrio_sp._Sal1D_NZ_CP062500
Vibrio_sp._Scap24_NZ_CP041332
Vibrio_splendidus_LGP32_NC_011753
Vibrio_chagasii_ECSMB14107NZ_CP034970
Rhodobacterales_bacterium_HKCCA1288_CP065161
Yoonia_vestfoldensis_SMR4r_NZ_CP021431
0
0.2
0.4
0.6
0.8
1
1.2
Identified genes
tssA
tssD
tssB
tssC(1)
tssC(2)
tssE
tssF
tssG
tssH
FHA domain protein
tssJ
tssK
tssL
tssM
tssI

Figure 3.6. (A) Phylogenetic relationship of T6SS i5 sequences based on the core TssB protein (168 aa) and (B) Genetic structure and homology among T6SS-core proteins (TssA-M). Phylogenetic tree was constructed using the maximum likelihood method implemented in CORASON. The blue branch highlights the minimal clade containing both plasmidic (T6SS2) and chromosomal T6SS (T6SS1) from *V. europaeus*. Tags with NCBI sequence IDs are highlighted in orange if the T6SS is encoded in a plasmid. Arrows indicated the *V. europaeus* T6SS sequences, with green arrows for T6SS2 and red arrows for T6SS1. Red circles denote bootstrap values above 70. Proteins homologous to the reference sequence are shown with an e-value cutoff of 1E-15 and are color-coded to represent different levels of homology. The intensity of the colours indicates the degree of homology with the reference sequence.

3.2.2 Identification and characterization of chromosomic RGPs

We have obtained a dataset composed by a total of 1135 chromosomic RGPs from *V. europaeus* genomes, 531 had a size between 3-10kb, 335 between 10-19kb, 180 between 19-35kb, 81 between 36-50kb, and 8 between 50-66kb.Among those chromosomic RGPs, 895 were assigned to a spot of insertion. RGPs not assigned to any spot (n=241), referred as decontextualized RGPs, were predominant in no fully-resolved genomes. Thus, a genomes fragmentation was positively correlated with the number of decontextualized RGPs (tau = 0.6738, p-value = 6.708e-09; Fig. 3.7).

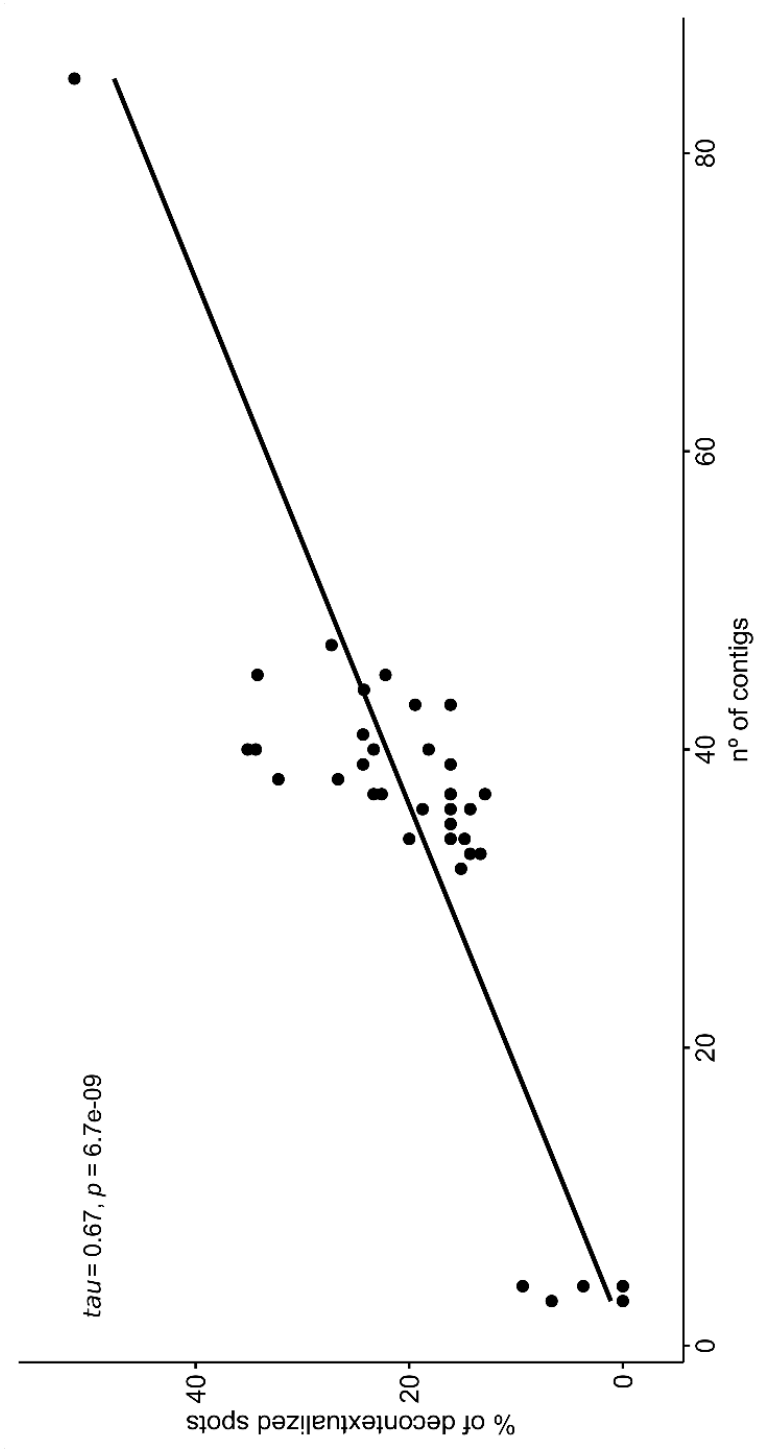

Fig 3.7. Correlation between genome fragmentation and number of decontextualized chromosomic RGPs. tau = 0.6738, p-value = 6.708e-09.

A total of 78 insertion spots were identified for RGPs, with 53 spots containing multiple RGPs (3-39 RGPs) and 25 spots containing single RGPs (Fig. 3.8). Based on mutation distances and applying a Jaccard Index cutoff of 0.394, a network of 228 RGP families was established. The spot of insertion was identified for 159 families whereas were assigned to 69 families were not assigned to any spot and, thus, composed of decontextualized RGPs (labelled as NS.1 to NS.69 on Fig. 3.8). Interestingly, three families contained RGPs from different insertion spots (24/55.1, 37/62.1, and 28/51/53.1) (Fig. 3.8). A total of 78 insertion spots were identified for RGPs, with 53 spots containing multiple RGPs (3-39) and 25 spots containing single RGPs (Fig. 3.8). Based on mutation distances and applying a Jaccard Index cutoff of 0.394, a network of 228 RGP families was established. The spot of insertion was identified for 159 families whereas were assigned to 69 families were not assigned to any spot and, thus, composed of decontextualized RGPs (labelled as NS.1 to NS.69 on Fig. 3.8). Interestingly, three families contained RGPs from different insertion spots (24/55.1, 37/62.1, and 28/51/53.1) (Fig. 3.8).

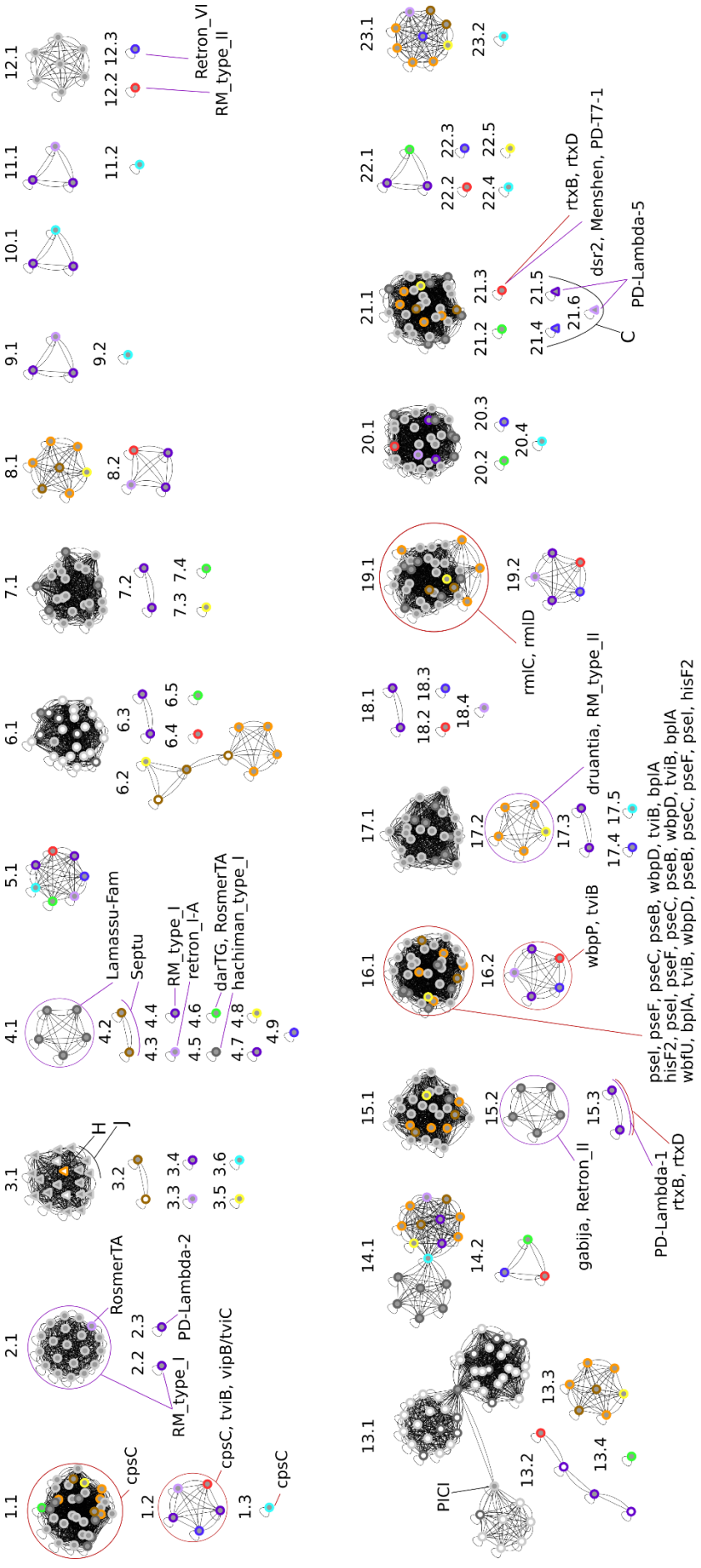

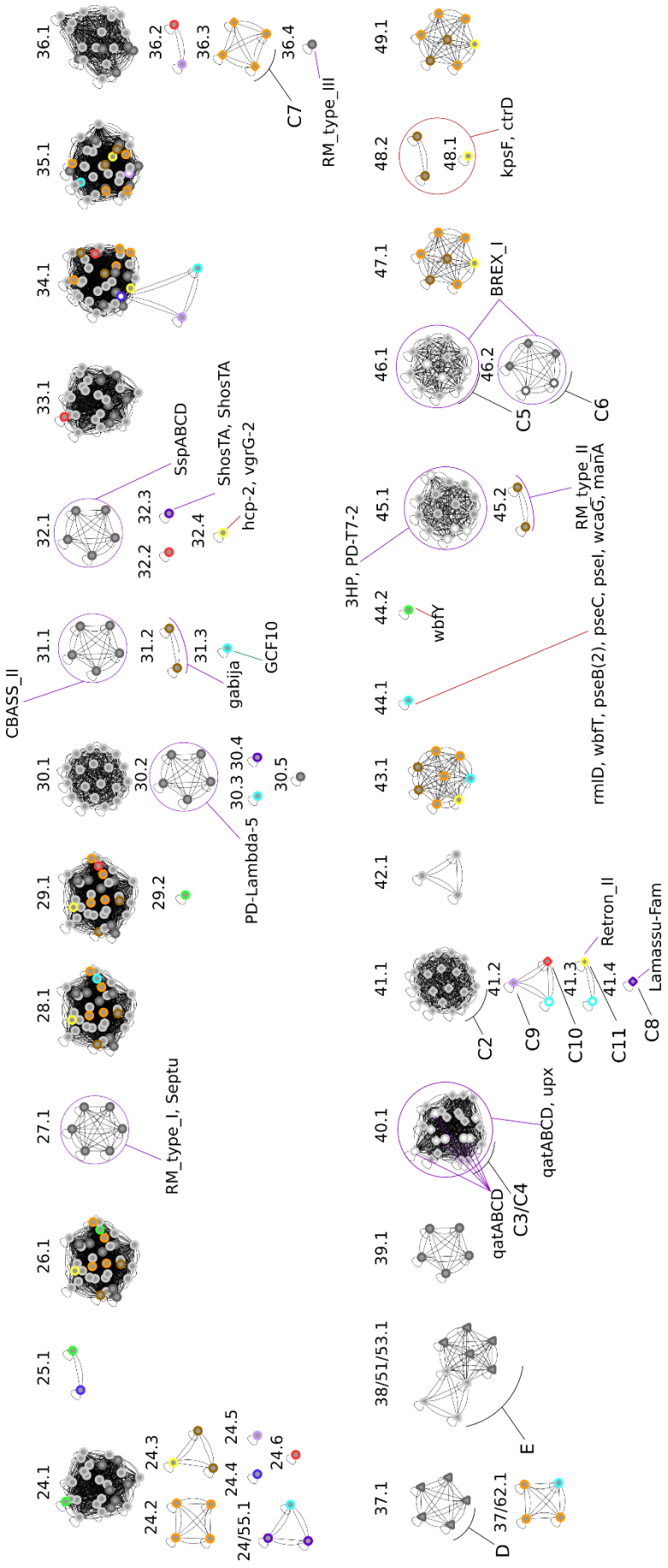
24.1
24.2
24.3
24.4
24/55.1
24.5
24.6
25.1
26.1
27.1
RM_type_I, Septu
28.1
29.1
29.2
30.1
30.2
30.3 30.4
30.5
PD-Lambda-5
CBASS_II
31.1
31.2
31.3
gabija
GCF10
32.1
32.2
32.3
SspABCD
32.4
ShosTA, ShosTA
hcp-2, vgrG-2
33.1
34.1
35.1
36.1
36.2
36.3
36.4
C7
RM_type_III
37.1
D
37/62.1
38/51/53.1
E
39.1
40.1
qatABCD
C3/C4
qatABCD, upx
41.1
41.2
C2
C9
41.3
C10
Retron_II
41.4
C11
C8
Lamassu-Fam
42.1
43.1
44.1
rmlD, wbfT, pseB(2), pseC, psel, wcaG, manA
44.2
wbfY
3HP, PD-T7-2
45.1
45.2
RM_type_II
46.1
46.2
C5
BREX_I
C6
47.1
48.1
48.2
kpsF, ctrD
49.1

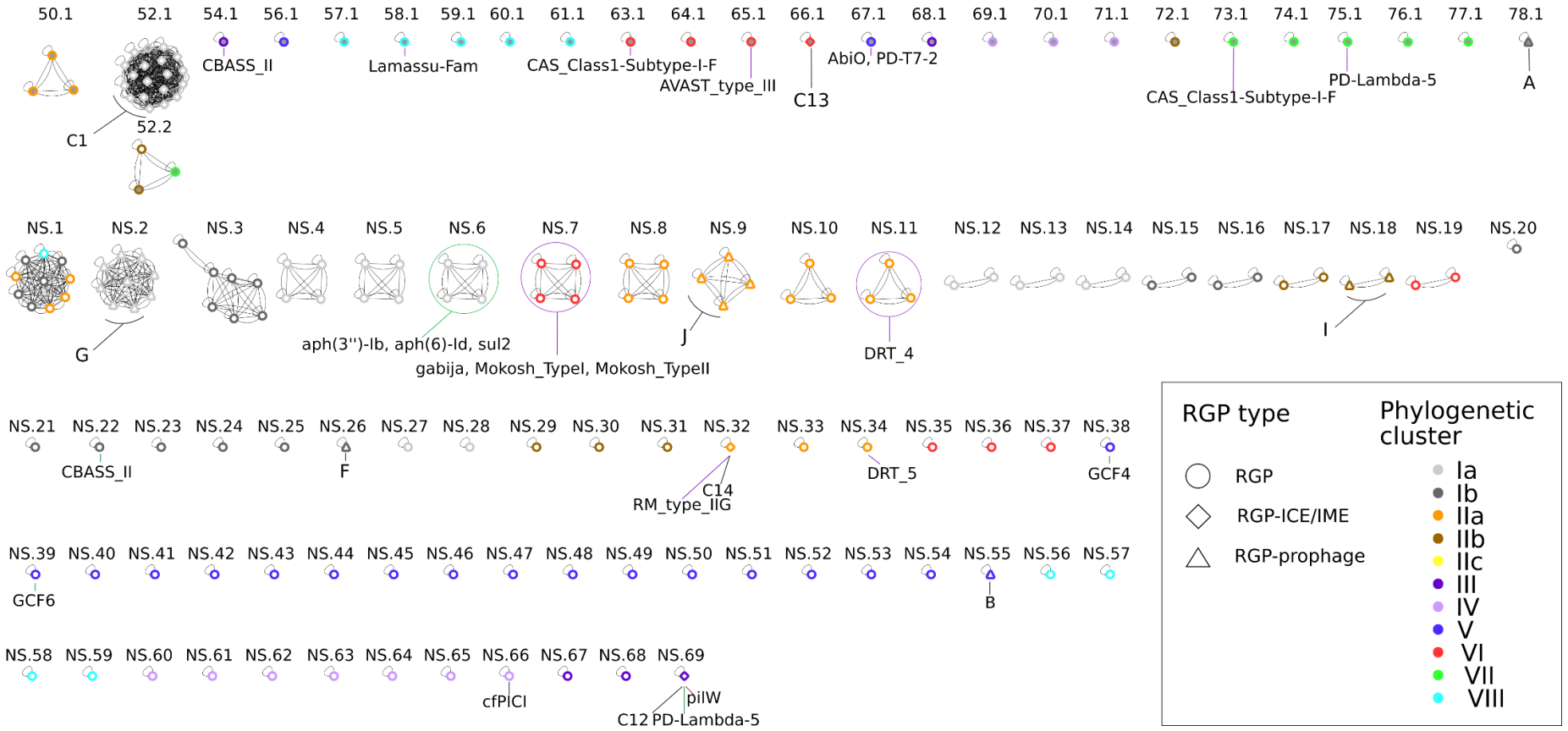
50.1
52.1
54.1
56.1
57.1
58.1
59.1
60.1
61.1
63.1
64.1
65.1
66.1
67.1
68.1
69.1
70.1
71.1
72.1
73.1
74.1
75.1
76.1
77.1
78.1
CBASS_II
Lamassu-Fam
CAS_Class1-Subtype-I-F
AVAST_type_III
C13
AbiO, PD-T7-2
PD-Lambda-5
CAS_Class1-Subtype-I-F
A
C1
52.2
NS.1
NS.2
NS.3
NS.4
NS.5
NS.6
NS.7
NS.8
NS.9
NS.10
NS.11
NS.12
NS.13
NS.14
NS.15
NS.16
NS.17
NS.18
NS.19
NS.20
G
aph(3'')-Ib, aph(6)-Id, sul2
gabija, Mokosh_TypeI, Mokosh_TypeII
J
DRT_4
I
NS.21
NS.22
NS.23
NS.24
NS.25
NS.26
NS.27
NS.28
NS.29
NS.30
NS.31
NS.32
NS.33
NS.34
NS.35
NS.36
NS.37
NS.38
CBASS_II
F
C14
RM_type_IIG
DRT_5
GCF4
NS.39
NS.40
NS.41
NS.42
NS.43
NS.44
NS.45
NS.46
NS.47
NS.48
NS.49
NS.50
NS.51
NS.52
NS.53
NS.54
NS.55
NS.56
NS.57
GCF6
B
NS.58
NS.59
NS.60
NS.61
NS.62
NS.63
NS.64
NS.65
NS.66
NS.67
NS.68
NS.69
cfPICI
pilW
C12
PD-Lambda-5
RGP type
RGP
RGP-ICE/IME
RGP-prophage
Phylogenetic cluster
Ia
Ib
IIa
IIb
IIc
III
IV
V
VI
VII
VIII

Figure 3.8. Network showing the different spot of insertions (1-78) with the associated RGPs families (named x.y, where x is the name of the spot and y is the number of the cluster) and the decontextualized RGPs (NS.1 to NS.69). Jaccard Index cutoff of 0.394 was used. Gray-filled nodes represent RGPs assigned to an insertion spot, while white-filled nodes represent decontextualized RGPs. The colour of each node border identifies its phylogenetic cluster origin. RGP families were grouped by their spot of insertion and. RGPs assigned to an ICE/IME or a prophage are represented as rhombuses or triangles.

From the perspective of the phylogenetic origin, most of the families are constituted by RGPs from a single cluster or sub-cluster (n= 178; Fig. 3.9A), while those shared between several groups (2 to 9) are less represented (n = 52). The most broadly distributed families are 34.1 (Ia, Ib, IIa, IIb, IIc, IV, V, VI, and VIII), 14.1 (Ia, IIa, IIb, IIc, IV, V, and VIII), and 35.1 (Ia, Ib, IIa, IIb, IIc, IV, and VIII) (Fig. 3.8). Among the decontextualized RGP families, only NS.1 is composed of RGPs from more than one phylogenetic origin (Ib, IIa, and VIII) (Fig. 3.8 and 3.9A).

On the other hand, most of the identified insertion spots (n = 44) are occupied by a single RGP family, while 34 spots are shared by more than one RGP family. The most variable spots of insertion, in terms of the diversity of RGP families present, were 4, 24, and 3, with 9, 7, and 6 RGP families, respectively (Fig. 3.8 and 3.9B).

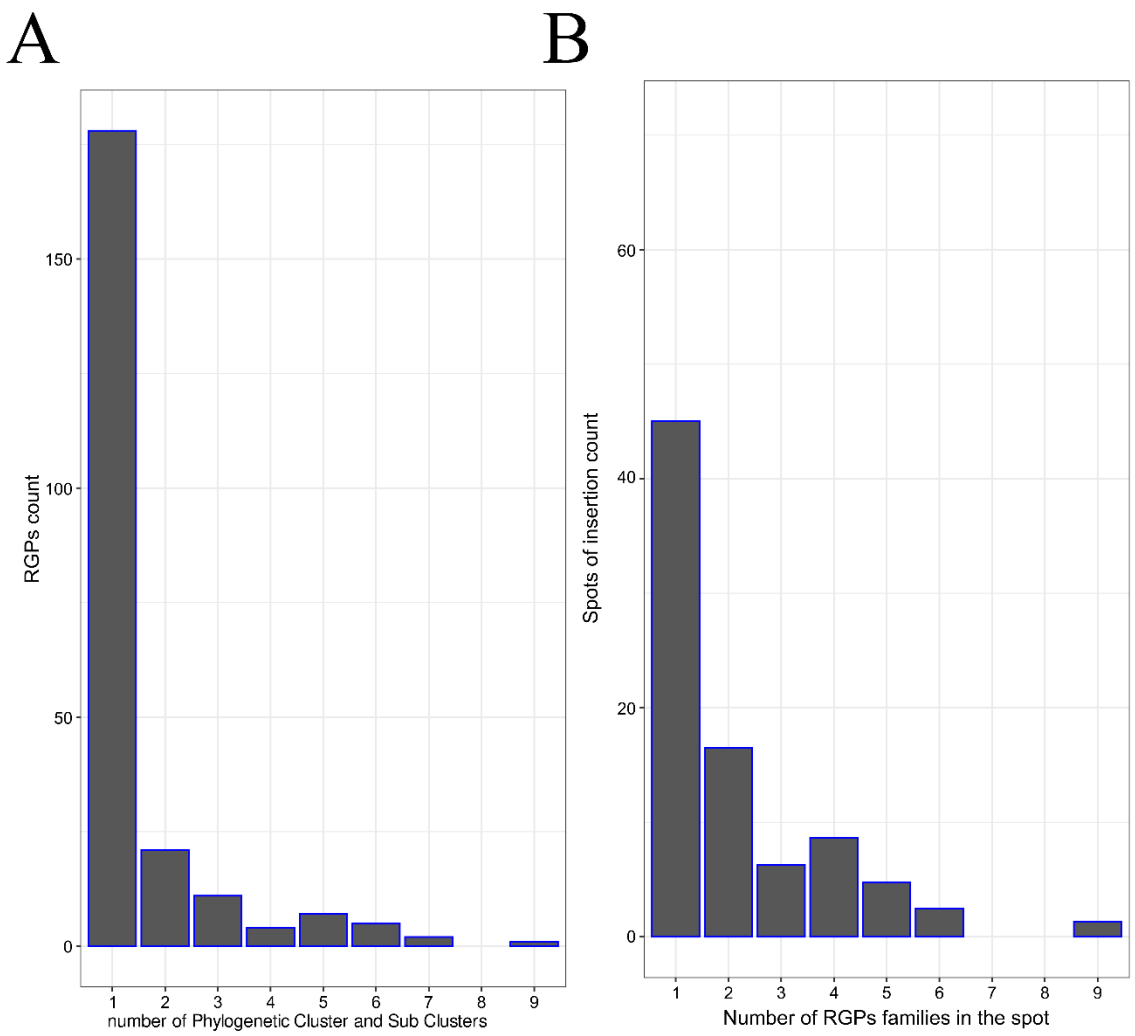

Figure 3.9. (A) Frequencies of RGP families according to the number of phylogenetic Clusters or SubClusters they share. (B) Frequencies of number of RGPs families sharing spot of insertion.

Chromosomic RGPs not associated with mobile elements harbour a wide variety of traits such as the 40.28% of the virulence-related genes, 49.51% of the defence systems, 100% of the ARGs, and 5.08% of the BGCs (Fig. 3.4).

A total of 396 genes related to virulence were located in chromosomic RGPs (Fig. 3.4). Virulence genes harboured by chromosomic RGPs are mainly related to antiphagocytosis (capsular polysaccharide: *wbfU*, *cpsC*, *rmlC*, *rmlD*, *wbfY*, *wbfT*, *pseC*, *tviB*(2), *vipB*/*tviC*), endotoxin (LPS, LOS: *bplA*, *kpsF*), adherence (LPS O-antigen, Type IV pili: *tviB*, *hisF2*), toxins (RTX toxins: *rtxB*, *rtxD*), and the glycosylation system (*pseB*). Virulence genes located in RGPs are distributed across 13 RGP families (1.1, 1.2, 1.3, 15.3, 16.1, 16.2, 19.1, 21.3, 32.4, 44.1, 44.2, 48.1, and 48.2), which were allocated in 8 insertion spots (Fig. 3.7). Each RGP in families 1.1 (phylogenetic clusters I, II, and VII) and 1.3 (phylogenetic cluster VIII) harboured a single copy of *cpsC*, while RGPs from family 1.2 (phylogenetic clusters III, IV, V, and VI) contain *cpsC*, *tviB*, and *vipB*/*tviC*. Among the RGPs in spot 16, family 16.1 (phylogenetic clusters I and II) showed three similar sets of virulence genes (with a common core formed by the genes *pseI*, *pseF*, *wbpD*, *pseB*, *pseC*, *bplA*, *tviB*; two sets with *hisF2*; and one with *wbfU*), while family 16.2 (phylogenetic clusters III, IV, V, and VI) carried only *tviB* and *wbpP*. Both families 48.1 and 48.2 harboured *kpsF* and *ctrD*. Families 15.3 and 21.3 harboured *rtxB* and *rtxD*. Families 19.1 and 32.4 harboured *rmlD* and *rmlC*, and hcp-2 and vgrG-2, respectively (Fig. 3.7).

A total of 44 RGP families, of which five are partially composed of RGPs identified from ICEs/IMEs, showed defence systems (Fig. 3.8). Furthermore, spots of insertion usually contained multiple RGPs or ICE/IME families with distinct defence systems. For example, spot 2 includes families 2.1, 2.2, and 2.3 (RosmerTA, RM_type_I, and PD-Lambda-2, respectively); spot 4 families 4.1, 4.2, 4.3, 4.4, 4.5, and 4.6 (Lamassu-Fam, Septu, retron_I-A, RM_type_I, Hachiman_type_I, and darTG and RosmerTA, respectively); spot 12 families 12.2 and 12.3 (RM_type_II and Retron_VI, respectively); spot 15 families 15.2 and 15.3 (Gabija and retron II, and PD-Lambda-1, respectively); spot 31 families 31.1 and 31.2 (CBASS_II and Gabija, respectively); spot 32 families 32.1 and 32.3 (SspABCD, and ShosTA, respectively); spot 41 families 41.1 and 41.2 (both with BREX_I); spot 45 families 45.1 and 45.2 (3HP and PD-T7-2, and

RM_type_II, respectively); and spot 46 families 46.1 and 46.2 (both with BREX_I) (Fig. 3.8).

On the other hand, families 17.2 (druantia and RM_type_II), 27.1 (RM_type_I and Septu), 30.2 (PD-Lambda-5), 36.4 (RM_type_III), 40.1 (qatABCD and upx), 54.1 (CBASS_II), 58.1 (Lamassu-Fam), 63.1 (CAS_Class1-Subtype-I-F), 65.1 (AVAST_type_III), 67.1 (AbiO and PD-T7-2), 73.1 (CAS_Class1-Subtype-I-F), and 75.1 (PD-Lambda-5) are the only families that harbour defence systems in their respective spots.

Decontextualized RGP families NS.7, NS.11, NS.22, and NS.34 also carry defence systems (Gabija, Mokosh_TypeI and Mokosh_TypeII, DRT_4, CBASS_II, and DRT_5, respectively) (Fig. 3.7).

The ARG genes aph(3")-Ib, aph(6)-Id, and sul2, which were responsible for resistance to streptomycin and sulfonamide detected in strains 3454, 3492, 3610, and 3614 (see Chapter 1), were located in RGP family NS.6 (Fig. 3.8).

The 3 BGC singletons (see Chapter 2) were detected in RGPs: GCF10, which produces butyrolactone in strain 07/108 T1, constituted RGP family 31.3; GCF4 and GCF6 (which produced RiPPs and NRPS, respectively, in strain 071316f) appeared in the decontextualized families NS39 and NS38, respectively (Fig. 3.8).

3.2.3 Identification of ICEs/IMEs

A total of 78 chromosomic RGPs, with a size range from 7.86 to 57.45 kb, were designated as ICE/IMEs based on the detection of both integrases and relaxases in their sequences, and they were detected in 25 of the 39 *V. europaeus* genomes (Table 3.2). ICE/IMEs were grouped into 14 ICE/IMEs clusters (C1-C14) using a Jaccard Index threshold of 0.95 (Fig. 3.10A, Table 3.2). Those belonging to ICE/IME clusters C1 and C2 were in all strains of the phylogenetic sub-cluster Ia. ICE/IME clusters C3 and C4 were partially distributed in sub-cluster Ia: C3 was identified in most of the strains belonging to this sub-cluster with the exception of the strains 3610 and 3614 the only ones with C4 (Table 3.2). The average Jaccard Index value between these two groups was 0.84. ICE/IME cluster C5 was present in a subset of strains from the phylogenetic sub-cluster Ia (3614, 2975, 2971, 2969, 2968, 2951, 2945, and 2895).C6 is found in a

subset of the phylogenetic sub-cluster Ib (PP2-978, PP2-843, and 2967). C7 was identified in 75% of strains from sub-cluster IIa (07_121_1T1, 07_116_T1, and 07_112_T1). The remaining putative ICE/IME clusters corresponded to singletons: C8 and C12 were found in 07/117 T1; C9 in 07/038 2T2; C10 and C13 in 07/115 T2; C11 in NPI-1; and C14 in 07/116 T1 (Fig. 3.10A and B).

Of the 78 ICEs/IMEs detected, 54 matched with a closely related ICE/IME deposited in the ICEberg3 database, namely for ICE/IME clusters C2, C3, C4, C5, C6, C8, C9, C10, C11, and C12 (Table 3.2). Only C5 and C6 obtained a total score higher than 5, which were found to be similar to ARG-carrier ICEs/IMEs (SXT) such as ICEVchBan9 from *V. cholerae* MJ-1236, ICEPmiCHN3300 from *Proteus mirabilis* TJ3300, ICEVchInd4 from *V. cholerae* Ind4 (9.5 and 10 TS, for each, respectively), SXT_MO10 from *V. cholerae* STX, and ICEPdaSpa1 from *Photobacterium damselae* subsp. *Piscicida* (9 and 10 TS, for each, respectively), and R391 from *Providencia rettgeri* (9.5 TS, both). The Multigenblast results showed that the similarity between C5 and C6 with the SXT ICEs/IMEs is limited to the genes belonging to the BREX_I defence system, with aminoacidic homologies ranging from 40% for BrxA to 78% BrxL for both C5 and C6 ICEs/IMEs to its ICEVchBan9 homologs.

RGPs identified as putative ICEs/IMEs are distributed in specific insertion spots. ICEs/IMEs cluster C1 made up the RGP family 52.1; however, only one RGP from the fully resolved genome CECT8136 was assigned to insertion point 52 (Fig. 3.8), while the others are decontextualized. Spot 41 contains the putative ICEs/IMEs C2 (family 41.1), C8 (family 41.4), C10 and C9 (family 41.2), and C11 (family 41.3) (Fig. 3.8). Both RGP families 41.2 and 41.3 also include decontextualized RGPs from strain 07/108 T1 (07/108_T1_scaffold24_RGP_0 and 07_108_T1_scaffold25_RGP_3, respectively). ICE/IME cluster C3 and C4 made up a single family at spot 40 (40.1) (Fig. 3.8). ICE/IME cluster C7 made up family 36.3 together with an RGP not identified as mobile (07_110_T1_scaffold18_RGP_2). C12, C13, and C14 constitute singletons (NS.69, 66.1, and NS.32, respectively) (Fig. 3.8).

ICEs/IMEs encoded only 0.10% of the virulence-related genes in the accessory genome of *V. europaeus* but the16.93% of the accessory defence systems (Fig. 3.4). Thus, the only ICE/IME with a gene related to virulence was NS.69, which harboured a *pilW* gene (related to adherence; Type IV pili) (Fig. 3.8).

ICEs/IMEs from seven RGP families (corresponding to 8 identified ICEs/IMEs) contained antiphage defence systems, and two were composed exclusively of these mobile elements. Defence systems have been found in ICEs/IMEs cluster C3 and C4 (qatABCD, and qatABCD and upx, respectively), C11 (Retron II), C8 (Lamassu-Fam), C5 and C6 (BREX I), C14 (RM_type_2G), and C12 (PD-Lambda-5) (Fig. 3.8).

Table 3.2. List of ICEs/IMEs identified from the *V. europaeus* genomes, including the ICE/IME cluster (C1-C14), the integrase and the relaxase. Best hits, attending to total score (TS) and Cumulative Blast bit score (CBBS), ICEs/IMEs identified with ICEberg3 are indicated, being referenced the ICEberg ID between parentheses.

ICE/IME Cluster	RGP	Lenght (kb)	Integrase	Relaxase	Match	TS	CBBS
C1	PP-660_scaffold28_RGP_0	8.15	Phage_integrase	T4SS_MOBV	-	-	-
	PP-654_scaffold28_RGP_0	8.15	Phage_integrase	T4SS_MOBV		-	-
	CECT8136T_contig_3_RGP_11	8.15	Phage_integrase	T4SS_MOBV		-	-
	PP-635_scaffold25_RGP_0	8.15	Phage_integrase	T4SS_MOBV		-	-
	L4_scaffold25_RGP_0	8.15	Phage_integrase	T4SS_MOBV		-	-
	L3_scaffold43_RGP_0	8.15	Phage_integrase	T4SS_MOBV		-	-
	L20_scaffold32_RGP_0	8.15	Phage_integrase	T4SS_MOBV		-	-
	3614_scaffold22_RGP_0	8.15	Phage_integrase	T4SS_MOBV		-	-
	3610_scaffold29_RGP_0	8.15	Phage_integrase	T4SS_MOBV		-	-
	3492_scaffold38_RGP_0	8.15	Phage_integrase	T4SS_MOBV		-	-
	3454_scaffold39_RGP_0	8.15	Phage_integrase	T4SS_MOBV		-	-
	2975_scaffold24_RGP_0	8.15	Phage_integrase	T4SS_MOBV		-	-
	2971_scaffold23_RGP_0	8.15	Phage_integrase	T4SS_MOBV		-	-
	2969_scaffold29_RGP_0	8.15	Phage_integrase	T4SS_MOBV		-	-
	2968_scaffold31_RGP_0	8.15	Phage_integrase	T4SS_MOBV		-	-
	2951_scaffold15_RGP_0	8.15	Phage_integrase	T4SS_MOBV		-	-
	2945_scaffold30_RGP_0	8.15	Phage_integrase	T4SS_MOBV		-	-
	2930_scaffold32_RGP_0	8.15	Phage_integrase	T4SS_MOBV		-	-
	2895_scaffold22_RGP_0	8.15	Phage_integrase	T4SS_MOBV		-	-
C2	PP-660_scaffold22_RGP_0	15.13	Phage_integrase	profile_MOBM	Trb-1 (1091)	1	263
	PP-654_scaffold20_RGP_0	15.13	Phage_integrase	profile_MOBM		1	263

	CECT8136T_contig_3 _RGP_6	15.13	Phage_integrase	profile_MOBM		1	263
	PP-635_scaffold23_RGP_0	15.13	Phage_integrase	profile_MOBM		1	263
	L4_scaffold18_RGP_0	15.13	Phage_integrase	profile_MOBM		1	263
	L3_scaffold37_RGP_0	15.13	Phage_integrase	profile_MOBM		1	263
	L20_scaffold30_RGP_1	15.13	Phage_integrase	profile_MOBM		1	263
	3614_scaffold31_RGP_0	15.13	Phage_integrase	profile_MOBM		1	263
	3610_scaffold22_RGP_0	15.13	Phage_integrase	profile_MOBM		1	263
	3492_scaffold22_RGP_0	15.13	Phage_integrase	profile_MOBM		1	263
	3454_scaffold25_RGP_0	15.13	Phage_integrase	profile_MOBM		1	263
	2975_scaffold26_RGP_0	15.13	Phage_integrase	profile_MOBM		1	263
	2971_scaffold25_RGP_0	15.13	Phage_integrase	profile_MOBM		1	263
	2969_scaffold22_RGP_0	15.13	Phage_integrase	profile_MOBM		1	263
	2968_scaffold27_RGP_0	15.13	Phage_integrase	profile_MOBM		1	263
	2951_scaffold29_RGP_0	15.13	Phage_integrase	profile_MOBM		1	263
	2945_scaffold25_RGP_1	15.13	Phage_integrase	profile_MOBM		1	263
	2930_scaffold26_RGP_0	15.13	Phage_integrase	profile_MOBM		1	263
	2895_scaffold23_RGP_0	15.13	Phage_integrase	profile_MOBM		1	263
C3	PP-660_scaffold12_RGP_0	47.42	Phage_integrase	T4SS_MOBP1	CMGI-3 (338)	4.5	953
	PP-654_scaffold16_RGP_0	47.42	Phage_integrase	T4SS_MOBP1		4.5	953
	CECT8136T_contig_1 _RGP_1	47.42	Phage_integrase	T4SS_MOBP1		4.5	953
	PP-635_scaffold19_RGP_0	47.42	Phage_integrase	T4SS_MOBP1		4.5	953
	L4_scaffold20_RGP_0	47.42	Phage_integrase	T4SS_MOBP1		4.5	953
	L3_scaffold23_RGP_0	47.42	Phage_integrase	T4SS_MOBP1		4.5	953
	L20_scaffold19_RGP_0	47.42	Phage_integrase	T4SS_MOBP1		4.5	953
	3614_scaffold19_RGP_0	47.42	Phage_integrase	T4SS_MOBP1		4.5	953
	3492_scaffold30_RGP_0	47.42	Phage_integrase	T4SS_MOBP1		4.5	953

	2975_scaffold16_RGP_0	47.42	Phage_integrase	T4SS_MOBP1		4.5	953
	2971_scaffold15_RGP_0	47.42	Phage_integrase	T4SS_MOBP1		4.5	953
	2969_scaffold13_RGP_0	47.42	Phage_integrase	T4SS_MOBP1		4.5	953
	2968_scaffold16_RGP_0	47.42	Phage_integrase	T4SS_MOBP1		4.5	953
	2951_scaffold17_RGP_0	47.42	Phage_integrase	T4SS_MOBP1		4.5	953
	2945_scaffold15_RGP_0	47.42	Phage_integrase	T4SS_MOBP1		4.5	953
	2930_scaffold18_RGP_0	47.42	Phage_integrase	T4SS_MOBP1		4.5	953
	2895_scaffold12_RGP_0	47.42	Phage_integrase	T4SS_MOBP1		4.5	953
C4	3610_scaffold19_RGP_0	40.31	Phage_integrase	T4SS_MOBP1	CMGI-3(338)	4.5	953
	3454_scaffold14_RGP_0	40.31	Phage_integrase	T4SS_MOBP1		4.5	953
C5	3614_scaffold30_RGP_1	31.02	Phage_integrase	T4SS_MOBP1	ICE*Vch*Ban 9(16)	9.5	4884
	2975_scaffold28_RGP_1	31.02	Phage_integrase	T4SS_MOBP1		9.5	4884
	2971_scaffold27_RGP_2	31.02	Phage_integrase	T4SS_MOBP1		9.5	4884
	2969_scaffold26_RGP_1	31.02	Phage_integrase	T4SS_MOBP1		9.5	4884
	2968_scaffold28_RGP_0	31.02	Phage_integrase	T4SS_MOBP1		9.5	4884
	2951_scaffold20_RGP_0	31.02	Phage_integrase	T4SS_MOBP1		9.5	4884
	2945_scaffold20_RGP_0	31.02	Phage_integrase	T4SS_MOBP1		9.5	4884
	2895_scaffold25_RGP_1	31.02	Phage_integrase	T4SS_MOBP1		9.5	4884
C6	PP2-978_scaffold23_RGP_0	38.16	Phage_integrase	T4SS_MOBP1	ICE*Vch*Ban 9(16)	10	5784
	PP2-843_contig_2_RGP_1	38.16	Phage_integrase	T4SS_MOBP1		10	5784
	2967_scaffold26_RGP_0	38.16	Phage_integrase	T4SS_MOBP1		10	5784
C7	07_121_1T1_scaffold13_RGP_2	7.86	Phage_integrase	T4SS_MOBV	-	-	-
	07_116_T1_scaffold11_RGP_2	7.86	Phage_integrase	T4SS_MOBV		-	-
	07_112_T1_scaffold17_RGP_2	7.86	Phage_integrase	T4SS_MOBV		-	-

C8	07_117_T1_scaffold15_RGP_0	15.40	Phage_integrase	profile_MOBM	ICEKpnSMU 18037509-1(1388)	2.5	366
C9	07_038_2T2_scaffold28_RGP_0	15.10	Phage_integrase	profile_MOBM	ICETn*4371_6067 (196)*	2.5	449
C10	07_115_T2_scaffold37_RGP_0	13.94	Phage_integrase	profile_MOBM	IE*Vch*Rus1(590_IME)	2.5	437
C11	NPI-1_contig_1_pilon_RGP_5	13.60	Phage_integrase	profile_MOBM	IE*Vch*Rus1(590_IME)	2.5	415
C12	07_117_T1_scaffold20_RGP_0	57.45	Phage_integrase	profile_MOBF	ICE*Vpa*Can 1(1071)	5.5	791
C13	07_115_T2_scaffold20_RGP_2	10.01	Phage_integrase	profile_MOBF	-	-	-
C14	07_116_T1_scaffold22_RGP_6	8.78	Phage_integrase	T4SS_MOBP1	-	-	-

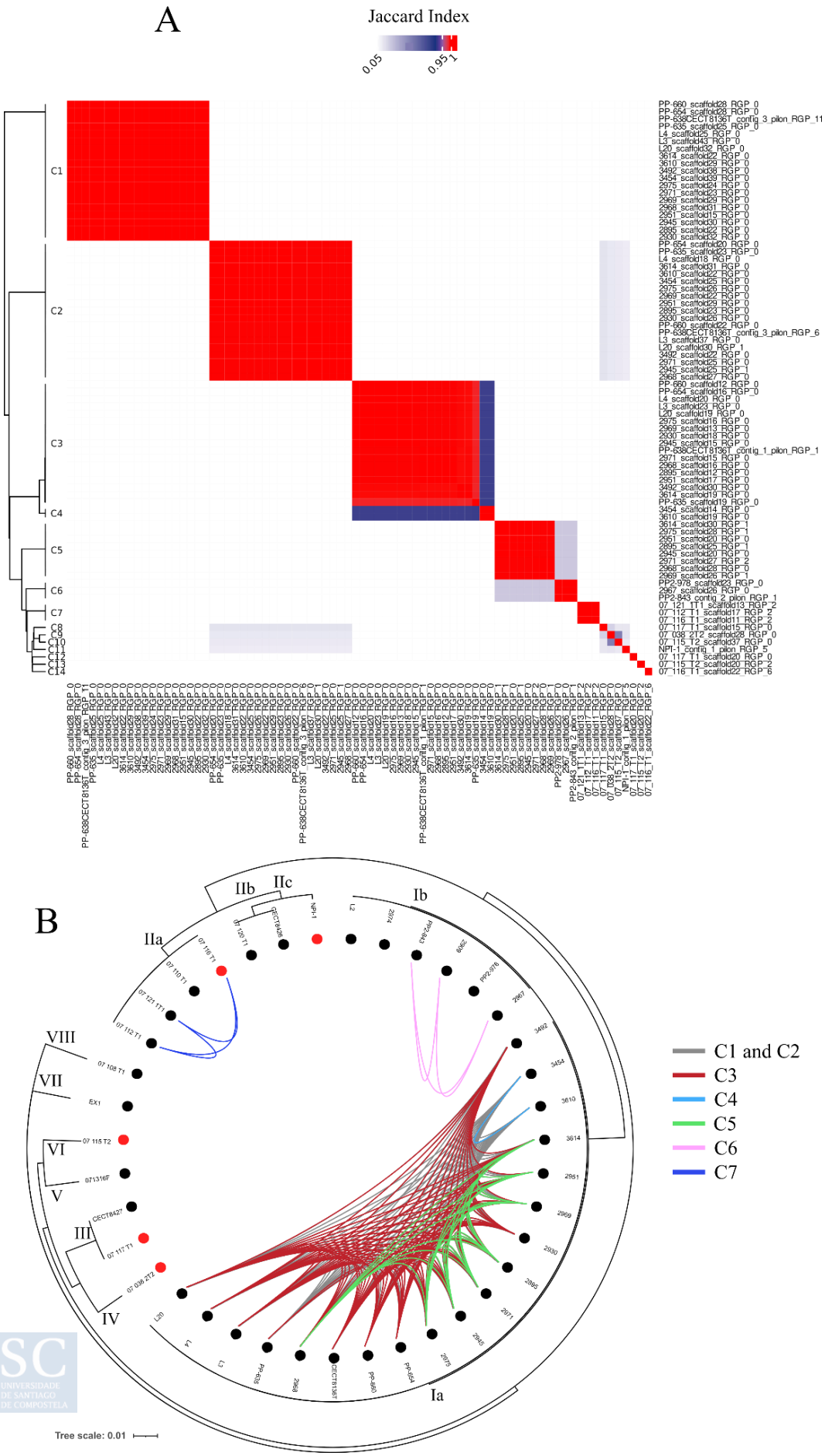
A
Jaccard Index
0.05
0.95
1
C1
C2
C3
C4
C5
C6
C7
C8
C9
C10
C11
C12
C13
C14
B
IIb
IIc
Ib
IIa
VIII
VII
VI
V
III
IV
Ia
C1 and C2
C3
C4
C5
C6
C7
Tree scale: 0.01

Figure 3.10. ICE/IMEs identified in *V. europaeus* genomes. (A) Heatmap showing the results of the Jaccard Index comparisons for the ICE/IME pairs found. (B) Distribution of ICEs/IMEs across *V. europaeus* strains. The clusters, labelled on the left (C1–14), were established using an index cutoff of 0.95. The strains are ordered according to the phylogeny obtained through the comparison of core genes (Chapter 1), which is represented in the outer ring as a circular tree. The red dot indicates the presence of unique ICEs/IMEs in the strain.

3.2.4 Prophages identification

A total of 55 intact prophages were identified with Phaster but they were detected only in 34 *V. europaeus* genomes out of 39 studied (Table 3.3). These prophages were clustered into 10 different groups (prophage clusters A-J) using a cutoff similarity Jaccard index of 0.95 (Fig. 3.11A, Table 3.3). Some clusters were represented by only one prophage, such as: (i) cluster A (VE-PP42; length: 41 kb), B (VE-PP36; length: 33.6 kb), F (VE-PP41; length: 43.7 kb), and H (VE-PP4; length: 5.9 kb) (Table 3.3). In contrast, the remaining clusters were made up by at least two prophages (Fig. 3.11B, Table 3.3): clusters C (n= 3 prophages; length: 36.3-39,9 kb), D (n=5 prophages; length: 46 kb), E (n=9 prophages; length: 31.3-31.9 kb), G (n=9 prophages; length: 41.2 kb), I (n=2 prophages; length: 8.5 kb), and J (n=23 prophages; length: 6-14.6 kb).

Among the Spanish strains, only the oldest Spanish strain (EX-1) did not harbour any prophage in its genome. All the 19 Spanish strains from sub-cluster Ia were infected by prophages from cluster J (Table 3.3; Fig. 3.11B), only parasitized by those phages (strains L20, L4, L3, 2930, 2895) or also by other cluster phages such as (Fig. 3.11B; Table 3.3): (i) the strains isolated in 2001 (PP-635, PP-660, PP-654, and CECT8136) were infected by prophages from clusters J and E; (ii) strains 3492, 3454, 3610, 3614, 2951, 2969, 2971, 2975, and 2968 parasitized by phages from cluster J and G.

Prophages from clusters A, D and F exclusively infected strains of sub-cluster Ib (Fig. 3.11B & B): (i) A and F prophages parasitized only the strain L2; and (ii) strains PP2-843, PP2-978, 2909, 2967, and 2974 were infected by prophages from clusters D. The prophages from cluster E infected only some Spanish strains but associated to both sub-clusters (Fig. 3.11B; Table 3.3): sub-cluster Ia (PP-635, PP-660, PP-654, CECT8136) and sub-cluster Ib (2967, 2974, 2909, PP2-843 and PP2-978) (Fig. 3.11A and 9B, Table 3.3).

Table 3.3. List of prophages identified from the *V. europaeus* genomes, including clusters (A-J) and similar prophages.

Cluster	Host	Phage code	Lenght (kb)	Match	Accession	Q cover	E- value	% Ident
A	L2	VE-P42	41	*Vibrio* phage L9-1	OR762784.1	27%	0.0	85.40%
B	071316F	VE-P36	33.6	-	-	-	-	-
C	CECT8427	VE-P40	38.9	-	-	-	-	-
	07_038_2T2	VE-P1	39.9	-	-	-	-	-
	071316F	VE-P35	36.3	-	-	-	-	-
D	2967	VE-P16	46	-	-	-	-	-
	PP2-978	VE-P49	46	-	-	-	-	-
	2909	VE-P10	46	-	-	-	-	-
	PP2-843	VE-P46	46	-	-	-	-	-
	2974	VE-P23	46	-	-	-	-	-
E	CECT8136T	VE-P37	31.3	*Vibrio* phage 1.159.O._10N.261.46.F12	MG592527.1	77%	0.0	90.30%
	PP-635	VE-P51	31.3			77%	0.0	90.30%
	PP-660	VE-P55	31.3			77%	0.0	90.30%
	PP-654	VE-P53	31.3			77%	0.0	90.30%
	PP2-843	VE-P47	31.9			73%	0.0	95.51%
	2967	VE-P15	31.9			73%	0.0	95.51%
	2974	VE-P24	31.9			73%	0.0	95.51%
	2909	VE-P9	31.9			73%	0.0	95.51%
	PP2-978	VE-P48	31.9			73%	0.0	95.51%
F	L2	VE-P41	43.7	*Vibrio* phage ST2-2pr	MZ496294.1	22%	0.0	95.08%
G	3454	VE-P27	41.2	*Vibrio* phage ST2-2pr	MZ496294.1	25%	0.0	93.21%
	2968	VE-P17	41.2			25%	0.0	93.21%
	3492	VE-P29	41.2			25%	0.0	93.21%
	3614	VE-P33	41.2			25%	0.0	93.21%
	2969	VE-P19	41.2			25%	0.0	93.21%
	2971	VE-P21	41.2			25%	0.0	93.21%

	2975	VE-P25	41.2			25%	0.0	93.21%
	3610	VE-P31	41.2			25%	0.0	93.21%
	2951	VE-P13	41.2			25%	0.0	93.21%
H	07_116_T1	VE-P4	5.9	Inoviridae sp.	MH649021.1	6%	9,00E-17	71.91%
I	07_120_T1	VE-P6	8.5	-	-	-	-	-
	CECT8426	VE-P39	8.5	-	-	-	-	-
J	L3	VE-P43	14.6	Inoviridae sp.	MH649021.1	0%	0.035	96.97%
	L4	VE-P44	14.6			0%	0.035	96.97%
	L20	VE-P45	14.6			0%	0.035	96.97%
	07_121_1T1	VE-P7	6			6%	9,00E-17	71.91%
	07_110_T1	VE-P2	6			6%	9,00E-17	71.91%
	07_112_T1	VE-P3	6			6%	9,00E-17	71.91%
	07_116_T1	VE-P5	6			6%	9,00E-17	71.91%
	CECT8136T	VE-P38	8.4			0%	0.007	96.97%
	3614	VE-P34	8.4			0%	0.007	96.97%
	2895	VE-P8	8.4			0%	0.007	96.97%
	2945	VE-P12	8.4			0%	0.007	96.97%
	2969	VE-P20	8.4			0%	0.007	96.97%
	PP-660	VE-P54	8.4			0%	0.007	96.97%
	3492	VE-P30	8.4			0%	0.007	96.97%
	PP-654	VE-P52	8.4			0%	0.007	96.97%
	PP-635	VE-P50	8.4			0%	0.007	96.97%
	3454	VE-P28	8.4			0%	0.007	96.97%
	3610	VE-P32	8.4			0%	0.007	96.97%
	2930	VE-P11	8.4			0%	0.007	96.97%
	2975	VE-P26	8.4			0%	0.007	96.97%
	2968	VE-P18	8.4			0%	0.007	96.97%
	2951	VE-P14	8.4			0%	0.007	96.97%

2971	VE-P22	8.4			0%	0.007		96.97%

Among the French strains, no prophages were detected in strains 07/108 T1, 07/115 T2, and 07/117 T1 (Fig. 3.11B). The French strain 07/116 T1 was infected by two prophages (clusters H and J) (Fig. 3.11B and Table 3.3), while the remaining strains were only infected by one prophage (Fig. 3.11B and Table 3.3). Cluster I prophages parasitized only French strains affiliated to sub-cluster IIb (CECT8426 and 07/120 T1) (Table 3.3; Fig. 3.11B). In contrast, prophages in cluster C exhibit the highest intra-cluster diversity among the identified prophage clusters, with an average Jaccard Index of 0.96 (Fig. 3.11A; Table 3.3).

Only phages from clusters C and J infected strains isolated from different countries (Fig. 3.11B; Table 3.3). Phages from cluster C parasitized French and American strains (bacterial clusters III and IV) and American strains (cluster V). Prophages from cluster J were the only ones found in the Spanish and French strains, specifically among all strains in sub-cluster Ia and sub-cluster IIa (07/121 T1, 07/110 T1, and 07/116 T1) (Fig. 3.11B). However, there was intra-specific variability between the prophages of J cluster, supported by size differences (prophages infecting French strains, 6 kb; prophages infecting Spanish strains, 14,6 kb) and the Jaccard Index (0.97-0.99) (Table 3.3).

Regarding to the taxonomic affiliation of those prophages, prophages of clusters A, E, F, G, H, and the French subset of cluster J were aligned with known prophages (Table 3.3).

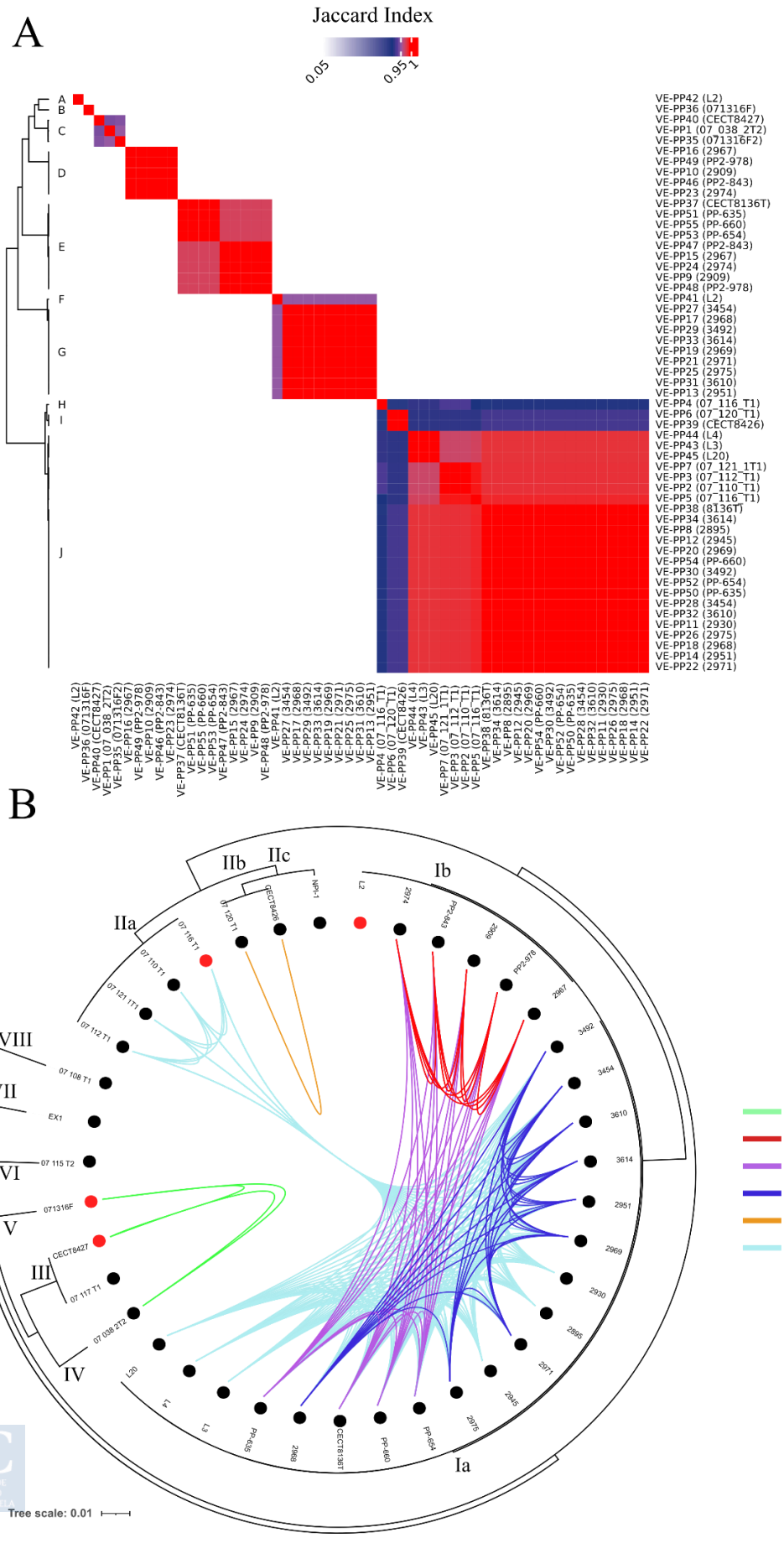

Figure 3.11. Prophages identified in *V. europaeus* genomes. (A) Heatmap showing the results of the Jaccard Index comparisons for the prophage pairs found. (B) Distribution of prophages across *V. europaeus* strains. The clusters labelled on the left (A-J) were established using an index cutoff of 0.95. The strains are ordered according to the core-genome phylogeny obtained in the Chapter 1, which is represented in the outer ring as a circular tree. The red dot indicates the presence of unique prophages in the strain.

Prophages represents the 4.84% of the chromosomic RGPs of *V. europaeus*. Regarding the distribution of the identified prophages in the defined RGP families, RGPs associated to prophages from clusters A, B, and F were found as singletons (78.1, NS.55, and NS.26, respectively) (Fig. 3.8). The three prophages forming cluster C included RGPs separated in different RGP families despite those RGPs were inserted in the same spot (RGP families 21.4, 21.5, and 21.6; Fig. 3.8). Prophages from clusters D, G, and I included RGP families 37.1, NS.2, and NS.18, respectively (Fig. 3.8). Prophages from cluster E included RGPs classified into one RGP family but inserted in three different insertion spots (38, 51, and 53.1) (Fig. 3.8). Prophages from cluster J included RGPs divided into two families infecting different bacterial hosts (RGP 3.1 and NS.9 found in prophages infecting hosts from the phylogenetic clusters Ia and IIa respectively (Fig. 3.8; Table 3.3). RGP 3.1 contained, in addition to part of cluster J, the only prophage from cluster H, associated with a decontextualized RGP, although it presents an average Jaccard Index of 0.62 with the other components (Fig. 3.8).

Some prophages were associated with decontextualized RGPs, as is the case of prophages B (1/1), F (1/1), G (9/9), H (1/1), I (2/2) and J (6/23).

No virulence factors, ARGs, or BGCs were encoded by the prophages and only encoded antiphage defence systems (Fig. 3.4). Prophages VE-P40 and VE-P1 (cluster C) encoded the PD-Lambda-5 anti-phage defence system associated to RGP 21.5 and 21.6 (Fig. 3.8).

3.2.5 Phage satellites

Only two phage satellites were identified: (i) cfPICI family microsatellite in the strain 07/038 2T2, including RGPs classified in the single RGP family NS.66 (Fig. 3.8);

(i) a PICI family microsatellite in the PP-635 strain, with RGPs included in the large RGP family 13.1 (Fig. 3.8).

3.2.6 Distribution of the pangenome accessory fractions among the different genetic elements.

The 72.49% (n=4391 genes, 44.53% of the pangenome genes) of the accessory genome was assigned to the genetic elements studied in this chapter (unclassified chromosomic RGPs, plasmids, ICEs/IMEs, prophages or phage satellites). Most of those genes (68%) were associated to unclassified chromosomal RGPs (Fig. 3.12). Mobile plasmids (mobilizable and conjugative) harboured the 26% of the accessory genes The remaining 6% were found in ICEs/IMEs (5%), prophages (0.8%), and phage satellites (0.2%) (Fig. 3.12).

Any known mobility genes, homologs for relaxases and integrases/recombinases, were identified from unclassified chromosomic RGPs sequences and, thus, they were not included in the well-characterized *V. europaeus* mobilome. Therefore, we assigned the 19.88% of the accessory genes to the well-characterized mobilome – e.g., mobile plasmids, ICEs/IMEs, prophages and phage satellites-, corresponding to the 12.12% of the total pangenome genes.

The assignation of each accessory fraction (cloud, shell or soft core) to all genetic elements identified in this study revealed that 53% (n=2206) of the cloud genes and the 24% (n= 732 genes) of the shell genes were found in unclassified chromosomic RGPs (Fig. 3.12). In fact, unclassified chromosomic RGPs were mainly formed by genes belonging to both fractions: 74% and 25% of the unclassified chromosomic RGPs genes were assigned the cloud and shell gene fraction respectively (Fig. 3.12).

Plasmids harboured the 17% (n=731) of the cloud genes and the 19% (n=305) of the shell genes (Fig. 3.12). However, the relative gene fraction was similar to unclassified chromosomic RGPs and plasmid genes were mainly constituted by cloud genes (64%) and shell genes (26%) (Fig. 3.12). Similar proportions were found in ICEs/IMEs and phage satellites (Fig. 3.12). For instance, cloud and shell genes constituted respectively the 60% and 36% of the genes associated to ICES/IMEs and the

73% and 19% in the case of phage satellites (Fig. 3.12). In contrast, genes associated to prophages were mainly cloud genes (97%) (Fig. 3.12).

Interestingly, the 46% of the soft-core genes were encoded by plasmids whereas the remaining 53% could not assigned to any genetic element (Fig. 3.12).

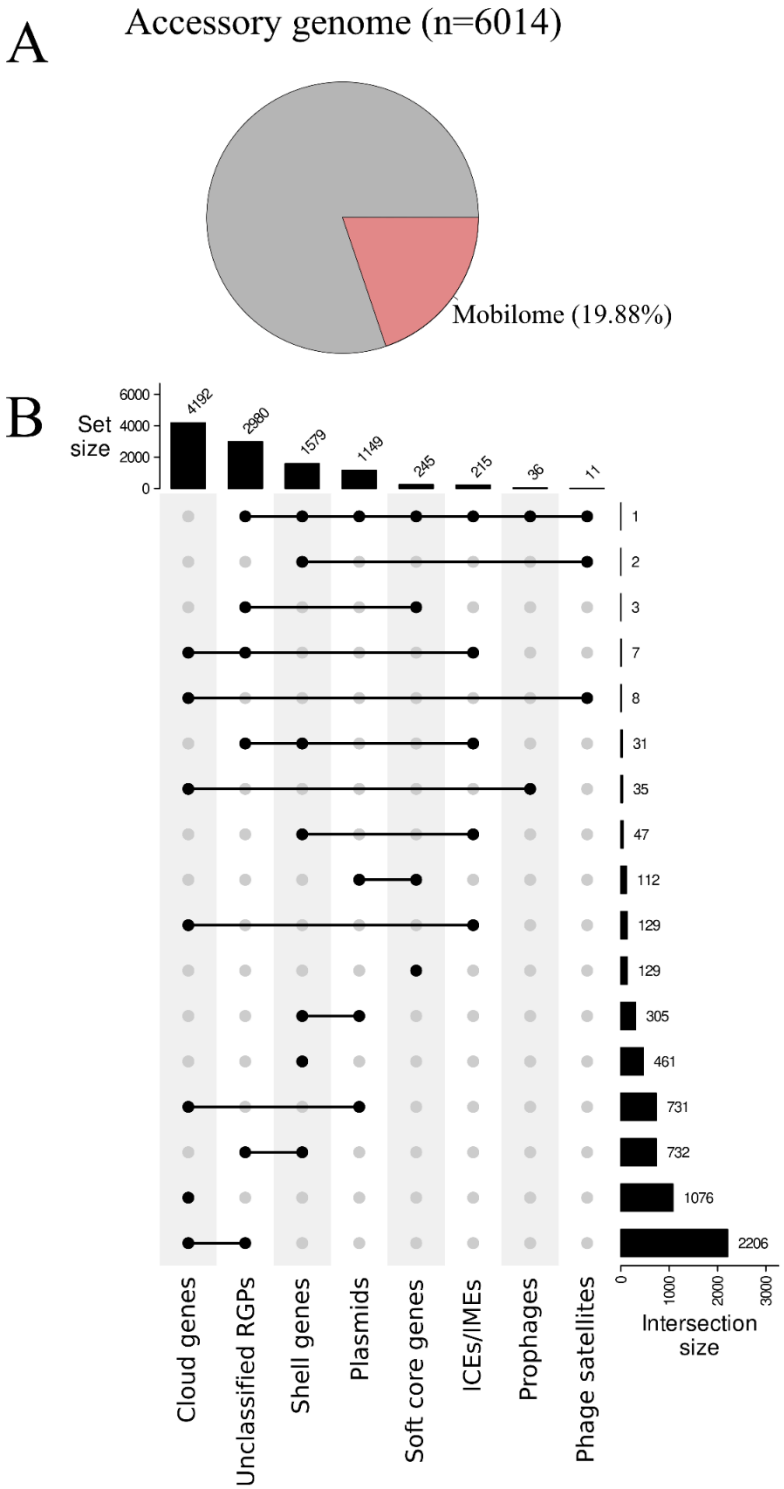

Figure 3.12. Characterization of the accessory genome of *V. europaeus*. (A) Percentage of the accessory genome assigned to mobilome; (B) Scatter plot showing homologous proteins between the different fractions of the accessory genome and the different elements thereof identified.

3.3 Discussion

As we have seen in Chapter 1, the accessory genome constituted the largest fraction (61%) of the *V. europaeus* pangenome and this has been found in many bacterial pangenomes (Azarian, Huang, and Hanage 2020). In this report most of the accessory genes (72%) have been assigned to the genetic elements (e.g. ICEs/IMEs, plasmids, prophages, phage satellites and unclassified chromosomic RGPs) identified from the *V: europaeus* pangenome. Thus, the structural organization of the accessory genome has been defined for first time in a pathogenic *Vibrio* species for shellfish aquaculture using a large -and high quality- genome collection.

Unclassified chromosomic RGPs were the most abundant genetic elements associated to the accessory genome (63%). However, those RGPs did not encode any known mobility genes and, thus, they were not included as the part of the well-characterized mobilome. However, unclassified chromosomic RGPs were mostly formed by genes associated to the cloud (74%) and shell (25%) gene fractions and both accessory fractions are expected to arise from HGT events (Bazim et al., 2020). HGT is a major source of variability in prokaryotic genomes and is, due to the absence of sexual reproduction in bacteria, the main force that drives bacterial evolution (Narra and Ochman 2006; Dobrindt et al. 2010). In *V. europaeus*, the fraction of genes in the pangenome originated putatively by HGT -and associated to genetic elements such as ICEs/IMEs, plasmids, prophages, phages satellites or unclassified chromosomic RGPs- was more than double that found for another bivalve pathogen such as *V. crassostreae* (44.53 and 19%, respectively) (Piel et al., 2022). Those authors classified the 47% of the RGPs into putative MGEs, accounting for less than 10% of the total genes in the pangenome similar to the 12% of total associated to mobilome obtained in our case (Piel et al. 2022).

The mobility of unclassified chromosomic RGPs was not clear because the absence of mobile related genes may correspond to their inactivation by random mutations or deletions (Bellanger et al. 2014). It is also possible that some RGPs are mobilized through mechanisms that remain unidentified and, thus, they could be classified as putative MGEs (Hochhauser, Millman, and Sorek 2023). In any case, many chromosomic RGPs may represent ancient prophage insertions or recombination events

that have undergone mutation decay (Casjens 2003; Bellanger et al. 2014). Despite this, it has been shown that these immobilized components, such as defective prophages, can endow significant biological traits to their bacterial hosts (Casjens 2003; Ogier et al. 2010).

On the other hand, undetected mobile elements could exist due to the loss of genes from RGPs located at the edges of contigs (Bazin et al. 2020). In our case, this underestimation could be one of the causes of the lower proportion of prophages (4.84%) found in the *V. europaeus* chromosomic RGPs than other pathogenic species (32%) ((Botelho, Cazares, and Schulenburg 2023). However, we cannot rule out the existence of the prophage as a non-integrated form of a plasmid prophage (Canchaya et al. 2003). The presence of plasmid prophages in *V. europaeus* genomes is suggested by the presence of a decontextualized prophage (I) in the chromosome-level assembled genome of CECT8426. Undetected or defective plasmid prophages could explain the existence of decontextualized RGPs in other fully-resolved *V. europaeus* genomes, such as in PP2-843 and CECT8427, belonging to NS.3, NS.5, and NS.68.

Similarly, the detection of ICEs/IMEs could be affected by this bias, being a possible explanation of the presence of decontextualized RGPs in families clearly associated with ICEs/IMEs clusters such as 40.1, 46.1, and 46.2. The fragmentation of complete sequences also accounted for the underestimation of a single phage satellite in the large RGP family 13.1, where we only detected PICI clusters with several decontextualized RGPs. As discussed in Chapter 1, the existence of structural RNAs may be related to the higher likelihood of contig fragmentation, with a larger number of these elements detected in full-resolved genomes in our case (Miyamoto et al. 2014). Since mobile elements are prone to inserting into specific tRNA sites (Hudson, Lau, and Williams 2015), it is expected that there may be a loss of information in the RGPs, including those associated with MGEs, in the contig-level genomes analysed.

Distinct RGPs were inserted in the same spot of insertion. The RGP families identified in *V. europaeus* suggested that at least two recombination events occurred involving different spots of insertion reflected in the two phylogenetic clusters of strains identified. Remarkably these strains coexist in the same environment, which represents a nice example of adaptive convergence. For instance, the prophage from cluster C is found in both the 38/51/53.1 spot (Hatchery A) and the 24/55.1 spot (Hatchery D).

Network analyses using RGP sequences revealed that various RGP family clusters consist of a mix of sequences from at least two different phylogenetic clusters. This observation indicates that recombination events between strains from different phylogenetic clusters may have occurred (Botelho et al. 2023).

V. europaeus frequently harboured RGPs with various anti-phage defence systems at specific insertion sites, a characteristic also observed in other species such as *Escherichia coli* and *Pseudomonas aeruginosa*, which are well known for their defence hotspots (Hochhauser, Millman, and Sorek 2023; Johnson et al. 2023). This clustering of defence systems along mobile elements is likely influenced by selective pressures that favour the host's fitness in environments rich in phages and promote the co-dispersion of these elements across genomes (Rocha and Bikard 2022; Botelho et al. 2023; Hochhauser, Millman, and Sorek 2023). Consequently, chromosomal RGPs encode the majority of defence systems and resulting in highly diverse defence profiles between the different strains (Botelho et al. 2023). Among all the defence systems identified this study, the PD-Lambda-1, PD-Lambda-2, PD-Lambda-5, PD-T7_1, PD-T7_2, and DarTG systems are characteristic of prophages (Patel and Maxwell 2023). Notably, only two out of eight PD-Lambda-5 systems were encoded prophages, reinforcing the notion that defective prophage sequences are prevalent among the RGPs in *V. europaeus*.

The virulence genes encoded by the *V. europaeus* RGPs are primarily associated with the synthesis of polysaccharides. These polysaccharides play crucial roles in forming cell surface structures such as the O-chain of lipopolysaccharides (LPS) and capsular polysaccharides, as well as glycosylating external features like flagella. In Gram-negative bacteria, glyco-type variability is influenced by three key components present in replacement-type RGPs: the O-chain (O-antigen) of the LPS, and optionally, the exopolysaccharide or capsular polysaccharide, and flagellar glycosylation. These RGPs undergo recombination events that contribute to glyco-type variability (López-Pérez and Rodriguez-Valera 2016; Puente-Sánchez et al. 2023). As discussed in Chapter 2, this glyco-type variability within pathogenic species enhances their ability to evade host immune defences and ensures survival. Additionally, glyco-types are involved in the specific recognition of phages, thereby contributing to population regulation through a process of negative selection (Chatzidaki-Livanis, Jones, and Wright 2006; Shu et al. 2009; Nakhamchik et al. 2010; López-Pérez and Rodriguez-Valera 2016). Further

analyses should be performed about the spot of insertion 16, which included the RGPs encoding LPS genes, due to its possible implication in the development of vibriosis prevention strategies through immune priming (Wildschutte et al. 2010; Yang et al. 2021).

We have shown that virulence genes, anti-phage defence systems, secondary metabolite biosynthetic gene and antibiotic resistance genes can be rapidly turned over on the *V. europaeus* populations linked to well-characterized MGEs such as ICEs/IMEs, plasmids, prophages and phage satellites. Encoding those genes on MGEs can make a fast-changing phenotypic trait independent of physiological or metabolic traits encoded by the core genome (Hussain et al. 2021). Anti-phage defence systems were the unique genes found in those MGEs, although mainly in plasmids and ICEs/IMEs, harbouring the 37% of the defence systems found in *V. europaeus* genomes. If we also consider unclassified chromosomic RGPs as -putative or ancient- MGEs, this percentage rises to 73%, similar to the 72% found in *V. crassostreae* and confirming that HGT events play a major role in the emergence of phage resistance by acquisition of MGEs (Piel et al. 2022). Phage resistance is the most important selective force determining clonal bacterial diversity, with anti-phage defence systems explaining a very large portion of the accessory genome (Hussain et al. 2021). This allows the core genome to be maintained over the long term even in the face of phage predation. Although phages may exert negative frequency-dependent selection on their hosts, this selection is largely acting at the level of MGEs containing anti-phage defence systems (Hussain et al. 2021). Interestingly, some prophages also encoded known anti-phage defence systems. Prophages are vulnerable to predation of their host bacterium by exogenous phages. Different anti-phage systems have been encoded by prophages to defend host cells against exogenous phage attack without sacrificing the ability to replicate lytically (Patel and Maxwell 2023).

The presence of numerous traits related to virulence, anti-phage defence systems, and secondary metabolite biosynthetic genes -but not antibiotic resistance genes- distinguished pVE1-like plasmids from other MGEs found from *V. europaeus* pangenome. These genes are associated with survival in novel environments and conditions and may provide an advantage for adaptation in certain environments (Carroll and Wong 2018). These plasmids were the most common MGE in our bacterial collection

(97,4% of *V. europaeus* strains harboured pVE1-like plasmids), highlighting the significance of the pVE1-like plasmids in the biology of *V. europaeus*. Despite most of pVE1-like plasmids were conjugative, some pVE1 plasmids such as those harboured by the strains NPI-1 or 07/108 T1 were mobilizable due to the absence of MPF and T4CP (Smillie et al. 2010). This transition from conjugative to mobilizable often involved gene loss and a reduction of plasmid size, which is associated with the presence of transposable elements within the plasmid (Coluzzi et al. 2022). In fact, pVE1 in NPI-1 was the smallest plasmid within its phylogenetic cluster or pVE1 in the strain 07/108 T1, which also lacked BGCs, supported this hypothesis.

Presence of different anti-phage defence systems encoded in the same pVE1 plasmid could be explained by: (i) preventing the entry of alien DNA, providing protection against invasion by prophages and other mobile elements (Picton et al. 2021), and (ii) preventing plasmid loss during bacterial division through post-segregation killing or addiction mechanisms (Hall et al. 2022). In last example, several studies indicated that RM (restriction-modification) systems are responsible for maintaining plasmid stability within their host (Mochizuki et al. 2006; Shaw, Rocha, and MacLean 2023). However, it has been found that only 10.50% of a large set of plasmids harbour RM systems, with a higher prevalence in conjugative and mobilizable plasmids (Oliveira, Touchon, and Rocha 2014). In the case of pVE1 from *V. europaeus*, RM_Type_I systems were detected in strains 07/108 T1, CECT8426, and 07/120 T1. Toxin-Antitoxin (TA) systems have also been identified as contributors to the stabilization of mobile elements (Makarova et al. 2011; Hall et al. 2022), but only an AbiE/SanTA system was found in the pVE1 plasmid of strain EX1. Most of the defence systems in pVE1-like plasmids were encoded within a flexible region characterized by highly conserved flanks that encompass multiple anti-phage defence islands. The homology of certain anti-phage defence system genes across all pVE1-like sequences, such as the flanking Gao_Hhe in all strains, suggested that this flexible region is additive, resulting from multiple discrete integrations (Rodriguez-Valera, Martin-Cuadrado, and López-Pérez 2016). Moreover, the presence of PD-T7_1 and PD-Lambda-1 in some pVE1 plasmids suggested possible integration of prophages into its flexible defence islands (Rodriguez-Valera, Martin-Cuadrado, and López-Pérez 2016; Patel and Maxwell 2023).

Further analyses are needed to confirm the role of the second T6SSi5 (T6SS2) encoded by pVE1-like plasmids in *V. europaeus*. T6SS1, encoded in the Chromosome I, and T6SS2 were two different systems supported by the low aminoacidic similarity among homologous genes found in most cases. Genetic structure of T6SS1 and T6SS2 was very similar among them and to other T6SSi5s found in pathogenic vibrios such as the bivalve pathogens *V. crassostreae*, *V. aestuarianus* or *V. coralliilyticus* (Piel et al. 2020; Mass, Cohen, Gerlic, et al. 2024). Interestingly, T6SS2 was closely related to the only T6SSi5 found in *V. crassostreae* J5-20 genome which it was also encoded in a plasmid (pGV) (Piel et al. 2020). The pathogenicity of *V. crassostreae* depends on a novel transcriptional regulator, which activates the bidirectional promoter of a T6SS genes cluster and caused haemocyte (oyster immune cell) cytotoxicity (Piel et al. 2020). Those authors proposed that haemocyte cytotoxicity was a lethality trait shared by a broad range of mollusc pathogens such as *V. aestuarianus* or *V. tapetis* and suggested that T6SS was involved in parallel evolution of pathogen for molluscs. It is important to remark that T6SS1 was similar to the T6SS found in *V. coralliilyticus* OCN008, which mediated anti-eukaryotic toxicity and contributes to mortality during infection of an aquatic model organism, *Artemia salina* (Mass et al., 2024). In basis of both reports, T6SS1 and T6SS2 would have a cytotoxic activity. However, the role of T6SS2 in bacteria-bacteria competition could not be discarded because the virulence towards Manila clam juveniles was similar between the unique *V. europaeus* strain without a pVE-1 plasmid (07/115 T2) and to strains with pVE1-like plasmids (see Chapter 2). In any case, the distribution of the T6SSs in the genome of *V. europaeus* is noteworthy, given the general absence of chromosomal T6SS in bacteria harbouring T6SS-encoding plasmids (Morgado and Vicente 2022).

pVE1-like plasmids encoded the most of BGCs associated to MGEs, supporting the significance of those plasmids for the adaptation of *V. europaeus* to its ecological niche. While the ecological role of PKS-NRP hybrids (GCF1 and GCF2) will require further investigation, the arylpolyene-NRPS hybrid (GCF9) is likely associated with colonization through utilization of chitin (Giubergia et al. 2017).

Plasmids are prone to be lost when selective pressure diminishes, thereby being irrelevant or slightly detrimental for bacterial fitness due to metabolic energy waste (Smith and Bidochka 1998; Chen et al. 2017; Carroll and Wong 2018). The lack of the

pVE1 plasmid in strain 07/115 T2 suggests it may have been lost by this reason. Bacterial fitness is a multifactorial trait influenced by the strain's genetic background, including prophages, horizontally transferred genes, and other traits (Andersson and Hughes 2010; Gordo, Perfeito, and Sousa 2012; Bondy-Denomy and Davidson 2014; Knöppel et al. 2014; Taylor et al. 2019). Although the impact of plasmid presence on bacterial fitness varies depending on the genetic context of both the host and the plasmid, it is generally accepted that carrying a plasmid incurs a fitness cost (Dionisio et al. 2005; Vogwill y MacLean 2015; Carroll y Wong 2018; Alonso-del Valle et al. 2021). The specific reasons for this cost are not fully understood but may involve increased resource demands for replication and gene expression, potential misexpression of chromosomal genes, and interference with host structures and functions (Carroll and Wong 2018; Alonso-del Valle et al. 2021).

CONCLUSIONS

Through the analysis of the pangenome of *V. europaeus* presented in this work, new insights into the species have been provided, enhancing the understanding of its intraspecific variability and ecology, and laying a foundation for the development of novel prevention and control strategies. The key conclusions drawn from this analysis are as follows:

1. *V. europaeus* has an open pangenome, indicating the acquisition of external genes. This pangenome is mainly composed by accessory genes (61%), with those belonging to the cloud genome standing out, highlighting the versatility for adaptation to specific ecological niches of the species.
2. *V. europaeus* strains isolated from Spanish hatcheries exhibited lower genetic diversity than French strains, suggesting a monophyletic radiation event followed by subsequent dispersal across Spanish hatcheries. Also, the exchange of phytoplankton stocks and broodstock among hatcheries can justify the finding of clonal strains in different Spanish hatcheries.
3. The American strains, particularly the Chilean one, were closely related to French strains, pointing to an intercontinental movement of *V. europaeus*, likely facilitated by the trade of spat, juveniles or adult bivalves.
4. The study of clonal strains isolated in Hatchery B allowed us to hypothesize that the phytoplankton is the main bacterial source of *V. europaeus*, at least in this facility.
5. Virulence is probably due to the core virulence factors. This is supported because most virulence genes (>60%) were encoded in the core genome and all *V. europaeus* strains were virulent in infection assays.
6. All *V. europaeus* strains were resistant to cephalexin and erythromycin, being sensitive to most of the tested antibiotics. However, the presence of a subgroup of strains were also resistant to streptomycin and sulfonamide. This demonstrated the additional acquisition of antibiotic resistance and highlighted the risk of using antibiotics as preventive tool in hatchery environments.

7. Most of the studied *V. europaeus* strains shared biosynthetic gene clusters such as NRPS, RiPP-like, betalactone, arylpolyene, and ectoine types, suggesting their importance for the proper ecological performance of the species.
8. All *V. europaeus* strains encoded an important repertoire of anti-phage defence systems. The accessory nature of the defence systems demonstrated the rapid adaptation of *V. europaeus* in the arm-race against phage predation, allowing the core genome to remain unchanged. Thus, the use of phage therapy to control this pathogen is questionable.
9. The 72% of the accessory genome of *V. europaeus* came from HGT and mobilome (ICEs/IMEs, mobile plasmids, prophages, phage satellites) comprised the 20% of the accessory genome. Unclassified chromosomal RGPs constituted the most abundant genetic element, however, they could not be assigned to mobilome despite their HGT origin.
10. The broad presence of virulence genes, anti-phage defence systems, BGCs, and ARGs in the mobilome and in the unclassified chromosomal RGPs supported the ability of *V. europaeus* to rapidly acquire or transfer these traits.
11. The pVE1-like plasmid stood out among the genetic elements identified in the pangenome of *V. europaeus* due to its size, abundance, prevalence, and the presence of important traits (e.g., defence systems, BGCs, T6SS2…), suggesting an important role in the bacterial survival and competition.

REFERENCES

1. Aagesen, A. M., and C. C. Häse. 2012. “Sequence Analyses of Type IV Pili from *Vibrio cholerae*, *Vibrio parahaemolyticus*, and *Vibrio vulnificus*.” *Microbial Ecology* 64 (2): 509–24. https://doi.org/10.1007/s00248-012-0021-2.
2. Abby, S. S., J. Cury, J. Guglielmini, B. Néron, M. Touchon, and E. P. C. Rocha. 2016. “Identification of Protein Secretion Systems in Bacterial Genomes.” *Scientific Reports* 6 (1): 23080. https://doi.org/10.1038/srep23080.
3. Abby, S. S., B. Néron, H. Ménager, M. Touchon, and E. P. C. Rocha. 2014. “MacSyFinder: A Program to Mine Genomes for Molecular Systems with an Application to CRISPR-Cas Systems.” *PLOS ONE* 9 (10): e110726. https://doi.org/10.1371/journal.pone.0110726.
4. Akhtar, A. A., and D. PJ. Turner. 2022. “The Role of Bacterial ATP-Binding Cassette (ABC) Transporters in Pathogenesis and Virulence: Therapeutic and Vaccine Potential.” *Microbial Pathogenesis* 171 (October):105734. https://doi.org/10.1016/j.micpath.2022.105734.
5. Akter, S., M. L. Wos-Oxley, S. R. Catalano, M. M. Hassan, X. Li, J. G. Qin, and A. Oxley. 2023. “Host Species and Environment Shape the Gut Microbiota of Cohabiting Marine Bivalves.” *Microbial Ecology* 86 (3): 1755. https://doi.org/10.1007/s00248-023-02192-z.
6. Albini, E., M. Orso, F. Cozzolino, L. Sacchini, F. Leoni, and C. F. Magistrali. 2022. “A Systematic Review and Meta-Analysis on Antimicrobial Resistance in Marine Bivalves.” *Frontiers in Microbiology* 13 (December):1040568. https://doi.org/10.3389/fmicb.2022.1040568.
7. Alex, A., V. Pratheepa, J. Martins, and A. Antunes. 2021. “Draft Genome Sequences of Six *Vibrio* Strains Isolated from the Atlantic Intertidal Marine Sponge *Ophlitaspongia papilla*.” *Microbiology Resource Announcements* 10 (1): 10.1128/mra.01259-20. https://doi.org/10.1128/mra.01259-20.
8. Almatroudi, A., I. B. Gosbell, H. Hu, S. O. Jensen, B. A. Espedido, S. Tahir, T. O. Glasbey, et al. 2016. “*Staphylococcus aureus* Dry-Surface Biofilms Are Not Killed by Sodium Hypochlorite: Implications for Infection Control.” *The Journal of Hospital Infection* 93 (3): 263–70. https://doi.org/10.1016/j.jhin.2016.03.020.
9. Alonso-del Valle, A., R. León-Sampedro, J. Rodríguez-Beltrán, J. DelaFuente, M. Hernández-García, P. Ruiz-Garbajosa, R. Cantón, R. Peña-Miller, and A. San Millán. 2021. “Variability of Plasmid Fitness Effects Contributes to Plasmid Persistence in Bacterial Communities.” *Nature Communications* 12 (1): 2653. https://doi.org/10.1038/s41467-021-22849-y.
10. Andersson, D. I., and D. Hughes. 2010. “Antibiotic Resistance and Its Cost: Is It Possible to Reverse Resistance?” *Nature Reviews Microbiology* 8 (4): 260–71. https://doi.org/10.1038/nrmicro2319.
11. Andrey, K., B. Haegeman, N. H. Bergman, and J. Weitz. 2011. “Genomic Fluidity: An Integrative View of Gene Diversity within Microbial Populations.” *BMC Genomics* 12 (January). https://doi.org/10.1186/1471-2164-12-32.
12. Anguiano-Beltrán, C., M. L. Lizárraga-Partida, and R. Searcy-Bernal. 2004. “Effect of *Vibrio alginolyticus* on Larval Survival of the Blue Mussel *Mytilus galloprovincialis*.” *Diseases of Aquatic Organisms* 59 (2): 119–23. https://doi.org/10.3354/dao059119.
13. Antonova, E. S., and B. K. Hammer. 2011. 2011. “Quorum-Sensing Autoinducer Molecules Produced by Members of a Multispecies Biofilm Promote Horizontal Gene Transfer to *Vibrio cholerae*.” *FEMS Microbiology Letters* 322 (1): 68–76. https://doi.org/10.1111/j.1574-6968.2011.02328.x.

14. APROMAR (2023). Aquaculture in Spain 2023. 106 pp. https://apromar.es/wp-content/uploads/2023/10/Aquaculture_in_Spain_2023_APROMAR.pdf.
15. Arfatahery, N., C. Rafaluk, J. Rolff, and K. M. Wegner. 2024. "Evidence for Immune Priming Specificity and Cross-Protection against Sympatric and Allopatric *Vibrio splendidus* Strains in the Oyster *Magalana (Crassostrea) gigas*." *Developmental & Comparative Immunology* 159 (October):105221. https://doi.org/10.1016/j.dci.2024.105221.
16. Arndt, D., Jason R. Grant, A. Marcu, T. Sajed, A. Pon, Y. Liang, and D. S. Wishart. 2016. "PHASTER: A Better, Faster Version of the PHAST Phage Search Tool." *Nucleic Acids Research* 44 (W1): W16-21. https://doi.org/10.1093/nar/gkw387.
17. Azam, F., T. Fenchel, J. G. Field, J. S. Gray, L. A. Meyer-Reil, and F. Thingstad. 1983. "The Ecological Role of Water-Column Microbes in the Sea." In *Foundations of Ecology II: Classic Papers with Commentaries*, edited by Thomas E. Miller and Joseph Travis, 384–90. University of Chicago Press. https://doi.org/10.7208/chicago/9780226125534-024.
18. Azarian, T., I-T. Huang, and W. P. Hanage. 2020. "Structure and Dynamics of Bacterial Populations: Pangenome Ecology." In *The Pangenome: Diversity, Dynamics and Evolution of Genomes*, edited by Hervé Tettelin and Duccio Medini, 115–28. Cham: Springer International Publishing. https://doi.org/10.1007/978-3-030-38281-0_5.
19. Balbi, T., R. Fabbri, K. Cortese, A. Smerilli, C. Ciacci, C. Grande, L. Vezzulli, C. Pruzzo, and L. Canesi. 2019. "Responses of *Mytilus galloprovincialis* to Challenge with the Emerging Marine Pathogen *Vibrio coralliilyticus*." *Fish & Shellfish Immunology* 84 (January):352–60. https://doi.org/10.1016/j.fsi.2018.10.011.
20. Balbi, T., M. Auguste, K. Cortese, M. Montagna, A. Borello, C. Pruzzo, L. Vezzulli, and L. Canesi. 2013. "Interactions between *Mytilus galloprovincialis* Hemocytes and the Bivalve Pathogens *Vibrio aestuarianus* 01/032 and *Vibrio splendidus* LGP32." *Fish & Shellfish Immunology* 35 (6): 1906–15. https://doi.org/10.1016/j.fsi.2013.09.027.
21. Baralla, E., M. P. Demontis, F. Dessì, and M. V. Varoni. 2021. "An Overview of Antibiotics as Emerging Contaminants: Occurrence in Bivalves as Biomonitoring Organisms." *Animals: An Open Access Journal from MDPI* 11 (11): 3239. https://doi.org/10.3390/ani11113239.
22. Barja, J. L., S. Novoa, J. Ojea, D. Martinez-Patiño, and S. Prado. 2023. "Biofilm Formation by Pathogenic Vibrios Oh Hatchery Surfaces." In. Viena.
23. Bauer, J., F. Teitge, L. Neffe, M. Adamek, A. Jung, C. Peppler, D. Steinhagen, and V. Jung-Schroers. 2021. "Impact of a Reduced Water Salinity on the Composition of *Vibrio* spp. in Recirculating Aquaculture Systems for Pacific White Shrimp (*Litopenaeus vannamei*) and Its Possible Risks for Shrimp Health and Food Safety." *Journal of Fish Diseases* 44 (1): 89–105. https://doi.org/10.1111/jfd.13270.
24. Bazin, A., G. Gautreau, C. Médigue, D. Vallenet, and A. Calteau. 2020. "panRGP: A Pangenome-Based Method to Predict Genomic Islands and Explore Their Diversity." *Bioinformatics* 36 (Supplement_2): i651–58. https://doi.org/10.1093/bioinformatics/btaa792.
25. Beaubrun, J. J.-G., G. Gopinath, M. H. Kothary, A. Franco, S. K. Curtis, B. E. Eribo, and B. D. Tall. 2011. "Influence of Iron-Chelated Growth Conditions on Outer Membrane Protein Production and Virulence of *Vibrio tubiashii*." *Food Microbiology* 28 (7): 1409–13. https://doi.org/10.1016/j.fm.2011.04.003.
26. Beavogui, A., A. Lacroix, N. Wiart, J. Poulain, T. O. Delmont, L. Paoli, P. Wincker, and P. H. Oliveira. 2024. "The Defensome of Complex Bacterial Communities." *Nature Communications* 15 (1): 2146. https://doi.org/10.1038/s41467-024-46489-0.
27. Beaz-Hidalgo, R., S. Balboa, J. L. Romalde, and M. J. Figueras. 2010. "Diversity and Pathogenecity of *Vibrio* Species in Cultured Bivalve Molluscs." *Environmental Microbiology Reports* 2 (1): 34–43. https://doi.org/10.1111/j.1758-2229.2010.00135.x.
28. Bellanger, X., S. Payot, N. Leblond-Bourget, and G. Guédon. 2014. "Conjugative and Mobilizable Genomic Islands in Bacteria: Evolution and Diversity." *FEMS Microbiology Reviews* 38 (4): 720–60. https://doi.org/10.1111/1574-6976.12058.

29. Bernheim, A., and R. Sorek. 2020. “The Pan-Immune System of Bacteria: Antiviral Defence as a Community Resource.” *Nature Reviews Microbiology* 18 (2): 113–19. https://doi.org/10.1038/s41579-019-0278-2.
30. Betcher, M. A., Jennifer M. F., A. W. Han, R. O’Connor, R. Seronay, G. P. Concepcion, D.l L. Distel, and M. G. Haygood. 2012. “Microbial Distribution and Abundance in the Digestive System of Five Shipworm Species (Bivalvia: *Teredinidae*).” *PLOS ONE* 7 (9): e45309. https://doi.org/10.1371/journal.pone.0045309.
31. Bhatty, M., J. A. L. Gomez, and P. J. Christie. 2013. “The Expanding Bacterial Type IV Secretion Lexicon.” *Research in Microbiology*, Bacterial secretion systems: function and structural biology, 164 (6): 620–39. https://doi.org/10.1016/j.resmic.2013.03.012.
32. Bik, E. M., E. K. Costello, A.D. Switzer, B. J. Callahan, S. P. Holmes, R. S. Wells, K. P. Carlin, E. D. Jensen, S.Venn-Watson, and D. A. Relman. 2016. “Marine Mammals Harbor Unique Microbiotas Shaped by and yet Distinct from the Sea.” *Nature Communications* 7 (1): 10516. https://doi.org/10.1038/ncomms10516.
33. Binesse, J., C. Delsert, D. Saulnier, M-C. Champomier-Vergès, M. Zagorec, H. Munier-Lehmann, D. Mazel, and F. Le Roux. 2008. “Metalloprotease Vsm Is the Major Determinant of Toxicity for Extracellular Products of *Vibrio splendidus*.” *Applied and Environmental Microbiology* 74 (23): 7108–17. https://doi.org/10.1128/AEM.01261-08.
34. Biswas, A., R. H.J. Staals, S. E. Morales, P. C. Fineran, and C. M. Brown. 2016. “CRISPRDetect: A Flexible Algorithm to Define CRISPR Arrays.” *BMC Genomics* 17 (1): 356. https://doi.org/10.1186/s12864-016-2627-0.
35. Bjørndal, T., M. Dey, and A. Tusvik. 2024. “Economic Analysis of the Contributions of Aquaculture to Future Food Security.” *Aquaculture* 578 (January):740071. https://doi.org/10.1016/j.aquaculture.2023.740071.
36. Bolger, A. M., M. Lohse, and B. Usadel. 2014. “Trimmomatic: A Flexible Trimmer for Illumina Sequence Data.” *Bioinformatics (Oxford, England)* 30 (15): 2114–20. https://doi.org/10.1093/bioinformatics/btu170.
37. Bondy-Denomy, J., and A. R. Davidson. 2014. “When a Virus Is Not a Parasite: The Beneficial Effects of Prophages on Bacterial Fitness.” *Journal of Microbiology* 52 (3): 235–42. https://doi.org/10.1007/s12275-014-4083-3.
38. Bortolaia, V., R. S. Kaas, E. Ruppe, M. C. Roberts, S. Schwarz, V. Cattoir, A. Philippon, et al. 2020. “ResFinder 4.0 for Predictions of Phenotypes from Genotypes.” *The Journal of Antimicrobial Chemotherapy* 75 (12): 3491–3500. https://doi.org/10.1093/jac/dkaa345.
39. Botelho, J., A. Cazares, and H. Schulenburg. 2023. “The ESKAPE Mobilome Contributes to the Spread of Antimicrobial Resistance and CRISPR-Mediated Conflict between Mobile Genetic Elements.” *Nucleic Acids Research* 51 (1): 236–52. https://doi.org/10.1093/nar/gkac1220.
40. Botelho, J., L. Tüffers, J. Fuss, F. Buchholz, C. Utpatel, J. Klockgether, S. Niemann, B. Tümmler, and H. Schulenburg. 2023. “Phylogroup-Specific Variation Shapes the Clustering of Antimicrobial Resistance Genes and Defence Systems across Regions of Genome Plasticity in *Pseudomonas zeruginosa*.” *eBioMedicine* 90 (April):104532. https://doi.org/10.1016/j.ebiom.2023.104532.
41. Braun, V., and K. Hantke. 2011. “Recent Insights into Iron Import by Bacteria.” *Current Opinion in Chemical Biology*, Biocatalysis and Biotransformation/Bioinorganic Chemistry, 15 (2): 328–34. https://doi.org/10.1016/j.cbpa.2011.01.005.
42. Brown, N. F., and B. B. Finlay. 2011. “Potential Origins and Horizontal Transfer of Type III Secretion Systems and Effectors.” *Mobile Genetic Elements* 1 (2): 118–21. https://doi.org/10.4161/mge.1.2.16733.
43. Brown, N. E. M., T. W. Therriault, and C. D. G. Harley. 2016. “Field-Based Experimental Acidification Alters Fouling Community Structure and Reduces Diversity.” *The Journal of Animal Ecology* 85 (5): 1328–39. https://doi.org/10.1111/1365-2656.12557.
44. Bruto, M., A. James, B. Petton, Y. Labreuche, S. Chenivesse, M. Alunno-Bruscia, M. F. Polz, and F. Le Roux. 2017. “*Vibrio crassostreae*, a Benign Oyster Colonizer Turned into a

Pathogen after Plasmid Acquisition." *The ISME Journal* 11 (4): 1043–52. https://doi.org/10.1038/ismej.2016.162.
45. Bruto, M., Y. Labreuche, A. James, D. Piel, S. Chenivesse, B. Petton, M. F. Polz, and F. Le Roux. 2018. "Ancestral Gene Acquisition as the Key to Virulence Potential in Environmental *Vibrio* Populations." *The ISME Journal* 12 (12): 2954–66. https://doi.org/10.1038/s41396-018-0245-3.
46. Burks, D. J., S. Norris, K. M. Kauffman, A. Joy, P. Arevalo, R. K. Azad, and H. Wildschutte. 2017. "Environmental Vibrios Represent a Source of Antagonistic Compounds That Inhibit Pathogenic *Vibrio cholerae* and *Vibrio parahaemolyticus* Strains." *MicrobiologyOpen* 6 (5): e00504. https://doi.org/10.1002/mbo3.504.
47. Cabello, A. E., R. T. Espejo, and J. Romero. 2005. "Tracing *Vibrio parahaemolyticus* in Oysters (*Tiostrea chilensis*) Using a Green Fluorescent Protein Tag." *Journal of Experimental Marine Biology and Ecology* 327 (2): 157–66. https://doi.org/10.1016/j.jembe.2005.06.009.
48. Cai, J., H. L. Chan, X. Yan, and P. Leung. 2023. "A Global Assessment of Species Diversification in Aquaculture." *Aquaculture* 576 (November):739837. https://doi.org/10.1016/j.aquaculture.2023.739837.
49. Calder, T., M. de Souza Santos, V. Attah, J. Klimko, J. Fernandez, D. Salomon, A.-M. Krachler, and K. Orth. 2014. "Structural and Regulatory Mutations in *Vibrio parahaemolyticus* Type III Secretion Systems Display Variable Effects on Virulence." *FEMS Microbiology Letters* 361 (2): 107–14. https://doi.org/10.1111/1574-6968.12619.
50. Camacho, C., G. Coulouris, V. Avagyan, N. Ma, J. Papadopoulos, K. Bealer, and T. L. Madden. 2009. "BLAST+: Architecture and Applications." *BMC Bioinformatics* 10 (1): 421. https://doi.org/10.1186/1471-2105-10-421.
51. Campa-Córdova, A. I., A. Luna-González, F. Ascencio, E. Cortés-Jacinto, and C. J. Cáceres-Martínez. 2006. "Effects of Chloramphenicol, Erythromycin, and Furazolidone on Growth of *Isochrysis galbana* and *Chaetoceros gracilis*." *Aquaculture* 260 (1): 145–50. https://doi.org/10.1016/j.aquaculture.2006.06.014.
52. Campa-Córdova, A. I., A. Luna-González, M. Zarain-Herzberg, and C. J. Cáceres-Martinez. 2005. "Prophylactic Use of Antibiotics in Larval Culture of *Argopecten ventricosus* (Sowerby, 1835)." *Journal of Shellfish Research* 24 (4): 923–30. https://doi.org/10.2983/0730-8000(2005)24[923:PUOAIL]2.0.CO;2.
53. Campbell, A. M., R. G. Gavilan, M. A. Marin, C. Yang, C. Hauton, R. van Aerle, and J. Martinez-Urtaza. 2024. "Evolutionary Dynamics of the Successful Expansion of Pandemic *Vibrio parahaemolyticus* ST3 in Latin America." *Nature Communications* 15 (1): 7828. https://doi.org/10.1038/s41467-024-52159-y.
54. Canchaya, C., C. Proux, G. Fournous, A. Bruttin, and H. Brüssow. 2003. "Prophage Genomics." *Microbiology and Molecular Biology Reviews* 67 (2): 238–76. https://doi.org/10.1128/MMBR.67.2.238-276.2003.
55. Carella, F., N. Carrasco, K. B. Andree, B. Lacuesta, D. Furones, and G. De Vico. 2013. "Nocardiosis in Mediterranean Bivalves: First Detection of *Nocardia crassostreae* in a New Host *Mytilus galloprovincialis* and in *Ostrea edulis* from the Gulf of Naples (Italy)." *Journal of Invertebrate Pathology* 114 (3): 324–28. https://doi.org/10.1016/j.jip.2013.10.001.
56. Carr, V. R., A. Shkoporov, C. Hill, P. Mullany, and D. L. Moyes. 2021. "Probing the Mobilome: Discoveries in the Dynamic Microbiome." *Trends in Microbiology* 29 (2): 158–70. https://doi.org/10.1016/j.tim.2020.05.003.
57. Carroll, A. C., and A. Wong. 2018. "Plasmid Persistence: Costs, Benefits, and the Plasmid Paradox." *Canadian Journal of Microbiology* 64 (5): 293–304. https://doi.org/10.1139/cjm-2017-0609.
58. Casadevall, A., and L-A. Pirofski. 2009. "Virulence Factors and Their Mechanisms of Action: The View from a Damage-Response Framework." *Journal of Water and Health* 7 Suppl 1:S2–18. https://doi.org/10.2166/wh.2009.036.
59. Casjens, S. 2003. "Prophages and Bacterial Genomics: What Have We Learned so Far?" *Molecular Microbiology* 49 (2): 277–300. https://doi.org/10.1046/j.1365-2958.2003.03580.x.

60. Castagna, M. 1983. “Review of Recent Bivalve Culture Methods.” *Journal of the World Mariculture Society* 14 (1–4): 567–75. https://doi.org/10.1111/j.1749-7345.1983.tb00109.x.
61. Cavallo, R., M. Acquaviva, and L. Stabili. 2008. “Culturable Heterotrophic Bacteria in Seawater and *Mytilus galloprovincialis* from a Mediterranean Area (Northern Ionian Sea – Italy).” *Environmental Monitoring and Assessment* 149 (March):465–75. https://doi.org/10.1007/s10661-008-0223-8.
62. Chan, P. P., B. Y. Lin, A. J. Mak, and T. M. Lowe. 2021. “tRNAscan-SE 2.0: Improved Detection and Functional Classification of Transfer RNA Genes.” *Nucleic Acids Research* 49 (16): 9077–96. https://doi.org/10.1093/nar/gkab688.
63. Chatzidaki-Livanis, M., M. K. Jones, and A. C. Wright. 2006. “Genetic Variation in the *Vibrio vulnificus* Group 1 Capsular Polysaccharide Operon.” *Journal of Bacteriology* 188 (5): 1987–98. https://doi.org/10.1128/JB.188.5.1987-1998.2006.
64. Cheikh, Y. B., M.-A. Travers, B. Morga, Y. Godfrin, D. Rioult, and F. Le Foll. 2016. “First Evidence for a *Vibrio* Strain Pathogenic to *Mytilus edulis* Altering Hemocyte Immune Capacities.” *Developmental and Comparative Immunology* 57 (April):107–19. https://doi.org/10.1016/j.dci.2015.12.014.
65. Chen, S., M. Larsson, R. C. Robinson, and S. L. Chen. 2017. “Direct and Convenient Measurement of Plasmid Stability in Lab and Clinical Isolates of *E. coli*.” *Scientific Reports* 7 (1): 4788. https://doi.org/10.1038/s41598-017-05219-x.
66. Cheng, W., F.-M. Juang, and J.-C. Chen. 2004. “The Immune Response of Taiwan Abalone *Haliotis diversicolor supertexta* and Its Susceptibility to *Vibrio parahaemolyticus* at Different Salinity Levels.” *Fish & Shellfish Immunology* 16 (3): 295–306. https://doi.org/10.1016/S1050-4648(03)00111-6.
67. Chevallereau, A., and E. R. Westra. 2022. “Bacterial Immunity: Mobile Genetic Elements Are Hotspots for Defence Systems.” *Current Biology* 32 (17): R923–26. https://doi.org/10.1016/j.cub.2022.07.075.
68. Choi, G., and S. H. Choi. 2022. “Complex Regulatory Networks of Virulence Factors in *Vibrio vulnificus*.” *Trends in Microbiology* 30 (12): 1205–16. https://doi.org/10.1016/j.tim.2022.05.009.
69. Cianciotto, N. P., and R. C. White. 2017. “Expanding Role of Type II Secretion in Bacterial Pathogenesis and Beyond.” *Infection and Immunity* 85 (5): e00014-17. https://doi.org/10.1128/IAI.00014-17.
70. Cimermancic, P., M. H. Medema, J. Claesen, K. Kurita, L. C. W. Brown, K. Mavrommatis, A. Pati, et al. 2014. “Insights into Secondary Metabolism from a Global Analysis of Prokaryotic Biosynthetic Gene Clusters.” *Cell* 158 (2): 412–21. https://doi.org/10.1016/j.cell.2014.06.034.
71. Coluzzi, C., M. P. Garcillán-Barcia, F. de la Cruz, and E. P.C. Rocha. 2022. “Evolution of Plasmid Mobility: Origin and Fate of Conjugative and Nonconjugative Plasmids.” *Molecular Biology and Evolution* 39 (6): msac115. https://doi.org/10.1093/molbev/msac115.
72. Conceição, M. V. R., S. S. Costa, A. P. Schaan, Â. K. C. Ribeiro-dos-Santos, A. Silva, D. A. das Graças, M. P. C. Schneider, and R. A. Baraúna. 2021. “Amazonia Seasons Have an Influence in the Composition of Bacterial Gut Microbiota of Mangrove Oysters (*Crassostrea gasar*).” *Frontiers in Genetics* 11 (February). https://doi.org/10.3389/fgene.2020.602608.
73. Cornelis, G. R., and F. van Gijsegem. 2000. “Assembly and Function of Type III Secretory Systems.” *Annual Review of Microbiology* 54:735–74. https://doi.org/10.1146/annurev.micro.54.1.735.
74. Coyle, N. M., C. O’Toole, J. C. L. Thomas, D. Ryder, E. J. Feil, M. Geary, T. P. Bean, et al. 2023. “*Vibrio aestuarianus* Clade A and Clade B Isolates Are Associated with Pacific Oyster (*Magallana gigas*) Disease Outbreaks across Ireland.” *Microbial Genomics* 9 (8): 001078. https://doi.org/10.1099/mgen.0.001078.
75. Czech, L., L. Hermann, N. Stöveken, A.A. Richter, A. Höppner, S. H. J. Smits, J. Heider, and E. Bremer. 2018. “Role of the Extremolytes Ectoine and Hydroxyectoine as Stress

Protectants and Nutrients: Genetics, Phylogenomics, Biochemistry, and Structural Analysis." *Genes* 9 (4): 177. https://doi.org/10.3390/genes9040177.
76. Dagan, T., Y. Artzy-Randrup, and W. Martin. 2008. "Modular Networks and Cumulative Impact of Lateral Transfer in Prokaryote Genome Evolution." *Proceedings of the National Academy of Sciences* 105 (29): 10039–44. https://doi.org/10.1073/pnas.0800679105.
77. Dai, C., X. Li, D. Luo, Q. Liu, Y. Sun, Z. Tu, and M. Shen. 2022. "Gut Microbiome Composition Likely Affects the Growth of Razor Clam *Sinonovacula constricta*." *Aquaculture* 550 (March):737847. https://doi.org/10.1016/j.aquaculture.2021.737847.
78. Dai, C., X. Li, D. Luo, Q. Liu, Y. Sun, Z. Tu, and M. Shen. 2022. "First Report on Genome Analysis and Pathogenicity of *Vibrio tubiashii* FP17 from Farmed Ivory Shell (*Babylonia areolata*)." *Fishes* 7 (6): 396. https://doi.org/10.3390/fishes7060396.
79. Dai, W., Z. Zhang, Y. Dong, L. He, Q. Xue, and Z. Lin. 2023. "Acute Salinity Stress Disrupts Gut Microbiota Homeostasis and Reduces Network Connectivity and Cooperation in Razor Clam *Sinonovacula constricta*." *Marine Biotechnology* 25 (6): 1147–57. https://doi.org/10.1007/s10126-023-10267-8.
80. Darling, A. C. E., B. Mau, F. R. Blattner, and N. T. Perna. 2004. "Mauve: Multiple Alignment of Conserved Genomic Sequence with Rearrangements." *Genome Research* 14 (7): 1394–1403. https://doi.org/10.1101/gr.2289704.
81. de Sousa, J. A. M., A. Fillol-Salom, J. R Penadés, and E. P. C. Rocha. 2023. "Identification and Characterization of Thousands of Bacteriophage Satellites across Bacteria." *Nucleic Acids Research* 51 (6): 2759–77. https://doi.org/10.1093/nar/gkad123.
82. Defoirdt, T. 2014. "Virulence Mechanisms of Bacterial Aquaculture Pathogens and Antivirulence Therapy for Aquaculture." *Reviews in Aquaculture* 6 (2): 100–114. https://doi.org/10.1111/raq.12030.
83. Dégremont, L., P. Azéma, E. Maurouard, and M.-A. Travers. 2020. "Enhancing Resistance to *Vibrio aestuarianus* in *Crassostrea gigas* by Selection." *Aquaculture* 526 (September):735429. https://doi.org/10.1016/j.aquaculture.2020.735429.
84. Delavat, F., R. Miyazaki, N. Carraro, N. Pradervand, and J. R.f van der Meer. 2017. "The Hidden Life of Integrative and Conjugative Elements." *FEMS Microbiology Reviews* 41 (4): 512–37. https://doi.org/10.1093/femsre/fux008.
85. Destoumieux-Garzón, D., L. Canesi, D. Oyanedel, M.-A. Travers, G. M. Charrière, C. Pruzzo, and L. Vezzulli. 2020. "*Vibrio*-Bivalve Interactions in Health and Disease." *Environmental Microbiology* 22 (10): 4323–41. https://doi.org/10.1111/1462-2920.15055.
86. Dias, G. M., A. Bidault, P. Le Chevalier, G. Choquet, C. Der Sarkissian, L. Orlando, C. Medigue, et al. 2018. "*Vibrio tapetis* Displays an Original Type IV Secretion System in Strains Pathogenic for Bivalve Molluscs." *Frontiers in Microbiology* 9. https://doi.org/10.3389/fmicb.2018.00227
87. Dietrich, J. P., M. B. R. Hicks, J. J. Hard, K. M. Nichols, C. J. Langdon, K. Divilov, B. Schoolfield, and M. R. Arkoosh. 2022. "Heritability Estimates of Disease Resistance to *Vibrio coralliiyticus* in Pacific Oyster (*Crassostrea gigas*) Larvae from a Selective Broodstock Program." *Aquaculture* 560 (November):738492. https://doi.org/10.1016/j.aquaculture.2022.738492.
88. Dijk, M. van, T. Morley, M. L. Rau, and Y. Saghai. 2021. "A Meta-Analysis of Projected Global Food Demand and Population at Risk of Hunger for the Period 2010–2050." *Nature Food* 2 (7): 494–501. https://doi.org/10.1038/s43016-021-00322-9.
89. Dionisio, F., I. C. Conceição, A. C. R. Marques, L. Fernandes, and I. Gordo. 2005. "The Evolution of a Conjugative Plasmid and Its Ability to Increase Bacterial Fitness." *Biology Letters* 1 (2): 250–52. https://doi.org/10.1098/rsbl.2004.0275.
90. Dobrindt, U., J. Zdziarski, E. Salvador, and J. Hacker. 2010a. "Bacterial Genome Plasticity and Its Impact on Adaptation during Persistent Infection." *International Journal of Medical Microbiology: IJMM* 300 (6): 363–66. https://doi.org/10.1016/j.ijmm.2010.04.010.
91. Doron, S., S. Melamed, G. Ofir, A. Leavitt, A. Lopatina, M. Keren, G. Amitai, and R. Sorek. 2018. "Systematic Discovery of Antiphage Defence Systems in the Microbial

Pangenome." *Science (New York, N.Y.)* 359 (6379): eaar4120. https://doi.org/10.1126/science.aar4120.
92. Du, Y., Y. Jin, B. Li, J. Yue, and Z. Yin. 2022. "Comparative Genomic Analysis of *Vibrio cincinnatiensis* Provides Insights into Genetic Diversity, Evolutionary Dynamics, and Pathogenic Traits of the Species." *International Journal of Molecular Sciences* 23 (9): 4520. https://doi.org/10.3390/ijms23094520.
93. Dubert, J., J. A. Aranda-Burgos, J. Ojea, J. L. Barja, and S. Prado. 2017. 2017. "Mortality Event Involving Larvae of the Carpet Shell Clam *Ruditapes decussatus* in a Hatchery: Isolation of the Pathogen *Vibrio tubiashii* subsp. *europaeus*." *Journal of Fish Diseases* 40 (9): 1185–93. https://doi.org/10.1111/jfd.12593.
94. Dubert, J., Juan L. Barja, and J. L. Romalde. 2017. "New Insights into Pathogenic Vibrios Affecting Bivalves in Hatcheries: Present and Future Prospects." *Frontiers in Microbiology* 8. https://www.frontiersin.org/articles/10.3389/fmicb.2017.00762.
95. Dubert, J., D. R. Nelson, Edward J. Spinard, L. Kessner, M. Gomez-Chiarri, F. da Costa, S. Prado, and J. L. Barja. 2016. "Following the Infection Process of Vibriosis in Manila Clam (*Ruditapes philippinarum*) Larvae through GFP-Tagged Pathogenic *Vibrio* Species." *Journal of Invertebrate Pathology* 133 (January):27–33. https://doi.org/10.1016/j.jip.2015.11.008.
96. Dubert, J., C. R. Osorio, S. Prado, and J. L. Barja. 2016. "Persistence of Antibiotic Resistant *Vibrio* spp. in Shellfish Hatchery Environment." *Microbial Ecology* 72 (4): 851–60. https://doi.org/10.1007/s00248-015-0705-5.
97. Dubert, J., J. L. Romalde, S. Prado, and J. L. Barja. 2016. "*Vibrio bivalvicida* sp. nov., a Novel Larval Pathogen for Bivalve Molluscs Reared in a Hatchery." *Systematic and Applied Microbiology* 39 (1): 8–13. https://doi.org/10.1016/j.syapm.2015.10.006.
98. Dubert, J., J. L. Romalde, E. J. Spinard, D. R. Nelson, M. Gomez-Chiarri, and J. L. Barja. 2016. "Reclassification of the Larval Pathogen for Marine Bivalves *Vibrio tubiashii* subsp. *europaeus* as *Vibrio europaeus* sp. Nov." *International Journal of Systematic and Evolutionary Microbiology* 66 (11): 4791–96. https://doi.org/10.1099/ijsem.0.001431.
99. Duperthuy, M., P. Schmitt, E. Garzón, A. Caro, R. D. Rosa, F. Le Roux, N. Lautrédou-Audouy, et al. 2011. "Use of OmpU Porins for Attachment and Invasion of *Crassostrea gigas* Immune Cells by the Oyster Pathogen *Vibrio splendidus*." *Proceedings of the National Academy of Sciences* 108 (7): 2993–98. https://doi.org/10.1073/pnas.1015326108.
100. Elston, R., and L. Leibovitz. 1980. "Pathogenesis of Experimental Vibriosis in Larval American Oysters, *Crassostrea virginica*." *Canadian Journal of Fisheries and Aquatic Sciences* 37 (6): 964–78. https://doi.org/10.1139/f80-126.
101. Elston, R. A., H. Hasegawa, K. L. Humphrey, I. K. Polyak, and C. C. Häse. 2008. "Re-Emergence of *Vibrio tubiashii* in Bivalve Shellfish Aquaculture: Severity, Environmental Drivers, Geographic Extent and Management." *Diseases of Aquatic Organisms* 82 (2): 119–34. https://doi.org/10.3354/dao01982.
102. Engelsma, M. Y., I. Roozenburg, and J.-P. Joly. 2008. "First Isolation of *Nocardia crassostreae* from Pacific Oyster *Crassostrea gigas* in Europe." *Diseases of Aquatic Organisms* 80 (3): 229–34. https://doi.org/10.3354/dao01938.
103. Estes, R. M., C. S. Friedman, R. A. Elston, and R. P. Herwig. 2004. "Pathogenicity Testing of Shellfish Hatchery Bacterial Isolates on Pacific Oyster *Crassostrea gigas* Larvae." *Diseases of Aquatic Organisms* 58 (2–3): 223–30. https://doi.org/10.3354/dao058223.
104. Fan, C., S. Liu, W. Dai, L. He, H. Xu, H. Zhang, and Q. Xue. 2023. "Characterization of *Vibrio mediterranei* Isolates as Causative Agents of Vibriosis in Marine Bivalves." *Microbiology Spectrum* 11 (2): e04923. https://doi.org/10.1128/spectrum.04923-22.
105. FAO. 2024a. "FishStat: Global Aquaculture Production 1950–2022." FishStatJ. 2024. https://www.fao.org/fishery/en/statistics/software/fishstatj.
106. FAO. 2024b. *The State of World Fisheries and Aquaculture 2024*. FAO. https://doi.org/10.4060/cd0683en.

107. Farmer III, J. J., J. M. Janda, F. W. Brenner, D. N. Cameron, and K. M. Birkhead. 2015. "*Vibrio*." In *Bergey's Manual of Systematics of Archaea and Bacteria*, 1–79. John Wiley & Sons, Ltd. https://doi.org/10.1002/9781118960608.gbm01078.
108. Federici, S., S. P. Nobs, and E. Elinav. 2021. "Phages and Their Potential to Modulate the Microbiome and Immunity." *Cellular and Molecular Immunology* 18 (4): 889–904. https://doi.org/10.1038/s41423-020-00532-4.
109. Feria, J. M., and M. A. Valvano. 2020. "An Overview of Anti-Eukaryotic T6SS Effectors." *Frontiers in Cellular and Infection Microbiology* 10. https://www.frontiersin.org/articles/10.3389/fcimb.2020.584751.
110. Fernández-Juárez, V., D. J. Riedinger, J. B. Gusmao, L. F. Delgado-Zambrano, G. Coll-García, V. Papazachariou, D. P. R. Herlemann, et al. 2024. "Temperature, Sediment Resuspension, and Salinity Drive the Prevalence of *Vibrio vulnificus* in the Coastal Baltic Sea." *mBio* 15 (10): e0156924. https://doi.org/10.1128/mbio.01569-24.
111. Ferri, G., V. Olivieri, A. Olivastri, L. Pennisi, and A. Vergara. 2024. "Multidrug Resistant *Vibrio* spp. Identified from Mussels Farmed for Human Consumption in Central Italy." *Journal of Applied Microbiology* 135 (4): lxae098. https://doi.org/10.1093/jambio/lxae098.
112. Forberg, T., R. Vestrum, A. Arukwe, and O. Vadstein. 2012. "Bacterial Composition and Activity Determines Host Gene-Expression Responses in Gnotobiotic Atlantic Cod (*Gadus morhua*) Larvae." *Veterinary Microbiology* 157 (January):420–27. https://doi.org/10.1016/j.vetmic.2012.01.007.
113. Frans, I., C. W. Michiels, P. Bossier, K. A. Willems, B. Lievens, and H. Rediers. 2011. "*Vibrio anguillarum* as a Fish Pathogen: Virulence Factors, Diagnosis and Prevention." *JOURNAL OF FISH DISEASES* 34 (9): 643–61.
114. Froelich, B. A., T. C. Williams, R. T. Noble, and J. D. Oliver. 2012. "Apparent Loss of *Vibrio vulnificus* from North Carolina Oysters Coincides with a Drought-Induced Increase in Salinity." *Applied and Environmental Microbiology* 78 (11): 3885–89. https://doi.org/10.1128/AEM.07855-11.
115. Fu, X., L. Gong, Y. Liu, Q. Lai, G. Li, and Z. Shao. 2021. "*Bacillus pumilus* Group Comparative Genomics: Toward Pangenome Features, Diversity, and Marine Environmental Adaptation." *Frontiers in Microbiology* 12. https://www.frontiersin.org/articles/10.3389/fmicb.2021.571212.
116. Galvis, F., L. Ageitos, D. Martínez-Matamoros, J. L. Barja, J. Rodríguez, M. L. Lemos, C. Jiménez, and M. Balado. 2020. "The Marine Bivalve Molluscs Pathogen *Vibrio neptunius* Produces the Siderophore Amphibactin, Which Is Widespread in Molluscs Microbiota." *Environmental Microbiology* 22 (12): 5467–82. https://doi.org/10.1111/1462-2920.15312.
117. Galvis, F., J. L. Barja, M. L. Lemos, and M. Balado. 2021. "The Vibriolysin-Like Protease VnpA and the Collagenase ColA Are Required for Full Virulence of the Bivalve Molluscs Pathogen *Vibrio neptunius*." *Antibiotics* 10 (4): 391. https://doi.org/10.3390/antibiotics10040391.
118. Galvis, F., L. Ageitos, J. Rodríguez, C. Jiménez, J. L. Barja, M. L. Lemos, and M. Balado. 2021. "*Vibrio neptunius* Produces Piscibactin and Amphibactin and Both Siderophores Contribute Significantly to Virulence for Clams." *Frontiers in Cellular and Infection Microbiology* 11 (October). https://doi.org/10.3389/fcimb.2021.750567.
119. García, M. J., P. W. D'Alvise, A. M. Rygaard, and L. Gram. 2014. "Biofilm Formation Is Not a Prerequisite for Production of the Antibacterial Compound Tropodithietic Acid in *Phaeobacter inhibens* DSM17395." *Journal of Applied Microbiology* 117 (6): 1592–1600. https://doi.org/10.1111/jam.12659.
120. Garcia, C., A. Mesnil, D. Tourbiez, M. Moussa, C. Dubreuil, A. G. de Sa, B. Chollet, et al. 2021. "*Vibrio aestuarianus* subsp. *cardii* subsp. nov., Pathogenic to the Edible Cockles *Cerastoderma edule* in France, and Establishment of *Vibrio aestuarianus* subsp. *aestuarianus* subsp. nov. and *Vibrio aestuarianus* subsp. *francensis* subsp. nov." *International Journal of Systematic and Evolutionary Microbiology* 71 (2): 004654. https://doi.org/10.1099/ijsem.0.004654.

121. Garcillán-Barcia, M. P., S. Redondo-Salvo, L. Vielva, and F. de la Cruz. 2020. "MOBscan: Automated Annotation of MOB Relaxases." *Methods in Molecular Biology (Clifton, N.J.)* 2075:295–308. https://doi.org/10.1007/978-1-4939-9877-7_21.
122. Garnier, M., Y. Labreuche, C. Garcia, M. R., and J.-L. Nicolas. 2007. "Evidence for the Involvement of Pathogenic Bacteria in Summer Mortalities of the Pacific Oyster *Crassostrea gigas*." *Microbial Ecology* 53 (2): 187–96. https://doi.org/10.1007/s00248-006-9061-9.
123. Geng, Z., L. Gao, Z. Yu, Q. Fu, R. Liu, X. Lin, L. Wang, and L. Song. 2022. "The Isolation and Identification of a Pathogenic *Vibrio neocaledonicus* from Yesso Scallop (*Patinopecten yessoensis*)." *Invertebrate Survival Journal*, July, 91–104.
124. Gianazza, E., I. Eberini, L. Palazzolo, and I. Miller. 2021. "Hemolymph Proteins: An Overview across Marine Arthropods and Molluscs." *Journal of Proteomics* 245 (August):104294. https://doi.org/10.1016/j.jprot.2021.104294.
125. Gignoux-Wolfsohn, S., M. G. Ruiz, D. P. Barron, G. Ruiz, and K. Lohan. 2024. "Bivalve Microbiomes Are Shaped by Host Species, Size, Parasite Infection, and Environment." *PeerJ* 12 (October):e18082. https://doi.org/10.7717/peerj.18082.
126. Giljan, G., S. Brown, C. C. Lloyd, S. Ghobrial, R. Amann, and C. Arnosti. 2023. "Selfish Bacteria Are Active throughout the Water Column of the Ocean." *ISME Communications* 3 (1): 1–8. https://doi.org/10.1038/s43705-023-00219-7.
127. Giubergia, S., C. Phippen, C. H. Gotfredsen, K. F. Nielsen, and L. Gram. 2016. "Influence of Niche-Specific Nutrients on Secondary Metabolism in *Vibrionaceae*." *Applied and Environmental Microbiology* 82 (13): 4035–44. https://doi.org/10.1128/AEM.00730-16.
128. Giubergia, S., C. Phippen, K. F. Nielsen, and L. Gram. 2017. "Growth on Chitin Impacts the Transcriptome and Metabolite Profiles of Antibiotic-Producing *Vibrio coralliilyticus* S2052 and *Photobacterium galatheae* S2753." Edited by Rachel J. Dutton. *mSystems* 2 (1): e00141-16. https://doi.org/10.1128/mSystems.00141-16.
129. Gobler, C. J., M. H. Doall, B. J. P.son, C. S. Young, F. DeLaney, R. B. Wallace, S. J. Tomasetti, et al. 2022. "Rebuilding A Collapsed Bivalve Population, Restoring Seagrass Meadows, and Eradicating Harmful Algal Blooms in a Temperate Lagoon Using Spawner Sanctuaries." *Frontiers in Marine Science* 9 (August). https://doi.org/10.3389/fmars.2022.911731.
130. Gomez-Gil, B., A. González-Castillo, M. J. Aguilar-Méndez, A. López-Cortés, J. Gómez-Gutiérrez, A. Roque, E. Lang, and J. Enciso-Ibarra. 2021. "*Veronia nyctiphanis* gen. nov., sp. nov., Isolated from the Stomach of the Euphausiid *Nyctiphanes simplex* (Hansen, 1911) in the Gulf of California, and Reclassification of *Enterovibrio pacificus* as *Veronia pacifica* comb. nov." *Current Microbiology* 78 (10): 3782–90. https://doi.org/10.1007/s00284-021-02627-1.
131. Gómez-León, J., L. Villamil, M. L. Lemos, B. Novoa, and A. Figueras. 2005. "Isolation of *Vibrio alginolyticus* and *Vibrio splendidus* from Aquacultured Carpet Shell Clam (*Ruditapes decussatus*) Larvae Associated with Mass Mortalities." *Applied and Environmental Microbiology* 71 (1): 98–104. https://doi.org/10.1128/AEM.71.1.98-104.2005.
132. Gordo, I., L. Perfeito, and A. Sousa. 2012. "Fitness Effects of Mutations in Bacteria." *Journal of Molecular Microbiology and Biotechnology* 21 (1–2): 20–35. https://doi.org/10.1159/000332747.
133. Gray, M. W., S. T. Alexander, B. F. Beal, T. Bliss, C. A. Burge, J. A. Cram, M. De Luca, et al. 2022. "Hatchery Crashes among Shellfish Research Hatcheries along the Atlantic Coast of the United States: A Case Study of Production Analysis at Horn Point Laboratory." *Aquaculture* 546 (January):737259. https://doi.org/10.1016/j.aquaculture.2021.737259.
134. Gu, Z. 2022. "Complex Heatmap Visualization." *iMeta* 1 (3): e43. https://doi.org/10.1002/imt2.43.
135. Guardiola-Avila, I., L. Sánchez-Busó, E. Acedo-Félix, B. Gomez-Gil, M. Zúñiga-Cabrera, F. González-Candelas, and L. Noriega-Orozco. 2021. "Core and Accessory Genome Analysis of *Vibrio mimicus*." *Microorganisms* 9 (1). https://doi.org/10.3390/microorganisms9010191.

136. Guédon, G., V. Libante, C. Coluzzi, S. Payot, and N. Leblond-Bourget. 2017. "The Obscure World of Integrative and Mobilizable Elements, Highly Widespread Elements That Pirate Bacterial Conjugative Systems." *Genes* 8 (11): 337. https://doi.org/10.3390/genes8110337.
137. Guo, X., and S. E. Ford. 2016. "Infectious Diseases of Marine Molluscs and Host Responses as Revealed by Genomic Tools." *Philosophical Transactions of the Royal Society of London. Series B, Biological Sciences* 371 (1689): 20150206. https://doi.org/10.1098/rstb.2015.0206.
138. Guo, X., and S. E. Ford. 2023. "Multi-Antibiotics Resistance Phenotype of Pathogenic *Vibrio parahaemolyticus* Isolated from Acute Hepatopancreatic Necrosis Disease in *Litopenaeus vannamei* Farmed in the Mekong Delta." *Journal of the World Aquaculture Society* 54 (4): 1070–87. https://doi.org/10.1111/jwas.12945.
139. Hall, J. P. J., João Botelho, A. Cazares, and D. A. Baltrus. 2022. "What Makes a Megaplasmid?" *Philosophical Transactions of the Royal Society B: Biological Sciences* 377 (1842): 20200472. https://doi.org/10.1098/rstb.2020.0472.
140. Hampton, H. G., B. N. J. Watson, and P. C. Fineran. 2020. "The Arms Race between Bacteria and Their Phage Foes." *Nature* 577 (7790): 327–36. https://doi.org/10.1038/s41586-019-1894-8.
141. Hansen, M. J., E. Kudirkiene, and I. Dalsgaard. 2020. "Analysis of 44 *Vibrio anguillarum* Genomes Reveals High Genetic Diversity." *PeerJ* 8 (December):e10451. https://doi.org/10.7717/peerj.10451.
142. Harbeitner, R. C., F. Wittmers, C. C. M. Yung, C. A. Eckmann, E. Hehenberger, M. Blum, D. M. Needham, and A.Z. Worden. 2024. "Gradients of Bacteria in the Oceanic Water Column Reveal Finely-Resolved Vertical Distributions." *PloS One* 19 (4): e0298139. https://doi.org/10.1371/journal.pone.0298139.
143. Hartwick, M. A., A. Berenson, C. A. Whistler, E. N. Naumova, and S. H. Jones. 2021. "The Seasonal Microbial Ecology of Plankton and Plankton-Associated *Vibrio parahaemolyticus* in the Northeast United States." *Applied and Environmental Microbiology* 87 (15): e02973-20. https://doi.org/10.1128/AEM.02973-20.
144. Hasegawa, H., E. J. Lind, M. A. Boin, and C. C. Häse. 2008. "The Extracellular Metalloprotease of *Vibrio tubiashii* Is a Major Virulence Factor for Pacific Oyster (*Crassostrea gigas*) Larvae." *Applied and Environmental Microbiology* 74 (13): 4101–10. https://doi.org/10.1128/AEM.00061-08.
145. He, X., F. Lu, F. Yuan, D. Jiang, P. Zhao, J. Zhu, H. Cheng, J. Cao, and G. Lu. 2015. "Biofilm Formation Caused by Clinical *Acinetobacter baumannii* Isolates Is Associated with Overexpression of the AdeFGH Efflux Pump." *Antimicrobial Agents and Chemotherapy* 59 (8): 4817–25. https://doi.org/10.1128/AAC.00877-15.
146. Helm, M.M., N. Bourne, and A. Lovatelli. 2004. "Hatchery Culture of Bivalves, a Practical Manual. FAO Fisheries Technical Paper 471. Food and Agriculture Organization of the in the Laboratory." *Mar. Biol.* 15 (January):350–55.
147. Hettiarachchi, S. A., S.-J. Lee, Y. Lee, Y.-K. Kwon, K. K. Kwon, S.-H. Yang, E. Jo, D.-H. Kang, and C. Oh. 2018. "*Corallibacterium pacifica* gen. nov., sp. nov., a Novel Bacterium of the Family *Vibrionaceae* Isolated from Hard Coral." *Current Microbiology* 75 (7): 835–41. https://doi.org/10.1007/s00284-018-1455-7.
148. Hiyoshi, H., T. Kodama, T. Iida, and T. Honda. 2010. "Contribution of *Vibrio parahaemolyticus* Virulence Factors to Cytotoxicity, Enterotoxicity, and Lethality in Mice." *Infection and Immunity* 78 (4): 1772–80. https://doi.org/10.1128/IAI.01051-09.
149. Hochhauser, D., A. Millman, and R. Sorek. 2023. "The Defence Island Repertoire of the *Escherichia coli* Pan-Genome." *PLOS Genetics* 19 (4). https://doi.org/10.1371/journal.pgen.1010694.
150. Hossain, A., M. Habibullah-Al-Mamun, I. Nagano, S. Masunaga, D. Kitazawa, and H. Matsuda. 2022. "Antibiotics, Antibiotic-Resistant Bacteria, and Resistance Genes in

Aquaculture: Risks, Current Concern, and Future Thinking." *Environmental Science and Pollution Research* 29 (8): 11054–75. https://doi.org/10.1007/s11356-021-17825-4.
151. Hossain, M. M., I. Uddin, H. Islam, J. Fardoush, A. H. Rupom, M. Hossain, N. Farjana, et al. 2020. "Diagnosis, Genetic Variations, Virulence, and Toxicity of AHPND-Positive *Vibrio parahaemolyticus* in *Penaeus monodon*." *Aquaculture International* 28 (6): 2531–46. https://doi.org/10.1007/s10499-020-00607-z.
152. Huan, P., G. Liu, H. Wang, and B. Liu. 2014. "Multiple Ferritin Subunit Genes of the Pacific Oyster *Crassostrea gigas* and Their Distinct Expression Patterns during Early Development." *Gene* 546 (1): 80–88. https://doi.org/10.1016/j.gene.2014.05.027.
153. Huang, L., L. Huang, Q. Yan, Y. Qin, Y. Ma, M. Lin, X. Xu, and J. Zheng. 2016. "The TCA Pathway Is an Important Player in the Regulatory Network Governing *Vibrio alginolyticus* Adhesion Under Adversity." *Frontiers in Microbiology* 7 (February). https://doi.org/10.3389/fmicb.2016.00040.
154. Huang, D., Z. Zhang, M. Sun, Z. Feng, and M. Ye. 2021. "Characterization and Ecological Function of Bacterial Communities in Seabed Sediments of the Southwestern Yellow Sea and Northwestern East China Sea, Western Pacific." *Science of The Total Environment* 761 (March):143233. https://doi.org/10.1016/j.scitotenv.2020.143233.
155. Huang, B., X. Zhang, C. Wang, C.-M. Bai, C. Li, C. Li, and L. Xin. 2021. "Isolation and Characterization of *Vibrio kanaloae* as a Major Pathogen Associated with Mass Mortalities of Ark Clam, *Scapharca broughtonii*, in Cold Season." *Microorganisms* 9 (10): 2161. https://doi.org/10.3390/microorganisms9102161.
156. Hudson, C. M., B. Y. Lau, and K. P. Williams. 2015. "Islander: A Database of Precisely Mapped Genomic Islands in tRNA and tmRNA Genes." *Nucleic Acids Research* 43 (Database issue): D48-53. https://doi.org/10.1093/nar/gku1072.
157. Hussain, F. A., J. Dubert, J. Elsherbini, M. Murphy, D. VanInsberghe, P. Arevalo, K. Kauffman, et al. 2021. "Rapid Evolutionary Turnover of Mobile Genetic Elements Drives Bacterial Resistance to Phages." *Science* 374 (6566): 488–92. https://doi.org/10.1126/science.abb1083.
158. Hyun, J. C., Jonathan M. M., and B. O. Palsson. 2022. "Comparative Pangenomics: Analysis of 12 Microbial Pathogen Pangenomes Reveals Conserved Global Structures of Genetic and Functional Diversity." *BMC Genomics* 23 (1): 7. https://doi.org/10.1186/s12864-021-08223-8.
159. Ishaq, S. L., S. Hosler, A. Dankwa, P. Jekielek, D. C. Brady, E. Grey, H. Haskell, et al. 2023. "Bacterial Community Trends Associated with Sea Scallop, *Placopecten magellanicus*, Larvae in a Hatchery System." *Aquaculture Reports* 32 (October):101693. https://doi.org/10.1016/j.aqrep.2023.101693.
160. Islam, S. S., S. Zhang, M. Eggermont, M. Bruto, F. Le Roux, and T. Defoirdt. 2022. "The Impact of the Multichannel Quorum Sensing Systems of *Vibrio tasmaniensis* and *Vibrio crassostreae* on Virulence towards Blue Mussel (*Mytilus edulis*) Larvae." *Aquaculture* 547 (January):737414. https://doi.org/10.1016/j.aquaculture.2021.737414.
161. Jackson, R. W., B. Vinatzer, D. L. Arnold, S. Dorus, and J. Murillo. 2011. "The Influence of the Accessory Genome on Bacterial Pathogen Evolution." *Mobile Genetic Elements* 1 (1): 55–65. https://doi.org/10.4161/mge.1.1.16432.
162. Jeffries, V. E. 1982. "Three *Vibrio* Strains Pathogenic to Larvae of *Crassostrea gigas* and *Ostrea edulis*." *Aquaculture* 29 (3): 201–26. https://doi.org/10.1016/0044-8486(82)90136-3.
163. Jiang, K., C. Chen, G. Jiang, Y. Chi, C. Xu, L. Kong, H. Yu, S. Liu, and Q. Li. 2024. "Genetic Improvement of Oysters: Current Status, Challenges, and Prospects." *Reviews in Aquaculture* 16 (2): 796–817. https://doi.org/10.1111/raq.12868.
164. Jiang, C., M. Tanaka, S. Nishikawa, S. Mino, J. L. Romalde, F. L. Thompson, B. Gomez-Gil, and T. Sawabe. 2021. "*Vibrio* Clade 3.0: New *Vibrionaceae* Evolutionary Units Using Genome-Based Approach." *Current Microbiology* 79 (1): 10. https://doi.org/10.1007/s00284-021-02725-0.

165. Johnson, M. C., E. Laderman, E. Huiting, C. Zhang, A. Davidson, and J. Bondy-Denomy. 2023. “Core Defence Hotspots within *Pseudomonas aeruginosa* Are a Consistent and Rich Source of Anti-Phage Defence Systems.” *Nucleic Acids Research* 51 (10): 4995–5005. https://doi.org/10.1093/nar/gkad317.
166. Jones, J. B. 2006. “Why Won’t They Grow? – Inhibitory Substances and Mollusc Hatcheries.” *Aquaculture International* 14 (4): 395–403. https://doi.org/10.1007/s10499-005-9040-z.
167. Jorquera, M. A., G. Valencia, M. Eguchi, M. Katayose, and C. Riquelme. 2002. “Disinfection of Seawater for Hatchery Aquaculture Systems Using Electrolytic Water Treatment.” *Aquaculture* 207 (3): 213–24. https://doi.org/10.1016/S0044-8486(01)00766-9.
168. Kalatzis, P. G., D. Castillo, P. Katharios, and M. Middelboe. 2018. “Bacteriophage Interactions with Marine Pathogenic Vibrios: Implications for Phage Therapy.” *Antibiotics* 7 (1): 15. https://doi.org/10.3390/antibiotics7010015.
169. Karlsen, C., S. M. Paulsen, H. S. Tunsjø, S. Krinner, H. Sørum, P. Haugen, and N.-P. Willassen. 2008. “Motility and Flagellin Gene Expression in the Fish Pathogen *Vibrio salmonicida*: Effects of Salinity and Temperature.” *Microbial Pathogenesis* 45 (4): 258–64. https://doi.org/10.1016/j.micpath.2008.06.002.
170. Karunasagar, I., S. K. Otta, and I. Karunasagar. 1996. “Biofilm Formation by *Vibrio harveyi* on Surfaces.” *Aquaculture* 140 (3): 241–45. https://doi.org/10.1016/0044-8486(95)01180-3.
171. Kesarcodi-Watson, A., P. Miner, J.-L. Nicolas, and R. Robert. 2012. “Protective Effect of Four Potential Probiotics against Pathogen-Challenge of the Larvae of Three Bivalves: Pacific Oyster (*Crassostrea gigas*), Flat Oyster (*Ostrea edulis*) and Scallop (*Pecten maximus*).” *Aquaculture* 344–349 (May):29–34. https://doi.org/10.1016/j.aquaculture.2012.02.029.
172. Kijewska, A., A. Koroza, K. Grudlewska-Buda, T. Kijewski, N. Wiktorczyk-Kapischke, K. Zorena, and K. Skowron. 2023. “Molluscs—A Ticking Microbial Bomb.” *Frontiers in Microbiology* 13. https://www.frontiersin.org/articles/10.3389/fmicb.2022.1061223.
173. Kim, H. J., J. W. Jun, S. S. Giri, C. Chi, S. Yun, S. G. Kim, S. W. Kim, et al. 2020. “Identification and Genome Analysis of *Vibrio coralliilyticus* Causing Mortality of Pacific Oyster (*Crassostrea gigas*) Larvae.” *Pathogens (Basel, Switzerland)* 9 (3): 206. https://doi.org/10.3390/pathogens9030206.
174. Kim, H. J., J.W. Jun, S. S. Giri, S. G. Kim, S. W. Kim, J. Kwon, S. B. Lee, C. Chi, and S. C. Park. 2020. “Bacteriophage Cocktail for the Prevention of Multiple-Antibiotic-Resistant and Mono-Phage-Resistant *Vibrio coralliilyticus* Infection in Pacific Oyster (*Crassostrea gigas*) Larvae.” *Pathogens* 9 (10): 831. https://doi.org/10.3390/pathogens9100831.
175. Kimes, N. E., C. J Grim, W. R. Johnson, N. A. Hasan, B. D. Tall, M. H. Kothary, H. Kiss, et al. 2012. “Temperature Regulation of Virulence Factors in the Pathogen *Vibrio coralliilyticus*.” *The ISME Journal* 6 (4): 835–46. https://doi.org/10.1038/ismej.2011.154.
176. Kirov, S. M. 2003. “Bacteria That Express Lateral Flagella Enable Dissection of the Multifunctional Roles of Flagella in Pathogenesis.” *FEMS Microbiology Letters* 224 (2): 151–59. https://doi.org/10.1016/S0378-1097(03)00445-2.
177. Kloska, A., G. M. Cech, D. Nowicki, M. Maciąg-Dorszyńska, A. E. Bogucka, S. Markert, D. Becher, K. Potrykus, P. Czaplewska, and A. Szalewska-Pałasz. 2022. “Three Microbial Musketeers of the Seas: *Shewanella baltica*, *Aliivibrio fischeri* and *Vibrio harveyi*, and Their Adaptation to Different Salinity Probed by a Proteomic Approach.” *International Journal of Molecular Sciences* 23 (2): 619. https://doi.org/10.3390/ijms23020619.
178. Knöppel, A., P. A. Lind, U. Lustig, J. Näsvall, and D. I. Andersson. 2014. “Minor Fitness Costs in an Experimental Model of Horizontal Gene Transfer in Bacteria.” *Molecular Biology and Evolution* 31 (5): 1220–27. https://doi.org/10.1093/molbev/msu076.
179. Kolmogorov, M., J. Yuan, Y. Lin, and P. A. Pevzner. 2019. “Assembly of Long, Error-Prone Reads Using Repeat Graphs.” *Nature Biotechnology* 37 (5): 540–46. https://doi.org/10.1038/s41587-019-0072-8.

180. Konieczna, I., P. Zarnowiec, M. Kwinkowski, B. Kolesinska, J. Fraczyk, Z. Kaminski, and W. Kaca. 2012. "Bacterial Urease and Its Role in Long-Lasting Human Diseases." *Current Protein & Peptide Science* 13 (8): 789–806.
181. Kopprio, G. A., M. E. Streitenberger, K. Okuno, M. Baldini, F. Biancalana, A. Fricke, A. Martínez, et al. 2017. "Biogeochemical and Hydrological Drivers of the Dynamics of *Vibrio* Species in Two Patagonian Estuaries." *Science of The Total Environment* 579 (February):646–56. https://doi.org/10.1016/j.scitotenv.2016.11.045.
182. Labreuche, Y., F. Le Roux, J. Henry, C. Zatylny, A. Huvet, C. Lambert, P. Soudant, D. Mazel, and J.-L. Nicolas. 2010. "*Vibrio aestuarianus* Zinc Metalloprotease Causes Lethality in the Pacific Oyster *Crassostrea gigas* and Impairs the Host Cellular Immune Defences." *Fish & Shellfish Immunology* 29 (5): 753–58. https://doi.org/10.1016/j.fsi.2010.07.007.
183. Labreuche, Y., P. Soudant, M. Gonçalves, C. Lambert, and J.-L. Nicolas. 2006. "Effects of Extracellular Products from the Pathogenic *Vibrio aestuarianus* Strain 01/32 on Lethality and Cellular Immune Responses of the Oyster *Crassostrea gigas*." *Developmental & Comparative Immunology* 30 (4): 367–79. https://doi.org/10.1016/j.dci.2005.05.003.
184. Lafont, M., B. Petton, A. Vergnes, M. Pauletto, A. Segarra, B. Gourbal, and C. Montagnani. 2017. "Long-Lasting Antiviral Innate Immune Priming in the Lophotrochozoan Pacific Oyster, *Crassostrea gigas*." *Scientific Reports* 7 (1): 13143. https://doi.org/10.1038/s41598-017-13564-0.
185. Laith, A. A., M. K. Ros-Amira, H. I. Sheikh, A. W. M. Effendy, and M. Najiah. 2021. "Histopathological and Immunological Changes in Green Mussel, *Perna viridis,* Challenged with *Vibrio alginolyticus*." *Fish & Shellfish Immunology* 118 (November):169–79. https://doi.org/10.1016/j.fsi.2021.08.032.
186. Lambert, C., J. L. Nicolas, V. Cilia, and S. Corre. 1998. "*Vibrio pectenicida* sp. nov., a Pathogen of Scallop (*Pecten maximus*) Larvae." *International Journal of Systematic and Evolutionary Microbiology* 48 (2): 481–87. https://doi.org/10.1099/00207713-48-2-481.
187. Le Roux, F., M. Gay, C. Lambert, M. Waechter, S. Poubalanne, B. Chollet, J.-L. Nicolas, and F. Berthe. 2002. "Comparative Analysis of *Vibrio splendidus*-Related Strains Isolated during *Crassostrea gigas* Mortality Events." *Aquatic Living Resources* 15 (January):251–58. https://doi.org/10.1016/S0990-7440(02)01176-2.
188. Le Roux, F., K. M. Wegner, and M. F. Polz. 2016. "Oysters and Vibrios as a Model for Disease Dynamics in Wild Animals." *Trends in Microbiology* 24 (7): 568–80. https://doi.org/10.1016/j.tim.2016.03.006.
189. Le Roux, F., M. Zouine, N. Chakroun, J. Binesse, D. Saulnier, C. Bouchier, N. Zidane, et al. 2009. "Genome Sequence of *Vibrio splendidus*: An Abundant Planctonic Marine Species with a Large Genotypic Diversity." *Environmental Microbiology* 11 (8): 1959–70. https://doi.org/10.1111/j.1462-2920.2009.01918.x.
190. Lee, K.-K., and K.-C. Yii. 1996. "A Comparison of Three Methods for Assaying Hydrophobicity of Pathogenic Vibrios." *Letters in Applied Microbiology* 23 (5): 343–46. https://doi.org/10.1111/j.1472-765X.1996.tb00204.x.
191. Lee, Y., H. Roh, A. Kim, J. Park, J.-Y. Lee, Y.-J. Kim, Y.-R. Kang, et al. 2023. "Molecular Mechanisms Underlying the Vulnerability of Pacific Abalone (*Haliotis discus hannai*) to *Vibrio harveyi* Infection at Higher Water Temperature." *Fish & Shellfish Immunology* 138 (July):108844. https://doi.org/10.1016/j.fsi.2023.108844.
192. Letunic, I., and P. Bork. 2021. "Interactive Tree Of Life (iTOL) v5: An Online Tool for Phylogenetic Tree Display and Annotation." *Nucleic Acids Research* 49 (W1): W293–96. https://doi.org/10.1093/nar/gkab301.
193. Li, Y.-F., Y.-W. Chen, J.-K. Xu, W.-Y. Ding, A.-Q. Shao, Y.-T. Zhu, C. Wang, X. Liang, and J.-L. Yang. 2019. "Temperature Elevation and *Vibrio cyclitrophicus* Infection Reduce the Diversity of Haemolymph Microbiome of the Mussel *Mytilus coruscus*." *Scientific Reports* 9 (1): 16391. https://doi.org/10.1038/s41598-019-52752-y.
194. Li, Z., S. Chen, C. Xu, L. Ju, and F. Li. 2018. "Rapid Subtyping of Pathogenic and Nonpathogenic *Vibrio parahaemolyticus* by Fourier Transform Infrared Spectroscopy with

Chemometric Analysis." *Journal of Microbiological Methods* 155 (December):70–77. https://doi.org/10.1016/j.mimet.2018.11.003.
195. Li, X., C. Shi, B. Yang, Q. Li, and S. Liu. 2023. "High Temperature Aggravates Mortalities of the Pacific Oyster (*Crassostrea gigas*) Infected with *Vibrio*: A Perspective from Homeostasis of Digestive Microbiota and Immune Response." *Aquaculture* 568 (April):739309. https://doi.org/10.1016/j.aquaculture.2023.739309.
196. Li, Q., Q. Wang, S. Liu, and L. Kong. 2011. "Selection Response and Realized Heritability for Growth in Three Stocks of the Pacific Oyster *Crassostrea gigas*." *Fisheries Science* 77 (4): 643–48. https://doi.org/10.1007/s12562-011-0369-0.
197. Li, X., Y. Xie, M. Liu, C. Tai, J. Sun, Z. Deng, and H.-Y. Ou. 2018. "oriTfinder: A Web-Based Tool for the Identification of Origin of Transfers in DNA Sequences of Bacterial Mobile Genetic Elements." *Nucleic Acids Research* 46 (W1): W229–34. https://doi.org/10.1093/nar/gky352.
198. Li, X., B. Yang, C. Shi, H. Wang, R. Yu, Q. Li, and S. Liu. 2022. "Synergistic Interaction of Low Salinity Stress With *Vibrio* Infection Causes Mass Mortalities in the Oyster by Inducing Host Microflora Imbalance and Immune Dysregulation." *Frontiers in Immunology* 13 (May). https://doi.org/10.3389/fimmu.2022.859975.
199. Liao, J., X. Guo, D. L. Weller, S. Pollak, D. H. Buckley, M. Wiedmann, and O. X. Cordero. 2021. "Nationwide Genomic Atlas of Soil-Dwelling *Listeria* Reveals Effects of Selection and Population Ecology on Pangenome Evolution." *Nature Microbiology* 6 (8): 1021–30. https://doi.org/10.1038/s41564-021-00935-7.
200. Lin, J., L. Xu, J. Yang, Z. Wang, and X. Shen. 2021. "Beyond Dueling: Roles of the Type VI Secretion System in Microbiome Modulation, Pathogenesis and Stress Resistance." *Stress Biology* 1 (1): 11. https://doi.org/10.1007/s44154-021-00008-z.
201. Liu, R., G. Han, Z. Li, S. Cun, B. Hao, J. Zhang, and X. Liu. 2022. "Bacteriophage Therapy in Aquaculture: Current Status and Future Challenges." *Folia Microbiologica* 67 (4): 573–90. https://doi.org/10.1007/s12223-022-00965-6.
202. Liu, M., X. Li, Y. Xie, D. Bi, J. Sun, J. Li, C. Tai, Z. Deng, and H.-Y. Ou. 2019. "ICEberg 2.0: An Updated Database of Bacterial Integrative and Conjugative Elements." *Nucleic Acids Research* 47 (D1): D660–65. https://doi.org/10.1093/nar/gky1123.
203. Liu, Sun, Li, Zhang, Cao, and Ma. 2015. "*Vibrio* Infections Associated with Yesso Scallop (*Patinopecten yessoensis*) Larval Culture." *Journal of Shellfish Research* 34 (August):213–16. https://doi.org/10.2983/035.034.0202.
204. Liu, X., H. Yao, X. Zhao, and C. Ge. 2023. "Biofilm Formation and Control of Foodborne Pathogenic Bacteria." *Molecules* 28 (6): 2432. https://doi.org/10.3390/molecules28062432.
205. Liu, B., D. Zheng, S. Zhou, L. Chen, and J. Yang. 2021. "VFDB 2022: A General Classification Scheme for Bacterial Virulence Factors." *Nucleic Acids Research* 50 (D1): D912–17. https://doi.org/10.1093/nar/gkab1107.
206. Lodeiros, C., J. Bolinches, C. P. Dopazo, and A. E. Toranzo. 1987. "Bacillary Necrosis in Hatcheries of *Ostrea edulis* in Spain." *Aquaculture* 65 (1): 15–29. https://doi.org/10.1016/0044-8486(87)90267-5.
207. Loor, A., P. Bossier, D. Wang, L. De Bels, W. Van den Broeck, N. Nevejan, and A. Declercq. 2023. "Effect of Continuous Dietary Administration of the *Saccharomyces cerevisiae* Yeast, Δ*Mnn9*, on Pacific Oyster (*Crassostrea gigas*) Juveniles: Immunological and Histopathological Findings after *Vibrio coralliilyticus* Challenge." *Aquaculture* 574 (September):739644. https://doi.org/10.1016/j.aquaculture.2023.739644.
208. López-Cervantes, G., P. Álvarez-Ruiz, S. Luna-Suárez, A. Luna-González, H. M. Esparza-Leal, C. Castro-Martínez, C. Gámez-Jiménez, and J. Soto-Alcalá. 2021. "Temperature and Salinity Modulate Virulence and PirA Gene Expression of *Vibrio parahaemolyticus*, the Causative Agent of AHPND." *Aquaculture International* 29 (2): 743–56. https://doi.org/10.1007/s10499-021-00654-0.

209. López-Hernández, K. M., V. T. Pardío-Sedas, L. Lizárraga-Partida, J. de J. Williams, D. Martínez-Herrera, A. Flores-Primo, R. Uscanga-Serrano, and K. Rendón-Castro. 2015. "Environmental Parameters Influence on the Dynamics of Total and Pathogenic *Vibrio parahaemolyticus* Densities in *Crassostrea virginica* Harvested from Mexico's Gulf Coast." *Marine Pollution Bulletin* 91 (1): 317–29. https://doi.org/10.1016/j.marpolbul.2014.11.015.
210. López-Pérez, M., and F. Rodriguez-Valera. 2016. "Pangenome Evolution in the Marine Bacterium *Alteromonas*." *Genome Biology and Evolution* 8 (5): 1556–70. https://doi.org/10.1093/gbe/evw098.
211. Lulijwa, R., E. J. Rupia, and A. C. Alfaro. 2020. "Antibiotic Use in Aquaculture, Policies and Regulation, Health and Environmental Risks: A Review of the Top 15 Major Producers." *Reviews in Aquaculture* 12 (2): 640–63. https://doi.org/10.1111/raq.12344.
212. Luo, Y., Z. Chen, S. Lian, X. Ji, C. Zhu, G. Zhu, and P. Xia. 2023. "The Love and Hate Relationship between T5SS and Other Secretion Systems in Bacteria." *International Journal of Molecular Sciences* 25 (1): 281. https://doi.org/10.3390/ijms25010281.
213. Luo, G., L. Huang, Y. Su, Y. Qin, X. Xu, L. Zhao, and Q. Yan. 2016. "flrA, flrB and flrC Regulate Adhesion by Controlling the Expression of Critical Virulence Genes in *Vibrio alginolyticus*." *Emerging Microbes & Infections* 5 (1): 1–11. https://doi.org/10.1038/emi.2016.82.
214. Maistrenko, O. M., D. R. Mende, M. Luetge, F. Hildebrand, T. S. B. Schmidt, S. S. Li, J. F. M. Rodrigues, et al. 2020. "Disentangling the Impact of Environmental and Phylogenetic Constraints on Prokaryotic Within-Species Diversity." *The ISME Journal* 14 (5): 1247–59. https://doi.org/10.1038/s41396-020-0600-z.
215. Makarova, K. S., Y. I. Wolf, S. Snir, and E. V. Koonin. 2011. "Defence Islands in Bacterial and Archaeal Genomes and Prediction of Novel Defence Systems." *Journal of Bacteriology* 193 (21): 6039–56. https://doi.org/10.1128/jb.05535-11.
216. Malara, D., C. Mielke, M. Oelgemöller, M. O. Senge, and K. Heimann. 2017. "Sustainable Water Treatment in Aquaculture – Photolysis and Photodynamic Therapy for the Inactivation of *Vibrio* Species." *Aquaculture Research* 48 (6): 2954–62. https://doi.org/10.1111/are.13128.
217. Maloy, A. P., S. E. Ford, R. C. Karney, and K. J. Boettcher. 2007. "*Roseovarius crassostreae*, the Etiological Agent of Juvenile Oyster Disease (Now to Be Known as *Roseovarius* Oyster Disease) in *Crassostrea virginica*." *Aquaculture* 269 (1): 71–83. https://doi.org/10.1016/j.aquaculture.2007.04.008.
218. Mao, F., K. Liu, N.-K. Wong, X. Zhang, W. Yi, Z. Xiang, S. Xiao, Z. Yu, and Y. Zhang. 2021. "Virulence of *Vibrio alginolyticus* Accentuates Apoptosis and Immune Rigor in the Oyster *Crassostrea hongkongensis*." *Frontiers in Immunology* 12 (September). https://doi.org/10.3389/fimmu.2021.746017.
219. Martinez, C., S. Rodriguez, A. Vences, J. L. Barja, A. E. Toranzo, and J. Dubert. 2022. "Role of the Vibriolysin VemA Secreted by the Emergent Pathogen *Vibrio europaeus* in the Colonization of Manila Clam Mucus." *Microorganisms* 10 (12): 2475. https://doi.org/10.3390/microorganisms10122475.
220. Masanja, F., K. Yang, Y. Xu, G. He, X. Liu, X. Xu, X. Jiang, et al. 2023. "Bivalves and Microbes: A Mini-Review of Their Relationship and Potential Implications for Human Health in a Rapidly Warming Ocean." *Frontiers in Marine Science* 10 (June). https://doi.org/10.3389/fmars.2023.1182438.
221. Mass, S., H. Cohen, R. Podicheti, D. B. Rusch, M.Gerlic, B. Ushijima, J. C. van Kessel, E. Bosis, and D. Salomon. 2024. "The Coral Pathogen *Vibrio coralliilyticus* Uses a T6SS to Secrete a Group of Novel Anti-Eukaryotic Effectors That Contribute to Virulence." *PLOS Biology* 22 (9): e3002734. https://doi.org/10.1371/journal.pbio.3002734.
222. Mass, S., H.r Cohen, M. Gerlic, B. Ushijima, J. C. van Kessel, E.Bosis, and D. Salomon. 2024. "A T6SS in the Coral Pathogen *Vibrio coralliilyticus* Secretes an Arsenal of Anti-Eukaryotic Effectors and Contributes to Virulence." bioRxiv. https://doi.org/10.1101/2024.03.20.584600.

223. Mateus, L., L. Costa, Y. J. Silva, C. Pereira, A. Cunha, and A. Almeida. 2014. "Efficiency of Phage Cocktails in the Inactivation of *Vibrio* in Aquaculture." *Aquaculture* 424–425 (March):167–73. https://doi.org/10.1016/j.aquaculture.2014.01.001.
224. McArthur, A. G., N. Waglechner, F. Nizam, A. Yan, M. A. Azad, A. J. Baylay, K. Bhullar, et al. 2013. "The Comprehensive Antibiotic Resistance Database." *Antimicrobial Agents and Chemotherapy* 57 (7): 3348–57. https://doi.org/10.1128/AAC.00419-13.
225. McCauley, M., T. L. Goulet, C. R. Jackson, and S. Loesgen. 2023. "Systematic Review of Cnidarian Microbiomes Reveals Insights into the Structure, Specificity, and Fidelity of Marine Associations." *Nature Communications* 14 (1): 4899. https://doi.org/10.1038/s41467-023-39876-6.
226. McInerney, J. O., A. McNally, and M. J. O'Connell. 2017. "Why Prokaryotes Have Pangenomes." *Nature Microbiology* 2 (4): 17040. https://doi.org/10.1038/nmicrobiol.2017.40.
227. Mckindsey, C. W., T. Landry, F. X. O'beirn, and I. M. Davies. 2007. "Bivalve Aquaculture and Exotic Species: a Review of Ecological Considerations and Management Issues." *Journal of Shellfish Research* 26 (2): 281–94. https://doi.org/10.2983/0730-8000(2007)26[281:BAAESA]2.0.CO;2.
228. Mersni-Achour, R., N. Imbert-Auvray, V. Huet, Y. B. Cheikh, N. Faury, I. Doghri, S. Rouatbi, et al. 2014a. "First Description of French *V. tubiashii* Strains Pathogenic to Mollusc: II. Characterization of Properties of the Proteolytic Fraction of Extracellular Products." *Journal of Invertebrate Pathology* 123 (November):49–59. https://doi.org/10.1016/j.jip.2014.09.006.
229. Mey, A.R., and S. M. Payne. 2001. "Haem Utilization in *Vibrio cholerae* Involves Multiple TonB-Dependent Haem Receptors." *Molecular Microbiology* 42 (3): 835–49. https://doi.org/10.1046/j.1365-2958.2001.02683.x.
230. Mey, A.R., E. E. Wyckoff, A. G. Oglesby, E. Rab, R. K. Taylor, and S. M. Payne. 2002. "Identification of the *Vibrio cholerae* Enterobactin Receptors VctA and IrgA: IrgA Is Not Required for Virulence." *Infection and Immunity* 70 (7): 3419–26. https://doi.org/10.1128/IAI.70.7.3419-3426.2002.
231. Miller, H. C., J. Wylie, G. Dejean, A. H. Kaksonen, D. Sutton, K. Braun, and G. J. Puzon. 2015. "Reduced Efficiency of Chlorine Disinfection of Naegleria Fowleri in a Drinking Water Distribution Biofilm." *Environmental Science & Technology* 49 (18): 11125–31. https://doi.org/10.1021/acs.est.5b02947.
232. Minich, J. J., A. Härer, J. Vechinski, B. W. Frable, Z. R. Skelton, E. Kunselman, M. A. Shane, et al. 2022. "Host Biology, Ecology and the Environment Influence Microbial Biomass and Diversity in 101 Marine Fish Species." *Nature Communications* 13 (1): 6978. https://doi.org/10.1038/s41467-022-34557-2.
233. Mira, A. 2010. "The Bacterial Pan-Genome: A New Paradigm in Microbiology." *International Microbiology*, no. 13, 45–57. https://doi.org/10.2436/20.1501.01.110.
234. Miyamoto, M., D. Motooka, K. Gotoh, T. Imai, K. Yoshitake, N. Goto, T. Iida, et al. 2014. "Performance Comparison of Second- and Third-Generation Sequencers Using a Bacterial Genome with Two Chromosomes." *BMC Genomics* 15 (1): 699. https://doi.org/10.1186/1471-2164-15-699.
235. Miyoshi, S.-I., and S. Shinoda. 2000. "Microbial Metalloproteases and Pathogenesis." *Microbes and Infection* 2 (1): 91–98. https://doi.org/10.1016/S1286-4579(00)00280-X.
236. Miyoshi, S.-I. 2013. "Extracellular Proteolytic Enzymes Produced by Human Pathogenic *Vibrio* Species." *Frontiers in Microbiology* 4. https://www.frontiersin.org/articles/10.3389/fmicb.2013.00339.
237. Mo, Z., D. Guo, Y. Mao, X. Ye, Y. Zou, P. Xiao, and B. Hao. 2010. "Identification and Characterization of the *Vibrio anguillarum prtV* Gene Encoding a New Metalloprotease." *Chinese Journal of Oceanology and Limnology* 28 (1): 55–61. https://doi.org/10.1007/s00343-010-9246-4.
238. Mochizuki, A., K. Yahara, I. Kobayashi, and Y. Iwasa. 2006. "Genetic Addiction: Selfish Gene's Strategy for Symbiosis in the Genome." *Genetics* 172 (2): 1309–23. https://doi.org/10.1534/genetics.105.042895.

239. Modak, T. H., and M. Gomez-Chiarri. 2020. “Contrasting Immunomodulatory Effects of Probiotic and Pathogenic Bacteria on Eastern Oyster, *Crassostrea virginica*, Larvae.” *Vaccines* 8 (4): 588. https://doi.org/10.3390/vaccines8040588.
240. Modolon, F., A.R. Barno, H.D.M. Villela, and R.S. Peixoto. 2020. “Ecological and Biotechnological Importance of Secondary Metabolites Produced by Coral-associated Bacteria.” *Journal of Applied Microbiology* 129 (6): 1441–57. https://doi.org/10.1111/jam.14766.
241. Montánchez, I., E. Ogayar, A. H. Plágaro, A. Esteve-Codina, J. Gómez-Garrido, M. Orruño, I. Arana, and V. R. Kaberdin. 2019. “Analysis of *Vibrio harveyi* Adaptation in Sea Water Microcosms at Elevated Temperature Provides Insights into the Putative Mechanisms of Its Persistence and Spread in the Time of Global Warming.” *Scientific Reports* 9 (1): 289. https://doi.org/10.1038/s41598-018-36483-0.
242. Morgado, S., and A. Carolina Vicente. 2022. “Diversity and Distribution of Type VI Secretion System Gene Clusters in Bacterial Plasmids.” *Scientific Reports* 12 (1): 8249. https://doi.org/10.1038/s41598-022-12382-3.
243. Murtazalieva, K., A. Mu, A. Petrovskaya, and R. D. Finn. 2024. “The Growing Repertoire of Phage Anti-Defence Systems.” *Trends in Microbiology*, June. https://doi.org/10.1016/j.tim.2024.05.005.
244. Nakhamchik, A., C. Wilde, H. Chong, and D. A. Rowe-Magnus. 2010. “Evidence for the Horizontal Transfer of an Unusual Capsular Polysaccharide Biosynthesis Locus in Marine Bacteria.” *Infection and Immunity* 78 (12): 5214–22. https://doi.org/10.1128/IAI.00653-10.
245. Naknaen, A., K. Surachat, J. Manit, K. W. Jetwanna, J. Thawonsuwan, and R. Pomwised. 2024. “Virulent Properties and Genomic Diversity of *Vibrio vulnificus* Isolated from Environment, Human, Diseased Fish.” *Microbiology Spectrum* 12 (7): e00079-24. https://doi.org/10.1128/spectrum.00079-24.
246. Narra, H. P., and H. Ochman. 2006. “Of What Use Is Sex to Bacteria?” *Current Biology* 16 (17): R705–10. https://doi.org/10.1016/j.cub.2006.08.024.
247. Nathamuni, S., A. K. Jangam, V. K. Katneni, A. Selvaraj, K. Krishnan, S. Kumar, S. Avunje, et al. 2019. “Insights on Genomic Diversity of *Vibrio* spp. through Pan-Genome Analysis.” *Annals of Microbiology* 69 (13): 1547–55. https://doi.org/10.1007/s13213-019-01539-7.
248. Natrah, F. M. I., H. A. Darshanee Ruwandeepika, S. Pawar, I. Karunasagar, P. Sorgeloos, P. Bossier, and T. Defoirdt. 2011. “Regulation of Virulence Factors by Quorum Sensing in *Vibrio harveyi*.” *Veterinary Microbiology* 154 (1): 124–29. https://doi.org/10.1016/j.vetmic.2011.06.024.
249. Navarro-Muñoz, J. C., N. Selem-Mojica, M. W. Mullowney, S. A. Kautsar, J. H. Tryon, E. I. Parkinson, E. L. C. De Los Santos, et al. 2020. “A Computational Framework to Explore Large-Scale Biosynthetic Diversity.” *Nature Chemical Biology* 16 (1): 60–68. https://doi.org/10.1038/s41589-019-0400-9.
250. Neu, A. T., I. V. Hughes, E. E. Allen, and K. Roy. 2021. “Decade-Scale Stability and Change in a Marine Bivalve Microbiome.” *Molecular Ecology* 30 (5): 1237–50. https://doi.org/10.1111/mec.15796.
251. Nguyen, T. V., A. C. Alfaro, F. Merien, and T. Young. 2019. “In Vitro Study of Apoptosis in Mussel (*Perna canaliculus*) Haemocytes Induced by Lipopolysaccharide.” *Aquaculture* 503 (March):8–15. https://doi.org/10.1016/j.aquaculture.2018.12.086.
252. Nguyen, T. V., A. C. Alfaro, T. Young, S. Ravi, and F. Merien. 2018. “Metabolomics Study of Immune Responses of New Zealand Greenshell™ Mussels (*Perna canaliculus*) Infected with Pathogenic *Vibrio* sp.” *Marine Biotechnology* 20 (3): 396–409. https://doi.org/10.1007/s10126-018-9804-x.
253. Nguyen, L.-T., H. A. Schmidt, A. von Haeseler, and B. Quang Minh. 2015. “IQ-TREE: A Fast and Effective Stochastic Algorithm for Estimating Maximum-Likelihood Phylogenies.” *Molecular Biology and Evolution* 32 (1): 268–74. https://doi.org/10.1093/molbev/msu300.

254. Nordio, D., N. Khtikian, S. Andrews, D. Bertotto, K. Leask, and T. Green. 2021. "Adaption Potential of *Crassostrea gigas* to Ocean Acidification and Disease Caused by *Vibrio harveyi*." *ICES Journal of Marine Science* 78 (1): 360–67. https://doi.org/10.1093/icesjms/fsaa080.
255. Nørstebø, S. F., E. Paulshus, A. Mohn Bjelland, and H. Sørum. 2017. "A Unique Role of Flagellar Function in *Aliivibrio salmonicida* Pathogenicity Not Related to Bacterial Motility in Aquatic Environments." *Microbial Pathogenesis* 109 (August):263–73. https://doi.org/10.1016/j.micpath.2017.06.008.
256. Nurhafizah, W. W. I., K. Leong Lee, A. Razzak Laith, M. Nadirah, M. Danish-Daniel, S. C. Zainathan, and M. Najiah. 2021. "Virulence Properties and Pathogenicity of Multidrug-Resistant *Vibrio harveyi* Associated with Luminescent Vibriosis in Pacific White Shrimp, *Penaeus vannamei*." *Journal of Invertebrate Pathology* 186 (November):107594. https://doi.org/10.1016/j.jip.2021.107594.
257. Ogier, J.-C., A.Calteau, S, Forst, H. Goodrich-Blair, D. Roche, Z. Rouy, G. Suen, et al. 2010. "Units of Plasticity in Bacterial Genomes: New Insight from the Comparative Genomics of Two Bacteria Interacting with Invertebrates, *Photorhabdus* and *Xenorhabdus*." *BMC Genomics* 11 (1): 568. https://doi.org/10.1186/1471-2164-11-568.
258. Olifirenko, V.V., and O.V. Rutta. 2024. "Site Selection, Design and Economic Considerations for the Establishment of a Bivalve Mollusc Hatchery." *Water Bioresources and Aquaculture*, no. 1, 30–46. https://doi.org/10.32782/wba.2024.1.3.
259. Olivares-Bañuelos, T. 2018. "How Important It Is to Produce Seeds for The Aquaculture of Bivalve Molluscs?" *Oceanography & Fisheries Open Access Journal* 8 (3). https://doi.org/10.19080/OFOAJ.2018.08.555740.
260. Oliveira, J., F. Castilho, A. Cunha, and M. J. Pereira. 2012. "Bacteriophage Therapy as a Bacterial Control Strategy in Aquaculture." *Aquaculture International* 20 (5): 879–910. https://doi.org/10.1007/s10499-012-9515-7.
261. Oliveira, P. H., M. Touchon, and E. P.C. Rocha. 2014. "The Interplay of Restriction-Modification Systems with Mobile Genetic Elements and Their Prokaryotic Hosts." *Nucleic Acids Research* 42 (16): 10618–31. https://doi.org/10.1093/nar/gku734.
262. Osei-Adjei, G., X. Huang, and Y. Zhang. 2018. "The Extracellular Proteases Produced by *Vibrio parahaemolyticus*." *World Journal of Microbiology and Biotechnology* 34 (5): 68. https://doi.org/10.1007/s11274-018-2453-4.
263. Osorio, C. R. 2018. "T3SS Effectors in Vibrios: Homology in Sequence, Diversity in Biological Functions?" *Virulence* 9 (1): 721–23. https://doi.org/10.1080/21505594.2018.1435965.
264. Page, A. J., C. A. Cummins, M. Hunt, V. K. Wong, S. Reuter, M. T.G. Holden, M. Fookes, D. Falush, J. A. Keane, and J. Parkhill. 2015. "Roary: Rapid Large-Scale Prokaryote Pan Genome Analysis." *Bioinformatics* 31 (22): 3691–93. https://doi.org/10.1093/bioinformatics/btv421.
265. Paillard, C., and P. Maes. 1990. "Etiology of the Brown Ring Disease in *Tapes philippinarum*: Pathogenicity of a *Vibrio* sp." *Comptes Rendus de l'Academie Des Sciences - Serie III* 310 (1): 15–20.
266. Paillard, C., Y. Gueguen, K. M. Wegner, D. Bass, A. Pallavicini, L. Vezzulli, and I. Arzul. 2022. "Recent Advances in Bivalve-Microbiota Interactions for Disease Prevention in Aquaculture." *Current Opinion in Biotechnology* 73 (February):225–32. https://doi.org/10.1016/j.copbio.2021.07.026.
267. Paillard, C., F. Le Roux, and J. J. Borrego. 2004. "Bacterial Disease in Marine Bivalves, a Review of Recent Studies: Trends and Evolution." *Aquatic Living Resources* 17 (4): 477–98. https://doi.org/10.1051/alr:2004054.
268. Pajares, S., and R. Ramos. 2019. "Processes and Microorganisms Involved in the Marine Nitrogen Cycle: Knowledge and Gaps." *Frontiers in Marine Science* 6 (November). https://doi.org/10.3389/fmars.2019.00739.

269. Palace, S. G., Y. Wang, D. H. Rubin, M. A. Welsh, T. D. Mortimer, K. Cole, D. W. Eyre, S. Walker, and Y. H. Grad. 2020. "RNA Polymerase Mutations Cause Cephalosporin Resistance in Clinical *Neisseria gonorrhoeae* Isolates." *eLife* 9 (February):e51407. https://doi.org/10.7554/eLife.51407.
270. Paranjpye, R.N., and M.S. Strom. 2005. "Colonization of Shellfish by Pathogenic Vibrios." In *Proceedings of OCEANS 2005 MTS/IEEE*, 1099-1103 Vol. 2. https://doi.org/10.1109/OCEANS.2005.1639903.
271. Paranjpye, R. N., A. B. Johnson, A. E. Baxter, and M. S. Strom. 2007. "Role of Type IV Pilins in Persistence of *Vibrio vulnificus* in *Crassostrea virginica* Oysters." *Applied and Environmental Microbiology* 73 (15): 5041–44. https://doi.org/10.1128/AEM.00641-07.
272. Parizadeh, L., D. Tourbiez, C. Garcia, P. Haffner, L. Dégremont, F. Le Roux, and M.-A. Travers., Le Roux, and Travers. 2018. "Ecologically Realistic Model of Infection for Exploring the Host Damage Caused by *Vibrio aestuarianus*." *Environmental Microbiology* 20 (12): 4343–55. https://doi.org/10.1111/1462-2920.14350.
273. Park, K.-S., T. Ono, M. Rokuda, M.-H. Jang, K. Okada, T. Iida, and T. Honda. 2004. "Functional Characterization of Two Type III Secretion Systems of *Vibrio parahaemolyticus*." *Infection and Immunity* 72 (11): 6659–65. https://doi.org/10.1128/IAI.72.11.6659-6665.2004.
274. Parte, A. C., J. S. Carbasse, J. P. Meier-Kolthoff, L. C. Reimer, and M. Göker. 2020. "List of Prokaryotic Names with Standing in Nomenclature (LPSN) Moves to the DSMZ." *International Journal of Systematic and Evolutionary Microbiology* 70 (11): 5607–12. https://doi.org/10.1099/ijsem.0.004332.
275. Patel, P. H., and K. L. Maxwell. 2023. "Prophages Provide a Rich Source of Antiphage Defence Systems." *Current Opinion in Microbiology* 73 (June):102321. https://doi.org/10.1016/j.mib.2023.102321.
276. Patel, S. 2016. "Drivers of Bacterial Genomes Plasticity and Roles They Play in Pathogen Virulence, Persistence and Drug Resistance." *Infection, Genetics and Evolution* 45 (November):151–64. https://doi.org/10.1016/j.meegid.2016.08.030.
277. Payne, L. J., S. Meaden, M. R. Mestre, C. Palmer, N. Toro, P. C. Fineran, and S. A. Jackson. 2022. "PADLOC: A Web Server for the Identification of Antiviral Defence Systems in Microbial Genomes." *Nucleic Acids Research* 50 (W1): W541–50. https://doi.org/10.1093/nar/gkac400.
278. Pena, R. T., L. Blasco, A. Ambroa, B. González-Pedrajo, L. Fernández-García, M. López, I. Bleriot, et al. 2019. "Relationship Between Quorum Sensing and Secretion Systems." *Frontiers in Microbiology* 10 (June). https://doi.org/10.3389/fmicb.2019.01100.
279. Peng, H.-B., Y.-C. Chan, T. J. Compton, X.-F. Cheng, D. S. Melville, S.-D. Zhang, Z. Zhang, G. Lei, Z. Ma, and T. Piersma. 2021. "Mollusc Aquaculture Homogenizes Intertidal Soft-Sediment Communities along the 18,400 Km Long Coastline of China." *Diversity and Distributions* 27 (8): 1553–67. https://doi.org/10.1111/ddi.13302.
280. Pepi, M., and S. Focardi. 2021. "Antibiotic-Resistant Bacteria in Aquaculture and Climate Change: A Challenge for Health in the Mediterranean Area." *International Journal of Environmental Research and Public Health* 18 (11): 5723. https://doi.org/10.3390/ijerph18115723.
281. Picton, D. M, Y. A. Luyten, R. D. Morgan, A. Nelson, D. L. Smith, D. T. F. Dryden, J. C. D. Hinton, and T. R. Blower. 2021. "The Phage Defence Island of a Multidrug Resistant Plasmid Uses Both BREX and Type IV Restriction for Complementary Protection from Viruses." *Nucleic Acids Research* 49 (19): 11257–73. https://doi.org/10.1093/nar/gkab906.
282. Piel, D., M. Bruto, A. James, Y. Labreuche, C. Lambert, A. Janicot, S. Chenivesse, et al. 2020. "Selection of *Vibrio crassostreae* Relies on a Plasmid Expressing a Type 6 Secretion System Cytotoxic for Host Immune Cells." *Environmental Microbiology* 22 (10): 4198–4211. https://doi.org/10.1111/1462-2920.14776.
283. Piel, D., M. Bruto, Y. Labreuche, F. Blanquart, D. Goudenège, R. Barcia-Cruz, S. Chenivesse, et al. 2022. "Phage–Host Coevolution in Natural Populations." *Nature Microbiology* 7 (7): 1075–86. https://doi.org/10.1038/s41564-022-01157-1.

284. Pierce, M. L., and J. E. Ward. 2018. “Microbial Ecology of the *Bivalvia*, with an Emphasis on the Family *Ostreidae*.” *Journal of Shellfish Research* 37 (4): 793–806. https://doi.org/10.2983/035.037.0410.
285. Pierce, M. L., J. E. Ward. 2019. “Gut Microbiomes of the Eastern Oyster (*Crassostrea virginica*) and the Blue Mussel (*Mytilus edulis*): Temporal Variation and the Influence of Marine Aggregate-Associated Microbial Communities.” *mSphere* 4 (6): 10.1128/msphere.00730-19. https://doi.org/10.1128/msphere.00730-19.
286. Potts, R. W. A., A. P. Gutierrez, C. S. Penaloza, T. Regan, T. P. Bean, and R. D. Houston 2021. “Potential of Genomic Technologies to Improve Disease Resistance in Molluscan Aquaculture.” *Philosophical Transactions of the Royal Society B: Biological Sciences* 376 (1825): 20200168. https://doi.org/10.1098/rstb.2020.0168.
287. Prado, P., N. Carrasco, G. Catanese, A. Grau, P. Cabanes, F. Carella, J. R. García-March, et al. 2020. “Presence of *Vibrio mediterranei* Associated to Major Mortality in Stabled Individuals of *Pinna nobilis* L.” *Aquaculture* 519 (March):734899. https://doi.org/10.1016/j.aquaculture.2019.734899.
288. Prado, S., J. Dubert, and J. L. Barja. 2015. “Characterization of Pathogenic Vibrios Isolated from Bivalve Hatcheries in Galicia, NW Atlantic Coast of Spain. Description of *Vibrio tubiashii* subsp. *europaeus* [Corrected] Subsp. nov.” *Systematic and Applied Microbiology* 38 (1): 26–29. https://doi.org/10.1016/j.syapm.2014.11.005.
289. Prado, S., J. Dubert, J. L. Romalde, A. E. Toranzo, and J. L. Barja.2014. “*Vibrio ostreicida* sp. nov., a New Pathogen of Bivalve Larvae.” *International Journal of Systematic and Evolutionary Microbiology* 64 (Pt_5): 1641–46. https://doi.org/10.1099/ijs.0.051417-0.
290. Prado, S., J. L. Romalde, and J. L. Barja. 2010. “Review of Probiotics for Use in Bivalve Hatcheries.” *Veterinary Microbiology* 145 (3): 187–97. https://doi.org/10.1016/j.vetmic.2010.08.021.
291. Prado, S, J. L. Romalde, J. Montes, and J. L Barja. 2005. “Pathogenic Bacteria Isolated from Disease Outbreaks in Shellfish Hatcheries. First Description of *Vibrio neptunius* as an *Oyster* Pathogen.” *Diseases of Aquatic Organisms* 67 (3): 209–15. https://doi.org/10.3354/dao067209.
292. Pritchard, L., R. H. Glover, S. Humphris, J. G. Elphinstone, and I. K. Toth. 2016. “Genomics and Taxonomy in Diagnostics for Food Security: Soft-Rotting Enterobacterial Plant Pathogens.” *Analytical Methods* 8 (1): 12–24. https://doi.org/10.1039/C5AY02550H.
293. Prjibelski, A., D. Antipov, D. Meleshko, A. Lapidus, and A. Korobeynikov. 2020. “Using SPAdes De Novo Assembler.” *Current Protocols in Bioinformatics* 70 (1): e102. https://doi.org/10.1002/cpbi.102.
294. Pu, M., and D. A. Rowe-Magnus. 2018. “A Tad Pilus Promotes the Establishment and Resistance of *Vibrio vulnificus* Biofilms to Mechanical Clearance.” *Npj Biofilms and Microbiomes* 4 (1): 1–8. https://doi.org/10.1038/s41522-018-0052-7.
295. Puente-Sánchez, F., M. Hoetzinger, M. Buck, and S. Bertilsson. 2023. “Exploring Environmental Intra-Species Diversity through Non-Redundant Pangenome Assemblies.” *Molecular Ecology Resources* 23 (7): 1724–36. https://doi.org/10.1111/1755-0998.13826.
296. Qi, X., X. Xu, H. Li, Y. Pan, E. K. Kraco, J. Zheng, M. Lin, and X. Jiang.2022. “fliA, flrB, and fliR Regulate Adhesion by Controlling the Expression of Critical Virulence Genes in *Vibrio harveyi*.” *Gene* 839 (September):146726. https://doi.org/10.1016/j.gene.2022.146726.
297. Quinlan, A. R., and I. M. Hall. 2010. “BEDTools: A Flexible Suite of Utilities for Comparing Genomic Features.” *Bioinformatics (Oxford, England)* 26 (6): 841–42. https://doi.org/10.1093/bioinformatics/btq033.
298. Rahmani, A., F. Delavat, C. Lambert, N. Le Goic, E. Dabas, C. Paillard, and V. Pichereau. 2021. “Implication of the Type IV Secretion System in the Pathogenicity of *Vibrio tapetis*, the Etiological Agent of Brown Ring Disease Affecting the Manila Clam *Ruditapes philippinarum*.” *Frontiers in Cellular and Infection Microbiology* 11:634427. https://doi.org/10.3389/fcimb.2021.634427.

299. Ramisetty, B. C. M., and P. A. Sudhakari. 2019. “Bacterial ‘Grounded’ Prophages: Hotspots for Genetic Renovation and Innovation.” *Frontiers in Genetics* 10 (February):65. https://doi.org/10.3389/fgene.2019.00065.
300. Randa, M. A., M. F. Polz, and E. Lim. 2004. “Effects of Temperature and Salinity on *Vibrio vulnificus* Population Dynamics as Assessed by Quantitative PCR.” *Applied and Environmental Microbiology* 70 (9): 5469–76. https://doi.org/10.1128/AEM.70.9.5469-5476.2004.
301. Redondo-Salvo, S., R. Bartomeus-Peñalver, L. Vielva, K. A. Tagg, H. E. Webb, R. Fernández-López, and F. de la Cruz.2021. “COPLA, a Taxonomic Classifier of Plasmids.” *BMC Bioinformatics* 22 (1): 390. https://doi.org/10.1186/s12859-021-04299-x.
302. Richards, G. P., M. A. Watson, D. Madison, N. Soffer, D. S. Needleman, D. S. Soroka, J. Uknalis, et al. 2021. “Bacteriophages against *Vibrio coralliilyticus* and *Vibrio tubiashii*: Isolation, Characterization, and Remediation of Larval Oyster Mortalities.” *Applied and Environmental Microbiology* 87 (10): e00008-21. https://doi.org/10.1128/AEM.00008-21.
303. Richards, G. P., M. A. Watson, D. S. Needleman, K. M. Church, and C. C. Häse. 2015. “Mortalities of Eastern and Pacific Oyster Larvae Caused by the Pathogens *Vibrio coralliilyticus* and *Vibrio tubiashii*.” *Applied and Environmental Microbiology* 81 (1): 292–97. https://doi.org/10.1128/AEM.02930-14.
304. Richards, G. P. 2014. “Bacteriophage Remediation of Bacterial Pathogens in Aquaculture: A Review of the Technology.” *Bacteriophage* 4 (4): e975540. https://doi.org/10.4161/21597081.2014.975540.
305. Ringø, E. 2020. “Probiotics in Shellfish Aquaculture.” *Aquaculture and Fisheries* 5 (1): 1–27. https://doi.org/10.1016/j.aaf.2019.12.001.
306. Roch, P. 1999. “Defence Mechanisms and Disease Prevention in Farmed Marine Invertebrates.” *Aquaculture* 172 (1): 125–45. https://doi.org/10.1016/S0044-8486(98)00439-6.
307. Rocha, E. P. C., and D. Bikard. 2022. “Microbial Defences against Mobile Genetic Elements and Viruses: Who Defends Whom from What?” *PLOS Biology* 20 (1): e3001514. https://doi.org/10.1371/journal.pbio.3001514.
308. Rodriguez-Valera, F., A.-B. M.-C., and M. López-Pérez. 2016. “Flexible Genomic Islands as Drivers of Genome Evolution.” *Current Opinion in Microbiology*, Environmental microbiology * Special Section: Megaviromes, 31 (June):154–60. https://doi.org/10.1016/j.mib.2016.03.014.
309. Rojas, R., A. Blanco-Hortas, H. Kehlet-Delgado, A. Lema, C. D. Miranda, J. Romero, P. Martínez, J. L. Barja, and J. Dubert. 2021. “First Description Outside Europe of the Emergent Pathogen *Vibrio europaeus* in Shellfish Aquaculture.” *Journal of Invertebrate Pathology* 180 (March):107542. https://doi.org/10.1016/j.jip.2021.107542.
310. Rojas, R., C. D. Miranda, R. Opazo, and J. Romero. 2015. “Characterization and Pathogenicity of *Vibrio splendidus* Strains Associated with Massive Mortalities of Commercial Hatchery-Reared Larvae of Scallop *Argopecten purpuratus* (Lamarck, 1819).” *Journal of Invertebrate Pathology* 124 (January):61–69. https://doi.org/10.1016/j.jip.2014.10.009.
311. Rojas, R., C. D. Miranda, J. Romero, J. L. Barja, and J. Dubert. 2019. “Isolation and Pathogenic Characterization of *Vibrio bivalvicida* Associated With a Massive Larval Mortality Event in a Commercial Hatchery of Scallop *Argopecten purpuratus* in Chile.” *Frontiers in Microbiology* 10 (May). https://doi.org/10.3389/fmicb.2019.00855.
312. Romalde, J. L. 2012. “Héroes y villanos: bacterias asociadas al cultivo de moluscos.” *AquaTIC*, no. 37, 45–59.
313. Romero, A., M. del Costa, G. Forn-Cuni, P. Balseiro, R. Chamorro, S. Dios, A. Figueras, and B. Novoa. 2014. “Occurrence, Seasonality and Infectivity of *Vibrio* Strains in Natural Populations of Mussels *Mytilus galloprovincialis*.” *Diseases of Aquatic Organisms* 108 (2): 149–63. https://doi.org/10.3354/dao02701.
314. Rouli, L., V. Merhej, P.-E. Fournier, and D. Raoult. 2015. “The Bacterial Pangenome as a New Tool for Analysing Pathogenic Bacteria.” *New Microbes and New Infections* 7 (September):72–85. https://doi.org/10.1016/j.nmni.2015.06.005.

315. Rubio, T., D. Oyanedel, Y. Labreuche, E. Toulza, X. Luo, M. Bruto, C. Chaparro, et al. 2019. "Species-Specific Mechanisms of Cytotoxicity toward Immune Cells Determine the Successful Outcome of *Vibrio* Infections." *Proceedings of the National Academy of Sciences of the United States of America* 116 (28): 14238–47. https://doi.org/10.1073/pnas.1905747116.
316. Ruiz-Ponte, C., J. F. Samain, J. L. Sánchez, and J. L. Nicolas. 1999. "The Benefit of a *Roseobacter* Species on the Survival of Scallop Larvae." *Marine Biotechnology (New York, N.Y.)* 1 (1): 52–59. https://doi.org/10.1007/pl00011751.
317. Salazar, G., and S. Sunagawa. 2017. "Marine Microbial Diversity." *Current Biology* 27 (11): R489–94. https://doi.org/10.1016/j.cub.2017.01.017.
318. Sampaio, A., V. Silva, P. Poeta, and F. Aonofriesei. 2022. "*Vibrio* spp.: Life Strategies, Ecology, and Risks in a Changing Environment." *Diversity* 14 (2): 97. https://doi.org/10.3390/d14020097.
319. Sanches-Fernandes, G. M. M., I. Sá-Correia, and R. Costa. 2022. "Vibriosis Outbreaks in Aquaculture: Addressing Environmental and Public Health Concerns and Preventive Therapies Using Gilthead Seabream Farming as a Model System." *Frontiers in Microbiology* 13 (July):904815. https://doi.org/10.3389/fmicb.2022.904815.
320. Sandkvist, M. 2001. "Type II Secretion and Pathogenesis." *Infection and Immunity* 69 (6): 3523–35. https://doi.org/10.1128/IAI.69.6.3523-3535.2001.
321. Santos, M. N. M., S.-T. Cho, C.-F. Wu, C.-J. Chang, C.-H. Kuo, and E.-M. Lai. 2020. "Redundancy and Specificity of Type VI Secretion *vgrG* Loci in Antibacterial Activity of *Agrobacterium tumefaciens* 1D1609 Strain." *Frontiers in Microbiology* 10. https://www.frontiersin.org/articles/10.3389/fmicb.2019.03004.
322. Sarris, P. F., C. Zoumadakis, N. J. Panopoulos, and E. V. Scoulica. 2011. "Distribution of the Putative Type VI Secretion System Core Genes in *Klebsiella* spp." *Infection, Genetics and Evolution* 11 (1): 157–66. https://doi.org/10.1016/j.meegid.2010.09.006.
323. Saulnier, D., S. De Decker, P. Haffner, L. Cobret, M. Robert, and C. Garcia. 2010. "A Large-Scale Epidemiological Study to Identify Bacteria Pathogenic to Pacific Oyster *Crassostrea gigas* and Correlation between Virulence and Metalloprotease-like Activity." *Microbial Ecology* 59 (4): 787–98. https://doi.org/10.1007/s00248-009-9620-y.
324. Sawabe, T. 2006. "The Mutual Partnership between *Vibrio halioticoli* and Abalones." In *The Biology of Vibrios*, 219–30. John Wiley & Sons, Ltd. https://doi.org/10.1128/9781555815714.ch15.
325. Schar, D., C. Zhao, Y. Wang, D. G. Joakim Larsson, M. Gilbert, and T. P. Van Boeckel. 2021. "Twenty-Year Trends in Antimicrobial Resistance from Aquaculture and Fisheries in Asia." *Nature Communications* 12 (1): 5384. https://doi.org/10.1038/s41467-021-25655-8.
326. Schulze, A. D., A. O. Alabi, A. R. Tattersall-Sheldrake, and K. M. Miller. 2006. "Bacterial Diversity in a Marine Hatchery: Balance between Pathogenic and Potentially Probiotic Bacterial Strains." *Aquaculture* 256 (1): 50–73. https://doi.org/10.1016/j.aquaculture.2006.02.008.
327. Seemann, T. 2014. "Prokka: Rapid Prokaryotic Genome Annotation." *Bioinformatics* 30 (14): 2068–69. https://doi.org/10.1093/bioinformatics/btu153.
328. Sem, N. A. D., S. A. Gani, C. M. Chong, I. Natrah, and S. Shamsi. 2023. "Management and Mitigation of Vibriosis in Aquaculture: Nanoparticles as Promising Alternatives." *International Journal of Molecular Sciences* 24 (16): 12542. https://doi.org/10.3390/ijms241612542.
329. Sequeira, J. C., M. Rocha, M. M. Alves, and A. F. Salvador. 2022. "UPIMAPI, reCOGnizer and KEGGCharter: Bioinformatics Tools for Functional Annotation and Visualization of (Meta)-Omics Datasets." *Computational and Structural Biotechnology Journal* 20 (January):1798–1810. https://doi.org/10.1016/j.csbj.2022.03.042.
330. Shannon, P., A. Markiel, O. Ozier, N. S. Baliga, J. T. Wang, D. Ramage, N. Amin, B. Schwikowski, and T. Ideker. 2003. "Cytoscape: A Software Environment for Integrated Models of Biomolecular Interaction Networks." *Genome Research* 13 (11): 2498–2504. https://doi.org/10.1101/gr.1239303.

331. Shapiro-Ilan, D. I., J. R. Fuxa, L. A. Lacey, D. W. Onstad, and H. K. Kaya. 2005. "Definitions of Pathogenicity and Virulence in Invertebrate Pathology." *Journal of Invertebrate Pathology* 88 (1): 1–7. https://doi.org/10.1016/j.jip.2004.10.003.
332. Sharma, M. H., S. Palamae, M. Yingkajorn, S. Benjakul, A. Singh, and J. Buatong. 2024. "Multidrug-Resistance of *Vibrio* Species in Bivalve Molluscs from Southern Thailand: Isolation, Identification, Pathogenicity, and Their Sensitivity toward Chitooligosaccharide-Epigallocatechin-3-Gallate Conjugate." *Foods* 13 (15): 2375. https://doi.org/10.3390/foods13152375.
333. Shaw, L. P., E. P. C. Rocha, and R. Craig MacLean. 2023. "Restriction-Modification Systems Have Shaped the Evolution and Distribution of Plasmids across Bacteria." *Nucleic Acids Research* 51 (13): 6806–18. https://doi.org/10.1093/nar/gkad452.
334. Shen, W., S. Le, Y. Li, and F. Hu. 2016. "SeqKit: A Cross-Platform and Ultrafast Toolkit for FASTA/Q File Manipulation." *PLOS ONE* 11 (10): e0163962. https://doi.org/10.1371/journal.pone.0163962.
335. Shu, H.-Y., C.-P. Fung, Y.-M. Liu, K.-M. Wu, Y.-T. Chen, L.-H. Li, T.-T. Liu, R. Kirby, and S.-F. Tsai. 2009. "Genetic Diversity of Capsular Polysaccharide Biosynthesis in *Klebsiella pneumoniae* Clinical Isolates." *Microbiology* 155 (12): 4170–83. https://doi.org/10.1099/mic.0.029017-0.
336. Siefert, J. L. 2009. "Defining the Mobilome." *Methods in Molecular Biology (Clifton, N.J.)* 532:13–27. https://doi.org/10.1007/978-1-60327-853-9_2.
337. Simonsen, A. K. 2022. "Environmental Stress Leads to Genome Streamlining in a Widely Distributed Species of Soil Bacteria." *The ISME Journal* 16 (2): 423–34. https://doi.org/10.1038/s41396-021-01082-x.
338. Smillie, C., M. P. Garcillán-Barcia, M. V. Francia, E. P. C. Rocha, and F. de la Cruz. 2010. "Mobility of Plasmids." *Microbiology and Molecular Biology Reviews : MMBR* 74 (3): 434–52. https://doi.org/10.1128/MMBR.00020-10.
339. Smith, M. A., and M. J. Bidochka. 1998. "Bacterial Fitness and Plasmid Loss: The Importance of Culture Conditions and Plasmid Size." *Canadian Journal of Microbiology* 44 (4): 351–55.
340. Smith, W. P. J., A. Vettiger, J. Winter, T. Ryser, L. E. Comstock, M. Basler, and K. R. Foster. 2020. "The Evolution of the Type VI Secretion System as a Disintegration Weapon." *PLOS Biology* 18 (5): e3000720. https://doi.org/10.1371/journal.pbio.3000720.
341. Snipen, L., and K. H. Liland. 2015. "Micropan: An R-Package for Microbial Pan-Genomics." *BMC Bioinformatics* 16 (1): 79. https://doi.org/10.1186/s12859-015-0517-0.
342. Sohn, S., K. M. Lundgren, K. Tammi, R. Smolowitz, D. R. Nelson, D. C. Rowley, and M. Gómez-Chiarri. 2016. "Efficacy of Probiotics in Preventing Vibriosis in the Larviculture of Different Species of Bivalve Shellfish." *Journal of Shellfish Research* 35 (2): 319–28. https://doi.org/10.2983/035.035.0206.
343. Souza, D. P., G. U. Oka, C. E. Alvarez-Martinez, A. W. Bisson-Filho, G. Dunger, L. Hobeika, N. S. Cavalcante, et al. 2015. "Bacterial Killing via a Type IV Secretion System." *Nature Communications* 6 (1): 6453. https://doi.org/10.1038/ncomms7453.
344. Spinard, E. J., J. Dubert, D. R. Nelson, M. Gomez-Chiarri, and J. L. Barja. 2016. "Draft Genome Sequence of the Emerging Bivalve Pathogen *Vibrio tubiashii* subsp. *europaeus*." *Genome Announcements* 4 (4): 10.1128/genomea.00625-16. https://doi.org/10.1128/genomea.00625-16.
345. Tan, K., P. Ya, K. Tan, K.-L. Cheong, and H. Fazhan. 2023. "Ecological Impact of Invasive Species and Pathogens Introduced through Bivalve Aquaculture." *Estuarine, Coastal and Shelf Science* 294 (November):108541. https://doi.org/10.1016/j.ecss.2023.108541.
346. Tanguy, M., P. McKenna, S. Gauthier-Clerc, J. Pellerin, J.-M. Danger, and A. Siah. 2013. "Functional and Molecular Responses in *Mytilus edulis* Hemocytes Exposed to Bacteria, *Vibrio splendidus*." *Developmental and Comparative Immunology* 39 (4): 419–29. https://doi.org/10.1016/j.dci.2012.10.015.

347. Taniguchi, C. N., J. Dobbs, and M. A. Dunn. 2017. “Heme Iron, Non-Heme Iron, and Mineral Content of Blood Clams (*Anadara* spp.) Compared to Manila Clams (*V. philippinarum*), Pacific Oysters (*C. gigas*), and Beef Liver (*B. taurus)*.” *Journal of Food Composition and Analysis* 57 (April):49–55. https://doi.org/10.1016/j.jfca.2016.12.018.
348. Taylor, V. L., A. D. Fitzpatrick, Z. Islam, and K. L. Maxwell. 2019. “The Diverse Impacts of Phage Morons on Bacterial Fitness and Virulence.” In *Advances in Virus Research*, 103:1–31. Elsevier. https://doi.org/10.1016/bs.aivir.2018.08.001.
349. Teitge, F., C. Peppler, D. Steinhagen, and V. Jung-Schroers. 2020. “Water Disinfection by Ozonation Has Advantages over UV Irradiation in a Brackish Water Recirculation Aquaculture System for Pacific White Shrimp (*Litopenaeus vannamei*).” *Journal of Fish Diseases* 43 (10): 1259–85. https://doi.org/10.1111/jfd.13238.
350. Tesson, F., A. Hervé, E. Mordret, M. Touchon, C. d’Humières, J. Cury, and A. Bernheim. 2022. “Systematic and Quantitative View of the Antiviral Arsenal of Prokaryotes.” *Nature Communications* 13 (1): 2561. https://doi.org/10.1038/s41467-022-30269-9.
351. Tetreau, G., J. Dhinaut, B. Gourbal, and Y. Moret. 2019. “Trans-Generational Immune Priming in Invertebrates: Current Knowledge and Future Prospects.” *Frontiers in Immunology* 10 (August). https://doi.org/10.3389/fimmu.2019.01938.
352. Thomas, C. M., and K. M. Nielsen. 2005. “Mechanisms of, and Barriers to, Horizontal Gene Transfer between Bacteria.” *Nature Reviews Microbiology* 3 (9): 711–21. https://doi.org/10.1038/nrmicro1234.
353. Tian, J., D. Wang, H. Wang, P. Huan, and B. Liu. 2024. “The Combination of High Temperature and *Vibrio* Infection Worsens Summer Mortality in the Clam *Meretrix petechialis* by Increasing Apoptosis and Oxidative Stress.” *Fish & Shellfish Immunology* 149 (June):109542. https://doi.org/10.1016/j.fsi.2024.109542.
354. Timmins-Schiffman, E., S. J. White, R. E. Thompson, B. Vadopalas, B. Eudeline, B. L. Nunn, and S. B. Roberts. 2021. “Coupled Microbiome Analyses Highlights Relative Functional Roles of Bacteria in a Bivalve Hatchery.” *Environmental Microbiome* 16 (1): 7. https://doi.org/10.1186/s40793-021-00376-z.
355. Tirapé, A., C. Bacque, R. Brizard, F. Vandenbulcke, and V. Boulo. 2007. “Expression of Immune-Related Genes in the Oyster *Crassostrea gigas* during Ontogenesis.” *Developmental and Comparative Immunology* 31 (9): 859–73. https://doi.org/10.1016/j.dci.2007.01.005.
356. Travers, M.-A., R. Mersni Achour, P. Haffner, D. Tourbiez, A.-L. Cassone, B. Morga, I. Doghri, et al. 2014. “First Description of French *V. tubiashii* Strains Pathogenic to Mollusc: I. Characterization of Isolates and Detection during Mortality Events.” *Journal of Invertebrate Pathology* 123 (November):38–48. https://doi.org/10.1016/j.jip.2014.04.009.
357. Urtubia, R., C. D. Miranda, S. Rodríguez, J. Dubert, J. L. Barja, and R. Rojas. 2023. “First Report, Characterization and Pathogenicity of *Vibrio chagasii* Isolated from Diseased Reared Larvae of Chilean Scallop, *Argopecten purpuratus* (Lamarck, 1819).” *Pathogens* 12 (2): 183. https://doi.org/10.3390/pathogens12020183.
358. Ushijima, B., G. P. Richards, M. A. Watson, C. B. Schubiger, and C. C. Häse. 2018. “Factors Affecting Infection of Corals and Larval Oysters by *Vibrio coralliilyticus*.” *PLOS ONE* 13 (6): e0199475. https://doi.org/10.1371/journal.pone.0199475.
359. Ushijima, B., J. H. Saw, P. Videau, and C. C. Häse. 2022. “Comparison of *Vibrio coralliilyticus* Virulence in Pacific Oyster Larvae and Corals.” *Microbiology* 168 (4): 001169. https://doi.org/10.1099/mic.0.001169.
360. Vaitkevicius, K., B. Lindmark, G. Ou, T. Song, C. Toma, M. Iwanaga, J. Zhu, et al. 2006. “A *Vibrio cholerae* Protease Needed for Killing of *Caenorhabditis elegans* Has a Role in Protection from Natural Predator Grazing.” *Proceedings of the National Academy of Sciences* 103 (24): 9280–85. https://doi.org/10.1073/pnas.0601754103.
361. Vandeputte, M., A. Kashem, P. Bossier, and D. Vanrompay. 2024. “*Vibrio* Pathogens and Their Toxins in Aquaculture: A Comprehensive Review.” *Reviews in Aquaculture* 16 (4): 1858–78. https://doi.org/10.1111/raq.12926.

362. Varina, M., S. M. Denkin, A. M. Staroscik, and D. R. Nelson. 2008. “Identification and Characterization of Epp, the Secreted Processing Protease for the *Vibrio anguillarum* EmpA Metalloprotease.” *Journal of Bacteriology* 190 (20): 6589–97. https://doi.org/10.1128/JB.00535-08.
363. Vaser, R., I. Sović, N. Nagarajan, and M. Šikić. 2017. “Fast and Accurate de Novo Genome Assembly from Long Uncorrected Reads.” *Genome Research* 27 (5): 737–46. https://doi.org/10.1101/gr.214270.116.
364. Vassallo, C. N., C. R. Doering, M. L. Littlehale, G. I. C. Teodoro, and M. T. Laub. 2022. “A Functional Selection Reveals Previously Undetected Anti-Phage Defence Systems in the *E. coli* Pangenome.” *Nature Microbiology* 7 (10): 1568–79. https://doi.org/10.1038/s41564-022-01219-4.
365. Verschuere, L., G. Rombaut, P. Sorgeloos, and W. Verstraete. 2000. “Probiotic Bacteria as Biological Control Agents in Aquaculture.” *Microbiology and Molecular Biology Reviews: MMBR* 64 (4): 655–71. https://doi.org/10.1128/MMBR.64.4.655-671.2000.
366. Vezzulli, L., E. Pezzati, M. Stauder, L. Stagnaro, P. Venier, and C. Pruzzo. 2015. “Aquatic Ecology of the Oyster Pathogens *Vibrio splendidus* and *Vibrio aestuarianus*.” *Environmental Microbiology* 17 (4): 1065–80. https://doi.org/10.1111/1462-2920.12484.
367. Vezzulli, L., M. Previati, C. Pruzzo, A. Marchese, D. G Bourne, and C. Cerrano, and the VibrioSea Consortium. 2010. “*Vibrio* Infections Triggering Mass Mortality Events in a Warming Mediterranean Sea.” *Environmental Microbiology* 12 (7): 2007–19. https://doi.org/10.1111/j.1462-2920.2010.02209.x.
368. Vogwill, T., and R. C. MacLean. 2015. “The Genetic Basis of the Fitness Costs of Antimicrobial Resistance: A Meta-Analysis Approach.” *Evolutionary Applications* 8 (3): 284–95. https://doi.org/10.1111/eva.12202.
369. Walker, B. J., T. Abeel, T. Shea, M. Priest, A. Abouelliel, S. Sakthikumar, C. A. Cuomo, et al. 2014. “Pilon: An Integrated Tool for Comprehensive Microbial Variant Detection and Genome Assembly Improvement.” *PloS One* 9 (11): e112963. https://doi.org/10.1371/journal.pone.0112963.
370. Wandersman, C., and P. Delepelaire. 2004. “Bacterial Iron Sources: From Siderophores to Hemophores.” *Annual Review of Microbiology* 58:611–47. https://doi.org/10.1146/annurev.micro.58.030603.123811.
371. Wang, L., L. Huang, Y. Su, Y. Qin, W. Kong, Y. Ma, X. Xu, M. Lin, and Q. Yan. 2015. “Involvement of the Flagellar Assembly Pathway in *Vibrio alginolyticus* Adhesion under Environmental Stresses.” *Frontiers in Cellular and Infection Microbiology* 5 (August). https://doi.org/10.3389/fcimb.2015.00059.
372. Wang, D., N. Mbewe, L. De Bels, L. Couck, G. Van Stappen, W. Van den Broeck, and N. Nevejan. 2021. “Pathogenesis of Experimental Vibriosis in Blue Mussel (*Mytilus edulis*) Larvae Based on Accurate Positioning of GFP-Tagged *Vibrio* Strains and Histopathological and Ultrastructural Changes of the Host.” *Aquaculture* 535 (March):736347. https://doi.org/10.1016/j.aquaculture.2021.736347.
373. Wang, H., B. Yang, Q. Li, and S. Liu. 2024. “Low-Dose of Formalin-Inactivated *Vibrio alginolyticus* Protects *Crassostrea gigas* from Secondary Infection and Confers Broad-Spectrum *Vibrio* Resistance on Offspring.” *Developmental & Comparative Immunology* 152 (March):105122. https://doi.org/10.1016/j.dci.2023.105122.
374. Waterhouse, A. M., J. B. Procter, D. M. A. Martin, M. Clamp, and G. J. Barton. 2009. “Jalview Version 2—a Multiple Sequence Alignment Editor and Analysis Workbench.” *Bioinformatics* 25 (9): 1189–91. https://doi.org/10.1093/bioinformatics/btp033.
375. Wei, Z., L. Xin, W. Zhang, C. Bai, C. Wang, and C. Li. 2019. “Isolation and Characterization of *Vibrio harveyi* as a Major Pathogen Associated with Mass Mortalities of Ark Clam, *Scapharca broughtonii*, in Summer.” *Aquaculture* 511 (September):734248. https://doi.org/10.1016/j.aquaculture.2019.734248.

376. Wickham, H. 2016. “Data Analysis.” In *Ggplot2: Elegant Graphics for Data Analysis*, edited by Hadley Wickham, 189–201. Use R! Cham: Springer International Publishing. https://doi.org/10.1007/978-3-319-24277-4_9.
377. Wildschutte, H., S. P. Preheim, Y. Hernandez, and M. F. Polz. 2010. “O-Antigen Diversity and Lateral Transfer of the Wbe Region among *Vibrio splendidus* Isolates.” *Environmental Microbiology* 12 (11): 2977–87. https://doi.org/10.1111/j.1462-2920.2010.02274.x.
378. Woude, M. van der, and A. J. Bäumler. 2004. “Phase and Antigenic Variation in Bacteria.” *Clinical Microbiology Reviews* 17 (3): 581–611. https://doi.org/10.1128/cmr.17.3.581-611.2004.
379. Xu, D., Z. Zhao, Z. Zhou, Y. Lin, X. Zhang, Y. Zhang, Y. Zhang, et al. 2020. “Mechanistic Molecular Responses of the Giant Clam *Tridacna crocea* to *Vibrio coralliilyticus* Challenge.” *PLOS ONE* 15 (4): e0231399. https://doi.org/10.1371/journal.pone.0231399.
380. Yang, W., N. T. Tran, C.-H. Zhu, D.-F. Yao, J. J. Aweya, Y. Gong, H.-Y. Ma, Y.-L. Zhang, G.-L. Li, and S.-K. Li. 2021. “Immune Priming in Shellfish: A Review and an Updating Mechanistic Insight Focused on Cellular and Humoral Responses.” *Aquaculture* 530 (January):735831. https://doi.org/10.1016/j.aquaculture.2020.735831.
381. Yang, B., S. Zhai, X. Li, J. Tian, Q. Li, H. Shan, and S. Liu. 2021. “Identification of *Vibrio alginolyticus* as a Causative Pathogen Associated with Mass Summer Mortality of the Pacific Oyster (*Crassostrea gigas*) in China.” *Aquaculture* 535 (March):736363. https://doi.org/10.1016/j.aquaculture.2021.736363.
382. Zannella, C., F. Mosca, F. Mariani, G. Franci, V. Folliero, M. Galdiero, P. G. Tiscar, and M. Galdiero. 2017. “Microbial Diseases of Bivalve Molluscs: Infections, Immunology and Antimicrobial Defence.” *Marine Drugs* 15 (6): 182. https://doi.org/10.3390/md15060182.
383. Zboralski, A., and M. Filion. 2020. “Genetic Factors Involved in Rhizosphere Colonization by Phytobeneficial *Pseudomonas* spp.” *Computational and Structural Biotechnology Journal* 18 (January):3539–54. https://doi.org/10.1016/j.csbj.2020.11.025.
384. Zhai, S., B. Yang, F. Zhang, Q. Li, and S. Liu. 2021. “Estimation of Genetic Parameters for Resistance to *Vibrio alginolyticus* Infection in the Pacific Oyster (*Crassostrea gigas*).” *Aquaculture* 538 (May):736545. https://doi.org/10.1016/j.aquaculture.2021.736545.
385. Zhang, J., J. Guan, M. Wang, G. Li, M. Djordjevic, C. Tai, H. Wang, Z. Deng, Z. Chen, and H.-Y. Ou. 2023. “SecReT6 Update: A Comprehensive Resource of Bacterial Type VI Secretion Systems.” *Science China Life Sciences* 66 (3): 626–34. https://doi.org/10.1007/s11427-022-2172-x.
386. Zhang, T., L. Qiu, Z. Sun, L. Wang, Z. Zhou, R. Liu, F. Yue, R. Sun, and L. Song. 2014. “The Specifically Enhanced Cellular Immune Responses in Pacific Oyster (*Crassostrea gigas*) against Secondary Challenge with *Vibrio splendidus*.” *Developmental & Comparative Immunology* 45 (1): 141–50. https://doi.org/10.1016/j.dci.2014.02.015.
387. Zhao, X. 2019. “BinDash, Software for Fast Genome Distance Estimation on a Typical Personal Laptop.” *Bioinformatics* 35 (4): 671–73. https://doi.org/10.1093/bioinformatics/bty651.
388. Zheng, H., Y. Huang, P. Liu, L. Yan, Y. Zhou, C. Yang, Y. Wu, et al. 2022. “Population Genomics of the Food-Borne Pathogen *Vibrio fluvialis* Reveals Lineage Associated Pathogenicity-Related Genetic Elements.” *Microbial Genomics* 8 (2): 000769. https://doi.org/10.1099/mgen.0.000769.
389. Zhu, S., S. Kojima, and M. Homma. 2013. “Structure, Gene Regulation and Environmental Response of Flagella in *Vibrio*.” *Frontiers in Microbiology* 4. https://www.frontiersin.org/articles/10.3389/fmicb.2013.00410.

ANNEX 1. IMAGES PERMISSIONS

Introduction

Figure 1: Explicit permission from the editor

Figure 2: Elsevier 5925830163124

Figure 3: Springer Nature 5925830830104

Figure 4: Creative Commons Attribution (CC BY 4.0)

Figure 5: Elsevier 5925840589316

SPRINGER NATURE LICENSE
TERMS AND CONDITIONS

Dec 11, 2024

This Agreement between Sergio Rodríguez Rodríguez ("You") and Springer Nature ("Springer Nature") consists of your license details and the terms and conditions provided by Springer Nature and Copyright Clearance Center.

License Number	5925830830104
License date	Dec 11, 2024
Licensed Content Publisher	Springer Nature
Licensed Content Publication	Current Microbiology
Licensed Content Title	Vibrio Clade 3.0: New VibrionaceaeEvolutionary Units Using Genome-BasedApproach
Licensed Content Author	Chunqi Jiang et al
Licensed Content Date	Dec 14, 2021
Type of Use	Thesis/Dissertation
Requestor type	academic/university or research institute
Format	print and electronic
Portion	figures/tables/illustrations
Number of figures/tables/illustrations	1
Will you be translating?	no
Circulation/distribution	1 - 29
Author of this Springer Nature content	no
Title of new work	GENOMIC CHARACTERIZATION OF THEBIVALVE PATHOGEN VIBRIO EUROPAEUS
Institution name	Universidad de Santiago de Compostela
Expected presentation date	Mar 2025
Portions	Fig. 1
The Requesting Person / Organization toAppear on the License	Sergio Rodríguez Rodríguez
Requestor Location	Sergio Rodríguez RodríguezRúa de Lope Gómez de Marzoa, 15Santiago De Compostela, A Coruña 15705Spain
Billing Type	Invoice
Billing Address	Sergio Rodríguez RodríguezRúa de Lope Gómez de Marzoa, 15Santiago De Compostela, Spain 15705
Total	0.00 EUR

ELSEVIER LICENSE
TERMS AND CONDITIONS

Dec 11, 2024

This Agreement between Sergio Rodríguez Rodríguez ("You") and Elsevier ("Elsevier") consists of your license details and the terms and conditions provided by Elsevier and Copyright Clearance Center.

License Number	5925840589316
License date	Dec 11, 2024
Licensed Content Publisher	Elsevier
Licensed Content Publication	Aquaculture
Licensed Content Title	Pathogenesis of experimental vibriosis in blue mussel(Mytilus edulis) larvae based on accurate positioningof GFP-tagged Vibrio strains and histopathologicaland ultrastructural changes of the host
Licensed Content Author	Dongdong Wang,Nelia Mbewe,Lobke DeBels,Liesbeth Couck,Gilbert Van Stappen,Wim Vanden Broeck,Nancy Nevejan
Licensed Content Date	Mar 30, 2021
Licensed Content Volume	535
Licensed Content Issue	n/a
Licensed Content Pages	1
Start Page	736347
End Page	0
Type of Use	reuse in a thesis/dissertation
Portion	figures/tables/illustrations
Number offigures/tables/illustrations	1
Format	both print and electronic
Are you the author of this Elsevierarticle?	No
Will you be translating?	No
Title of new work	GENOMIC CHARACTERIZATION OF THEBIVALVE PATHOGEN VIBRIO EUROPAEUS
Institution name	Universidad de Santiago de Compostela
Expected presentation date	Mar 2025
Portions	Fig. 3
The Requesting Person /Organization to Appear on theLicense	Sergio Rodríguez Rodríguez
Requestor Location	Sergio Rodríguez RodríguezRúa de Lope Gómez de Marzoa, 15Santiago De Compostela, A Coruña 15705Spain
Publisher Tax ID	GB 494 6272 12
Total	0.00 EUR

ELSEVIER LICENSE
TERMS AND CONDITIONS

Dec 11, 2024

This Agreement between Sergio Rodríguez Rodríguez ("You") and Elsevier ("Elsevier") consists of your license details and the terms and conditions provided by Elsevier and Copyright Clearance Center.

License Number	5925830163124
License date	Dec 11, 2024
Licensed Content Publisher	Elsevier
Licensed Content Publication	Current Opinion in Biotechnology
Licensed Content Title	Recent advances in bivalve-microbiotainteractions for disease prevention in aquaculture
Licensed Content Author	Christine Paillard,Yannick Gueguen,K MathiasWegner,David Bass,Alberto Pallavicini,LuigiVezzulli,Isabelle Arzul
Licensed Content Date	Feb 1, 2022
Licensed Content Volume	73
Licensed Content Issue	n/a
Licensed Content Pages	8
Start Page	225
End Page	232
Type of Use	reuse in a thesis/dissertation
Portion	figures/tables/illustrations
Number of figures/tables/illustrations	1
Format	both print and electronic
Are you the author of this Elsevier article?	No
Will you be translating?	No
Title of new work	GENOMIC CHARACTERIZATION OF THEBIVALVE PATHOGEN VIBRIO EUROPAEUS
Institution name	Universidad de Santiago de Compostela
Expected presentation date	Mar 2025
Portions	Graphical abstract
The Requesting Person / Organizationto Appear on the License	Sergio Rodríguez Rodríguez
Requestor Location	Sergio Rodríguez RodríguezGeneral DeliverySantiago de Compostela, 15782Spain

Publisher Tax ID	GB 494 6272 12
Total	0.00 EUR

ANNEX 2. URL TO FULL RESOLUTION IMAGES

Figure 1.2	1.2.png
Figure 1.3	1.3.png
Figure 1.4	1.4.png
Figure 1.5	1.5.png
Figure 1.6	1.6.png
Figure 2.1	2.1.png
Figure 2.2	2.2.png
Figure 2.3	2.3.png
Figure 2.4	2.4.png
Figure 2.5	2.5.png
Figure 2.6	2.6.png
Figure 2.7	2.7.png
Figure 3.3	3.3.png
Figure 3.4	3.4.png
Figure 3.6	3.6.png
Figure 3.8	3.8.png
Figure 3.10	3.10.png
Figure 3.11	3.11.png
Figure 3.12	3.12.png

Pathogens of the Vibrio genus represent one of the main threats to bivalve hatchery production, often leading to the loss of entire batches. The high virulence of these infections renders control methods ineffective once mortality is detected, focusing efforts instead on preventive strategies that are limited, environmentally costly, and often ineffective. Vibrio europaeus is an emerging pathogen reported in both Europe and the Americas, capable of causing mortalities across various developmental stages of multiple bivalve species. This study presents a genomic characterization of all available V. europaeus strains to date, including pangenome analysis, phylogeny, characterization of key genes and elements, and a study of the accessory genome.